JUSTUS-LIEBIG-UNIVERSITÄT GIESSEN

DLR

Microbial burden in public transport: Detection and prevention of bacterial contaminants based on an *in vitro* bacterial community

Dissertation for the degree of *Doctor rerum naturalium* (Dr. rer. nat.)

submitted by
Yen-Tran Ly-Sauerbrey

To the Faculty of Biology and Chemistry of the Justus Liebig University Giessen, prepared at the Institute of Aerospace Medicine at the German Aerospace Center (DLR)

Bonn 2026

Reviewers

First reviewer:	Prof. Dr. Alexander Goesmann, Justus Liebig University, Giessen
Second reviewer:	Prof. Dr. Stefan Janssen, Justus Liebig University, Giessen
Examiner:	PD Dr. med. vet. Christine E. Hellweg, German Aerospace Center, Cologne
Examiner:	PD Dr. Torsten Hain, Justus Liebig University, Giessen

Declaration of Authorship

„Ich erkläre: Ich habe die vorgelegte Dissertation selbstständig und ohne unerlaubte fremde Hilfe und nur mit den Hilfen angefertigt, die ich in der Dissertation angegeben habe. Alle Textstellen, die wörtlich oder sinngemäß aus veröffentlichten Schriften entnommen sind, und alle Angaben, die auf mündlichen Auskünften beruhen, sind als solche kenntlich gemacht. Ich stimme einer evtl. Überprüfung meiner Dissertation durch eine Antiplagiat-Software zu. Bei den von mir durchgeführten und in der Dissertation erwähnten Untersuchungen habe ich die Grundsätze guter wissenschaftlicher Praxis, wie sie in der „Satzung der Justus-Liebig-Universität Gießen zur Sicherung guter wissenschaftlicher Praxis“ niedergelegt sind, eingehalten.“

Angaben zu auf künstlicher Intelligenz (KI) basierender Hilfen wie ChatGPT oder SchulKI von OpenAI oder Gemini von Google zur Erstellung meiner Dissertation (Zutreffendes angekreuzt):

☐ Ich habe bei der Erstellung dieses Textes kein KI-Tool verwendet.

☑ Ich habe ein KI-Tool in den folgenden Bereichen eingesetzt (Mehrfachnennungen möglich):

- ☐ Ideen finden, meine Kreativität anregen
- ☐ Verstehen von Konzepten, Recherche von Fakten und Definitionen
- ☑ Optimierung eines von mir verfassten Textes
- ☐ Erstellen ganzer Textpassagen nach meinen Vorgaben

Folgende KI-Tools habe ich verwendet, damit aufgeführte Teile meines Textes von dem Tool wie folgt profitiert haben: DeepL Write (zur Prüfung der Grammatik)

Bonn, 4. März 2026 _____

Yen-Tran Ly-Sauerbrey

„Wer abbeißt, muss auch kauen“ – Chris Sommer

Contents

Abstract 1

Zusammenfassung 3

1 Introduction 5

1.1 Risks of microbial communities 7

1.1.1 Importance of microbial communities 7

1.1.2 Pathogen outbreaks 8

1.2 Microbial spread and infection routes 9

1.2.1 Airborne transmission 11

1.2.2 Contact transmission 12

1.3 Passenger cabins as transmission hotspots 13

1.3.1 The subway and aircraft cabin microbiome 14

1.3.2 *In vitro* public transport bacterial community for improved research 15

1.4 Antimicrobial materials as a preventive strategy 16

1.4.1 Antimicrobial mechanisms of copper 17

1.4.2 Bacterial defense mechanisms against copper 18

1.5 Air curtains against bioaerosol propagation 20

1.6 Investigating microbial communities: Microbial monitoring and detection 21

1.6.1 Broad microbial detection – 16S rRNA Sequencing 22

1.6.2 Species-specific detection of low-biomass samples 23

1.7 Research questions 25

1.8 Document structure 27

2 Results 28

2.1 An overview of the bacterial microbiome of public transportation systems – risks, detection, and countermeasures 28

2.2 Microbial communities in local train cabins remain stable through the seasons during one year of monitoring 36

2.3 Modeling the public transport microbiome: Development of a microbial reference community 67

2.4 Comparative assessment of bioaerosol propagation through an air curtain using microbiological methods and particulate matter sensors 79

2.5 Comparison of single bacteria and a bacterial reference community in a test against coated surfaces of varying copper content 102

2.6 Short-time thermal inactivation of surrogates of the public transport microbiome with a low-cost thermoresistometer 122

2.7 Other publications 137

3 Discussion 139

3.1 Microbial surveillance as a preventive measure 140

3.1.1 The public transport microbiome 140

3.1.2 Microbial detection – lack of standards and limited by resources 142

3.2 *In vitro* bacterial community of the public transport microbiome 144

3.2.1 Suitability & applicability as a reference 144

3.2.2 Single vs. bacterial community testing 147

3.3 Reduction of microbial load in passenger cabins 148

3.3.1 Intervention of airborne transmission 148

3.3.2 Intervention of contact transmission 151

3.3.3 Safe passenger cabin of the future 155

4 Conclusion and outlook 158

5 Acknowledgements 161

6 Bibliography 163

Abstract

Passenger cabins of public transport represent environments in which humans reside for short or long periods. Together with them, microorganisms they carry shape the public transport microbiome. Among the microbiome, mostly human-associated microbes exist, that are unharmful or opportunistic for healthy humans. However, particularly vulnerable groups of the population with weakened immune system are at higher risk for severe infections. The confined and, especially during rush hours, crowded space poses an environment that facilitates microbial transmission. Measures that reduce the spread of potential pathogens should be addressed to interfere with airborne and surface transmission, the two main pathways of microbial transmission in such spaces.

To contribute to the research of microbial burden in public transport, this thesis addressed approaches to detect and reduce bacterial contaminants. For that, the train cabin microbiome was monitored and investigated by regular sampling through one year. Based on present data, most abundant and relevant genera of the public transport microbiome were identified to develop an *in vitro* bacterial community. It includes surrogates of high abundant or healthcare relevant genera, namely *Pseudomonas, Staphylococcus, Streptococcus, Propionibacterium, Corynebacterium, Sphingomonas, Flavobacterium, Burkholderia* and *Enterococcus*. All nine species were biosafety level 1 organisms and were the main tool to test microbial interventions in this thesis. The aim was to create a reference bacterial community, that can more realistically represent effects of potential microbial interventions compared to single model organisms, that are mostly used in research. After a first characterization of the *in vitro* bacterial community, two main interventions were investigated: (I) Antibacterial surface coatings based on copper and copper-aluminum alloys, and (II) Reduced bioaerosol propagation through an air curtain. As a third microbial countermeasure, thermal inactivation of members of the bacterial community was investigated, with the perspective of reducing microbial burden in the passenger cabin air.

Characterization of the developed public transport ***in vitro* bacterial community** showed that the DNA remained largely intact after various stress treatments. The bacterial community was further used for the **detection of bioaerosols**, using both particle-based measurements and assessments of bacterial survival. This enabled the identification of a maximum **air curtain** effectivity of 66 % in reducing particle and bacterial concentrations. The importance of using

not only single species for investigations was highlighted by the observed protective effect of the *in vitro* bacterial community during the experiments on **antibacterial surfaces**. The novel surfaces with a copper content of 79 at.% and 100 at.% demonstrated their antibacterial potential after wet contact killing. **Thermal inactivation** of members of the *in vitro* bacterial community and a bacteriophage also proved to be an effective microbial countermeasure, with all of the tested microorganisms exhibiting no detectable survival after exposure to 85 °C for 2 s.

Overall, this thesis highlights the importance of incorporating a broader range of test organisms to investigate their detection and strategies to reduce bacterial contaminations. The *in vitro* bacterial community was successfully established and applied to multiple research questions, demonstrating its potential as a reference for studies on bacterial detection and microbial intervention.

Zusammenfassung

Fahrgastkabinen öffentlicher Verkehrsmittel sind von Menschen und ihren Mikroorganismen geprägte Umgebungen. Im Mikrobiom öffentlicher Verkehrsmittel kommen überwiegend human-assoziierte Organismen vor, die für gesunde Menschen harmlos oder opportunistisch sind. Besonders gefährdete Bevölkerungsgruppen mit geschwächtem Immunsystem sind jedoch einem höheren Risiko für schwere Infektionen ausgesetzt. Die räumlich begrenzte und, insbesondere zu Stoßzeiten, überfüllte Umgebung begünstigt dabei die Übertragung von Mikroben. Antimikrobielle Maßnahmen werden in dieser Arbeit thematisiert, welche auf die Hauptübertragungswege über die Luft und Oberflächen abzielen.

Um einen Beitrag zur Erforschung der mikrobiellen Belastung in öffentlichen Verkehrsmitteln zu leisten, befasste sich diese Arbeit mit Ansätzen zur Detektion und Reduzierung bakterieller Kontaminanten. Zu diesem Zweck wurde das Mikrobiom in Zugkabinen ein Jahr lang durch regelmäßige Probenahmen überwacht und untersucht. Auf Grundlage der vorliegenden Daten wurden die häufigsten und relevantesten Gattungen des Mikrobioms in öffentlichen Verkehrsmitteln identifiziert, um eine in-vitro-Bakteriengemeinschaft zu entwickeln. Diese umfasst Surrogate von häufig vorkommenden oder für die öffentliche Gesundheit relevanten Gattungen: *Pseudomonas*, *Staphylococcus*, *Streptococcus*, *Propionibacterium*, *Corynebacterium*, *Sphingomonas*, *Flavobacterium*, *Burkholderia* und *Enterococcus*. Alle neun verwendeten Spezies sind der Biosicherheitsstufe 1 zugeordnet und dienten in dieser Arbeit als Hauptinstrument zur Untersuchung mikrobieller Interventionen. Das Ziel war es, eine Referenz-Bakteriengemeinschaft zu schaffen, die die Auswirkungen potenzieller mikrobieller Interventionen realistischer darstellen kann als einzelne Modellorganismen, die meist in der Forschung verwendet werden. Nach einer ersten Charakterisierung der in-vitro-Bakteriengemeinschaft wurden zwei Hauptinterventionen untersucht: (I) Antibakterielle Oberflächenbeschichtungen auf Basis von Kupfer und Kupfer-Aluminium-Legierungen und (II) Reduzierte Bioaerosolausbreitung durch einen Luftvorhang. Als dritte mikrobielle Gegenmaßnahme wurde die thermische Inaktivierung von verschiedenen Mikroorganismen untersucht, mit dem weitreichenden Ziel, die mikrobielle Belastung in der Luft von Passagierkabinen zu reduzieren.

Die Charakterisierung der entwickelten **in-vitro-Bakteriengemeinschaft** des öffentlichen Nahverkehrs zeigte, dass die DNA nach verschiedenen Stress-Tests weitgehend intakt blieb.

Die Bakteriengemeinschaft wurde weiterführend für den **Nachweis von Bioaerosolen** eingesetzt, gemeinsam durch partikelbasierte Messungen als auch durch Bewertung der Überlebensrate der Bakterien. Dadurch konnte eine maximale Wirksamkeit des Luftvorhangs von 66 % bei der Reduzierung der Konzentration von Partikeln und Bakterien festgestellt werden. Die Bedeutung der Verwendung einer Bakteriengemeinschaft anstelle von Einzelorganismen wurde durch die beobachtete Schutzwirkung der in-vitro-Bakteriengemeinschaft im Zuge der Untersuchungen der **antibakteriellen Oberflächen** unterstrichen. Die neuartigen Oberflächen mit einem Kupfergehalt von 79 at.% und 100 at.% zeigten ihr Potenzial für die Abtötung von Bakterien. Auch die **thermische Inaktivierung** von Teilen der in-vitro-Bakteriengemeinschaft sowie die Verwendung eines Bakteriophagen erwiesen sich als wirksame mikrobielle Gegenmaßnahme, da nach einer Exposition bei 85 °C für 2 Sekunden kein Überleben der getesteten Mikroorganismen mehr festgestellt wurde.

Insgesamt unterstreicht diese Arbeit die Bedeutung der Einbeziehung eines breiteren Spektrums von Testorganismen, um deren Nachweis und Strategien zur Verringerung bakterieller Kontaminationen zu untersuchen. Die in-vitro-Bakteriengemeinschaft wurde erfolgreich etabliert und demonstrierte ihr Potential für die Beantwortung zahlreicher Forschungsfragen, die auch in Zukunft weiter adressiert werden können.

1 Introduction

Many remember wearing masks, taking tests, curfews, and social distancing. It reminds us of a time at the beginning and in the middle of the COVID-19 pandemic, which started in 2020 (1). Measures were influencing social and work life in many fields, for example, because travelling was put under caution. It was recommended that crowded and confined spaces with little fresh air supply should be avoided. This description, however, fits the environment of various types of public transportation. Hence, public transportation has not only been highly impacted by the pandemic, but it remains to be an environment favoring the spread of airborne pathogens. Further, fomites play a crucial role in microbial spread. These are inanimate objects, such as surfaces that carry microbial contaminations and contribute to their transmission. It is known, that the COVID-19 pandemic will not be the last pandemic (1, 2). Even now, we are caught in a pandemic of antimicrobial resistance (AMR), often called the "silent pandemic", since medial popularity is not as strong as during the COVID-19 pandemic (3, 4).

Given the issues described above, this work addresses different measures to counteract microbial burden in public transport (see **Figure 1**). Chapter 1.1 describes the general risks of **microbial burden** and pathogen outbreaks. Further, the passenger cabin and its role in microbial transmission (1.3) is introduced, with a particular focus on the subway and aircraft cabin microbiome (1.3.1). There are different methods to interfere with bacterial contaminants in such environments. **Investigating microbial communities** through monitoring and detection (1.6) is important for understanding and reflecting what microorganisms are present, and for identifying possible threats. As **thesis contribution**, the public transport microbiome was investigated and microbial monitoring was conducted in train cabins. Based on the gathered data, an *in vitro* bacterial community representative of the public transport was created (1.3.2), which was applied to test a range of **countermeasures**, including copper-based antimicrobial materials (1.4.), an air curtain (1.5.) and thermal inactivation. These approaches address airborne and surface transmission, which are the main **transmission routes** for microorganisms within passenger cabins (1.2).

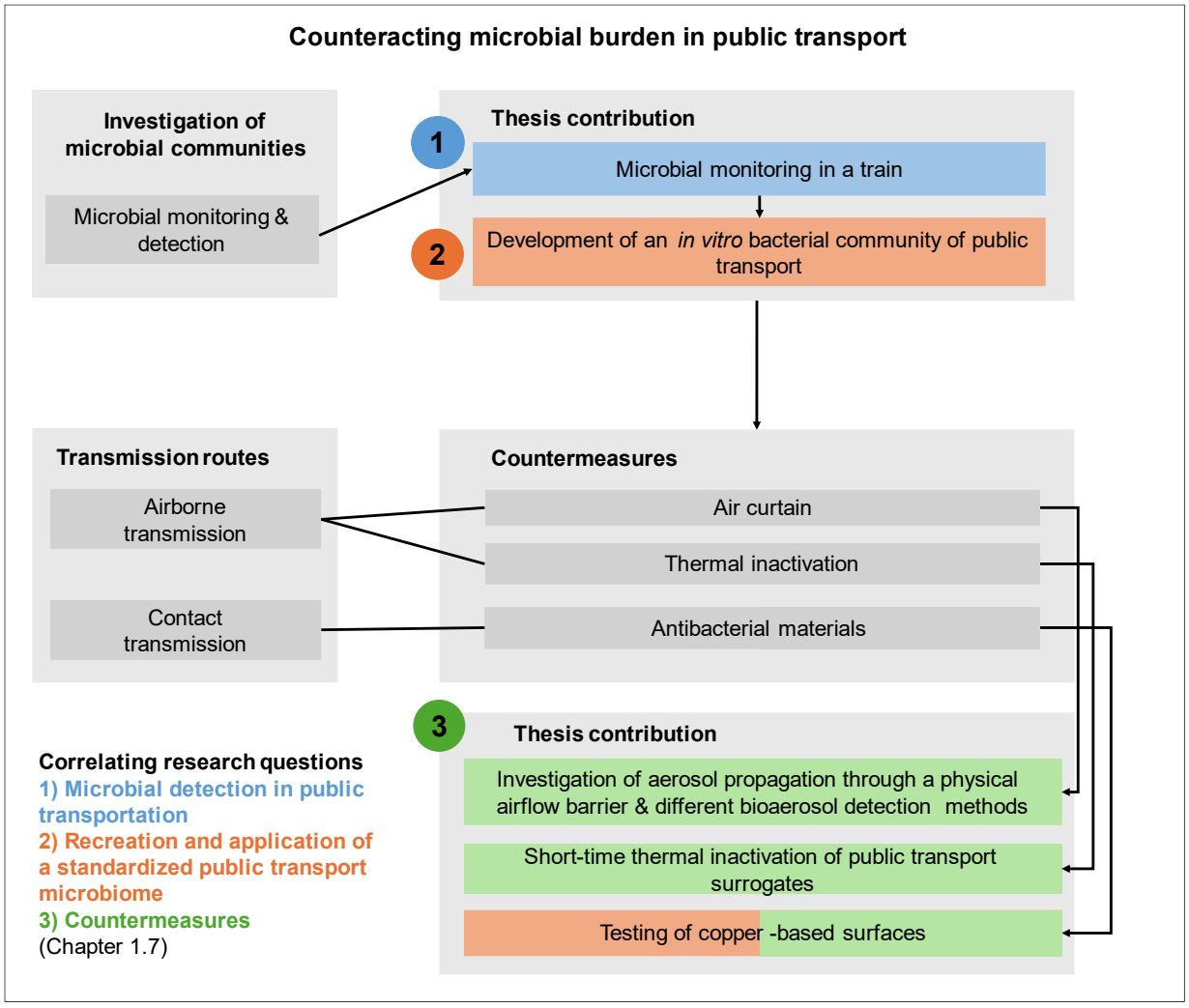

Figure 1: Overview of this works motivation and investigated topics.

1.1 Risks of microbial communities

Microbial communities are naturally inhabiting living organisms (e.g. human skin, gut) and environments (e.g. plants, soil). They are composed of microorganisms, which are microscopic organisms, including bacteria, viruses, fungi, protozoa, microalgae, and archaea. Their applications are versatile, ranging from the synthesis of antibiotics by fungi and bacteria to the production of food, such as bread and cheese. The composition of microbial communities is dynamic, influenced by various factors, such as climate, nutrient availability, antimicrobials, radiation, surface materials, and more. Different habitats result in different microbial communities, and consequently in a varying stress response. Therefore, microbial communities can act as an indicator for risk assessment (5, 6). Reducing the microbial spread in environments and potential subsequent transmission to humans is important to protect vulnerable populations, such as immunocompromised people. Opportunistic pathogens can become pathogenic and therefore cause infection, when the host immune system is weakened. This issue must be addressed by considering the role of microorganisms in human health.

1.1.1 Importance of microbial communities

Commensal microorganisms are required for the host immune response. These can be found within the gut and on the skin (7-9). For instance, commensal skin bacteria *Staphylococcus epidermidis* induces antimicrobial peptides, modulates cytokines, and inhibits the growth of competing or pathogenic bacteria (10, 11). In addition, gut microbiota and their bacteria are essential for gut health and metabolism, including the production of vitamins, amino acids and short-chain fatty acids, as concluded by Thursby and Juge (2017) (12). Therefore, the complete eradication of microorganisms in our environment is unreasonable. Diminished exposure to certain commensal and environmental microorganisms has been shown to facilitate the development of immune disorders such as allergies and autoimmune diseases, especially in industrialized countries (13). This topic is addressed by the Old Friends Hypothesis. It implies that microorganisms that were once abundant and trained the individual immune system are no longer exposed to appropriately, contributing to immune disorders (14). Those microorganisms derive from environmental microbiota, such as plants, animals, and soil. In addition, close contact and interactions between people, for example through skin, contribute to individual microbiota and immunoregulation (15-17). Therefore, a balanced approach is needed to prevent the reinforcement of rising immune disorders by using targeted interventions, while

simultaneously minimizing pathogen outbreaks, without the complete elimination of microorganisms.

1.1.2 Pathogen outbreaks

Pathogen outbreaks, such as the recent COVID-19 pandemic, are not only caused by viruses, but also parasites (e.g. malaria) or bacteria (e.g. tuberculosis). Furthermore, transmission is not limited to airborne, but, for example, also includes fecal- oral transmitted bacteria like *Vibrio cholerae* (18). A pandemic that was reinforced during COVID-19, was the AMR pandemic (19, 20). The misuse and overuse of antimicrobials, particularly in livestock (21) results in an increase in acquired resistances against antibiotics. Although AMR is not a virulence factor, it aggravates the treatment of infections in environments with selective antibiotic pressure, leading to prolonged illness and higher mortality, as concluded by Huemer et al. (2020) (22). This problem is further enhanced by the slow development of new antibiotics, leading to narrowed or no treatment possibilities, ultimately causing death of patients. By now, numbers of AMR-associated deaths are at 4.71 million worldwide in 2021, of which 1.14 million are directly traced back to AMR (23). For the year 2050, it has been estimated that 8.22 million deaths will be associated with AMR, therefore ~1.7 times more than in 2021. With 1.91 million deaths attributable to AMR globally, numbers are rising by 770.000 compared to 1.14 million deaths in 2021 (23).

Most deaths by AMR can be assigned to the so-called ESKAPE pathogens. The abbreviation stands for the species *Enterococcus faecium, Staphylococcus aureus, Klebsiella pneumoniae, Acinetobacter baumannii, Pseudomonas aeruginosa,* and *Enterobacter* species (24). Those pathogens are characterized by their high virulence and the ability to carry or transfer antibiotic resistances (25, 26). The ESKAPE pathogens represent a group of organisms that are a public health risk and, therefore, the subject of many studies. Additionally, the World Health Organization (WHO) published lists of bacterial priority pathogens in 2017 and 2024 which provide guidance for the investigation and analysis of new antibacterials (27, 28). Millions of patients that get infected with those pathogens cannot be treated easily and succumb to the consequences of their infections. Beside the high mortality, massive economic damage is caused by this crisis, as reviewed by Ahmad and Khan (2019) (29). In hospitals, various outbreaks have been often associated with ESKAPE pathogens (30-35). However, the spread is

not only limited to hospital settings. In public transport environments, various ESKAPE pathogens were detected before, as summarized by Ly et al. (2024) (36).

Future pandemics are certain. They are favored by global warming and human intrusion into nature, from where initially hidden pathogens could expand (e.g. zoonosis). To prevent future outbreaks, it is of great importance to understand microbial spread. For instance, during the COVID-19 pandemic, the key to reduce infections was to understand that the pathogen is airborne. Since public transport poses an environment that favors microbial spread and is part of the daily routine for a majority of people, I concentrate on the public transport microbiome and preventive measures, focusing on selected ESKAPE species as relevant AMR risks. To counteract this problem, it is important to understand microbial spread, investigate and apply suitable detection methods and countermeasures against microbial contaminants.

1.2 Microbial spread and infection routes

An infection is defined as the colonization and reproduction of microorganisms in a host organism. If a colonization leads to an infection of the host or not, depends on the infectious agent (pathogenicity, virulence) and the immunological status of the host. Another aspect is the infection risk, which also depends on different factors and has to be investigated for each microorganism to point out measures to minimize infections. This was extensively investigated for SARS-CoV-2 (37). The steps of an infection can be summarized into six categories (38) and are illustrated in **Figure 2**.

Microorganisms, which cause infections, can be bacteria, fungi, viruses, or parasites. Those can occur or settle, and multiply in a *reservoir*, which can be various places, such as humans, food, water, soil or animals, and not be neglected, environments, for instance, passenger cabins. The microorganisms or infectious agents can then be released from the reservoir via a *port of exit*. The port of exit is either secretions, such as saliva, or excretions (stool, urine), or fomites (e.g. contaminated areas, such as surfaces or hands). The released microorganisms are then transmitted through *modes of transport*, which can be direct or indirect contact. Direct contact is, e.g. the touching of contaminated surfaces or interaction with infected organisms, or the inhalation of bioaerosols, while indirect contact can occur through vectors, such as mosquitoes. The infectious agents then enter the body through the *port of entry*, possibly the respiratory tract (mouth, nose), eyes, wounds or the urinary tract. The infectious agents in the *susceptible host* can then settle and multiply. From the susceptible host, the infection chain continues again.

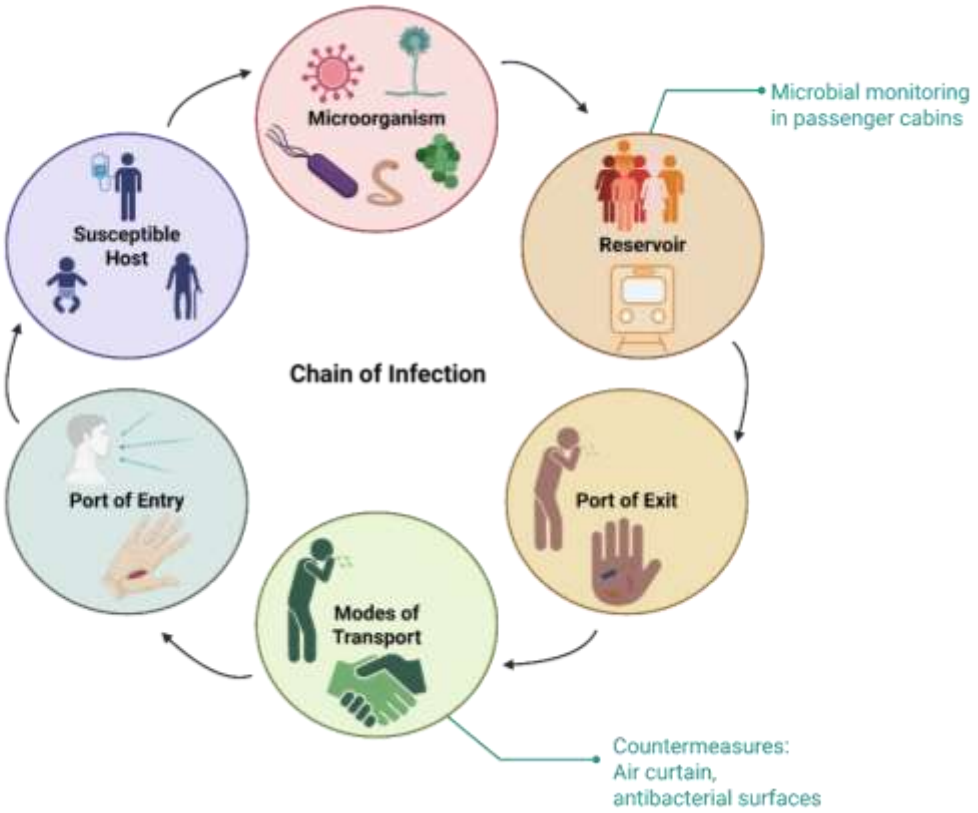

Figure 2: Chain of infection (based on NIOSH, (38)), with focus on the public transport environment. The chain of infection includes the microorganism or pathogens, a reservoir, which can be a passenger cabin, were pathogens can multiply. The port of exit describes secretions or excretions, which then lead to the modes of transport, being contact to surfaces (e.g. door bars), inhalation of droplets and airborne transmission. This is where countermeasures, such as those discussed in this paper, can come into effect. These include air curtains against air transmission and antibacterial surfaces against contact transmission. The port of entry can be the respiratory tract, oral, or open wounds. The susceptible host commuting gets infected and becomes the reservoir by spreading infectious agents during sickness. Created with BioRender.

A factor that facilitates the spread of infectious diseases, which is the focus of this work, is the microbial transmission during travel. Within the chain of infection, there are possibilities to interfere and reduce infection transmission. One measure, that was performed in this work, was microbial monitoring of the reservoir, that is the train passenger cabin. With the detection of anomalies, further measures can be taken, such as targeted elimination or reduction of occurring pathogens. In addition, this work focusses on different countermeasures to reduce the mode of transport in public environments. One mode of transport are aerosols, which can carry

pathogenic organisms. Especially in crowded passenger cabins without proper ventilation and low amount of fresh air, transmission of infectious diseases is facilitated (39, 40). Several of these aspects are part of the presented work, and will be explored in more detail in the following chapters. Besides aerosols, specific fomites in the train cabin can lead to contact transmission, such as frequently touched seat handles. Both airborne and contact transmission are further described in the following sections.

1.2.1 Airborne transmission

Airborne transmission can be either direct droplet transmission (sneezing, coughing, talking) or indirect (aerosolized particles containing infectious agents).

In a study by Knobling et al. (2022) it is suggested that bioaerosol assessment may be of importance for the modelling and investigation of airborne infectious disease particles (41). Bioaerosols can be described as airborne particulate matter (PM) of biological origin, containing microorganisms and their products with a particle diameter between 10 nm and 100 µm (42). Sneezing can disperse large droplets (300-900 µm) up to 5 meters, while small droplets (100-200 µm) have been shown to reach a distance of up to 18 meters (43). However, it is highly dependent on individual human physiology, how far droplets travel after sneezing (44). As described in 1.2, bioaerosols present one mode of transmission of pathogens. The number of cells that are transmitted during an infection, is variable and depends on factors, such as the host's immune system, the pathogen itself, current disease progression, and environmental settings. Therefore, it is of interest to investigate this specific mode of transmission and the possible detection methods of bioaerosols. Through decent detection, the development and assessment of countermeasures for bioaerosol spread is possible.

1.2.2 Contact transmission

Humans conduct frequent face-touching, which promotes the transmission of infectious agents. In a study by Kwok et al. (2014), test subjects unknowingly touched their face with their hands 23 times per hour (45). As described earlier, fomites contribute to microbial spread. Norovirus is a good example for an easily spread pathogen by contaminated surfaces, among other transmission routes (46). The transmission of infectious agents via surfaces has been known for a long time (47), and hygiene concepts have been developed ever since. These concepts include the use of disinfectants and cleaning agents, which reduce the microbial burden. Although cleaning agents and biocides are important for protection against pathogens, they have to be handled with care: Indications of increased resistance against disinfectants exist and are a concern, as concluded by Rozman et al. (2021) (48). Therefore, a responsible application is important to reduce the risks of arising antimicrobial resistance (49).

The risk of infectious disease transmission through surfaces is known. And the risk is not unfounded. Many nosocomial pathogens can survive for months on dry surfaces, such as *Staphylococcus aureus* (including methicillin resistant *S. aureus*, MRSA), *Enterococcus* spp. (including vancomycin resistant enterococci, VRE), *Acinetobacter* spp., *Pseudomonas aeruginosa*, and many more (50). Long survival periods allow the nosocomial pathogens to be spread even more, if no proper cleaning is performed. As a result, immunocompromised patients are at high risk for infections by direct or indirect contact, further compromising their health critically. Therefore, surfaces present a suitable target to reduce or even completely disrupt transmission.

1.3 Passenger cabins as transmission hotspots

The threat of rising and intensifying pandemics exists and is promoted by global transport networks. These include shipping, air travel, and public transportation via subway, train, and bus. Travel has increased substantially both locally and globally over the past few decades. This rise can be traced back to different factors. Over time, traveling became more affordable and, partially due to the media, touristic locations were promoted. The increased demand of travelling is pictured by the growth of prognosticated international tourist arrivals by the World Tourism Organization (UNWTO), which proposes an increase from 1.4 billion in 2020 to 1.8 billion in 2030 worldwide (51). Similar, in local public transport, passenger growth has shown further increase, until 2020, when the COVID-19 pandemic hit (52, 53). During the pandemic a decline was also observed for air travel due to travel restrictions (54). In Germany, passenger numbers of October 2024 in regional public transport and air travel have not fully recovered to pre-pandemic levels of October 2019 (55, 56). In the European Union, however, air traffic showed even more passengers compared to 2019 levels (57).

Transmission of pathogens and microorganisms in general is facilitated by many factors, especially in environments with large crowds of people and confined spaces, which do not allow proper ventilation. This scenario can be found in public transportation in large cities, where millions of people commute daily. The potential risks call for the implementation of countermeasures. Since air travel can be controlled more easily compared to commuting via train, more data to its impact to disease transmission are available. It has been traced back and investigated, that the spread of different types of diseases is facilitated by air travel. These include respiratory diseases (Influenza, COVID-19, Tuberculosis), vector-borne diseases (Malaria, Dengue, Chikungunya), and gastrointestinal diseases (Salmonellosis, Cholera), as summarized by Findlater and Bogoch (2018) (58).

Since data is still lacking on the current state of public transport systems, it is important to investigate its microbiome. Some studies conducted microbiome analysis of public transportation, such as subway systems and aircraft cabins. The following sections will highlight key characteristics of those environments and their relevance to this work.

1.3.1 The subway and aircraft cabin microbiome

To investigate public transport cabins and possible countermeasures to reduce microbial transmission, the current state of knowledge on this environment is of interest. Due to the risk of airborne and contact transmission, monitoring the aircraft microbiome is highly relevant. A unique feature of aircrafts and air travel is its potential contribution to the development of pandemics. Investigations on the transmission of different infectious diseases in aircraft cabins have been conducted. This includes airborne infections of SARS-CoV-1, SARS-CoV-2, Influenza and tuberculosis, but also foodborne and vector-borne infections (59). Although the train microbiome was subject of this present work, most studies existing on ground public transportation are based on the subway environment. The risks of subway systems for bacterial pathogens and their occurrence are further described in 2.1.

Both subway and aircraft cabin microbiomes consist of human-associated bacterial genera, such as *Staphylococcus, Corynebacterium*, and *Streptococcus*. Further, they share high contents of *Flavobacterium* and *Sphingomonas*. This is not surprising, since aircraft and subway passenger cabins are exposed to humans. Substantial differences between these two indoor scenarios are displayed in **Table 1**. Mostly, higher frequencies of passengers and a maximum travel time of one hour is expected in subways. On the other hand, commercial aircrafts are normally habiting passengers for more than 1 hour and no passenger fluctuation occurs during the travel. An even greater influence of the microbiome lies in the surface types within these environments (60). The surface microbiome is affected by different factors, such as the surface composition (e.g. Cu with antimicrobial properties) or topography (smooth or rough, influencing microbial attachment, biofilm formation).

Another difference between aircrafts and subways / trains is the ventilation. Aircraft cabins are equipped with high efficiency particulate air (HEPA) filters, where the recirculated air containing bacteria and other microbes, is filtrated (61). However, it does not ensure complete protection against airborne infectious agents.

Table 1 also displays an overview of the most abundant genera in aircraft cabins and subway systems. The studies were conducted using 16S rRNA sequencing, and focused on the detection up to genera-level. This provides a good overview of the existing bacteria. However, the identification of pathogens is not clear with this approach. Nonetheless, as indicated in red font, some of the most abundant genera in those settings, namely *Staphylococcus*, *Klebsiella*

(*Enterobacteriaceae*), *Pseudomonas*, and *Acinetobacter*, are genera of ESKAPE pathogens and deserve close attention.

Table 1: Travel mode variations and top ten abundant bacterial taxa (mostly genera) found in past microbiome studies within aircraft cabins and subways (based on surface and/or air samples). Ordered by abundance from top to bottom. Gray marked taxa display dissimilarities between the two environments. Red font highlights genera or family of ESKAPE pathogens.

Travel mode variations	**Aircraft cabin**	**Subway**
Ventilation system	HEPA filter, recirculating air	No HEPA filter, fresh air
Travel duration	~1- > 10 hours	~30 – 60 min
Passenger fluctuation	low	high
Bacterial taxa no.		
1	*Staphylococcus*	*Staphylococcus*
2	*Pseudomonas*	*Acinetobacter*
3	*Corynebacterium*	*Corynebacterium*
4	*Streptococcus*	*Micrococcus*
5	*Enterobacteriaceae*	*Propionibacterium*
6	*Flavobacterium*	*Pseudomonas*
7	*Kocuria*	*Sphingomonas*
8	*Micrococcus*	*Flavobacterium*
9	*Sphingomonas*	*Streptococcus*
10	*Stenotrophomonas*	*Kocuria*

References: Aircraft cabin – Weiss et al., 2019 (62), Liu et al., 2020 (63), Sun et al., 2020 (60). Subway – Afshinnekoo et al., 2018 (64), Kang et al., 2018 (65), Gohli et al., 2019 (66), Zhao et al., 2019 (67), Hernández et al., 2020 (68).

1.3.2 *In vitro* public transport bacterial community for improved research

Thinking about a next potential pandemic: Would we be prepared? To answer this question, microbial surveillance poses an important role to detect potential pathogens. Therefore, the comprised information in this section creates a fundament for the investigations conducted on the development and testing of microbial countermeasures: In this work, the train microbiome was investigated over a one-year study, to collect additional data and allow new insights, for example, regarding potential seasonality of the microbiome. Based on the gathered data, an *in*

vitro bacterial community was created, functioning as a reference tool for the test of different microbial countermeasures. This bacterial community is composed of nine bacterial species, which genera are abundant in public transport environments, or relevant genera of pathogens, e.g. *Enterococcus*, and carries an important role in this work. This specific *in vitro* bacterial community was applied to test the introduced detection methods and microbial countermeasures. This approach allows a closer insight to real-life environments, in comparison to single species model organisms. The idea is not new, since various *in vitro* microbial communities exist, resembling, for instance, the highly complex gut microbiome (69-71).

1.4 Antimicrobial materials as a preventive strategy

The aircraft cabin and its frequently touched surfaces, pose a risk for the transmission of pathogenic microorganisms (67). Therefore, one point of attack against microbial spread are antimicrobial surfaces, which can interfere contact transmission of pathogens. A variation of such materials exists and can act biocidal, as briefly described in the introduction of 2.5 "*Comparison of Single Bacteria and a Bacterial Reference Community in a Test Against Coated Surfaces of Varying Copper Content*".

In some cities, antimicrobial materials or coatings are already implemented on frequently-touched surfaces, e.g. on handrails (72, 73). The most known, studied and used material with antimicrobial properties is copper. Nonetheless, the mechanisms and effect of copper is not yet fully understood. Therefore, it is of interest to deepen the knowledge about the antimicrobial properties and (long-term) effects of copper to bacterial communities, but also work on innovative functionalization of this material.

Besides the research on copper as an antimicrobial material, searching and creating new alternatives to counter resistance development is important. The application of all sorts of antimicrobials harbors the risk of the emergence of resistances due to selective pressure. This includes antibiotics, as well as antimicrobial surfaces. It is already known for antibiotics, that after their application as such, the emergence of respective resistance is not far (74, 75). Resistant bacterial strains have been isolated from animal farms with resistance to copper, but also antibiotics and disinfectants (76, 77). This can be traced back to high use of antibiotics and copper sulfate as feed supplement in animal farming. Nevertheless, the development and application of novel countermeasures (in combination) are crucial to act against the

transmission of potential pathogens. This includes microbial surveillance, but also effective and efficient cleaning protocols, and other countermeasures.

1.4.1 Antimicrobial mechanisms of copper

Copper is an essential element for the cells of all aerobic organisms (78). However, copper tolerance is limited and copper concentrations in the cell can become toxic. For instance, the copper ions Cu^{+} and Cu^{2+} can cause membrane damage by inducing reactive oxygen species (ROS), which are involved in oxidative stress response (79, 80). ROS include singlet oxygen ($^1O_2$) and ozone (O_3) as well as partially reduced oxygen, such as superoxide anion ($O_2^{\bullet -}$), hydrogen peroxide (H_2O_2), and hydroxyl radicals ($^{\bullet}OH$) (81). They are generated by both Fenton (82) (some state also Fenton independent reactions (83)) and Haber-Weiss (84) reactions under aerobic conditions:

$$Cu^{+} + H_2O_2 \rightarrow Cu^{2+} + OH^{-} + \cdot OH \text{ (Fenton)}$$

$$\cdot O_2^{-} + H_2O_2 \overset{Cu}{\rightarrow} O_2 + OH^{-} + \cdot OH \text{ (Haber-Weiss)}$$

While it is not agreed on, what exactly causes the first-degree copper damage to the cells, the generation of ROS leads to oxidative stress. In bacteria, oxidative stress results in the damage of cells by membrane damage, lipid peroxidation, protein oxidation and DNA damage, ultimately ending in cell death (85-88). For instance, protein damage is caused by superoxide and hydrogen peroxide, that can oxidize Fe-S clusters of proteins, leading to the release of Fe^{2+}. Free Fe^{2+} can bind to the naturally negatively charged DNA, and with surrounding H_2O_2 and Fenton-like reactions, hydroxyl radicals form and react with the DNA. As a result, the DNA can acquire mutations, which can lead to cell death (89, 90). In addition to the induction of ROS generation and oxidative stress response, copper ions and copper nanoparticles (CuNPs) can cause direct membrane damage and altered permeabilization (91, 92). Besides copper surfaces and copper ions, CuNPs are subject of targeted antimicrobial strategies (93, 94).

Copper affects different microorganisms, i.e. fungi, bacteria and viruses in both, similar but also different ways (86). Interestingly, even between bacteria, the effects of copper and their defense mechanisms can differ. Bacteria can be divided into two groups, based on their cell wall structure, namely gram-positive and gram-negative bacteria. Gram-negative bacteria have an outer membrane, equipped with lipopolysaccharides alongside phospholipids and proteins (95). They have a thin peptidoglycan layer with a periplasm between the outer and inner

membrane, while gram-positive bacteria do not possess an outer membrane, but a cell wall composed of a thick layer of peptidoglycan (96). The periplasmatic space of gram-positive bacteria is not as pronounced as in gram-negative bacteria, and is considered as periplasmic-like compartment (97). Some studies indicate that gram-negative bacteria have better requirements to overcome antibacterial effects of copper due to their negatively charged cells (98). But this assumption does not account for all gram-positive and gram-negative bacteria, since there are exceptions, such as negatively charged *Bacillus subtilis* (compared to *Escherichia coli*) (99).

Within gram-negative bacteria, the negative effects of copper have been the subject of research. The main aspects of antibacterial effects of copper in both gram-positive and gram-negative bacteria are protein misfolding, interference of peptidoglycan maturation, displacement of metals from protein binding sites, disruption of cellular redox potential, and prevention of lipoprotein maturation in the cell envelope (88, 100).

1.4.2 Bacterial defense mechanisms against copper

Although copper is an essential element for bacteria, higher concentrations lead to a toxic shift within the cells. To counteract this, bacteria have developed a range of mechanisms to tolerate higher copper ion concentrations. So far, only a handful of species have been investigated in detail, such as *Escherichia coli* or *Salmonella enterica* (100). Due to the different cell wall structures, different defense mechanisms have been developed within gram-positive and gram-negative bacteria. For instance, periplasmic copper efflux is mediated through distinct genes of the *cus* or *cue* operon (101, 102). Other copper related operons exist, that contribute to copper defense and are related to regulation systems, copper efflux, copper oxidation, copper binding, and ROS defense, not necessarily attributed to gram-positive or gram-negative bacteria (103-105).

In this work, special focus was on the investigation of copper effects on selected gram-positive and gram-negative bacteria. As **Table 2** shows, there are some differences in coping with copper stress between gram-positive and gram-negative bacteria. Gram-negative bacteria are normally equipped with effective efflux pumps, which transport copper ions out of the cytoplasm and periplasm. Further, extracellular vesicles (EVs) have been reported to extrude copper at high concentrations (106). Gram-positive bacteria are also able to form EVs, but have

been only observed in relation to antibiotic resistance and not to transport excess copper from the cell (107).

Table 2: Mechanisms against copper induced and oxidative stress found in gram-negative and gram-positive bacteria.

Mechanism	**Gram-negative**	**Gram-positive**
Structural barrier	Outer membrane, periplasm	Thick peptidoglycan layer
Point of attack	Cytoplasm, periplasm	Cytoplasm
Copper efflux	Cytoplasmic (e.g. CopA) (108) Periplasmic (e.g. CusCBA) (108, 109) Extracellular vesicles (106) RND-type efflux systems (110, 111)	Cytoplasmic (e.g. CopA, CopB) (112-114)
Copper binding/chaperones	Intra- and extracellular sequestration (e.g. CusF) (108), regulation by copper-binding proteins (e.g. CsoR) (115)	Intracellular copper chaperoning (e.g. CopZ) (114)
Copper oxidation	Enzymatic detoxification (108), mainly periplasmic (e.g. CueO) (116, 117)	Membrane-associated or extracellular (114)
ROS defense	- Scavenging enzymes, regulated by SoxRS and OxyR (118): superoxide dismutases, catalases, peroxidases, terminal oxidases (119) - Glutathione (GSH) for H_2O_2 elimination (120, 121)	

1.5 Air curtains against bioaerosol propagation

Airborne transmission of pathogens (see 1.2.1) can potentially be prevented by air curtains: This countermeasure acts as a physical barrier for airborne pathogens, as visualized in **Figure 3**, and investigated within this thesis.

Air curtains are not a new invention for intervening airborne transmission of microorganisms. In operating rooms, they help to maintain sterile conditions in combination with HEPA filters and laminar air flow (122). A similar principle is given in clean benches of laboratories. The effectiveness of air curtains is also demonstrated in cold storages or in the entrance of large stores, functioning as a thermal barrier by maintaining stable air conditions and facilitating energy savings (123).

In addition, air curtains display a measure against airport malaria. Here, mosquitos carrying the malaria pathogen *Plasmodium falciparum* are imported by travelers or aircrafts from affected areas, which are then able to infect people in or nearby the airport that were not residing in malaria effecting regions (124). Air curtains installed in the entrance of aircrafts are suspected to be effective in keeping mosquitos outside the cabin and reduce the risk of distributing the vectors to the next destination (125). However, they are not commonly established, which can be attributed to constraints in their integration, maintenance, costs, and passenger comfort.

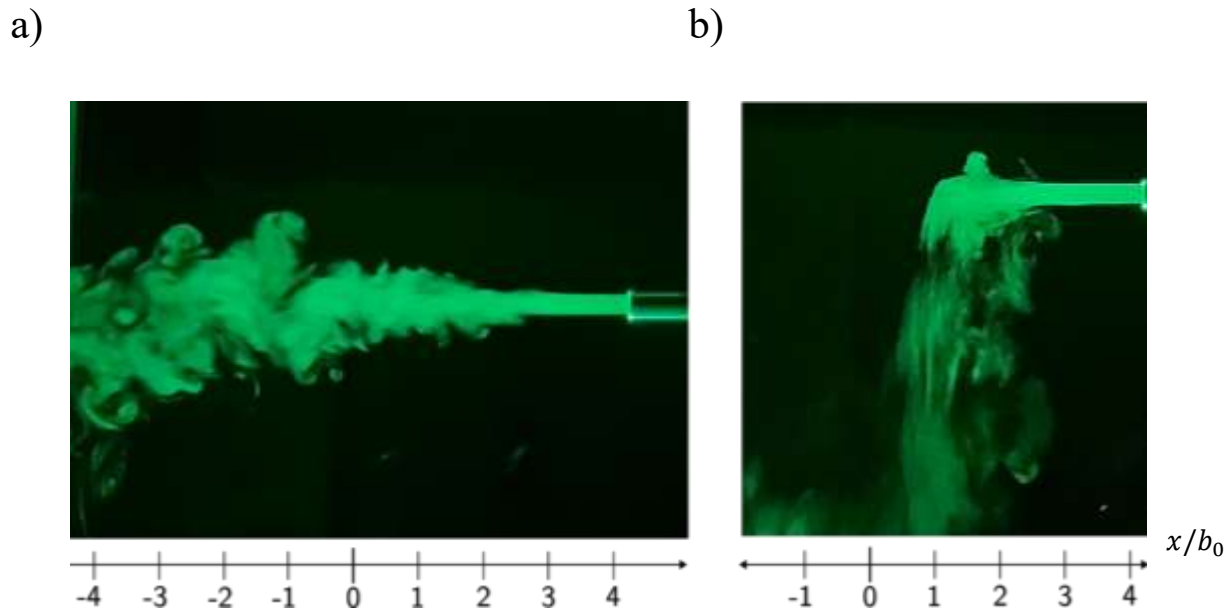

Figure 3: Air curtain effect on an aerosol jet visualized by a laser light sheet (from (126)). a) No air curtain, b) active air curtain. $b_0 = 0$ displays the nozzle of the air curtain.

As this work focuses on public transport cabins and reduced microbial spread, the air curtain was analyzed in regards to its ability to create a barrier and, therefore, prevent bioaerosol spread in passenger cabins. In order to understand the air curtain effectivity, great emphasis was placed on bioaerosol detection using particulate matter (PM) and culture-based methods. These methodologies and their importance are briefly described in the introduction of "*Comparative assessment of bioaerosol propagation through an air curtain using microbiological methods and particulate matter sensors*" (127) which is part of this thesis (see 2.4). To test bioaerosol detection and the effectivity of the air curtain against bioaerosol propagation, a standardized bacterial community was used. As described later in regards to microbial detection, standardized microbial communities greatly support the standardized testing of antimicrobial countermeasures, providing a novel insight into behavior of *in vivo* bacterial communities.

1.6 Investigating microbial communities: Microbial monitoring and detection

The thesis consists of two objects of investigation: 1) an unknown train microbiome and 2) an *in vitro* bacterial community, based on the public transport microbiome (aircraft, subway, train). To investigate both communities, different methods are necessary, which are described in the following.

Microbial monitoring and therefore microbial detection are common practice in many fields, including the food industry, biotechnology, drug industry (e.g. clean rooms), medicine and healthcare (e.g. diagnostics), water quality (e.g. sewage plants), and in the aerospace sector (e.g. planetary protection). With microbial monitoring, quality control is provided and can assure safe products. For example, in food industry, a certain level of colony forming units (CFU) must be below a limit, especially for health relevant species, such as *Listeria monocytogenes*, to provide a safe product (128). In space flight, planetary protection includes microbial quality control, which allows space craft and rovers to exit Earth only when it can be assured that no contamination of other planets will occur (129). Microbial monitoring deepens the understanding of baseline conditions and deviations, and contributes to the understanding of infection routes. In terms of public health, microbial monitoring is important for diagnostics, detection and containment of infectious diseases.

There are different approaches and methods to conduct microbial monitoring which are suitable for various purposes. All of the subsequent described detection techniques were used in this work and substantially contribute to a better understanding of microbial spread and the development of effective countermeasures (**Figure 4**).

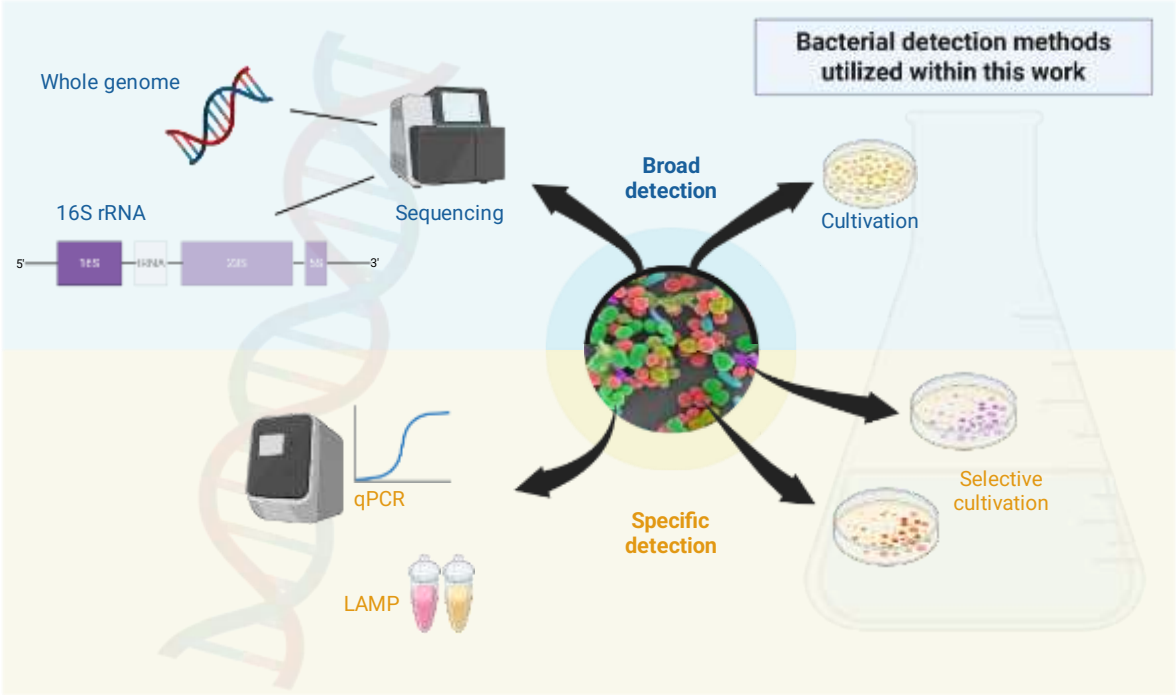

Figure 4: Microbial detection methods utilized within this work. Created with BioRender.

1.6.1 Broad microbial detection – 16S rRNA Sequencing

One used method is 16S rRNA amplicon sequencing, which was conducted for the investigation of the train cabin microbiome, whole genome sequencing for a detailed analysis of single species, and cultivation for the evaluation of microbial countermeasures in terms of cultivability.

The 16S rRNA gene is a highly conserved gene in bacteria and archaea, which is used for the identification and classification and, in addition to the conserved regions, contains hypervariable regions. It should be noted, that analysis of fungi and viruses is not possible, since the 16S rRNA gene is not found in these organisms. With the whole 16S rRNA gene, coding for the 16S rRNA as part of the small ribosomal subunit 30S, information on the species level are provided (130). Prior to sequencing, the gene can be amplified using universal primers. For 16S rRNA sequencing, different platforms exist. Some of the most used platforms are

Illumina (short-read, often used for distinct variable regions of the 16S rRNA gene), Pacific Biosciences (PacBio, long-read), Oxford Nanopore Technologies (ONT, long-read), and Sanger Sequencing (mainly used for single isolates). The reason for sequencing targeted variable regions of this gene with Illumina is its ability to sequence short sequence lengths of up to 2x300 bp via paired-end sequencing. Sequencing the whole 16S gene (~1500 bp) is possible with Illumina, but associated with increased data accumulation, requirement for data infrastructure and most limiting, higher material costs. Therefore, it is common practice to target the shorter variable regions (~250-500 bp), which mostly allow a reliable identification up to genus level (131). In total, nine variable regions (V1-V9) exist in the 16S rRNA gene, each with distinct features and carrying different information for phylogenetic identification (132).

The advantage of 16S rRNA sequencing is that it is a high-throughput technique, which is cost-effective compared to whole genome sequencing. It provides information on bacteria and archaea sufficiently down to genus level and covers both culturable and non-culturable organisms. In this work, the V1-V2 region was sequenced of samples originating from different locations of a train cabin to analyze existing taxa and their abundance as a microbial monitoring approach.

1.6.2 Species-specific detection of low-biomass samples

Low-biomass samples, as those retrieved from passenger cabins, are challenging to investigate. To monitor the microbial load, regular assessments are conducted. This can be achieved by cultivation, or DNA based methods. One disadvantage of cultivation is that it only detects organisms that can be cultivated. In addition, slow-growing species may be overlooked due to overgrowth by fast-growing species. A great challenge of detection within low-biomass samples is low DNA yield, which can be highly influenced by contaminations and results are prone to misrepresentation through PCR bias, which can be species-specific (133, 134). Requirements for species-specific detection from those samples include great sensitivity and specificity. To investigate the microbial taxonomy, diversity and abundance, amplicon sequencing (e.g. 16S rRNA) is a suitable approach. For a closer look into the genome up to species- and strain level, functional genes and metabolic pathways can be investigated by metagenome sequencing, which was not in scope of this work. For species-specific detection from low-biomass train cabin samples, real-time quantitative PCR (qPCR) was conducted for

environmental samples of the train. The widespread technique is utilizing a specific genetic region of an organism of choice, which is subsequently amplified and detected within a DNA sample in question (135). It is commonly used in routine laboratories as diagnostic tool, as highlighted by Maurin (2012) (136). To investigate the presence of specific bacterial species, different methods are also suitable, such as Loop-mediated isothermal amplification (LAMP), or fluorescence *in situ* hybridization (FISH). The description and application of LAMP is briefly summarized in Ly et al. (2024) (see 2.1) (36). The advantage of using qPCR instead of LAMP, is the fast primer design cost, since only two primers are needed. For LAMP, four to six primers are crucial, which are more complex in design (137). Other monitoring technologies exist, which are not dependent on DNA/RNA extraction. Warning systems, e.g. by laser-induced fluorescence (138, 139) are based on fluorescent emission spectra, which can be assigned to distinct pathogens within a sample.

1.7 Research questions

As exemplified in the introduction, we are likely to be facing pathogen outbreaks, that might bear the risk of causing a large number of ill patients and deaths. Although countermeasures exist, they must be studied more deeply, and new ones must be developed constantly. It is a race against time, as new resistances constantly develop, hence making it near impossible to solve this problem once and for all. This work aims to contribute to the fight against pandemic threats in public transport, as this environment is prone to promoting microbial transmission. As indicated in **Figure 1**, this was accomplished by 1) understanding what microbes and possible pathogens have to be targeted, 2) creating and testing tools for microbial detection and countermeasures, and 3) testing a variation of possible countermeasures, namely an air curtain against bioaerosol propagation, antibacterial surfaces coated with copper and copper-aluminum, and thermal inactivation of bioaerosols. Based on these aims, the following research questions were set.

RQ1) What microbiome are we facing in public transport systems, and how can we reliably detect it?

In order to create a reference tool to test detection and countermeasures, it is important to understand what the public transport microbiome is composed of. Studies that investigate the public transport microbiome focus mostly on the microbiome of subway environments, a few exist on the airplane cabin microbiome, only a handful of studies exist that analyze the bus microbiome, and no study has been done to date, which investigates the train microbiome. In the minireview "*An overview of the bacterial microbiome of public transportation systems – risks, detection, and countermeasures*", the findings of past studies were concluded and thus serve as the initial inventory of what is known about the public transport environment. In Germany, the train is high ranked for commuting. Therefore, this makes it the perfect environment for investigating the risk of infection transmission. Monitoring of the train microbiome provides knowledge on commonly found bacteria, and, with a series of sampling campaigns, the core microbiome was detected in scope of the study "*Microbial Communities in Local Train Cabins Remain Stable Through the Seasons During One Year of Monitoring*".

RQ2) From *in vivo* to *in vitro*: Is it possible to recreate and apply a standardized public transport microbiome as a simplified, yet realistic reference model for experimental testing?

Based on the findings of literature and the conducted train microbiome study, the development of an *in vitro* bacterial community was initialized. In this work, the creation and first characterization of this bacterial community was introduced in the conference proceeding "*Modeling the public transport microbiome: Development of a microbial reference community*" and additional data. With this tool, microbial dynamics can be considered when testing measures for microbial reduction or variations in microbial detection.

The behavior of microorganisms can be manifold. Although some species within a microbial community can be beneficial, others are able to comprise other bacterial species' survival through competition and selective pressure (140). To investigate this sort of behavior in a stress induced setting, antibacterial materials were tested with two bacterial species as pure cultures and the bacterial community. This experimental setup was applied in the study "*Comparison of Single Bacteria and a Bacterial Reference Community in a Test Against Coated Surfaces of Varying Copper Content*". With this approach, different factors could be compared, such as survival and metabolic activity.

RQ3) To what extent can physical and material-based interventions reduce microbial load in passenger cabins?

The developed bacterial community was tested as a bioaerosol, to investigate two methods for bioaerosol detection. For that, particulate matter measurement and culture-based methods were used in cooperation with the created bacterial community in the study "*Comparative Assessment of Bioaerosol Propagation Through an Air Curtain Using Microbiological Methods and Particulate Matter Sensors*". The same study was investigating the first microbial intervention in this work. Using different air curtain settings with and without HEPA filters attached, the bioaerosol dispersion within a closed chamber was tested. The bacterial growth of two of nine species of the bacterial community that were selected for cultivation was compared regarding their stability and detectability for the tested scenarios.

The current literature proposes that a copper content of ≥ 58 % has antibacterial effects. To confirm with the materials produced within this study, Cu-Al alloys with copper content between 24 at.% and 100 at.% were created by magnetron sputtering. We created controlled

settings with known bacterial inocula using the bacterial community developed within this work. In the study "*Comparison of Single Bacteria and a Bacterial Reference Community in a Test Against Coated Surfaces of Varying Copper Content*", the antibacterial activity of the materials was tested by wet contact killing assay, and addressing different behavior between single species and the bacterial community.

The last intervention strategy tested in this work was thermal inactivation. In food industry, it is already used for food safety (e.g. pasteurization), and can be applied in other settings too. Therefore, in the study "*Short-time thermal inactivation of surrogates of the public transport microbiome with a low-cost thermoresistometer*", the heat tolerance of different microorganisms was tested, among them three bacterial species of the bacterial community. The aim of application for the future would be the thermal inactivation of microorganism of the air in passenger cabins of electronic vehicles in winter or cold seasons, where heating is automatically conducted for passenger comfort.

1.8 Document structure

This thesis is comprised of six publications, of which three are counted as official thesis contribution (peer-reviewed journal articles, 2.1, 2.4, 2.5), one article is submitted (2.2), one article is a conference paper (2.3), and one article is a co-authored contribution (2.6). Nonetheless, all manuscripts contribute to the answer of the research questions.

2 Results

2.1 An overview of the bacterial microbiome of public transportation systems – risks, detection, and countermeasures

Title	**An overview of the bacterial microbiome of public transportation systems – risks, detection, and countermeasures**
Authors	**Yen-Tran Ly[1]**, Stefan Leuko[1], Ralf Möller[1]
Affiliation	[1] Department of Radiation Biology, Institute of Aerospace Medicine, German Aerospace Center, Cologne, Germany
Article type	Mini review
Authorship	Single-first author
Journal	Frontiers in Public Health
Year	2024
Volume	12
DOI	10.3389/fpubh.2024.1367324
Author Contributions	
Y-TL	Conceptualization, Visualization, Writing -original draft, Writing – review & editing
SL	Conceptualization, Writing – review & editing
RM	Conceptualization, Funding acquisition, Supervision, Writing – review & editing

frontiers | Frontiers in Public Health

TYPE Mini Review
PUBLISHED 11 March 2024
DOI 10.3389/fpubh.2024.1367324

OPEN ACCESS

EDITED BY
Faris Lami,
University of Baghdad, Iraq

REVIEWED BY
Hanan Khaleel,
University of Baghdad, Iraq
Batool Yassin,
University of Baghdad, Iraq

*CORRESPONDENCE
Ralf Moeller
ralf.moeller@dlr.de

RECEIVED 08 January 2024
ACCEPTED 27 February 2024
PUBLISHED 11 March 2024

CITATION
Ly Y-T, Leuko S and Moeller R (2024) An overview of the bacterial microbiome of public transportation systems—risks, detection, and countermeasures. *Front. Public Health* 12:1367324. doi: 10.3389/fpubh.2024.1367324

An overview of the bacterial microbiome of public transportation systems—risks, detection, and countermeasures

Yen-Tran Ly, Stefan Leuko and Ralf Moeller*

Department of Radiation Biology, Institute for Aerospace Medicine, German Aerospace Center, Cologne, Germany

When we humans travel, our microorganisms come along. These can be harmless but also pathogenic, and are spread by touching surfaces or breathing aerosols in the passenger cabins. As the pandemic with SARS-CoV-2 has shown, those environments display a risk for infection transmission. For a risk reduction, countermeasures such as wearing face masks and distancing were applied in many places, yet had a significant social impact. Nevertheless, the next pandemic will come and additional countermeasures that contribute to the risk reduction are needed to keep commuters safe and reduce the spread of microorganisms and pathogens, but also have as little impact as possible on the daily lives of commuters. This review describes the bacterial microbiome of subways around the world, which is mainly characterized by human-associated genera. We emphasize on healthcare-associated ESKAPE pathogens within public transport, introduce state-of-the art methods to detect common microbes and potential pathogens such as LAMP and next-generation sequencing. Further, we describe and discuss possible countermeasures that could be deployed in public transportation systems, as antimicrobial surfaces or air sterilization using plasma. Commuting in public transport can harbor risks of infection. Improving the safety of travelers can be achieved by effective detection methods, microbial reduction systems, but importantly by hand hygiene and common-sense hygiene guidelines.

KEYWORDS

microbial community, public transport, microbial detection, countermeasures, microbial spread

1 Introduction and discussion

Viruses play a major role in the spread of infectious diseases, most recently SARS-CoV-2, which was responsible for the COVID-19 pandemic. Even before the occurrence of SARS-CoV-2, the Influenza waves are causing 15,000–70,000 deaths of European citizens every year (1).

However, in addition to viruses, bacteria are also responsible for the spread of infectious diseases. More than half of emerging infectious diseases are caused by bacteria, many of which are drug-resistant (2). Antimicrobial resistance has long been recognized as an acute danger and is also referred to in the literature as a silent pandemic (3). The spread of microorganisms and thus also pathogens does not necessarily begin in hospitals, but rather where people move around.

1.1 Humans represent the main source of bacteria within subways

Subway systems are widely used, especially in big cities and carry millions of passengers every day. The high frequency of passengers using public transportation facilitates an exchange of microorganisms, especially when getting in contact with frequently touched surfaces such as handrails, and sharing the air within a confined space. In this review, the most common taxa within the subway microbiome of different cities are presented, and relevant risk factors are discussed. Further, a range of microbial detection methods are listed and countermeasures that may be applied in public transport are described.

Touching objects, such as handrails, leads to a transfer of the human hand microbiome to the touched object. In recent studies, the transfer of the hand microbiome from test subjects to objects was demonstrated (4, 5), which can also be transferred to the subway environment. The most abundant organisms found in subway microbiome studies in various cities are displayed in Table 1. Among those, most frequently occurring taxa were *Acinetobacter, Staphylococcus, Propionibacterium, Corynebacterium, Micrococcus, Streptococcus,* and *Kocuria,* which are common for the human skin microbiome (15–17). These studies were not specifically focused on the detection of pathogens, and only a few were found such as *Helicobacter pylori*, *Acinetobacter* species (sp.) (10) as well as opportunistic pathogenic isolates related to the species *Propionibacterium acnes* and *Staphylococcus epidermidis* or genera *Pseudonocardia* and *Nesterenkonia* (14). An important factor that should be considered is that in most of the studies listed, microbial detection was based on 16S rRNA sequencing, which does not provide adequate detection at the species level (18, 19) and therefore, no pathogenic strains were conclusively detected.

For this section, we reviewed 30 research articles, including nine studies on the subway microbiome, 12 studies on the occurrence of ESKAPE pathogens in public transportation environments, and 7 studies on general information on the human skin microbiome, the association with surfaces and the detection of pathogenic species in general.

1.1.1 ESKAPE pathogens—detected in public transport?

ESKAPE pathogens are the causative agents of most nosocomial infections worldwide. The abbreviation stands for the species *Escherichia coli, Staphylococcus aureus, Klebsiella pneumoniae, Acinetobacter baumannii, Pseudomonas aeruginosa*, and *Enterococcus faecium/faecalis*. Those organisms can be highly virulent and carry or transfer antibiotic resistances (20, 21).

Antibiotic resistance and the spread of multidrug-resistant bacteria (AMR) is a problem that was associated with about 4.9 million deaths worldwide in 2019 (22). However, the spread of these organisms does not occur in hospitals alone, but also in places with a high frequency of people, such as on public transportation. Notably, the following studies were focused on the detection of pathogenic species, mostly based on (selective) cultivation followed by PCR of pathogen-associated marker genes, e.g., the *mcr-1* gene for *E. coli* that mediates colistin resistance.

The most prominent ESKAPE species within the public transport studies is the (opportunistic) pathogen *Staphylococcus aureus*. In general, due to the natural passenger's microbiome, the skin-associated species are highly abundant in busses and subways. In a bus, serving both hospital and community routes, methicillin-resistant *S. aureus* (MRSA) was found (community-associated SCCmec type IV and healthcare-associated SCCmec type II). Of the detected MRSA strains, 65% were multidrug resistant (23). Within this study, seats and seat rails were most contaminated. In subways, *S. aureus* containing the *mecA* gene was detected, alongside natural skin-associated species of *S. aureus* (11). *mecA* is associated with methicillin-resistant *S. aureus* (MRSA) and nosocomial infections, but the study concludes no strong evidence for pathogenicity based on the obtained sequences. Other studies showed the prevalence of MRSA in public transport (24–27).

Escherichia coli with a multidrug resistance, including *mcr-1* which mediates colistin resistance, was found in public transportation in Guangzhou, China (28). Twenty-three isolates of 737 samples with bacterial growth were positive for *mcr-1*, most of them were resistant against ampicillin, cefotaxime, fosfomycin, and gentamicin.

For *Klebsiella pneumoniae*, there were less findings of drug resistant isolates. In the Beijing (China) subway environment, highly touched surfaces were sampled and from a total of 603 samples across 15 metro lines, 11 carbapenem-resistant *K. pneumoniae* isolates were detected (29).

Enterobacter species were also found in public transport studies. *E. faecium* was abundant throughout the subway in New York City, United States (11), and multidrug resistant *E. faecalis* was observed on shared bicycles in Chengdu, China (30).

No studies have been found on the occurrence of multidrug resistant *Acinetobacter baumannii* and *Pseudomonas aeruginosa* in public transport.

1.2 Microbial detection methods

There are a number of options for identifying bacteria. Classical biochemical or physiological methods such as microscopy are time-consuming and inefficient when it comes to examining a large number of samples and identifying the organism. Most studies reviewed within this work used the methodology of next-generation sequencing (1.2.1), which displays a modern and high-throughput detection approach, in contrast to cultivation on nutrient media. Latter allows the analysis of organisms that can grow under specific conditions. Several other methods exist, such as matrix-assisted laser desorption ionization coupled to time-of-flight mass spectrometry (MALDI-TOF MS) (31), or tandem mass spectrometry (19).

1.2.1 Next-generation-sequencing

Nowadays, next-generation-sequencing (NGS) is the most used technology for sequencing. With this approach, high throughput analysis is possible and enables the identification of microbes within a high sample size in a cost-effective manner, generating high amounts of data (32, 33). There is a big variation within the NGS DNA sequencing technologies, varying in amplification method, sequencing chemistry, sequencing speed, etc. (32, 33). The most established NGS platform was created by Illumina, followed by Oxford Nanopore, which revolutionized the field by releasing a first portable nanopore sequencing device in 2014. Each technology differs in its output, advantages and limitations. With NGS, not only the microbial identity can be detected, also the diversity within or of all samples can be determined, outshining the limited information obtained by cultivation. The possibilities within NGS and the bioinformatical analysis are rapidly evolving more and more.

TABLE 1 Overview of abundant bacteria across subways and subway stations found in multiple studies.

Organism			Location		Method	References
Five most abundant taxa (genus level): • *Acinetobacter* • *Corynebacterium* • *Streptococcus* • *Staphylococcus* • *Cutibacterium*	Ubiquitous in all samples: • *Acinetobacter* • *Corynebacterium* • *Streptococcus* • *Staphylococcus* • *Propionibacterium*	• *Kocuria* • *Pseudomonas* • *Micrococcaceae* • *Micrococcus*	Subway, Mexico city • Turnstiles • Stair handrails • Escalator handrails • Platform floor • Train poles • Seats		V3–V4 region of the 16S rRNA gene, MiSeq™ Illumina	(6)
Surfaces dominated by human skin and oral commensals: • *Propionibacterium* • *Corynebacterium* • *Staphylococcus* • *Streptococcus*			Subway, Boston • Grips • Poles • Seats • Seat backs	• Touchscreens • Sides of fare ticketing machines	V4 region of the 16S rRNA gene, MiSeq™ Illumina	(7)
Most abundant known genera: • *Propionibacterium* • *Corynebacterium* • *Streptococcus* • *Staphylococcus*			Metro, Mexico city • Station turnstiles • Vertical handrails inside the train		V3–V4 region of the 16S rRNA gene, MiSeq™ Illumina	(8)
Most commonly detected genera: • *Micrococcus* • *Enhydrobacter* • *Propionibacterium*	• *Staphylococcus* • *Corynebacterium*		Subway/MTR (Mass Transit Railway), Hong Kong • Aerosol samples		V4 region of the 16S rRNA gene, MiSeq™ Illumina	(9)
Bacterial species with the highest abundance: • *Propionibacterium acnes* • *Micrococcus luteus* • *Propionibacterium humerusii* • *Acinetobacter baumannii* • *Staphylococcus epidermidis* • *Escherichia coli* • *Staphylococcus aureus*			Subway/MTR (Mass Transit Railway), Hong Kong • Hands after handrail touching for 30 min		Metagenome sequencing with Illumina HiSeq™ 1,500	(10)
• *Pseudomonas stutzeri* • *Stenotrophomonas maltophilia* • *Enterobacter cloacae* • *Acinetobacter radioresistens* • *Acinetobacter nosocomialis*	• *Lysinibacillus sphaericus* • *Enterococcus casseliflavus* • *Brevundimonas diminuta* • *Acinetobacter lwoffii* • *Bacillus cereus*		Subway, NYC • Turnstiles • Emergency exits • Metro card kiosks • Benches • Stairwell handrails	• Trashcans • Doors • Poles • Handrails • Seats	HiSeq™ 2,500	(11)
High abundance: • *Paracoccus* • *Sphingomonas* • *Kocuria* • *Acinetobacter* • *Staphylococcus*	Lower abundance: • *Dietzia* • *Streptococcus* • *Enterobacter* • *Enterococcus* • *Anaerococcus*	• *Blautia* • *Burkholderia*	Metro, Athens • Bioaerosol of underground station		16S rRNA gene and ITS, MiSeq™ Illumina	(12)
• *Stenotrophomonas* • *Pseudomonas* • *Dietzia* • *Brevundimonas* • *Intrasporangiaceae_u*	• *(Arsenicicoccus/unclassified)* • *Comamonadaceae_u* • *Staphylococcus* • *Rhodococcus* • *Erwinia*		Subway, Moscow • Information stand • Bench • Floor	• Wall • Railings	V4 region of the 16S rRNA gene, MiSeq™ Illumina	(13)
Air: • *Unassigned* • *Micrococcus* • *Staphylococcus* • *Rubrobacter* • *Sphingomonas* • *Hymenobacter* • *Arthrobacter* • *Corynebacterium* • *Nocardioides*	• *Psychrobacter* • *Blastococcus* • *Kocuria* • *Streptococcus* • … Surface: • Unassigned • *Staphylococcus* • *Sphingomonas*	• *Streptococcus* • *Hymenobacter* • *Corynebacterium* • *Arthrobacter* • *Kocuria* • *Micrococcus* • *Psychrobacter* • *Flavobacterium* • …	Subway, Oslo • Air and surface samples from 16 stations • Across four seasons		V3–V4 region of the 16S rRNA gene, MiSeq™ Illumina	(14)

There have been studies that investigated the public transport microbiome within different cities. The most common method was the 16S rRNA sequencing, which provides taxa data of the genera found within samples more or less confidently. Interestingly, but not surprisingly, the genera of bacteria associated with humans are repeatedly listed as passengers leave their microbial footprints in the passenger cabins. These typically found bacterial genera may also be helpful in terms of suitable model organisms to study effective measures to reduce microbial load and pathogens in public transportation to reduce the transmission of infectious diseases.

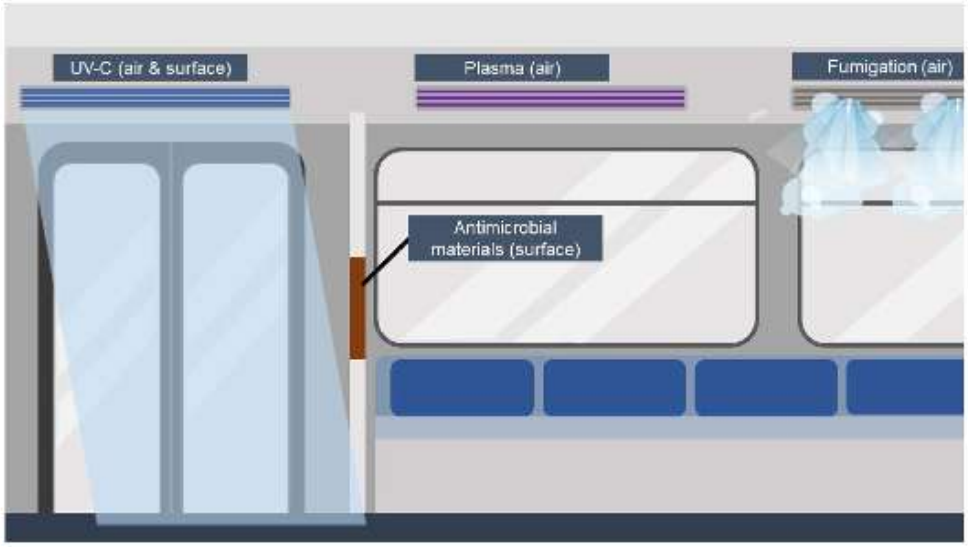

FIGURE 1
Overview of described microbial countermeasures in public transport. For air cleaning and disinfection, UV-C, fumigation of disinfectants, and plasma air sterilization can be used. Of those, plasma air cleaning is suitable for the use during passenger occurrence. For the reduced microbial burden on (highly) touched surfaces, antimicrobial surfaces can be implemented. UV-C can be installed during cleaning times without any passenger on board, as well as the fumigation of chemicals. Created with BioRender.com.

Nevertheless, there are some shortcomings when it comes to profiling uncharacterized species in environmental microbiomes, as strain-level analyses are usually tested for human metagenomes and the tools are tailored to human metagenomes (34).

1.2.2 Loop-mediated isothermal amplification

Metagenomics is a powerful tool to identify the microbiome of a sample. If specific organisms are to be screened for, such as potential pathogens, there are methods such as loop-mediated isothermal amplification (LAMP) that allow the targeted detection of species. LAMP is a fast, cost effective, and easy tool to detect specific organisms and requires only a few devices, while the evaluation occurs after 30 min.

Using marker genes, which differ for every organism, fast and detailed detection with a high specificity and sensitivity are possible (35). The potential of LAMP has already been established in relation to the detection of pathogens in the food industry (36). It is also useful for hospitals or in human high traffic environments to monitor microbial threats. During the SARS-CoV-2 pandemic, several publications showed the successful application of reverse transcription LAMP for this pathogen (37–39).

To this date and to our knowledge, there is no publication on the use of LAMP for pathogen detection in public transport as microbial monitoring measure. The detection of drug-resistant organisms is an important factor in monitoring the spread of pathogens and has yet to be implemented.

1.3 Countermeasures and feasibility in public transport

A summary of the mentioned countermeasures is displayed in Figure 1. The term antimicrobial includes not only bacteria, but also other groups such as viruses and fungi. But even within the group of bacteria, the effect of countermeasures varies depending on the bacterium, e.g., in the case of spore-forming bacteria, as their spores can be highly resistant to heat, for example (40, 41). Many of the mentioned countermeasures have been tested within hospital settings and in food industry, since the urge of clean and sterile environments is inevitable in those areas. Passenger cabins do not have to be sterile, but to provide an environment that does not promote the transmission of (opportunistic) pathogens, measures are needed.

1.3.1 Antimicrobial surfaces

The transmission of pathogens is especially meaningful when it occurs through surfaces in epidemic and endemic scenarios (42). Although the transmission of pathogens through contact surfaces can be reduced by antimicrobial surfaces, the long-term usage and consequences have to be evaluated. One important factor is the increased risk of the development and transmission of antibiotic resistances between bacteria, when such materials are overused (43).

One of the best investigated antimicrobial material is copper. It causes cell damage by releasing copper ions which causes the cell membrane to rupture, leading to a membrane potential loss and depletion of cytoplasmic subtances (44). Further, copper ions induce reactive oxygen species (ROS), which in turn cause DNA damage (45). While copper as a material is costly, surfaces using the antibacterial effect of copper and integrating it as metal nanoparticles within a polymer matrix makes it cost effective, as reviewed by Tamayo et al. (46), and therefore could be suitable for a broad use.

While the antimicrobial properties of copper have long been known and researched, there are many different antimicrobial surfaces available (47, 48). For example, anti-biofouling surfaces can reduce

microbial adhesion to the surfaces, biocidal nanocomposites kill microbes using biocidal species. Physical mechanisms as nanostructured surfaces can rupture bacterial cells, others can even prevent the attachment on the surfaces (49).

Some innovative antimicrobial materials were already tested in public transportation, such as antimicrobial photodynamic coatings, showing an absolute risk reduction of 22.6% for high bacterial counts (50). Other tested materials showed no significant reduction of the microbial burden, using photocatalyst-coated and uncoated hand-contact surfaces (51).

1.3.2 Fumigation of chemicals as an antimicrobial approach

In the process of fumigation, an antimicrobial solution is nebulized in an enclosed environment with the aim to reduce the microbial burden in the air and on surfaces. The nebulization of chemicals, e.g., hydrogen peroxide has been in use (52, 53). There are also different forms of fumigation, that even consider the application in public transport (54). Here, peracetic acid stabilized with acetic acid and hydrogen peroxide showed an effectiveness of disinfection of 81.7% in busses, and even worked against highly resistant spores. Hydrogen peroxide facilitates the penetration of peracetic acid, which contributes to a fortified sporicidal activity of the agents, as tested with *Bacillus subtilis* spores (55).

The effectiveness of fumigation is highly dependent on the materials to be disinfected (54, 56), e.g., the effect of fogged peracetic acid and hydrogen peroxide was shown to be particularly high on glass windows and doors, and low on fabric materials (56). Further, the efficacy depends on the type of microorganism, the fumigation device and technology and the substance (57–59). One downfall of the fumigation of chemicals is the safety measures, that have to be ensured. Therefore, the usage of fumigation can only occur while the passenger cabins are not in service, but could be performed during night times. Considering the costs of fumigation, it depends on the device and fumigation technologies used. Costs for consumables are low, e.g., ~2 € / L of hydrogen peroxide.

1.3.3 UV-C

Another method for disinfection in public transport, but more commonly employed in hospital settings, is UV-C disinfection. UV radiation causes DNA damage (60), which is mediated by the generation of ROS (61). UV-C operates in a spectrum of 200–280 nm. Because UV-C is also harmful to humans, some efforts have been made to employ mobile robots for disinfection with UV-C radiation (62, 63). In hospitals, there have been several systems using and testing UV-C disinfection, that are combined with disinfectant chemical agents (64, 65). One disadvantage of this approach is the material damage (66) and the incomplete light contact in all areas in a room or cabin. An advantage of UV-C disinfection is the economical aspect. Some low-cost UV-C light devices can be purchased with high efficacy against strains of *Candida auris*, MRSA, and bacteriophage Phi6 (67). Although UV-C disinfection shows effectiveness against some pathogens, it can cause bacterial mutations (68). A new, LED-based UV-irradiation technology has shown to be effective against some bacteria and viruses, but it is connected to high costs (69), which is uneconomical for use in public transport.

1.3.4 Plasma sterilization

A tool designed to provide both air purification and surface disinfection is plasma. Plasma is also known as the fourth state of matter, which is a particle mix with a high electrical conductivity and is chemically reactive. The use of plasma is well established in the food industry (70) and in the medical field (71, 72), but it may be useful for the application in public transport.

The antimicrobial effect of plasma has been long known and is created by the combination or single effect of charged particles (ions, electrons), reactive species (e.g., ozone, ROS), radiation of UV-C/Vacuum-UV (VUV) as well as heating (73–75).

There are different types of plasma that can be used for disinfection. In a study conducted by Liang and Wu (76), culturable bacterial aerosol diversity loss was observed after using non-thermal plasma. Tested with *Aspergillus niger, Bacillus subtilis,* and *Pseudomonas fluorescens* as test organisms, it was described as a highly efficient air decontamination method.

To date, no study has used plasma as a system to reduce the microbial load in public transport. Only plasma related methods, such as a needle-point bipolar ionization system was tested in trams to investigate the reduction of bioaerosols (77). It was shown that environmental bioaerosols were reduced with this method, but it was not sufficient for surfaces. Therefore, more research is needed to test the feasibility of plasma technologies in the public transport context. Regarding cost-efficiency, only publications are available on the use of plasma in water treatment plants or in food industry (78), using plasma activated water (79). But in general, the formation of non-thermal plasma is connected to low energy input, unlike thermal plasma (80).

All approaches that were introduced in this section have their advantages and disadvantages. Different factors have to be considered when finding a best suiting method for a specific environment, such as passenger cabins. These include cost-effectiveness, service life, operation of devices, combined with the effectiveness of microbial reduction. In the end, the aim to apply countermeasures within the passenger cabins is to reduce the microbial load and therefore decrease the spread of potential pathogens, and a combination of some methods may bring all advantages together and ensure passenger safety and comfort.

2 Conclusion

In this review, the most common bacterial organisms from studies of the public transport microbiome were presented. Most studies performed 16S rRNA sequencing to identify the microbiome. The results showed that the public transport microbiome is dominated by human-associated organisms, while no pathogens were detected. However, targeted studies have shown that many of the so-called ESKAPE organisms in particular are found in public transportation and that this can be the place for the transmission of pathogens.

The use of the presented countermeasures in public transport was classified in this review. The purpose of this research is to show what is shaping our microbiome in public transportation and how specific organisms can be detected, but also reduced, to create a safe environment where pathogen transmission is minimized. However, this review also shows that more research is still needed to establish microbial reduction measures in public transportation.

Author contributions

Y-TL: Conceptualization, Visualization, Writing – original draft, Writing – review & editing. SL: Conceptualization, Writing – review & editing. RM: Conceptualization, Funding acquisition, Supervision, Writing – review & editing.

Funding

The author(s) declare that financial support was received for the research, authorship, and/or publication of this article. Y-TL was supported by the DLR grant DLR-VO: GANDALF. RM and SL were supported by the DLR grants: FuE-Projekt "ISS LIFE" (Program RF-FuW, TP 475) and Traffic (RoSto and VMo4Orte). These data will be included in the Ph.D. thesis of Y-TL.

Conflict of interest

The authors declare that the research was conducted in the absence of any commercial or financial relationships that could be construed as a potential conflict of interest.

Publisher's note

References

1. ECDC. (2022). *Factsheet about seasonal influenza*. Available at: https://www.ecdc.europa.eu/en/seasonal-influenza/facts/factsheet (Accessed February 13, 2024).

2. Jones KE, Patel NG, Levy MA, Storeygard A, Balk D, Gittleman JL, et al. Global trends in emerging infectious diseases. *Nature*. (2008) 451:990–3. doi: 10.1038/nature06536

3. Rehman S. A parallel and silent emerging pandemic: antimicrobial resistance (AMR) amid COVID-19 pandemic. *J Infect Public Health*. (2023) 16:611–7. doi: 10.1016/j.jiph.2023.02.021

4. Hoisington AJ, Stamper CE, Bates KL, Stanislawski MA, Flux MC, Postolache TT, et al. Human microbiome transfer in the build environment differs based on occupants, objects, and buildings. *Sci Rep*. (2023) 13:6446. doi: 10.1038/s41598-023-33719-6

5. Meadow JF, Altrichter AE, Kembel SW, Moriyama M, O'Connor TK, Womack AM, et al. Bacterial communities on classroom surfaces vary with human contact. *Microbiome*. (2014) 2:2–7. doi: 10.1186/2049-2618-2-7

6. Vargas-Robles D, Gonzalez-Cedillo C, Hernandez AM, Alcaraz LD, Peimbert M. Passenger-surface microbiome interactions in the subway of Mexico City. *PLoS One*. (2020) 15:e0237272. doi: 10.1371/journal.pone.0237272

7. Hsu T, Joice R, Vallarino J, Abu-Ali G, Hartmann EM, Shafquat A, et al. Urban transit system microbial communities differ by surface type and interaction with humans and the environment. *mSystems*. (2016) 1:e00018-16. doi: 10.1128/mSystems.00018-16

8. Hernández AM, Vargas-Robles D, Alcaraz LD, Peimbert M. Station and train surface microbiomes of Mexico City's metro (subway/underground). *Sci Rep*. (2019) 10:8798. doi: 10.1101/735027

9. Leung MH, Wilkins D, Li EK, Kong FK, Lee PK. Indoor-air microbiome in an urban Subway network: diversity and dynamics. *Appl Environ Microbiol*. (2014) 80:6760–70. doi: 10.1128/AEM.02244-14

10. Kang K, Ni Y, Li J, Imamovic L, Sarkar C, Kobler MD, et al. The environmental exposures and inner- and intercity traffic flows of the metro system may contribute to the skin microbiome and Resistome. *Cell Rep*. (2018) 24:1190–202 e5. doi: 10.1016/j.celrep.2018.06.109

11. Afshinnekoo E, Meydan C, Chowdhury S, Jaroudi D, Boyer C, Bernstein N, et al. Geospatial resolution of human and bacterial diversity with City-scale metagenomics. *Cell Syst*. (2015) 1:72–87. doi: 10.1016/j.cels.2015.01.001

12. Grydaki N, Colbeck I, Mendes L, Eleftheriadis K, Whitby C. Bioaerosols in the athens metro: metagenetic insights into the PM(10) microbiome in a naturally ventilated subway station. *Environ Int*. (2021) 146:106186. doi: 10.1016/j.envint.2020.106186

13. Klimenko NS, Tyakht AV, Toshchakov SV, Shevchenko MA, Korzhenkov AA, Afshinnekoo E, et al. Co-occurrence patterns of Bacteria within microbiome of Moscow Subway. *Comput Struct Biotechnol J*. (2020) 18:314–22. doi: 10.1016/j.csbj.2020.01.007

14. Gohli J, Boifot KO, Moen LV, Pastuszek P, Skogan G, Udekwu KI, et al. The Subway microbiome: seasonal dynamics and direct comparison of air and surface bacterial communities. *Microbiome*. (2019) 7:160. doi: 10.1186/s40168-019-0772-9

15. Grice EA, Kong HH, Renaud G, Young AC, Program NCS, Bouffard GG, et al. A diversity profile of the human skin microbiota. *Genome Res*. (2008) 18:1043–50. doi: 10.1101/gr.075549.107

16. Byrd AL, Belkaid Y, Segre JA. The human skin microbiome. *Nat Rev Microbiol*. (2018) 16:143–55. doi: 10.1038/nrmicro.2017.157

17. Wang Y, Yu Q, Zhou R, Feng T, Hilal MG, Li H. Nationality and body location Alter human skin microbiome. *Appl Microbiol Biotechnol*. (2021) 105:5241–56. doi: 10.1007/s00253-021-11387-8

18. Winand R, Bogaerts B, Hoffman S, Lefevre L, Delvoye M, Braekel JV, et al. Targeting the 16S rRNA Gene for bacterial identification in complex mixed samples: comparative evaluation of second (Illumina) and third (Oxford Nanopore technologies) generation sequencing technologies. *Int J Mol Sci*. (2019) 21:298. doi: 10.3390/ijms21010298

19. Runzheimer K, Lozano C, Boy D, Boy J, Godoy R, Matus FJ, et al. Exploring Andean high-altitude Lake extremophiles through advanced Proteotyping. *J Proteome Res*. (2024). doi: 10.1021/acs.jproteome.3c00538

20. De Oliveira DM, Forde BM, Kidd TJ, Harris PN, Schembri MA, Beatson SA, et al. Antimicrobial resistance in ESKAPE pathogens. *Clin Microbiol Rev*. (2020) 33:10–1128. doi: 10.1128/CMR.00181-19

21. Denissen J, Reyneke B, Waso-Reyneke M, Havenga B, Barnard T, Khan S, et al. Prevalence of ESKAPE pathogens in the environment: antibiotic resistance status, community-acquired infection and risk to human health. *Int J Hyg Environ Health*. (2022) 244:114006. doi: 10.1016/j.ijheh.2022.114006

22. Murray CJ, Ikuta KS, Sharara F, Swetschinski L, Aguilar GR, Gray A, et al. Global burden of bacterial antimicrobial resistance in 2019: a systematic analysis. *Lancet*. (2022) 399:629–55. doi: 10.1016/S0140-6736(21)02724-0

23. Lutz JK, Van Balen J, Mac Crawford J, Wilkins JR III, Lee J, Nava-Hoet RC, et al. Methicillin-resistant *Staphylococcus aureus* in public transportation vehicles (buses): another piece to the epidemiologic puzzle. *Am J Infect Control*. (2014) 42:1285–90. doi: 10.1016/j.ajic.2014.08.016

24. Mendes Â, da Costa PM, Rego D, Beça N, Alves C, Moreira T, et al. Contamination of public transports by *Staphylococcus aureus* and its carriage by biomedical students: point-prevalence, related risk factors and molecular characterization of methicillin-resistant strains. *Public Health*. (2015) 129:1125–31. doi: 10.1016/j.puhe.2015.05.010

25. Lin JL, Peng Y, Ou QT, Lin DX, Li Y, Ye XH, et al. A molecular epidemiological study of methicillin-resistant *staphylococci* environmental contamination in railway stations and coach stations in Guangzhou of China. *Lett Appl Microbiol*. (2017) 64:131–7. doi: 10.1111/lam.12700

26. Angbuhang KB, Neupane M, Adhikari A, Binita K, Jha S. Detection of methicillin resistant *Staphylococcus aureus* in public transportation of Kathmandu Valley, Nepal. *Tribhuvan Univ J Microbiol*. (2018) 5:51–6. doi: 10.3126/tujm.v5i0.22312

27. Medveďová A, Györiová R. Prevalence of *Staphylococcus aureus* and antibiotic resistant *Staphylococcus aureus* in public transport in Bratislava, Slovakia. *Acta Chim Slov*. (2019) 12:41–5. doi: 10.2478/acs-2019-0007

28. Shen C, Feng S, Chen H, Dai M, Paterson DL, Zheng X, et al. Transmission of *mcr-1*-producing multidrug-resistant Enterobacteriaceae in public transportation in Guangzhou, China. *Clin Infect Dis*. (2018) 67:S217–24. doi: 10.1093/cid/ciy661

29. Cao T, Liu Y, Li Y, Wang Y, Shen Z, Shao B, et al. A public health concern: emergence of carbapenem-resistant *Klebsiella pneumoniae* in a public transportation environment. *J Antimicrob Chemother*. (2020) 75:2769–72. doi: 10.1093/jac/dkaa260

30. Gu J, Xie X-J, Liu J-X, Shui J-R, Zhang H-Y, Feng G-Y, et al. Prevalence and transmission of antimicrobial-resistant *staphylococci* and *enterococci* from shared bicycles in Chengdu, China. *Sci Total Environ*. (2020) 738:139735. doi: 10.1016/j.scitotenv.2020.139735

31. Torres-Sangiao E, Leal Rodriguez C, García-Riestra C. Application and perspectives of MADLI-TOF mass spectrometry in clinical microbiology laboratories. *Microorganisms*. (2021) 9:1539. doi: 10.3390/microorganisms9071539

32. Akintunde O, Tucker T, Carabetta VJ. *The evolution of next-generation sequencing technologies*. arXiv [preprint]. (2023). Available at: https://arxiv.org/abs/2305.08724 (Accessed December 2023).

33. Barba M, Czosnek H, Hadidi A. Historical perspective, development and applications of next-generation sequencing in plant virology. *Viruses*. (2014) 6:106–36. doi: 10.3390/v6010106

34. Zolfo M, Asnicar F, Manghi P, Pasolli E, Tett A, Segata N. Profiling microbial strains in urban environments using metagenomic sequencing data. *Biol Direct*. (2018) 13:9. doi: 10.1186/s13062-018-0211-z

35. Pooja S, Sudesh D, Poonam K, Joginder SD, Suresh KG. Loop-mediated isothermal amplification (LAMP) based detection of bacteria: a review. *Afr J Biotechnol*. (2014) 13:1920–8. doi: 10.5897/ajb2013.13459

36. Kokkinos P, Ziros P, Bellou M, Vantarakis A. Loop-mediated isothermal amplification (LAMP) for the detection of *Salmonella* in food. *Food Anal Methods*. (2014) 7:512–26. doi: 10.1007/s12161-013-9748-8

37. El-Kafrawy SA, El-Daly MM, Hassan AM, Harakeh SM, Alandijany TA, Azhar EI. Rapid and reliable detection of SARS-CoV-2 using direct RT-LAMP. *Diagnostics*. (2022) 12:828. doi: 10.3390/diagnostics12040828

38. dos Santos C, de Oliveira K, Mendes G, Silva L, de Souza JM, Estrela PF, et al. Detection of SARS-CoV-2 in saliva by RT-LAMP during a screening of Workers in Brazil, including pre-symptomatic carriers. *J Braz Chem Soc*. (2021). doi: 10.21577/0103-5053.20210098

39. Lamb LE, Bartolone SN, Ward E, Chancellor MB. Rapid detection of novel coronavirus/severe acute respiratory syndrome coronavirus 2 (SARS-CoV-2) by reverse transcription-loop-mediated isothermal amplification. *PLoS One*. (2020) 15:e0234682. doi: 10.1371/journal.pone.0234682

40. Setlow P. Spores of *Bacillus subtilis*: their resistance to and killing by radiation, heat and chemicals. *J Appl Microbiol*. (2006) 101:514–25. doi: 10.1111/j.1365-2672.2005.02736.x

41. Tu Z, Setlow P, Brul S, Kramer G. Molecular physiological characterization of a high heat resistant spore forming *Bacillus subtilis* food isolate. *Microorganisms*. (2021) 9:667. doi: 10.3390/microorganisms9030667

42. Otter JA, French GL. Bacterial contamination on touch surfaces in the public transport system and in public areas of a hospital in London. *Lett Appl Microbiol*. (2009) 49:803–5. doi: 10.1111/j.1472-765X.2009.02728.x

43. Llor C, Bjerrum L. Antimicrobial resistance: risk associated with antibiotic overuse and initiatives to reduce the problem. *Ther Adv Drug Saf*. (2014) 5:229–41. doi: 10.1177/2042098614554919

44. Grass G, Rensing C, Solioz M. Metallic copper as an antimicrobial surface. *Appl Environ Microbiol*. (2011) 77:1541–7. doi: 10.1128/AEM.02766-10

45. Hong Y, Zeng J, Wang X, Drlica K, Zhao X. Post-stress bacterial cell death mediated by reactive oxygen speciesProc. *Natl Acad Sci USA*. (2019) 116:10064–71. doi: 10.1073/pnas.1901730116

46. Tamayo L, Azócar M, Kogan M, Riveros A, Páez M. Copper-polymer nanocomposites: an excellent and cost-effective biocide for use on antibacterial surfaces. *Mater Sci Eng*. (2016) 69:1391–409. doi: 10.1016/j.msec.2016.08.04141

47. Cassidy SS, Sanders DJ, Wade J, Parkin IP, Carmalt CJ, Smith AM, et al. Antimicrobial surfaces: a need for stewardship? *PLoS Pathog*. (2020) 16:e1008880. doi: 10.1371/journal.ppat.1008880

48. Mahanta U, Khandelwal M, Deshpande AS. Antimicrobial surfaces: a review of synthetic approaches, applicability and outlook. *J Mater Sci*. (2021) 56:17915–41. doi: 10.1007/s10853-021-06404-0

49. Linklater DP, Baulin VA, Juodkazis S, Crawford RJ, Stoodley P, Ivanova EP. Mechano-bactericidal actions of nanostructured surfaces. *Nat Rev Microbiol*. (2021) 19:8–22. doi: 10.1038/s41579-020-0414-z

50. Kalb L, Bassler P, Schneider-Brachert W, Eckl DB. Antimicrobial photodynamic coatings reduce the microbial burden on environmental surfaces in public transportation-a field study in buses. *Int J Environ Res Public Health*. (2022) 19:2325. doi: 10.3390/ijerph19042325

51. Eicker R, Salomon W. Investigation of the effectiveness of antimicrobial photocatalyst-coated hand-contact surfaces in passenger transport vehicles under everyday conditions. *Int J Infect Control*. (2021) 17:20969. doi: 10.3396/ijic.v17.20969

52. Andersen B, Rasch M, Hochlin K, Jensen F-H, Wismar P, Fredriksen J-E. Decontamination of rooms, medical equipment and ambulances using an aerosol of hydrogen peroxide disinfectant. *J Hosp Infect*. (2006) 62:149–55. doi: 10.1016/j.jhin.2005.07.020

53. Møretrø T, Fanebust H, Fagerlund A, Langsrud S. Whole room disinfection with hydrogen peroxide mist to control *Listeria monocytogenes* in food industry related environments. *Int J Food Microbiol*. (2019) 292:118–25. doi: 10.1016/j.ijfoodmicro.2018.12.015

54. Kruszewska E, Czupryna P, Pancewicz S, Martonik D, Bukłaha A, Moniuszko-Malinowska A. Is Peracetic acid fumigation effective in public transportation? *Int J Environ Res Public Health*. (2022) 19:2526. doi: 10.3390/ijerph19052526

55. Leggett MJ, Schwarz JS, Burke PA, McDonnell G, Denyer SP, Maillard J-Y. Mechanism of sporicidal activity for the synergistic combination of Peracetic acid and hydrogen peroxide. *Appl Environ Microbiol*. (2016) 82:1035–9. doi: 10.1128/AEM.03010-15

56. Richter WR, Wood JP, Wendling MQ, Rogers JV. Inactivation of *Bacillus anthracis* spores to decontaminate subway railcar and related materials via the fogging of peracetic acid and hydrogen peroxide sporicidal liquids. *J Environ Manag*. (2018) 206:800–6. doi: 10.1016/j.jenvman.2017.11.027

57. Matys J, Gedrange T, Dominiak M, Grzech-Leśniak K. The impact of hydrogen peroxide (H_2O_2) fumigation on bacterial levels in dental office environments: a randomized clinical trial investigation. *J Clin Med*. (2023) 12:7551. doi: 10.3390/jcm12247551

58. Beswick AJ, Farrant J, Makison C, Gawn J, Frost G, Crook B, et al. Comparison of multiple systems for laboratory whole room fumigation. *Appl Biosaf*. (2011) 16:139–57. doi: 10.1177/153567601101600303

59. Rutala WA, Weber DJ. Disinfectants used for environmental disinfection and new room decontamination technology. *Am J Infect Control*. (2013) 41:S36–41. doi: 10.1016/j.ajic.2012.11.006

60. Murphy T. Nucleic acids: interaction with solar UV radiation. *Curr Top Radiat Res Q*. (1975) 10:199–228.

61. Peak MJ, Peak JG, Jones CA. Different (direct and indirect) mechanisms for the induction of DNA-protein crosslinks in human cells by far-and near-ultraviolet radiations (290 and 405 nm). *Photochem Photobiol*. (1985) 42:141–6. doi: 10.1111/j.1751-1097.1985.tb01552.x

62. Hurtado M, Marquez J, Sotelo P, Cornejo J, Palomares R. Mechanic design and kinematic simulation of tri-star wheeled Mobile robot for COVID-19 using UV-C disinfection for public transport. 2022 First International Conference on Electrical, Electronics, Information and Communication Technologies (ICEEICT) (2022). p. 1–8.

63. Rakib SH, Masum S, Farhana A, Islam MA, Islam MF, Reza MT. Design of a low cost ultraviolet disinfection unit to minimize the cross-contamination of COVID-19 in transport. 2022 International Conference on Advancement in Electrical and Electronic Engineering (ICAEEE) (2022).

64. Guettari M, Gharbi I, Hamza S. UVC disinfection robot. *Environ Sci Pollut Res Int*. (2021) 28:40394–9. doi: 10.1007/s11356-020-11184-2

65. Dos Santos T, de Castro LF. Evaluation of a portable ultraviolet C (UV-C) device for hospital surface decontamination. *Photodiagn Photodyn Ther*. (2021) 33:102161. doi: 10.1016/j.pdpdt.2020.102161

66. Teska P, Dayton R, Li X, Lamb J, Strader P. Damage to common healthcare polymer Surfaces from UV exposure. *Nano Life*. (2020) 10:2050001. doi: 10.1142/S1793984420500014

67. Pearlmutter BS, Haq MF, Cadnum JL, Jencson AL, Carlisle M, Donskey CJ. Efficacy of relatively low-cost ultraviolet-C light devices against *Candida auris*. *Infect Control Hosp Epidemiol*. (2022) 43:747–51. doi: 10.1017/ice.2021.206

68. Mora M, Mahnert A, Koskinen K, Pausan MR, Oberauner-Wappis L, Krause R, et al. Microorganisms in confined habitats: microbial monitoring and control of intensive care units, operating rooms, cleanrooms and the international space station. *Front Microbiol*. (2016) 7:1573. doi: 10.3389/fmicb.2016.01573

69. Schöbel H, Diem G, Kiechl J, Chistè D, Bertacchi G, Mayr A, et al. Antimicrobial efficacy and inactivation kinetics of a novel LED-based UV-irradiation technology. *J Hosp Infect*. (2023) 135:11–7. doi: 10.1016/j.jhin.2022.12.023

70. Deng L-Z, Tao Y, Mujumdar AS, Pan Z, Chen C, Yang X-H, et al. Recent advances in non-thermal decontamination technologies for microorganisms and mycotoxins in low-moisture foods. *Trends Food Sci Technol*. (2020) 106:104–12. doi: 10.1016/j.tifs.2020.10.012

71. Bernhardt T, Semmler ML, Schäfer M, Bekeschus S, Emmert S, Boeckmann L. Plasma medicine: applications of cold atmospheric pressure plasma in dermatology. *Oxidative Med Cell Longev*. (2019) 2019:1–10. doi: 10.1155/2019/3873928

72. Borges AC, Kostov KG, Pessoa RS, de Abreu GM, Lima GDM, Figueira LW, et al. Applications of cold atmospheric pressure plasma in dentistry. *Appl Sci*. (2021) 11:1975. doi: 10.3390/app11051975

73. Gallagher MJ, Vaze N, Gangoli S, Vasilets VN, Gutsol AF, Milovanova TN, et al. Rapid inactivation of airborne Bacteria using atmospheric pressure dielectric barrier grating discharge. *IEEE Trans Plasma Sci*. (2007) 35:1501–10. doi: 10.1109/TPS.2007.905209

74. Scholtz V, Pazlarova J, Souskova H, Khun J, Julak J. Non-thermal plasma—a tool for decontamination and disinfection. *Biotechnol Adv*. (2015) 33:1108–19. doi: 10.1016/j.biotechadv.2015.01.002

75. Laroussi M. Low temperature plasma-based sterilization: overview and state-of-the-art. *Plasma Process Polym*. (2005) 2:391–400. doi: 10.1002/ppap.200400078

76. Liang Y, Wu Y, Sun K, Chen Q, Shen F, Zhang J, et al. Rapid inactivation of biological species in the air using atmospheric pressure non-thermal plasma. *Environ Sci Technol*. (2012) 46:3360–8. doi: 10.1021/es203770q

2.2 Microbial communities in local train cabins remain stable through the seasons during one year of monitoring

Title	**Microbial Communities in Local Train Cabins Remain Stable Through the Seasons During One Year of Monitoring**
Authors	**Yen Ly-Sauerbrey[1]**, Anna Rehm[2], Denise Engel[1,3], Stefan Leuko[1], and Stefan Janssen[2]
Affiliation	[1] Department of Applied Biology, Institute of Aerospace Medicine, German Aerospace Center, Cologne, Germany [2] Department of Algorithmic Bioinformatics, Justus Liebig University Giessen, Giessen, Germany [3] Laboratory of Experimental Immunology, Institute of Virology, Faculty of Medicine and University Hospital Cologne, University of Cologne, Cologne, Germany
Article type	Original research article
Authorship	Single-first author
Journal	Microbiology (Microbiology Society), submitted
Year	2026
Author Contributions	
YL-S	Conceptualization, Data curation, Formal analysis, Investigation, Methodology, Visualization, Writing -original draft, Writing – review & editing
AR	Conceptualization, Data curation, Formal analysis, Visualization, Writing – review & editing

DE	Conceptualization, Data curation, Investigation, Writing – review & editing
SL	Conceptualization, Resources, Writing – review & editing
SJ	Conceptualization, Funding acquisition, Project administration, Supervision, Writing – review & editing

Microbial Communities in Local Train Cabins Remain Stable Through the Seasons During One Year of Monitoring

Author names

Yen Ly-Sauerbrey[1]: https://orcid.org/0009-0007-0048-0218

Anna Rehm[2]: https://orcid.org/0009-0000-5063-486X

Denise Engel[1,3]: no orcid

Stefan Janssen[2]: https://orcid.org/0000-0003-0955-0589

Stefan Leuko[1]*: https://orcid.org/0000-0002-0423-0896

*** Correspondence**

Affiliation(s)

[1] Department of Applied Aerospace Biology, Institute for Aerospace Medicine, German Aerospace Center, 51147 Cologne, Germany

[2] Department of Algorithmic Bioinformatics, Justus Liebig University Giessen, 35390 Giessen, Germany

[3] Laboratory of Experimental Immunology, Institute of Virology, Faculty of Medicine and University Hospital Cologne, University of Cologne, 50931 Cologne, Germany

Corresponding author and email address

Stefan Leuko: stefan.leuko@dlr.de

Keywords

public transportation, microbiome, surface, seasonal changes

1. Abstract

Millions of people commute daily by train and are exposed to the microbes brought by past and present passengers. Like other forms of public transportation, train cabins provide an environment that favors the spread of fomites due to high passenger frequency, confined space, and close contact, thereby putting the health of immunocompromised individuals at risk. The composition of environmental microbiomes can change over time. Monitoring of community shifts and in particular abundance of potential pathogens is relevant, when it comes to (targeted) application of microbial countermeasures. Only few studies exist, which focus on train cabins, and no such study was performed in Germany. To close this gap, we conducted a one-year microbial monitoring study of a German train line, taking surface and air samples from different locations inside train cabins. We profiled the train microbiome via 16S rRNA amplicon sequencing of the V1-V2 region. In addition, we used targeted qPCR to detect the opportunistic pathogen *Staphylococcus aureus* and the skin commensal *Staphylococcus capitis* in DNA samples from the train cabin samples. Our results show no significant seasonal changes in the train microbiome, despite varying outside temperatures; however, distinct sampling locations, differ significantly from others. The overall microbiome is mainly shaped by human-associated genera. *Staphylococcus aureus* was rarely detectable, while only a few sample locations showed positive detection of *Staphylococcus capitis*. The detection of (opportunistic) pathogens may indicate a need for more targeted and improved detection protocols from low biomass samples.

2. Impact statement

Studies that investigate the train microbiome are extremely rare. Most studies focus on subway microbiomes, particularly subway stations, which are often exposed to a constant outside climate. Public transportation is an environment favorable to microbial spread and needs to be investigated further.

We collected microbial samples at different indoor (and one outdoor) locations in trains over the course of one year. This is relevant for detecting sampling location specific microbiomes or identifying shifts in the microbiome, that visualize abnormal distributions or influences of the environment, such as changes in temperature and humidity.

As antimicrobial resistance is becoming an increasing threat, this study deepens our understanding of microbial transmission by determining the presence of the ESKAPE (1) pathogen *S. aureus* and the BSL-1 control strain *S. capitis* in train cabins. By investigating

selected sampling locations, possible countermeasures can be applied, e.g. for surfaces suspected with high microbial load.

We observed human- and environment associated genera. The detection of *S. capitis* showed more positive hits than *S. aureus*. Although seasonal differences did not reach statistical significance level, a certain trend was evident. This study will help to understand certain microbial dynamics and identify locations which can be targeted for increased microbial countermeasures.

3. Data summary

The authors confirm all supporting data, code and protocols have been provided within the article, through submission to publicly accessible repositories or through supplementary data files.

4. Introduction

Public transport plays a big role in the transmission of pathogens and is therefore target of many studies (2, 3). Infectious agents often spread through airborne (inhalation of contaminated air) or contact (fomites, e.g. contaminated surfaces) transmission. Focusing on microbial monitoring of the train cabin air and of frequently touched surfaces provides useful information to develop suitable intervention strategies within those transmission routes. The spread of opportunistic pathogens can create health risks for passengers and their contacts, especially for humans with compromised immune systems, such as the elderly. The implementation of measures for microbial reduction is needed. Prior to that, understanding composition and dynamics of the existing microbiome is necessary to create targeted countermeasures to shift the microbial stowaway into harmless configurations and not select for pathogens. Beside the overall detection of public transport microbiome and pathogenic species, long-term monitoring can provide valuable information on seasonal changes. Seasonal dynamics were previously observed in subway stations in Oslo, Norway, showing increased diversity in spring and summer (4). As extreme weather and temperatures are showing and are expected for the following years due to climate change (5, 6), it is important to keep monitoring microbial changes in the environment and human-shaped places. Besides, microbiomes differ geographically (7), and collecting data on unexplored microbiomes contributes to the overall microbiome knowledge.

So far, human transportation has been shown to constitute vehicles for infectious disease transmission in bus rides (8), air flight (9, 10), subways (3, 11), and trains (12). Studies which focus on the train cabin microbiome are rare, although they play a great role in commuting for millions of people daily. In Germany, trains were used 2.73 billion times in 2023 (13). One study on the train cabin microbiome exists, showing that handrails and straps are mostly inhabited by human-associated microorganisms (14). However, no long-term sampling was conducted.

In light of the growing threat of antimicrobial resistance (AMR), especially concerning the most relevant ESKAPE pathogens, it is crucial to monitor the presence of species that pose a health risk to understand transmission and develop countermeasures. Suitable methods must be applied to detect target species. Studies focusing on the detection of pathogenic microorganisms, used cultivation on selective media, PCR of pathogen-associated marker genes, or sequencing towards cultivation (16-19). Another approach to detect pathogenic species, is sequencing of the full 16S rRNA gene, or even the metagenome, which secures identification on species level (20). This would, however, not allow constant monitoring as these approaches are accompanied by higher costs due to increased work and material costs. An alternative, reliable and long-established method is qPCR, which is known for its high sensitivity, specificity and quantitative data, as well as high-throughput possibility.

Taking into account the stated knowledge gaps, the train cabin of a German train line was selected as the object of investigation in this study. The train microbiome was investigated over the course of all four seasons of one year, with sample collection every two months. We collected samples from surfaces that are suspected to be frequently touched by passengers, or are expected to inherit a characteristic microbial composition. Additionally, the train cabin air was analyzed to allow a comparison of these distinct sample types. These are expected to differ, as shown by several studies (4, 21, 22). We purposely selected surface locations with different surface materials, since they can harbor a varied microbiome (23, 24). In line with previous studies of subway (25, 26) and indoor microbiomes (27), we observed a similar pattern with predominantly human-associated taxa. Additionally, we tested targeted pathogen detection of two selected bacterial species using qPCR without prior cultivation as proof of principle, to compare the detection to 16S rRNA sequencing. This study complements data to previous work by Auerhammer et al. (2023) (28) on the cultivation and characterization of (potential) pathogens from the train cabin.

5. Methods

For this study, cabins of the train line Regional Express 6 (RE6, commuting a ~300km distance hourly from Minden to Cologne/Bonn Airport) from the Rhein-Ruhr-Express (RRX) were sampled every two month and in total six times throughout one year at the train station Cologne/Bonn Airport, Cologne, Germany. The sampling period was between March 2023 and February 2024. Sampling occurred on 2023-03-28, 2023-05-30, 2023-08-01, 2023-09-28, 2023-12-06, and 2024-02-01.

5.1 Sampling

Both, surface and air sampling were conducted. On each sampling day, 11 sampling positions (armrest, door button inside, door button outside, door bar, headrest, louvers, seat handle, 1st-class table, 2nd-class table, 1st-class under-seat handle, and train air) and blank control were processed (per sampling: 10 surface positions, 1 air sample,1 blank). In **Figure 1**, we display an overview of the sampling locations. To gain sufficient biomass and statistical stability for further processing, each surface sampling type was sampled six times (e.g. six different door bars for one, pooled DNA sample of sampling position “door bar”). Prior to sampling, swabs (C1052-50, Zymo Research) were wetted with ~20 µL of 0.8 % NaCl for optimal sampling efficiency. After sampling, the swabs were placed in a 1.5 mL tube and stored at -20 °C until further processing. In total, 60 pooled surface samples (6 swabs per pool), 6 air samples, and 6 pooled blanks (6 swabs per sampling day) were collected within this study.

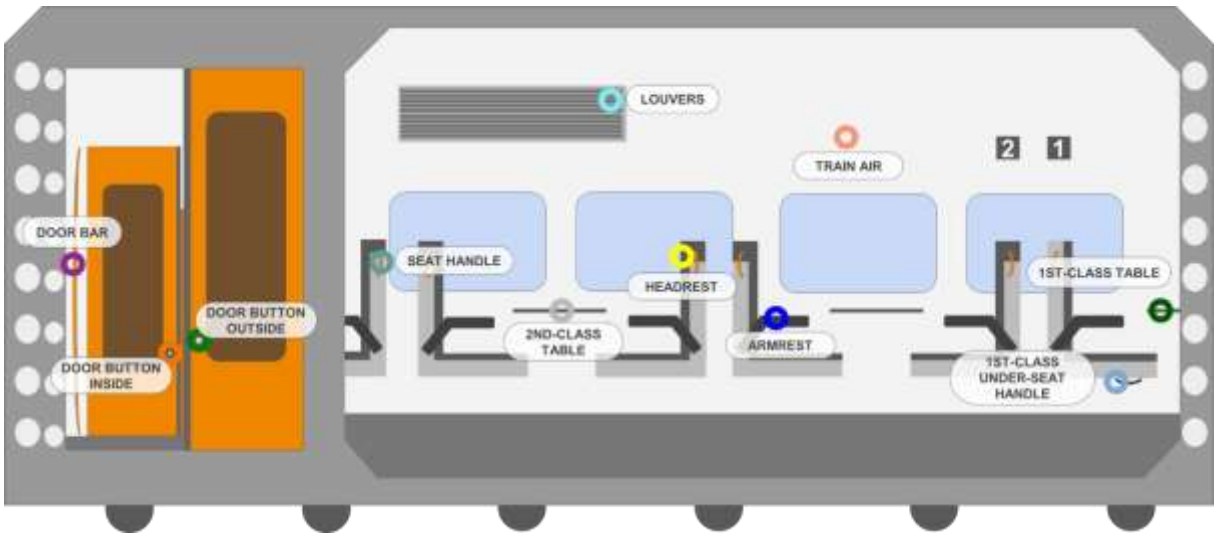

Figure 1: Overview of the sampling locations in the train cabin.

Air samples were collected for ~35 min using the AerosolSense™ (Thermo Scientific) with a flow rate of 200 L/min, by placing the air sampling device on a seat within the passenger cabin. Additionally, blank samples were taken as a control, using a wetted swab and by shortly exposing the swab in the train cabin air while taking few steps. No passengers were in the train during sampling.

The temperature and relative humidity were documented at each sampling using a TFA Dostmann Thermo Hygrometer. DNA extraction was performed within a month post-sampling.

5.2 DNA extraction

For DNA extraction from the swabs, the DNA Microprep Kit (D4301, Zymo Research) was used. The tip of the swab and 750 µL of lysis buffer from the kit were assembled in a ZR Bashing Lysis Tube prior to cell disruption for 5 min at 30 /s using the TissueLyzer (QIAGEN). Further steps of the DNA extraction were performed according to the manufacturer's instructions, with a modification to pool the samples of each sampling location (6 swabs). This was conducted by pooling after mixing the flow through with the binding buffer. The final DNA was eluted in 20 µL of nuclease free water.

To extract DNA of the air samples, the sponge within the sampling cartridge was removed under sterile conditions and placed into a ZR Bashing Lysis Tube before cell disruption as described above. Further steps were similar as described in previous paragraph, without the pooling step.

5.3 Library preparation & 16S rRNA sequencing

To prepare the DNA samples for sequencing, the *Quick*-16S Library Prep Kit (D6400, Zymo Research) was used as instructed by the manufacturer, except for the following modifications. For the targeted sequence amplification, 2 µL of the *Quick*-16S™ Primer Set V1-V2 and 6 µL of DNase/RNase free water was used for one reaction. In the final library clean-up, 20 µL of DNase/RNase free water was added to the beads before incubation for 2 min. The final library was quantified using Qubit™ 1X dsDNA assay kit with high sensitivity (Q33230, Invitrogen™) and adjusted to 4 nmol.

For 16S rRNA sequencing, the Illumina MiSeq™ system was used in combination with the MiSeq Reagent Nano Kit v2 (500 cycles). The final concentration of the denatured DNA was

set to 10 pM, and 510 µL of the library was mixed with 90 µL of the PhiX control before loading it onto the MiSeq reagent cartridge. All samples were included in one MiSeq run, which comprised a negative control and the ZymoBIOMICS Microbial Community Standard as positive control of the 16S rRNA gene amplification by qPCR.

5.4 Data processing & analysis

Basecalling was performed with bcl2fastq (v2.19.0.316), and cutadapt (v1.18) (29) was used to trim adapter sequences and generate fastq files. With fastqc (https://www.bioinformatics.babraham.ac.uk/projects/fastqc/) and multiqc (30), quality control was conducted. The trimmed fastq files were then uploaded to Qiita (31) for further processing (study ID 15480, https://qiita.ucsd.edu/study/description/15480). Processing included library split for demultiplexing, trimming to 150 bp and Deblur (v2021.09) (32). With Deblur, a reference hit table was generated, which was positively filtered for sequences being close enough to the Greengenes (v13.8) 88% sequence similarity alignment. Using Qiime2 (v2025.7), the following processes were conducted, based on Deblur's "reference hit table" (33): Reads that occurred with a frequency <10 were filtered out, taxonomy classification was conducted based on Greengenes2 (v2024.09) "2024.09.backbone.full-length.nb". Chloroplasts and mitochondria were excluded to avoid host- or plant-associated features. For alpha- and beta-diversity, a rarefaction was performed with 10 iterations. Alpha- and beta-diversity were calculated based on a rarefaction depth of 2,200 reads per sample. For alpha-diversity, Shannon, Observed Features and Faith's PD were computed (supplementary Table 1). Beta-diversity was calculated as weighted and unweighted UniFrac, and Bray-Curtis (34). Dissimilarities between samples were ordinated via PcoA and visualized as Emperor plots.

Statistical analyses were conducted as followed to determine differences between sampling groups. Significance testing of top ten genera (taxa bar plot) and of all groups in alpha-diversity was performed using Kruskal-Wallis and Post-hoc Dunn-test with Bonferroni correction. Beta-diversity group significance was assessed by PERMANOVA using 999 permutations (supplementary Table 2).

Microbial analysis notebook is available at: jlab/microbiome_leuko_train: The train microbiome: A one-year study on bacterial communities

5.5 Detection of *Staphylococcus aureus* and *Staphylococcus capitis* via qPCR

To detect the species *Staphylococcus capitis* and *Staphylococcus aureus*, qPCR was performed using the Luna® Universal qPCR Master Mix (New England BioLabs®) according to manufacturer's instruction. For each reaction, 2 µL of template DNA was used. Extension was performed at 58 °C (S. capitis) and 56 °C (S. aureus). Primer sequences were obtained from Kim, Yang (35). As positive control, extracted DNA from *Staphylococcus capitis* DSM 20326 and *Staphylococcus aureus* DSM 20231 was used. Prior to DNA extraction, the selected bacterial strains were grown in overnight cultures in TSB at 37 °C shaking at 120 rpm. DNA extraction was performed using the ZymoBIOMICS DNA Miniprep Kit (D4300). For quantification, the QubitTM fluorometer was used with the dsDNA BR Assay Kit (Invitrogen). qPCR was conducted in technical triplicates (n=3).

Table 1: Primer sequences from Kim, Yang (35).

Target species	**Sequence (5'-3')**	**Size (bp)**
S. capitis		150
Forward	CGC AAG GTG GTC AAC TTG AT	
Reverse	GCG CAT CGT GAA GTA ATT CC	
S. aureus		145
Forward	CAA GCA CAA GGC AGT GGT AT	
Reverse	GTG GCG TTG CAA TCT CCT TA	

6. Results

6.1 Seasonality

The taxonomic composition of the different sampling locations in the train during all sample collection times are presented at genus level as top ten most abundant genera in **Figure 2**. Those genera were *Cutibacterium*, *Corynebacterium*, *Acinetobacter*, *Staphylococcus*, *Streptococcus*, JC017, *Pseudomonas*, *Paracoccus*, and *Kocuria*. This finding was not surprising, since most of these genera are human-associated. The most abundant genus was unknown. In total, for 7,503 of 20,786 ASVs a genus level name could not reliably be assigned (~36.1 %).

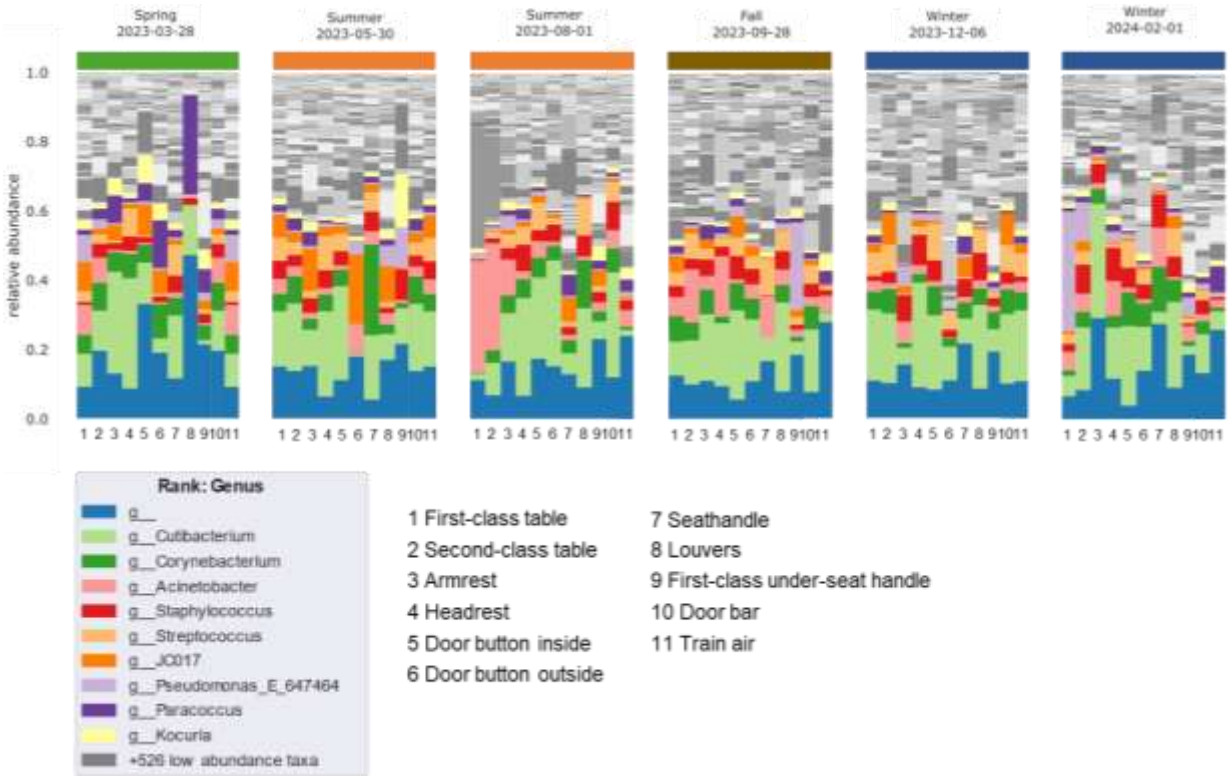

Figure 2: Top ten genera in various train locations during different seasons (n=6 per sampling position per sampling time).

The taxa bar plot in **Figure 2** displays the relative abundances in relation to the sampling seasons. No distinct pattern was observed for all seasons.

To investigate potential seasonal dynamics, the sample alpha-diversity was plotted in **Figure 3** in relation to the sampling seasons. Outside temperatures ranged from 10.2 °C to 26.5 °C (16.3 °C difference) (see **Figure 3A**). A similar trend was observed for the measured relative humidity within the train cabin. The temperature discrepancy was not significant within the

train cabin with 23.5 °C T_{min} and 26.9 °C as T_{max}, and a discrepancy of 3.4 °C. Subsequently, no significant influence on the indoor cabin microbiome was observed. The microbial composition of the train air was consistent throughout the whole year of sampling (see **Figure 5**), with not even half of the most abundant genera being similar to the surfaces' samples. This indicates that many abundant genera of the train air differed from surface samples, which is consistent with the literature (37).

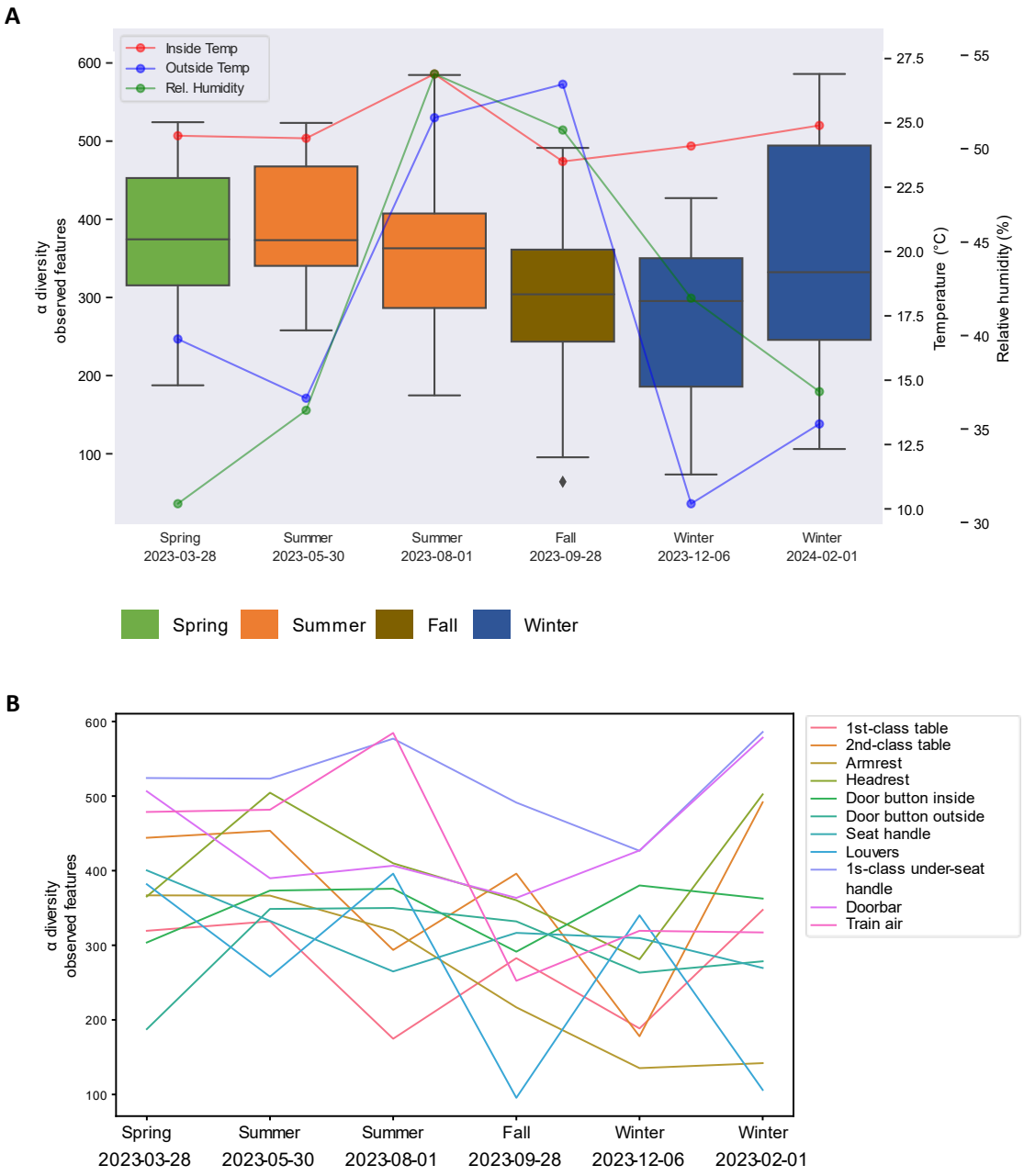

Figure 3: Alpha-diversity per **A** season and temperature at sampling location in- and outside the train cabin (no significant difference between seasons) and **B** per samples at each season.

The alpha-diversity over time (**Figure 3A** and suppl. **Figure S1**) shows a wave-like pattern. Sample numbers are low and in fact statistical testing did not reach significance level.

For each sampling location, alpha-diversity is displayed as observed features sorted after sampling season (**Figure 3B**). For most sampling locations, big fluctuation was observed throughout all sampling seasons. Interestingly, alpha-diversity increased in the final winter sampling for five out of eleven sampling positions. Even within the same season, there is a considerable difference in alpha-diversity, as demonstrated by comparing, for example, both winter samplings. However, no indication or explanation for this behavior was identified or suggested. In contrast, rather constant alpha-diversities were observed for the sampling locations door button inside and seat handle. Similar seasonal trends were shown for 1st-class table and 2nd-class table, which constitute the same surface material.

Bray-Curtis beta-diversity of the samples is displayed in **Figure 4**. According to seasons, no distinct pattern was observed. Samples collected in summer and winter showed most variability, which might be due to temperature differences.

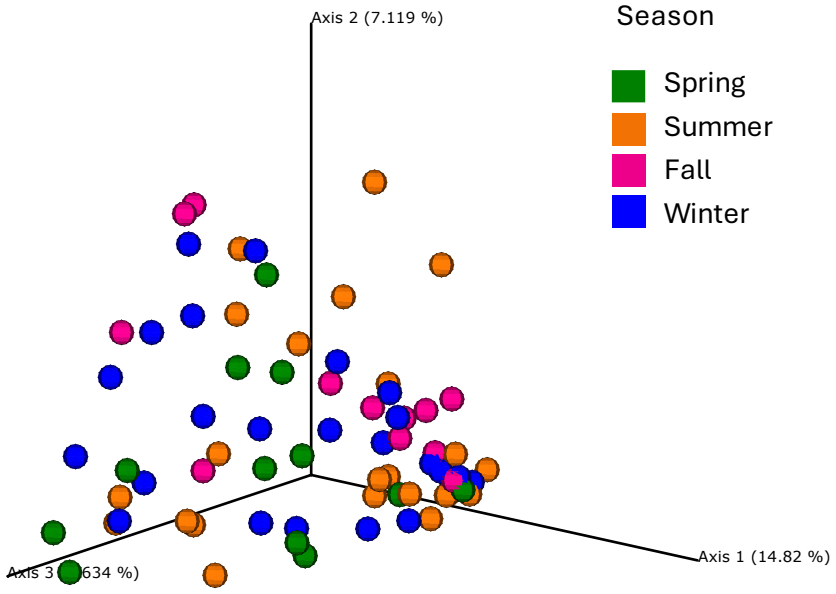

Figure 4: Train microbial diversity. PcoA of Bray-Curtis distances for samples organized after season.

6.2 Sampling location

The taxonomy bar plot in **Figure 5** displays the relative abundances in relation to the sampling locations, based on the same data as **Figure 2**.

Cutibacterium was abundant in most sampling locations, but showed significantly lower abundance in train air (vs. door bar (p=0.032), seat handle (p=0.020), headrest (p=0.029), door button inside (p=0.004)), louvers (vs. door button inside (p=0.046)), and 1st-class under-seat handle (vs. door button inside (p=0.029)). Significant differences were calculated by Kruskal-Wallis tests and Post-hoc-Dunn-tests with Bonferroni-correction. The locations train air, 1st-class under-seat handle, and louvers are all locations or surfaces which we expect to be either not or rarely touched, explaining the low abundance of this genus.

Acinetobacter was most abundant on 1st- and 2nd-class table – surfaces, which are likely cleaned less frequently than seat handles and door bars, allowing this desiccation tolerant genus to persist. It showed higher abundance on the locations armrest, headrest (fall, second winter sampling) and louvers (first summer sampling, fall, second winter sampling). However, there were no significant differences.

The occurrence of the human skin-associated *Corynebacterium* was evenly distributed and reasonably less abundant only in the train air, showing significantly lower abundance compared to the locations door button inside (p=0.006) and seat handle (p=0.028). As another skin-associated genus, *Staphylococcus* was less abundant on 1st-class table, train air, and for most sampling of the louvers, therefore showing similar trends as the relative abundance of skin-associated *Cutibacterium* and *Corynebacterium*. However, no significant differences in *Staphylococcus* abundance were found among sampling locations.

Streptococcus was most abundant within samples of door button inside and seat handle, whereas significantly lower abundance was observed in the train air (vs. seat handle (p=0.004), door button inside (p=0.002)).

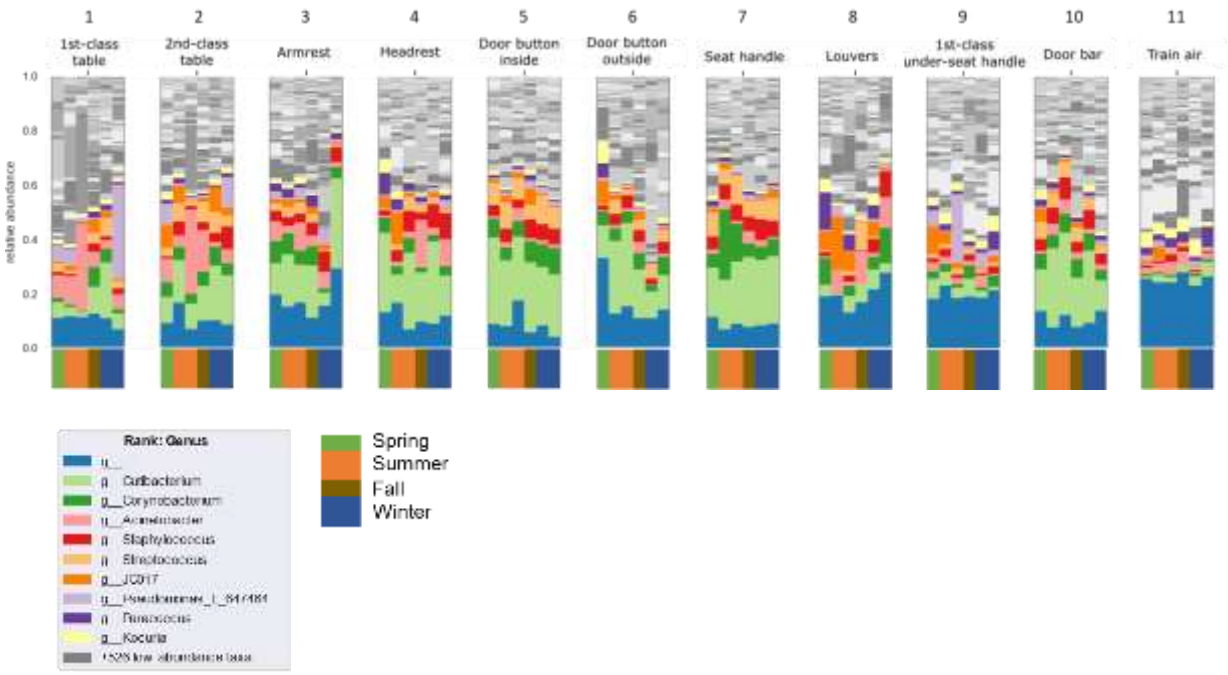

Figure 5: Different locations in the train harbor varying microbiomes. Top ten genera composition in different train areas (n=6).

Positions with higher *Pseudomonas* abundance were 1st-class table, 2nd-class table (spring, winter), and 1st-class under-seat handle. However, no significant differences in abundance were determined between sampling locations for *Pseudomonas,* and other genera, such as *JC017, Paracoccus,* and *Kocuria*. Distinct abundance of *Paracoccus* was observed on armrest, headrests (spring), door button outside (spring), louvers (spring, summer, winter), and constant abundance was shown in the train air. For *Kocuria,* the highest abundances were shown for the locations headrest (spring), door button outside (spring), 1st-class under-seat handle, and the train air.

Overall, we were not able to identify distinct connections between taxa abundance and surface materials. Most sampling locations were composed of plastic material (1st-class table, 2nd-class table, armrest, door buttons, 1st-class under-seat handle). The headrest material was synthetic leather. Seat handles and door bars had metallic (painted) surfaces.

Within a similar sampling campaign, cultivation and characterization of isolates was conducted by Auerhammer et al. (2023) (28). The most abundant cultivated genus was *Staphylococcus*, followed by *Moraxella,* and *Micrococcus*. Besides *Staphylococcus*, none of the cultured genera

were represented in the displayed sequencing data. In comparison, qPCR detection of *Staphylococcus* species is described in **6.4 qPCR detection**.

The sampling location-dependent alpha-diversity (Faith's PD) is displayed in **Figure 6**. Although the train air showed consistent relative abundance of the top ten genera (**Figure 5**), it was found to have a high in-sample diversity, which was also observed by Gohli et al. (2019) (4). Sampling locations with highest diversity within a sampling type were the 1st-class under-seat handle, the door bar and the train air. Comparison of sampling positions was performed using Kruskal-Wallis test, showing differences in alpha-diversity (H=33.442, p=0.0002). Post-hoc-Dunn-tests using Bonferroni-correction showed significant differences only between the 1st-class under-seat handle and louvers (p=0.03), as well as very significant compared to the armrest (p=0.008). Further, significant difference was observed between door bar and armrest (p=0.047). The different alpha-diversities could be explained by the surface materials, as demonstrated by Hsu et al. (2016) (23). The door bar is a metallic bar with varnish, whereas the armrest material is plastic. Another difference would be the touching frequency, which we expect to be higher for the armrest.

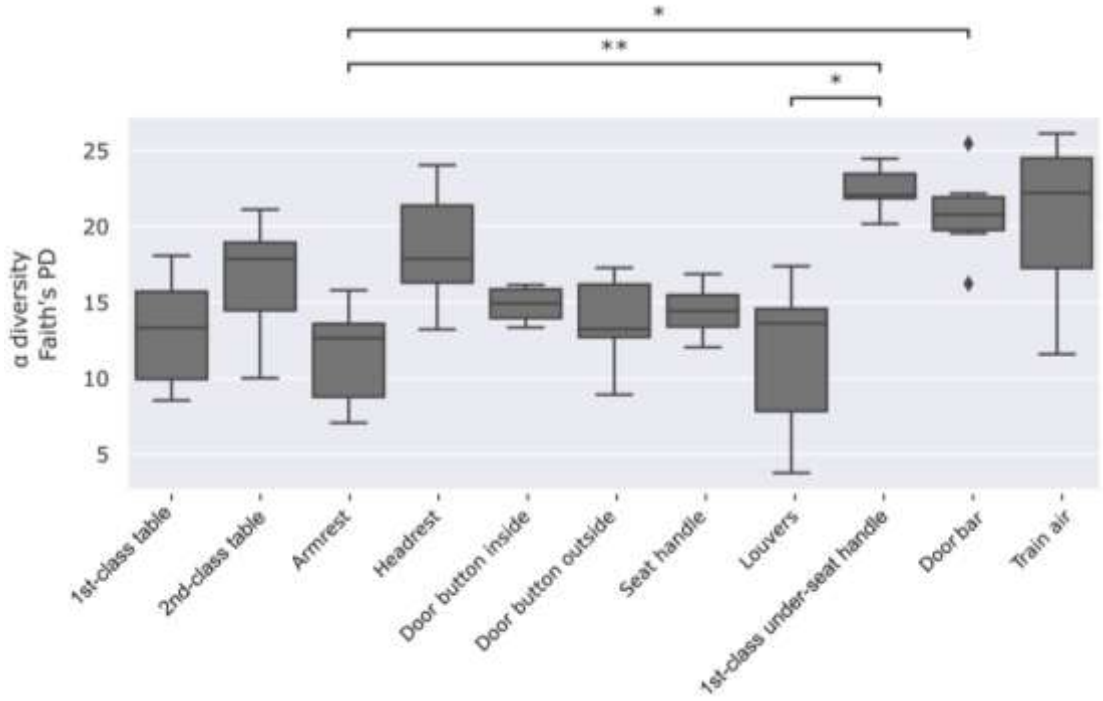

Figure 6: Alpha-diversity of sampling locations. Louvers vs. 1st-class under-seat handle (p=0.03), armrest vs. 1st-class under-seat handle (p=0.008), armrest vs. door bar (p=0.047).

A driving factor on microbial similarity is sample site, visible by the clustering in **Figure 7**. However, samples of locations like 1st-class table, armrest, and louvers are widely scattered, indicating high shifts in microbial communities. In contrast, especially door button inside and seat handle samples were clustered with high proximity to each other. The beta-diversity of door button inside, seat handle, and some samples of headrest and door bar was similar. This was not expected, since those positions are characterized by different surface materials.

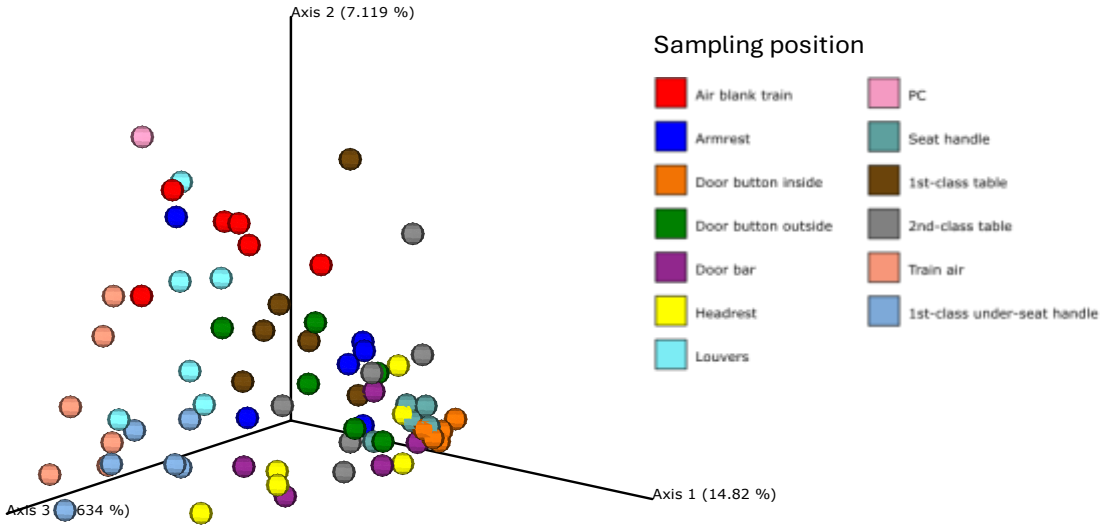

Figure 7: Train microbial diversity. PCoA of Bray-Curtis distances for samples organized after sampling position.

6.3 Effect size – sampling location > sampling time

Previous results already showed a distinct microbial pattern for each sampling position rather than sampling time. To analyze which component, sampling location or sampling time, had the most influence on the diversity (alpha and beta), forward step redundancy analysis was performed using Observed Features, Faith's PD and Shannon metrices for alpha-diversity, and unweighted unifrac, weighted unifrac, and Bray-Curtis for beta-diversity (**Figure 8,** supplementary **Figure S2**). It clearly showed, that the sampling locations harbored distinct microbial compositions. However, seasonal changes of the microbiome were not disproved at this point.

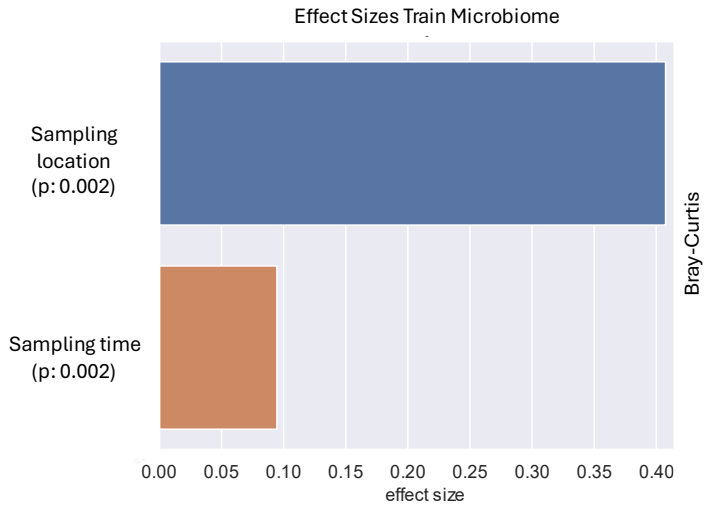

Figure 8: Sampling location has greater influence on beta-diversity compared to the sampling time. Effect size analysis using forward step redundancy analysis with a linear model composed of sampling position and sampling time on Bray-Curtis distances.

6.4 qPCR detection of *Staphylococcus* is limited – more *S. capitis* than *S. aureus*

Sequencing of variable regions of the 16S gene holds limitations which are reflected by the reliable determination of taxonomic levels until the genus level. Microbial detection via sequencing of the whole 16S gene can provide information on the species level, but is connected to higher cost. To investigate the occurrence of opportunistic pathogens, another methodology is needed. Therefore, qPCR was performed to aim for a species level detection within the DNA samples. Due to the limitation of DNA material, two target species were selected. *Staphylococcus aureus*, as one of the ESKAPE pathogens, and *Staphylococcus capitis*, as a

control as it is a skin commensal. Additionally, the results of each sampling time were concluded. qPCR results are represented by CT-values for each sampling position (**Figure 9**). Based on the results of the negative controls, the limit of detection was set to a CT of 35. It has to be noted that the calculated copy numbers were <0, therefore the data have to be considered with high caution. Overall, *S. capitis* was detected in all sampling positions but three, whereas *S. aureus* was only detected in three positions. This was expected due to *S. capitis*' natural occurrence on human skin. *S. aureus* was detected in samples of seat handle, door button inside and 2nd-class table, where *S. capitis* was also detected. On the other hand, *S. capitis* was not detected in louvers, armrest, and 1st-class table. Based on these results, no concerning concentrations of *S. aureus* were found. As many studies perform selective cultivation of samples for pathogen detection (2, 38), it would be of interest to test cultivation simultaneously to qPCR to compare outcomes. Cultivation of highly touched surfaces in trains was performed in another study (28), investigating the same train line as in our study with focus on cultivation. However, no *S. aureus* was identified, which can be the result of non-selective cultivation or low abundance of cultivable cells.

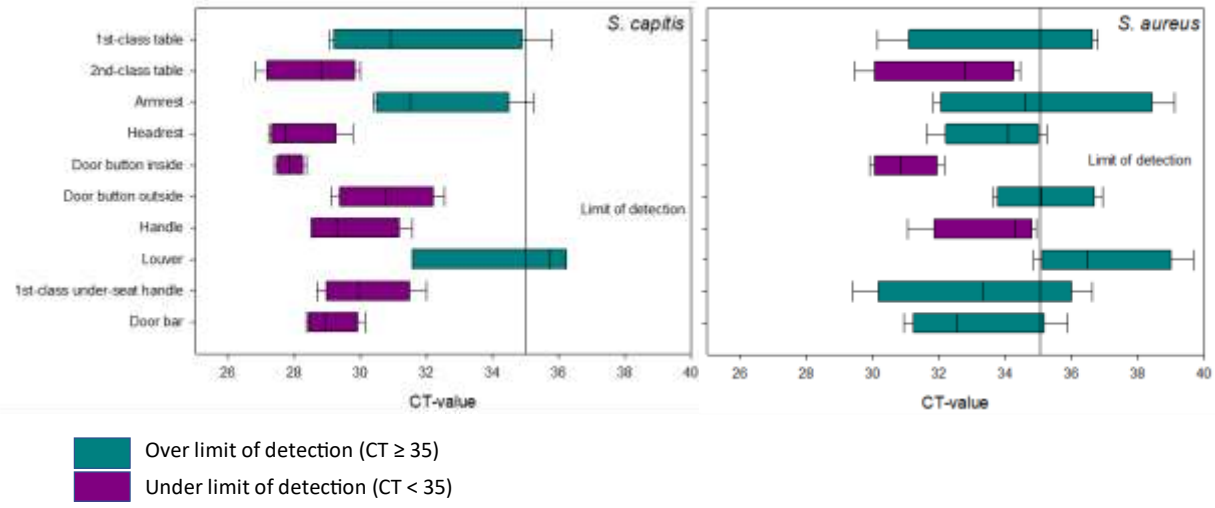

Figure 9: No quantitative detection of *S. capitis* and *S. aureus* in the train.

Additionally, CT-values were plotted for both species according to the sampling seasons (supplementary **Figure S3**). *S. capitis* detection was more prominent in winter and summer, while *S. aureus* showed only a slight tendency for better detection in one summer sampling.

As for future investigations, other relevant genera such as *Pseudomonas, Streptococcus* and *Acinetobacter* would be of interest as they occurred within the top ten sequenced genera.

7. Discussion

The train cabin is a public space, which is used by millions of passengers daily. It is shaped by the human microbiome, mostly by the contact from skin to surface. Further, airborne microorganisms can spread in such confined spaces, especially within full cabins. The train cabin environment is favoring the transmission of opportunistic pathogens, which poses public health concerns, especially due to the rising threat by AMRs. Therefore, we conducted a one-year study on the train microbiome, complemented by the detection of opportunistic pathogen *S. aureus* and control *S. capitis* via qPCR.

7.1 No significant seasonal dynamics in the train cabin microbiome

In this one-year study, no statistically significant difference in diversity was observed between the seasons. However, a distinct wave-like trend of alpha-diversity was visible throughout the sampling year. Other studies showed a higher alpha-diversity in different seasons. In Shanghai (39) metro stations, the highest alpha-diversity was observed in fall, whereas in Seoul (40), the fall season resulted in the lowest diversity and summer the highest. In Oslo, spring showed highest diversity (4). Therefore, even the comparison between roughly similar study designs with outdoor station analysis is not easy, as parameters such as geographic location, the temperature and relative humidity might create a striking difference (7, 36, 41).

Long term studies of other indoor environments have shown seasonal dynamics of microbial communities. However, the study design differed, since dust samples were taken in homes (42, 43), or active air sampling with filters was conducted, also focusing on dust collection (36). By collecting data on the train cabin microbiome, we contributed new information in this field, since no studies on the train or even subway cabin microbiome over long-term exist. Countermeasures to provide benign surface and air microbial communities might therefore not require seasonal adaptations, easing practical implementations significantly.

7.2 Sampling locations define the microbial composition

Our data show that sampling location has a higher influence on the microbial composition than sampling time. Our result matches findings of previous studies, which state that the surface material is defining the surface microbiome (23). However, no specific pattern according to surface material could be observed in our study. Therefore, we speculate that multiple influences together shape the microbial indoor cabin community: The surface material, type of contact (e.g. door bar by hand, headrest by head), and frequency of touching (44). Alongside the surface samples, air samples were retrieved in this study. Here, a clear difference of the top ten genera was shown compared to the surface samples. The indoor air microbiome has been already shown to be different to the surface microbiome, since the air microbiome is shaped by outdoor air and non-skin sources (37).

7.3 Pathogen detection in the train

The analysis of environmental samples of public transport is mostly conducted by 16S rRNA sequencing to create a picture of the microbial composition, as summarized by Ly et. al (2024) (45). Most studies of the subway microbiome conducted sequencing of distinct variable regions of the 16S gene. This approach allows reliable taxonomic identification up to the genus level (46). However, pathogenic species cannot be targeted by sequencing of variable regions of 16S rRNA. Therefore, we conducted qPCR detection of target species as proof of concept, without prior cultivation. The mentioned AMR crisis was subjected in this study by target detection of one ESKAPE pathogens, *S. aureus* and skin commensal *S. capitis* as a control. qPCR revealed three sampling locations as *S. aureus* positive, and seven positions as *S. capitis* positive. This was determined by a CT-value under a threshold of 35. However, the calculation of the copy numbers of each species and position showed no indication of infection risk of both species due to an extremely low copy number near zero. This low detection outcome is expected to be result of the low biomass, since in other studies, cultivation of isolates was performed prior to qPCR (17, 18).

In a study conducted by Auerhammer et al. in 2023 (28), samples were collected for cultivation in the same train line, which was investigated the present study. Different sampling locations, not all similar to those of this study were tested. Isolated species were identified by MALDI-TOF MS, followed by subsequent analysis and characterization by 16S rRNA sequencing,

growth curves, antimicrobial susceptibility testing, evaluation of cleaning and disinfection on isolates, among others, on selected bacterial species. Of tested isolates, only *E. cloacae* showed noteworthy antimicrobial resistance against five antibiotics. Among those, resistance against last resort antibiotic colistin was identified (28). For future studies, focusing on selective cultivation for antibiotic resistant bacteria would be beneficial for microbial risk assessment.

In the same study, the most abundant cultivated genera were *Staphylococcus, Moraxella,* and *Micrococcus*. Compared to our sequencing data, only *Staphylococcus* was abundant. An explanation would be, that abundant genera identified by 16S rRNA sequencing were not viable or "viable, but non-culturable" (VBNC), which is a common issue or downfall of cultivation (47). However, sequencing is subjected to certain restrictions. For instance, the selection of the target 16S sequence segment can influence the outcome. Even at the beginning, during DNA extraction, cells of some species or genera are more difficult to lyse than others (e.g. Gram-positive bacteria) (48), which influences the representation of the taxonomic results. Further, different extraction kits result in variable sequencing results (49).

7.4 The train microbiome shows high similarity to other public transport environments

The train cabin microbiome is a confined space, with high fluctuation of passengers, often times without highly efficient ventilation system (e.g. no HEPA filtration), with varying travel durations. Some of these factors are also present in other indoor environments, such as airplane cabins. However, airplane cabin ventilation systems are more sophisticated with the use of HEPA filters, which are not commonly found in trains. Another similar environment is displayed by the subway (16, 23, 25, 50), which is characterized by typical human- and environment-associated genera, as concluded by Ly et al. (2024) (51). The fact that human shape the indoor microbiome becomes clear considering the International Space Station (ISS) microbiome, as an isolated environment. Here, abundant taxa are *Corynebacterium*, *Streptococcus*, *Staphylococcus*, *Propionibacterium*, and *Pseudomonas*, among others (52-55), which are similar to the public transport microbiome. Nevertheless, as the previous section showed, collecting data and perform microbial monitoring is still important.

7.5 Limitations of this study

For statistical purposes, an increased number of samples would have been beneficial for the results. However, this was not feasible in with regard to the laboratory expense. We decided to take six samples of each sampling location to gather enough biomass for DNA extraction and analysis. In detail, e.g. for each seat handle sample, six different swabs and seat handles were sampled to moreover minimize sampling location bias. However, the obtained DNA was not detectable via Qubit measurement. Sequencing was possible, but the detection of specific species via qPCR constituted a challenge. Almost no *S. capitis* and even less *S. aureus* were detectable, which is a relieve in terms of microbial risk. To gain more information on the detection method, other target organisms with expected higher abundance according to sequencing results could be selected, such as *S. epidermidis* as a control and *Acinetobacter baumannii* as a pathogen. Another approach is the detection of specific genes, as previously conducted by Shen et al. (2018) (17). Although no prior cultivation for qPCR was intended in this study for time and feasibility, selective cultivation for antibiotic resistances would facilitate this approach by generating more output DNA.

7.6 Concluding comments

This study was the first to conduct long-term sampling in train cabins in Germany. We conclude, that the sampling locations within the train influence the microbial diversity in the train cabin the most, rather than the sampling time or seasons. Countermeasures might therefore work over the whole year and should be considered for each location/material in the cabin. Microbial detection via qPCR showed more hits for *Staphylococcus capitis* compared to *Staphylococcus aureus.* However, this approach has to be improved.

The combination of 16S rRNA amplicon sequencing of the V1-V2 region and qPCR allowed for a broad-spectrum analysis of the train microbiome, and the targeting of specific species of interest. This work provides basic knowledge for future studies exploring the indoor microbiome of public transportation and the development of suiting microbial countermeasures to reduce transmission of opportunistic pathogens.

8. Author statements

Author contributions

https://casrai.org/credit/]

Yen Ly-Sauerbrey: Conceptualization, Data curation, Formal analysis, Investigation, Methodology, Visualization, Writing – original draft.

Anna Rehm: Conceptualization, Data curation, Formal analysis, Visualization, Writing – review & editing

Denise Engel: Conceptualization, Data curation, Investigation, Writing – review & editing

Stefan Janssen: Conceptualization, Resources, Writing – review & editing

Stefan Leuko: Conceptualization, Funding acquisition, Project administration, Supervision, Writing – review & editing

Conflicts of interest

The authors declare that there are no conflicts of interest

Funding information

This work was supported by the DLR internal grant DLR-VO: GANDALF and the data will be included in the Ph.D. thesis of YLS. SL was supported by the German Aerospace Center (Deutsches Zentrum für Luft- und Raumfahrt, DLR) grant Traffic (RoSto, VmO4Orte and DiVe). We acknowledge the support of NFDI4Microbiota, which is funded by the Deutsche Forschungsgemeinschaft (DFG) - German Research Foundation (project number 460129525, NFDI 28/1).

Acknowledgements

We thank goRheinland and National Express for creating the possibility to conduct the sampling campaign, the whole aerospace microbiology research group for helping at every sampling day. The raw data was processed on JupyterHub, a platform for further data processing and analysis, which is coupled to the servers of the Justus-Liebig-University Giessen, Germany. Further, this project was initiated with Prof. Ralf Möller†, who we miss and thank the most for his unlimited support and passion throughout all past years.

9. References

1. Pendleton JN, Gorman SP, Gilmore BF. Clinical relevance of the ESKAPE pathogens. Expert review of anti-infective therapy. 2013;11(3):297-308.

2. Otter JA, French GL. Bacterial contamination on touch surfaces in the public transport system and in public areas of a hospital in London. Lett Appl Microbiol. 2009;49(6):803-5.

3. Zhou F, Wang Y. Characteristics of antibiotic resistance of airborne *Staphylococcus* isolated from metro stations. International Journal of Environmental Research and Public Health. 2013;10(6):2412-26.

4. Gohli J, Boifot KO, Moen LV, Pastuszek P, Skogan G, et al. The subway microbiome: seasonal dynamics and direct comparison of air and surface bacterial communities. Microbiome. 2019;7(1):160.

5. Stott P. How climate change affects extreme weather events. Science. 2016;352(6293):1517-8.

6. Hanlon HM, Bernie D, Carigi G, Lowe JA. Future changes to high impact weather in the UK. Climatic Change. 2021;166(3):50.

7. Leung M, Tong X, Bøifot KO, Bezdan D, Butler DJ, et al. Characterization of the public transit air microbiome and resistome reveals geographical specificity. Microbiome. 2021;9(1):112.

8. Shen Y, Li C, Dong H, Wang Z, Martinez L, et al. Community outbreak investigation of SARS-CoV-2 transmission among bus riders in eastern China. JAMA internal medicine. 2020;180(12):1665-71.

9. Sze To GN, Wan MP, Chao CYH, Fang L, Melikov A. Experimental study of dispersion and deposition of expiratory aerosols in aircraft cabins and impact on infectious disease transmission. Aerosol Science and Technology. 2009;43(5):466-85.

10. Kenyon TA, Valway SE, Ihle WW, Onorato IM, Castro KG. Transmission of multidrug-resistant *Mycobacterium tuberculosis* during a long airplane flight. New England Journal of Medicine. 1996;334(15):933-8.

11. Goscé L, Johansson A. Analysing the link between public transport use and airborne transmission: mobility and contagion in the London underground. Environmental Health. 2018;17:1-11.

12. Hu M, Lin H, Wang J, Xu C, Tatem AJ, et al. Risk of coronavirus disease 2019 transmission in train passengers: an epidemiological and modeling study. Clinical Infectious Diseases. 2021;72(4):604-10.

13. Statistisches Bundesamt (Destatis). Beförderte Personen in Deutschland [cited 2025-11-14]. Available from: https://www.destatis.de/DE/Themen/Branchen-Unternehmen/Transport-Verkehr/Personenverkehr/Tabellen/befoerderte-personen-verkehrstraeger.html.

14. Yoshie S, Ikehata M, Kawasaki T, Kyotani T, Ushiogi T. Evaluation of Environmental Hygiene in Railway Vehicles Using Microbiome Analysis. J-STAGE. 2022;63(4):283-8.

15. Sharma S, Jahanzaib M, Bakht A, Kim M-K, Lee H, et al. The composition of the bacterial communities collected from the PM10 samples inside the Seoul subway and railway station. Scientific Reports. 2024;14(1):6478.

16. Afshinnekoo E, Meydan C, Chowdhury S, Jaroudi D, Boyer C, et al. Geospatial Resolution of Human and Bacterial Diversity with City-Scale Metagenomics. Cell Syst. 2015;1(1):72-87.

17. Shen C, Feng S, Chen H, Dai M, Paterson DL, et al. Transmission of *mcr*-1-producing multidrug-resistant Enterobacteriaceae in public transportation in Guangzhou, China. Clinical Infectious Diseases. 2018;67(suppl_2):S217-S24.

18. Cao T, Liu Y, Li Y, Wang Y, Shen Z, et al. A public health concern: emergence of carbapenem-resistant *Klebsiella pneumoniae* in a public transportation environment. Journal of Antimicrobial Chemotherapy. 2020;75(10):2769-72.

19. Gu J, Xie X-J, Liu J-X, Shui J-R, Zhang H-Y, et al. Prevalence and transmission of antimicrobial-resistant Staphylococci and Enterococci from shared bicycles in Chengdu, China. Science of The Total Environment. 2020;738:139735.

20. Johnson JS, Spakowicz DJ, Hong B-Y, Petersen LM, Demkowicz P, et al. Evaluation of 16S rRNA gene sequencing for species and strain-level microbiome analysis. Nature communications. 2019;10(1):5029.

21. Weiss H, Hertzberg VS, Dupont C, Espinoza JL, Levy S, et al. The airplane cabin microbiome. Microbial ecology. 2019;77:87-95.

22. Yang J, Kim JS, Jeon HW, Lee J, Seo JH. Integrated Culture-Based and Metagenomic Profiling of Airborne and Surface-deposited Bacterial Communities in Residential Environments. Environmental Pollution. 2025:126703.

23. Hsu T, Joice R, Vallarino J, Abu-Ali G, Hartmann EM, et al. Urban Transit System Microbial Communities Differ by Surface Type and Interaction with Humans and the Environment. mSystems. 2016;1(3).

24. Zhao B, Dewald C, Hennig M, Bossert J, Bauer M, et al. Microorganisms@ materials surfaces in aircraft: Potential risks for public health?–A systematic review. Travel medicine and infectious disease. 2019;28:6-14.

25. Vargas-Robles D, Gonzalez-Cedillo C, Hernandez AM, Alcaraz LD, Peimbert M. Passenger-surface microbiome interactions in the subway of Mexico City. PLoS One. 2020;15(8):e0237272.

26. Pochtovyi AA, Vasina DV, Verdiev BI, Shchetinin AM, Yuzhakov AG, et al. Microbiological Characteristics of Some Stations of Moscow Subway. Biology (Basel). 2022;11(2).

27. Adams RI, Bateman AC, Bik HM, Meadow JF. Microbiota of the indoor environment: a meta-analysis. Microbiome. 2015;3:1-18.

28. Auerhammer A. Investigation and Characterization of Human-Health Related Microbes in Public Transport: University of Applied Sciences Bonn-Rhein-Sieg; 2023.

29. Martin M. Cutadapt removes adapter sequences from high-throughput sequencing reads. EMBnet journal. 2011;17(1):10-2.

30. Ewels P, Magnusson M, Lundin S, Käller M. MultiQC: summarize analysis results for multiple tools and samples in a single report. Bioinformatics. 2016;32(19):3047-8.

31. Gonzalez A, Navas-Molina JA, Kosciolek T, McDonald D, Vázquez-Baeza Y, et al. Qiita: rapid, web-enabled microbiome meta-analysis. Nature methods. 2018;15(10):796-8.

32. Amir A, McDonald D, Navas-Molina JA, Kopylova E, Morton JT, et al. Deblur rapidly resolves single-nucleotide community sequence patterns. MSystems. 2017;2(2):10.1128/msystems. 00191-16.

33. Bolyen E, Rideout JR, Dillon MR, Bokulich NA, Abnet CC, et al. Reproducible, interactive, scalable and extensible microbiome data science using QIIME 2. Nature biotechnology. 2019;37(8):852-7.

34. Bray JR, Curtis JT. An ordination of the upland forest communities of southern Wisconsin. Ecological monographs. 1957;27(4):326-49.

35. Kim E, Yang S-M, Won J-E, Kim D-Y, Kim D-S, et al. Real-time PCR method for the rapid detection and quantification of pathogenic *Staphylococcus* species based on novel molecular target genes. Foods. 2021;10(11):2839.

36. Frankel M, Beko G, Timm M, Gustavsen S, Hansen EW, et al. Seasonal variations of indoor microbial exposures and their relation to temperature, relative humidity, and air exchange rate. Appl Environ Microbiol. 2012;78(23):8289-97.

37. Wilkins D, Leung MH, Lee PK. Indoor air bacterial communities in Hong Kong households assemble independently of occupant skin microbiomes. Environmental microbiology. 2016;18(6):1754-63.

38. Mendes A, Martins da Costa P, Rego D, Beca N, Alves C, et al. Contamination of public transports by *Staphylococcus aureus* and its carriage by biomedical students: point-prevalence, related risk factors and molecular characterization of methicillin-resistant strains. Public Health. 2015;129(8):1125-31.

39. Zhang L, Li X, Shi L, Zheng Y, Ding Y, et al. Bacterial diversity and biomarkers screening of station and carriage surface in Shanghai metro system, China. Current Research in Microbial Sciences. 2025;8:100374.

40. Hassan ZU, Cho H, Park C, Yim Y-H, Kim S. Seasonal variations of the airborne microbial assemblages of the Seoul subway, South Korea from 16S and ITS gene profiles with chemical analysis. Scientific Reports. 2022;12(1):18456.

41. Kembel SW, Jones E, Kline J, Northcutt D, Stenson J, et al. Architectural design influences the diversity and structure of the built environment microbiome. The ISME journal. 2012;6(8):1469-79.

42. Rintala H, Pitkaranta M, Toivola M, Paulin L, Nevalainen A. Diversity and seasonal dynamics of bacterial community in indoor environment. BMC Microbiol. 2008;8:56.

43. Weikl F, Tischer C, Probst AJ, Heinrich J, Markevych I, et al. Fungal and Bacterial Communities in Indoor Dust Follow Different Environmental Determinants. PLoS One. 2016;11(4):e0154131.

44. Hoisington AJ, Stamper CE, Bates KL, Stanislawski MA, Flux MC, et al. Human microbiome transfer in the built environment differs based on occupants, objects, and buildings. Scientific Reports. 2023;13(1):6446.

45. Ly Y-T, Leuko S, Moeller R. An overview of the bacterial microbiome of public transportation systems-risks, detection, and countermeasures. Frontiers in Public Health. 2024;12:1367324.

46. Wang S, Sun B, Tu J, Lu Z. Improving the microbial community reconstruction at the genus level by multiple 16S rRNA regions. Journal of Theoretical Biology. 2016;398:1-8.

47. Rhoads DD, Cox SB, Rees EJ, Sun Y, Wolcott RD. Clinical identification of bacteria in human chronic wound infections: culturing vs. 16S ribosomal DNA sequencing. BMC infectious diseases. 2012;12:1-8.

48. Cabeen MT, Jacobs-Wagner C. Bacterial cell shape. Nat Rev Microbiol. 2005;3(8):601-10.

49. Sui HY, Weil AA, Nuwagira E, Qadri F, Ryan ET, et al. Impact of DNA Extraction Method on Variation in Human and Built Environment Microbial Community and Functional Profiles Assessed by Shotgun Metagenomics Sequencing. Front Microbiol. 2020;11:953.

50. Leung MH, Wilkins D, Li EK, Kong FK, Lee PK. Indoor-air microbiome in an urban subway network: diversity and dynamics. Appl Environ Microbiol. 2014;80(21):6760-70.

51. Ly Y-T, Wetzig N, Holtel J, Leuko S, Moeller R, editors. Modeling the Public Transport Microbiome: Development of a Microbial Reference Community. 18th International Conference on Indoor Air Quality and Climate, INDOOR AIR 2024; 2024.

52. Lang JM, Coil DA, Neches RY, Brown WE, Cavalier D, et al. A microbial survey of the International Space Station (ISS). PeerJ. 2017;5:e4029.

53. Mora M, Wink L, Kögler I, Mahnert A, Rettberg P, et al. Space Station conditions are selective but do not alter microbial characteristics relevant to human health. Nature communications. 2019;10(1):3990.

54. Venkateswaran K, Vaishampayan P, Cisneros J, Pierson DL, Rogers SO, et al. International Space Station environmental microbiome—microbial inventories of ISS filter debris. Applied microbiology and biotechnology. 2014;98(14):6453-66.

55. Avila-Herrera A, Thissen J, Urbaniak C, Be NA, Smith DJ, et al. Crewmember microbiome may influence microbial composition of ISS habitable surfaces. PLoS One. 2020;15(4):e0231838.

10. Supplements

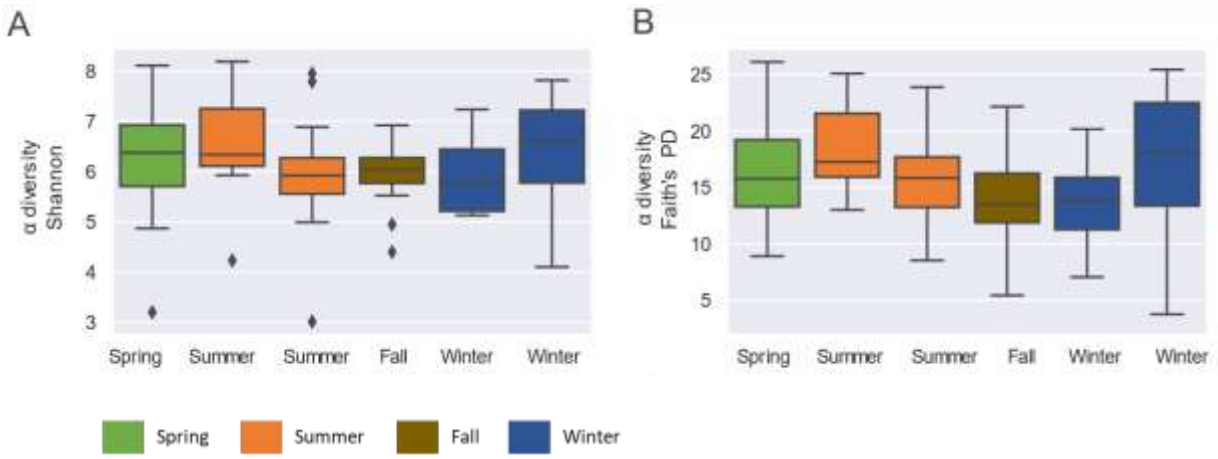

Figure S1: Alpha-diversity over the seasons occurs similar between metrices. A Shannon, B Faith's PD.

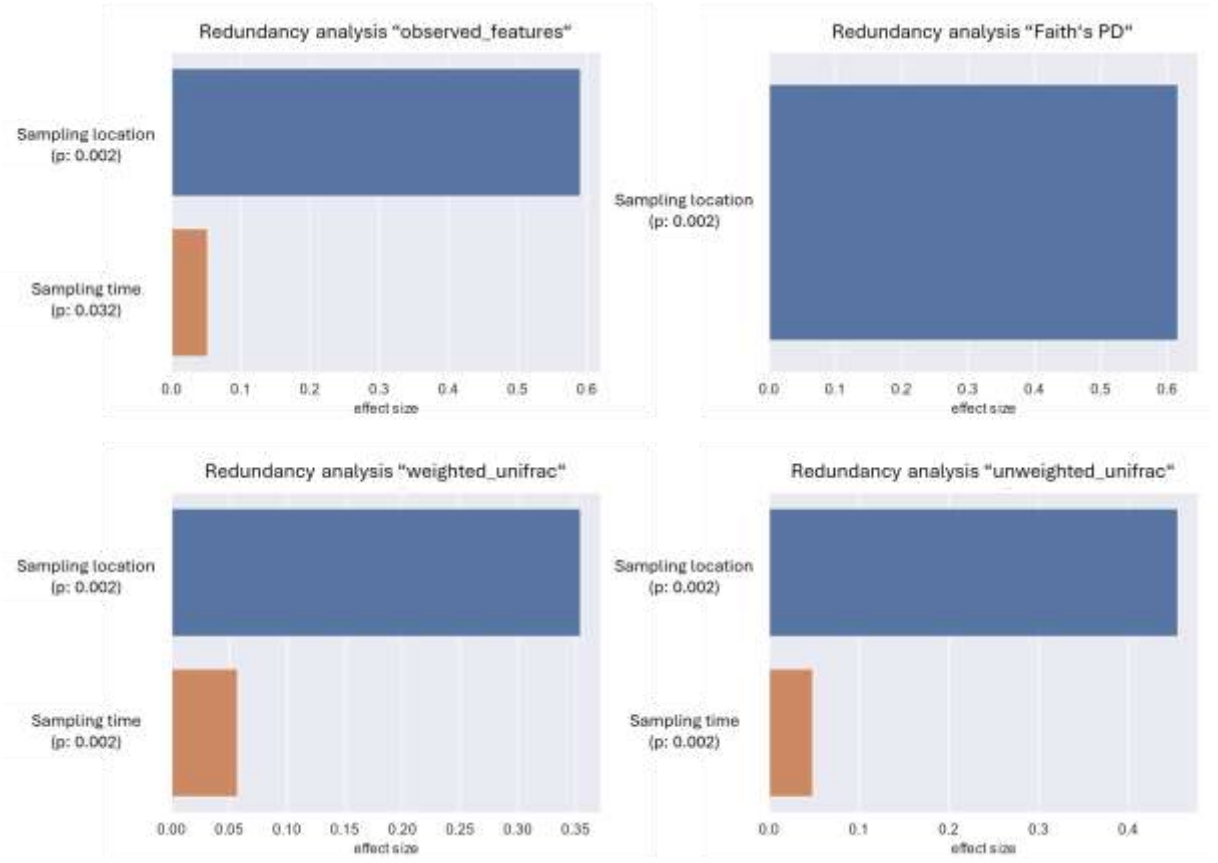

Figure S2: Sampling location has greater influence on alpha- and beta-diversity compared to sampling time. For Shannon, no significant findings were observed.

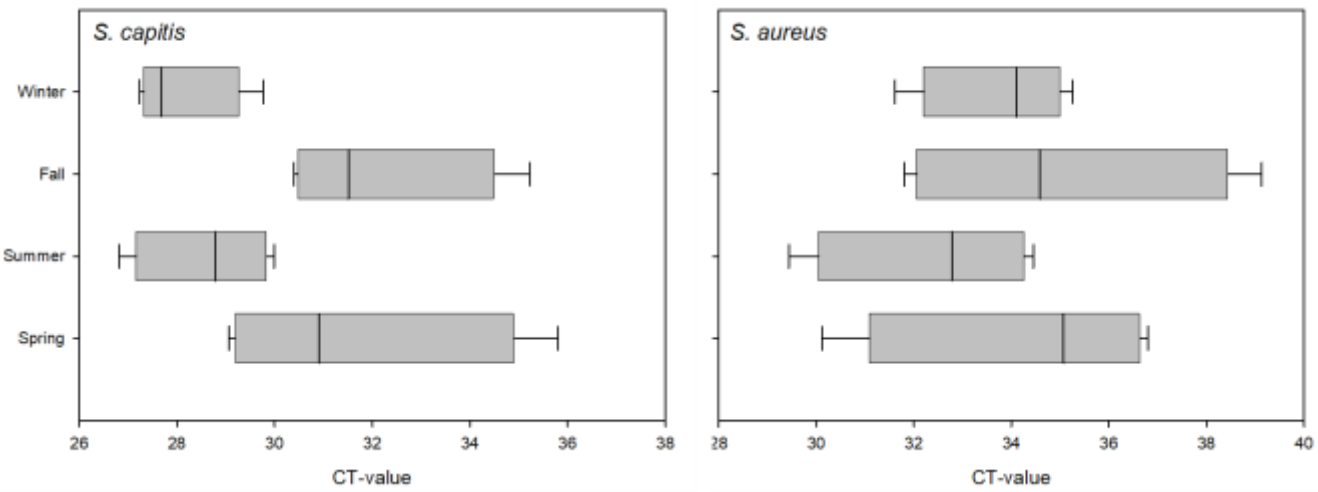

Figure S3: qPCR detection of *S. capitis* and *S. aureus* in different seasons. For this figure, data of the sample collection of 05/30/2023 (spring), 08/01/2023 (summer), 09/28/2023 (fall), and 02/01/2024 (winter) were used.

Available in microbial analysis notebook:

Supplementary Table 1: Alpha-diversity measures.

Supplementary Table 2: Beta-diversity measures.

2.3 Modeling the public transport microbiome: Development of a microbial reference community

Title	**Modeling the public transport microbiome: Development of a microbial reference community**
Authors	**Yen Ly-Sauerbrey[1]**, Nina Wetzig[2], Julia Holtel[2], Stefan Leuko[1] and Ralf Möller[1]
Affiliation	[1] Department of Applied Biology, Institute of Aerospace Medicine, German Aerospace Center, Cologne, Germany [2] Institute for Functional Gene Analytics, Bonn-Rhein-Sieg University of Applied Sciences, Sankt Augustin, Germany
Article type	Conference paper
Authorship	Single-first author
Journal	18th International Conference on Indoor Air Quality and Climate, INDOOR AIR
Year	2024
Author Contributions	
Y-TL	Conceptualization, Data curation, Formal analysis, Investigation, Visualization, Writing -original draft, Writing – review & editing
NW	Data curation, Formal analysis, Visualization, Writing – review & editing
JH	Resources, Writing – review & editing
SL	Writing – review & editing
RM	Conceptualization, Funding acquisition, Supervision, Writing – review & editing

Modeling the Public Transport Microbiome: Development of a Microbial Reference Community

Yen-Tran Ly[1],*, Nina Wetzig[2], Julia Holtel[2], Stefan Leuko[1], Ralf Moeller[1]

[1] Institute of Aerospace Medicine, Aerospace Microbiology Group, German Aerospace Center (DLR), Cologne, Germany

[2] Institute for Functional Gene Analytics, Bonn-Rhein-Sieg University of Applied Sciences, Grantham Allee 20, 53757 Sankt Augustin, Germany

**Corresponding email: yen-tran.ly@dlr.de*

Summary

A microbial community containing 9 bacterial species was created based on the most common bacteria in public transportation, which can be used as a reference microbiome for testing the efficiency of decontamination and detection methods, and also as a bioaerosol. In addition, the created microbial community was characterized with regard to its behavior and abundance of individual strains under the stress conditions of irradiation, desiccation and cold storage in order to investigate the stability of the product.

Keywords

Bioaerosol, microbial monitoring, indoor and build environment microbiome, public transport

1. Introduction

Public transport was particularly affected by the COVID-19 pandemic, as passengers no longer felt safe. There was a great concern of becoming infected in crowded, confined spaces. To investigate the influence of microbes to the indoor climate, a microbial community was developed that closely resembles the microbiome of public transport. This will be used to test methods for decontaminating vehicle cabins and reducing contamination. Furthermore, the simulated microbiome will also be used as a bioaerosol, for example to test new ventilation concepts (Kohl, Ly et al., 2024). Composite microbial communities are already available on the market, such as the ZymoBIOMICS^{TM} Microbial Community Standard cells (MC; Zymo Research Corp., Irvine, CA, United States). The difference to this work, however, is that here a microbiome was developed for a specific environment, namely public transport and passenger areas. There are already studies that have examined the microbiome in subways and airplanes (Weiss et al., 2019, Leung et al., 2014), which mostly consist of human-associated bacteria, but

also environmental-associated bacteria. Airplanes and subways share the most frequently occurring genera (see **Table 1**). Genera typical of skin microbes are represented, such as *Propionibacterium*, *Corynebacterium, Micrococcus* and *Staphylococcus*. However, genera of environmental representatives such as *Flavobacterium* and *Burkholderia* are also represented. The publications on which the data in the table are based on, used different methods to identify the microbes in the airplane and subway samples. For the airplane samples, 16S rRNA sequencing (Weiss et al., 2019, Liu et al., 2020) and shotgun metagenomics (Sun et al., 2020) were performed, and data were compiled from other literature (Zhao et al., 2019). For the subway samples, methods such as 16S rRNA sequencing (Gohli et al., 2019, Hernández et al., 2019), and Illumina HiSeq (Kang et al., 2018, Afshinnekoo et al., 2015) were used.

In this study, nine bacteria were used to create an artificial microbial community resembling the microbiome of public transportation. These are based on the most frequently occurring genera (see **Table 1**). They are all classified as biosafety level 1 and are used in this community as a reference model for various investigations and tests of decontamination and detection methods.

Table 1: Most abundant bacteria in aircraft cabins and subways. Based on studies that investigated the microbiome of aircraft cabin and subway air and surfaces.

	Aircraft cabin	**Subway**	**Reference**
1	*Staphylococcus*	*Staphylococcus*	**Aircraft cabin:** Weiss et al., 2019, Liu et al., 2020, Sun et al., 2020, Zhao et al., 2019 **Subway:** Afshinnekoo et al., 2015, Kang et al., 2018, Gohli et al., 2019, Hernández et al., 2019
2	*Pseudomonas*	*Acinetobacter*	
3	*Corynebacterium*	*Corynebacterium*	
4	*Streptococcus*	*Micrococcus*	
5	*Enterobacteriaceae*	*Propionibacterium*	
6	*Flavobacterium*	*Pseudomonas*	
7	*Kocuria*	*Sphingomonas*	
8	*Micrococcus*	*Flavobacterium*	
9	*Sphingomonas*	*Streptococcus*	
10	*Stenotrophomonas*	*Kocuria*	

2. Materials and methods

2.1 Test organisms and growth conditions

The organisms are listed in **Table 2** and were grown using 2x Reasoner's 2A broth (TEKnova; composition: yeast extract 0.5 g, peptone 0.5 g, casamino acids 0.5 g, glucose 0.5 g, soluble starch 0.5 g, sodium pyruvate 0.3 g, dipotassium phosphate 0.3 g, magnesium sulfate 0.05 g, per Liter), Tryptic Soy Broth (Sigma-Aldrich; composition: casein peptone (pancreatic) 17 g, dipotassium hydrogen phosphate 2.5 g, glucose 2.5 g, sodium chloride 5 g, soya peptone (papain digest.) 3 g, per Liter), and Brain Heart Infusion broth (Sigma-Aldrich; composition: brain extract 7.8 g, heart extract 9.7 g, proteose peptone 10 g, sodium chloride 5 g, D(+)-Glucose 2 g, disodium hydrogen phosphate 2.5 g, per Liter). The strains *Burkholderia lata* DSM 23089^T, *Enterococcus viikkiensis* DSM 24043^T, *Propionibacterium cyclohexanicum* DSM 16859^T, *Pseudomonas antarctica* DSM 1530^T, *Staphylococcus capitis* subsp. c*apitis* DSM 111179 and DSM 20326^T were grown for 18 h under constant shaking at 200 rpm, while the strains *Corynebacterium halotolerans* DSM 44683^T, *Flavobacterium frigoris* DSM 15719^T, *Sphingomonas rubra* DSM 26135^T, and *Streptococcus halotolerans* DSM 101996^T were grown for 48 h at 200 rpm. The composition of the microbial community in a solution depends on the desired concentration of the respective strains and can be adjusted individually. The composition of the bacterial strains used in this work is listed in **Table 2**. In addition, *S. capitis* subsp. *capitis* DSM 11179 was listed, which is used instead of *S. capitis* subsp. *capitis* DSM 20326^T in other experiments, depending on the type of experiment.

Table 2: List of utilized bacterial strains with growth conditions and reference.

Strain	Growth	Reference
Burkholderia lata **DSM 23089^{T}**	2xReasoner's 2A broth or agar 37 °C	Vanlaere et al., 2009
Corynebacterium halotolerans **DSM 44683^{T}**	Tryptic Soy Broth (TSB) or agar (TSA) 37 °C	Chen et al., 2004
Enterococcus viikkiensis **DSM 24043^{T}**	Brain Heart Infusion (BHI) broth or agar 37 °C	Rahkila et al., 2011
Flavobacterium frigoris **DSM 15719^{T}**	2xReasoner's 2A broth or agar 20 °C	Van Trappen et al., 2004
Propionibacterium cyclohexanicum **DSM 16859^{T}**	Brain Heart Infusion (BHI) broth or agar 37 °C	Kusano et al., 1997
Pseudomonas antarctica **DSM 1530^{T}**	Tryptic Soy Broth (TSB) or agar (TSA) 20 °C	Reddy et al., 2004
Sphingomonas rubra **DSM 26135^{T}**	2xReasoner's 2A broth or agar 20 °C	Huo et al., 2011
Staphylococcus capitis **subsp. capitis DSM 20326^{T}**	Tryptic Soy Broth (TSB) or agar (TSA) 37 °C	Kloos and Schleifer, 1975
Staphylococcus capitis **subsp. c*apitis* DSM 111179 / K1-2-2-23**	Tryptic Soy Broth (TSB) or agar (TSA) 37 °C	Sobisch et al., 2019, Siems et al., 2022
Streptococcus halotolerans **DSM 101996^{T}**	Brain Heart Infusion (BHI) broth or agar 37 °C	Niu et al., 2016

2.2 Stress tests

In order to characterize the developed microbial community as a product, three different treatments were tested. Irradiation was used to inactivate the microorganisms in order to be able to use the microbial community as a non-reproducible and inactive product while it is still molecularly detectable. **A) Irradiation** was applied on the microbial community using a dose of 10 kGy X-Ray (RS 225 A, Gulmay Medical). To test the stability of the microbial community after **B) desiccation**, 500 µL of the bacterial suspension with a total cell count of ~5 x 10^{9} cells

was dried under sterile conditions. The **C) stability stress test at 4 °C** was conducted by storing the samples at 4 °C for one week, to investigate the shelf life of the bacteria.

2.3 DNA extraction and 16S rRNA sequencing

For DNA extraction, the DNA/RNA Miniprep Kit (ZYMOBIOMICS) was used according to the provided protocol. Prior to 16S rRNA sequencing, the samples were preprocessed using the *Quick*-16S^{TM} NGS Library Prep Kit (ZYMO RESARCH) according to the corresponding protocol with minor modifications: the fluorescence standards were not used and instead, quantification was performed by the Quantus fluorometer (Promega). Further, AMPure XP Beads (Beckmann Coulter) were used for the clean-up of the DNA after index PCR. 16S rRNA sequencing was performed with the Illumina MiSeq Reagent Kit v3 (600 cycles).

2.4 Data analysis

Data obtained from sequencing was preprocessed using divisive amplicon denoising algorithm 2 (DADA2), the taxonomic classification was conducted using Quantitative Insights Into Microbial Ecology2 (QIIME2) with the plugin sklearn (scikit-learn), using a classifier connected to the SILVA rRNA database for 16S.

3. Results and discussion

The genera of the selected strains are known to be both human-associated and environmentally-associated bacteria, and at the same time related to pathogens (**Figure 1**). The study of these organisms in the community provides a reference for understanding microbial interactions and also serves as a realistic model for various applications.

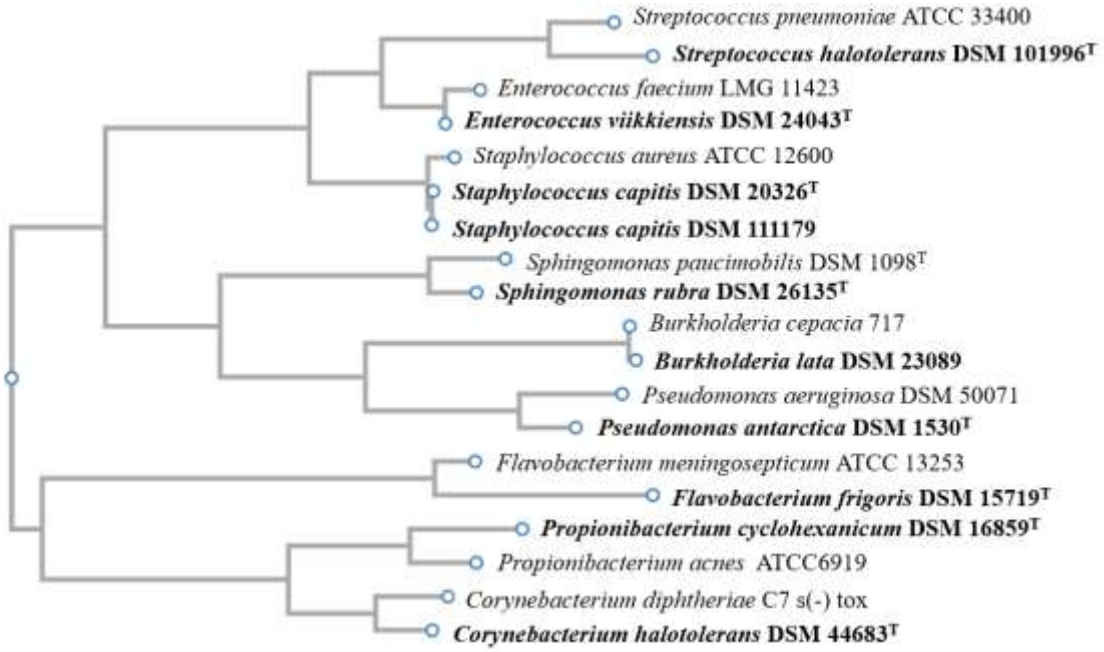

Figure 1: Phylogenetic tree of the developed public transport microbiome (bold) and related pathogens. The tree construction was performed with FastTree v2.1.8. based on 16S rRNA sequences. 16S rRNA of the strain *S. capitis* DSM 111179 was extracted from whole genome data using ContEst16S (Lee et al., 2017).

Various stress tests and storage conditions were performed for an initial characterization of the microbial community produced for the first time. This was followed by DNA extraction of the cells and 16S rRNA sequencing to check the abundances of the respective genera within the microbial community before and after the treatments. Comparing the taxonomic abundance within the microbial positive control model community with that of the treated samples, some differences and similarities can be seen. In the irradiated microbial community, only *Corynebacterium* showed a significantly higher abundance than in the positive control (**Figure 2A**). The inactivation of cells using X-rays has already been investigated and earlier studies have shown that amplifiable DNA is still present (Josephson et al., 1993) despite the double-strand breaks in the DNA induced by X-rays (Dean et al., 1969). This was confirmed by this work with 16S rRNA sequencing.

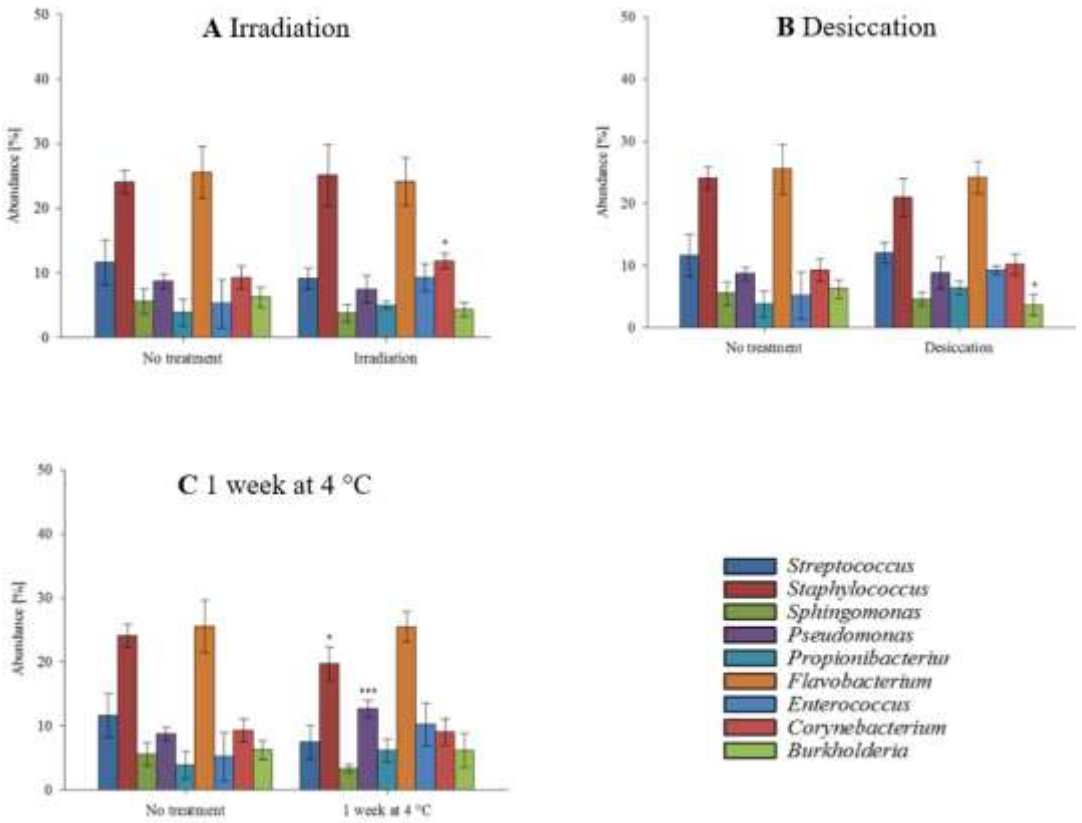

Figure 2: Changes within the microbial community after irradiation, desiccation and storage at 4 °C. Genera relative abundances were compared after treatments with the untreated microbial community. After (A) irradiation and (B) desiccation, the relative abundances were similar to the untreated microbial community. (C) Storing the microbial community at 4 °C for one week showed an increase of the genus *Pseudomonas*.

Desiccation of cells through air drying can cause hyperosmotic and matric stress, as well as damage of cell membranes (Potts, 1994). After desiccation, only a decrease in *Burkholderia* was observed (**Figure 2B**), indicating stability of the DNA while cells might be damaged. These results indicate the stability of the model community after irradiation and desiccation stress. Only when the microbial community was stored at 4 °C, significant increases in *Pseudomonas* were shown, which can be attributed to the growth characteristics of *P. antarctica* DSM 1530^{T} at such low temperatures (Reddy et al., 2004).

4. Conclusions

An artificial microbiome simulating that of public transport was developed and its behavior was tested under three stress conditions. Inactivation of the microbial community by X-ray irradiation (10 kGy), desiccation treatment and storage at 4 °C led to a change in the bacterial abundance of only three different strains. The microbial community was therefore mostly stable. In future work, the use of reference microorganisms, in particular customized microbiomes, will be relevant in order to achieve an approximately realistic behavior in the application of (novel) methods. It can be used in liquid or dry state to test microbial countermeasures such as antimicrobial surfaces or as a bioaerosol to test ventilation concepts. The microbial community presented in this work has already been used in other as a reference bioaerosol for the investigation of a ventilation concept to reduce the bacterial load in passenger cabins (Kohl, Ly et al., 2024). With regard to indoor air, this means finding and testing measures that are effective in improving the quality of indoor air and thus maintaining people's health.

Acknowledgement

Y.-T.L. received funding from the German Aerospace Center (DLR) grant DLR-VO: GANDALF. R.M. & S.L. were supported by the DLR grants: FuE-Projekt “ISS LIFE” (Program RF-FuW, TP 475) and Traffic (RoSto & VMo4Orte). Y-T. L. is participant of German Aerospace Center: interdisciplinary PhD graduate school GANDALF (“fighting current and future pandemic threats”). These results will be included in the PhD theses of Yen-Tran Ly.

5. References

Afshinnekoo, E., Meydan, C., Chowdhury, S., Jaroudi, D., Boyer, C., Bernstein, N., Maritz, J. M., Reeves, D., Gandara, J., Chhangawala, S., Ahsanuddin, S., Simmons, A., Nessel, T., Sundaresh, B., Pereira, E., Jorgensen, E., Kolokotronis, S. O., Kirchberger, N., Garcia, I., Gandara, D., Dhanraj, S., Nawrin, T., Saletore, Y., Alexander, N., Vijay, P., Henaff, E. M., Zumbo, P., Walsh, M., O'mullan, G. D., Tighe, S., Dudley, J. T., Dunaif, A., Ennis, S., O'halloran, E., Magalhaes, T. R., Boone, B., Jones, A. L., Muth, T. R., Paolantonio, K. S., Alter, E., Schadt, E. E., Garbarino, J., Prill, R. J., Carlton, J. M., Levy, S. & Mason, C. E. 2015. Geospatial Resolution of Human and Bacterial Diversity with City-Scale Metagenomics. Cell Syst, 1, 72-87.

Chen, H.-H., Li, W.-J., Tang, S.-K., Kroppenstedt, R. M., Stackebrandt, E., Xu, L.-H. & Jiang, C.-L. 2004. *Corynebacterium halotolerans* sp. nov., isolated from saline soil in the west of China. International journal of systematic and evolutionary microbiology, 54, 779-782.

Dean, C., Ormerod, M., Serianni, R. & Alexander, P. 1969. DNA strand breakage in cells irradiated with X-rays. Nature, 222, 1042-1044.

Fernández-Iriarte, A., Duchaine, C., Degois, J., Mbareche, H., Veillette, M., Moreno, N., Amato, F., Querol, X. & Moreno, T. 2021. Bioaerosols in public and tourist buses. Aerobiologia, 37**,** 525-541.

Gohli, J., Boifot, K. O., Moen, L. V., Pastuszek, P., Skogan, G., Udekwu, K. I. & Dybwad, M. 2019. The subway microbiome: seasonal dynamics and direct comparison of air and surface bacterial communities. Microbiome, 7, 160.

Hernández, A. M., Vargas-Robles, D., Alcaraz, L. D. & Peimbert, M. 2019. Station and train surface microbiomes of Mexico City's metro. Scientific Reports, 10.

Huo, Y.-Y., Xu, X.-W., Liu, S.-P., Cui, H.-L., Li, X. & Wu, M. 2011. *Sphingomonas rubra* sp. nov., isolated from bioreactor wastewater. International journal of systematic and evolutionary microbiology, 61, 1028-1032.

Josephson, K., Gerba, C. & Pepper, I. 1993. Polymerase chain reaction detection of nonviable bacterial pathogens. Applied and Environmental Microbiology, 59, 3513-3515.

Kang, K., Ni, Y., Li, J., Imamovic, L., Sarkar, C., Kobler, M. D., Heshiki, Y., Zheng, T., Kumari, S. & Wong, J. C. Y. 2018. The environmental exposures and inner-and intercity traffic flows of the metro system may contribute to the skin microbiome and resistome. Cell Reports, 24, 1190-1202. e5.

Kloos, W. E. & Schleifer, K. H. 1975. Isolation and characterization of staphylococci from human skin II. Descriptions of four new species: *Staphylococcus warneri*, *Staphylococcus capitis*, *Staphylococcus hominis*, and *Staphylococcus simulans*. International Journal of Systematic and Evolutionary Microbiology, 25, 62-79.

Kohl, A. & Ly, Y.-T., Leuko, S., Schmeling, D., Wagner, C., Moeller, R. 2024. Evaluation of bioaerosol propagation through an air curtain. 17th Conference of the International Society of Indoor Air Quality & Climate, Indoor Air. Honolulu, Hawaii, 7-11.07.2024.

Kusano, K., Yamada, H., Niwa, M. & Yamasato, K. 1997. *Propionibacterium cyclohexanicum* sp. nov., a new acid-tolerant ω-cyclohexyl fatty acid-containing propionibacterium isolated from spoiled orange juice. International Journal of Systematic and Evolutionary Microbiology, 47, 825-831.

Lee, I., Chalita, M., Ha, S.-M., Na, S.-I., Yoon, S.-H. & Chun, J. 2017. ContEst16S: an algorithm that identifies contaminated prokaryotic genomes using 16S RNA gene sequences. International journal of systematic and evolutionary microbiology, 67, 2053-2057.

Leung, M. H., Wilkins, D., Li, E. K., Kong, F. K. & Lee, P. K. 2014. Indoor-air microbiome in an urban subway network: diversity and dynamics. Appl Environ Microbiol, 80, 6760-70.

Liu, M., Liu, J., Ren, J., Liu, L., Chen, R. & Li, Y. 2020. Bacterial community in commercial airliner cabins in China. International Journal of Environmental Health Research, 30, 284-295.

Niu, L., Lu, S., Hu, S., Jin, D., Lai, X., Yang, J., Chen, C., Wang, Y., Bai, X. & Lan, R. 2016. *Streptococcus halotolerans* sp. nov. isolated from the respiratory tract of Marmota himalayana in Qinghai-Tibet Plateau of China. International journal of systematic and evolutionary microbiology, 66, 4211-4217.

Potts, M. 1994. Desiccation tolerance of prokaryotes. Microbiological reviews, 58, 755-805.

Rahkila, R., Johansson, P., Säde, E. & Björkroth, J. 2011. Identification of enterococci from broiler products and a broiler processing plant and description of *Enterococcus viikkiensis* sp. nov. Applied and Environmental Microbiology, 77, 1196-1203.

Reddy, G. S., Matsumoto, G. I., Schumann, P., Stackebrandt, E. & Shivaji, S. 2004. Psychrophilic pseudomonads from Antarctica: *Pseudomonas antarctica* sp. nov., *Pseudomonas meridiana* sp. nov. and *Pseudomonas proteolytica* sp. nov. International journal of systematic and evolutionary microbiology, 54, 713-719.

Siems, K., Runzheimer, K., Rehm, A., Schwengers, O., Heidler Von Heilborn, D., Kaser, L., Arndt, F., Neidhöfer, C., Mengel, J. P. & Parcina, M. 2022. Phenotypic and genomic assessment of the potential threat of human spaceflight-relevant *Staphylococcus capitis* isolates under stress conditions. Frontiers in Microbiology, 13, 1007143.

Sobisch, L.-Y., Rogowski, K. M., Fuchs, J., Schmieder, W., Vaishampayan, A., Oles, P., Novikova, N. & Grohmann, E. 2019. Biofilm forming antibiotic resistant gram-positive pathogens isolated from surfaces on the international space station. Frontiers in microbiology, 10, 543.

Sun, Y., Fu, X., Li, Y., Yuan, Q., Ou, Z., Lindgren, T., Deng, Y. & Norbäck, D. 2020. Shotgun metagenomics of dust microbiome from flight deck and cabin in civil aviation aircraft. Indoor Air, 30, 1199-1212.

Van Trappen, S., Vandecandelaere, I., Mergaert, J. & Swings, J. 2004. *Flavobacterium degerlachei* sp. nov., *Flavobacterium frigoris* sp. nov. and *Flavobacterium micromati* sp. nov., novel psychrophilic bacteria isolated from microbial mats in Antarctic lakes. International journal of systematic and evolutionary microbiology, 54, 85-92.

Vanlaere, E., Baldwin, A., Gevers, D., Henry, D., De Brandt, E., Lipuma, J. J., Mahenthiralingam, E., Speert, D. P., Dowson, C. & Vandamme, P. 2009. Taxon K, a complex within the *Burkholderia cepacia* complex, comprises at least two novel species, *Burkholderia* contaminans sp. nov. and *Burkholderia lata* sp. nov. International journal of systematic and evolutionary microbiology, 59, 102-111.

Weiss, H., Hertzberg, V. S., Dupont, C., Espinoza, J. L., Levy, S., Nelson, K., Norris, S. & Team, F. R. 2019. The airplane cabin microbiome. Microbial ecology, 77, 87-95.

Zhao, B., Dewald, C., Hennig, M., Bossert, J., Bauer, M., Pletz, M. W. & Jandt, K. D. 2019. Microorganisms@ materials surfaces in aircraft: Potential risks for public health?–A systematic review. Travel medicine and infectious disease, 28, 6-14.

2.4 Comparative assessment of bioaerosol propagation through an air curtain using microbiological methods and particulate matter sensors

Title	**Comparative Assessment of Bioaerosol Propagation Through an Air Curtain Using Microbiological Methods and Particulate Matter Sensors**
Authors	**Yen-Tran Ly**[1], **Andreas Kohl**[2,3], Daniel Schmeling[2], Stefan Leuko[1] and Claus Wagner[2,3]
Affiliation	[1] Institute of Aerospace Medicine, German Aerospace Center, Cologne, Germany [2] Institute of Aerodynamics and Flow Technology, German Aerospace Center, Göttingen, Germany [3] Institute of Thermodynamics and Fluid Mechanics, Technische Universität Ilmenau, Ilmenau, Germany
Article type	Original research article
Authorship	Shared-first author
Journal	Indoor Air
Year	2025
Volume	2025
DOI	10.1155/ina/8825442
Author contributions	

Y-TL	Shared first authorship, Conceptualization, Methodology, Formal analysis, Investigation, Data curation, Visualization, Writing -original draft, Writing – review & editing
AK	Shared first authorship, Conceptualization, Methodology, Formal analysis, Data curation, Visualization, Writing -original draft, Writing – review & editing
DS	Writing - review & editing, Conceptualization
CW	Writing - review & editing
SL	Writing - review & editing

Wiley
Indoor Air
Volume 2025, Article ID 8825442, 21 pages
https://doi.org/10.1155/ina/8825442

WILEY

Research Article

Comparative Assessment of Bioaerosol Propagation Through an Air Curtain Using Microbiological Methods and Particulate Matter Sensors

Yen-Tran Ly[1], **Andreas Kohl**[2,3], **Daniel Schmeling**[2], **Stefan Leuko**[1], **and Claus Wagner**[2,3]

[1]*Institute of Aerospace Medicine, German Aerospace Center (DLR), Cologne, Germany*
[2]*Institute of Aerodynamics and Flow Technology, German Aerospace Center (DLR), Göttingen, Germany*
[3]*Institute of Thermodynamics and Fluid Mechanics, Technische Universität Ilmenau, Ilmenau, Germany*

Correspondence should be addressed to Yen-Tran Ly; yen-tran.ly@dlr.de and Andreas Kohl; andreas.kohl@dlr.de

Received 6 February 2025; Accepted 29 May 2025

Academic Editor: Poulami Jha

An important route of transmission for potentially harmful bacteria is the spread of bioaerosols in indoor environments. In a chamber specially developed for particle dispersion tests, we created a defined bioaerosol to study the performance of two methods commonly used in biology and engineering studies: airborne bacterial detection and particulate matter (PM) analysis. A total of five ventilation cases were investigated in which an air curtain, operated at Reynolds numbers $Re < 11,000$, shielded the particles in one half of the test chamber from the other half. In two of these five cases, a HEPA filter was also installed to specifically reduce the particle concentration in the test chamber. In addition to active and passive air sampling measurements of bacteria, we took PM measurements in front of, beneath, and behind the air curtain under constant air temperature and relative humidity conditions. The bioaerosol contained nine bacterial species, evenly distributed in artificial saliva. Two species in the bioaerosol, *Staphylococcus capitis* DSM 111179 and *Burkholderia lata* DSM 23089^T, were selected for evaluation due to their antibiotic resistance, which makes them distinguishable from other species. The results show a similar trend in the concentrations of the detected particles and bacteria. The survival rates of the evaluated bacterial species differed; *S. capitis* exhibited a greater agreement with the PM measurements than *B. lata* did, which emphasizes the importance of using a various model organism in such experimental setups. We evaluated the effectiveness of the air curtain in reducing particle and bacterial spread, with values reaching up to 66% for both measurement approaches. This study highlights the key differences between the two detection methods and confirms the reproducibility and suitability of the standardized bioaerosol for future research applications. Both methods have demonstrated their potential for use in more realistic scenarios.

1. Introduction

Microbial spread is natural when people travel or reside indoors because microorganisms, especially bacteria, colonize the human body [1, 2]. These microorganisms can be transferred via surfaces [3, 4] as well as through the air [5]. The potential for microbial transmission is a significant issue when opportunistic or pathogenic agents cause infections. Therefore, it is essential to investigate a range of countermeasures for reducing microbes, particularly in indoor environments such as the passenger compartments of public transportation vehicles [6, 7], where there is a high potential for pathogen transmission due to long-duration and short-distance contact between passengers. Several studies have examined the air quality in the passenger compartments of underground trains and aircraft cabins [8, 9]. Using sequence-based methods, microorganisms in these environments were detected and identified. The detected organisms included common representatives of skin-

associated bacteria, such as the genera *Corynebacterium*, *Burkholderia*, *Staphylococcus*, and *Propionibacterium*. It should be noted that these environments can harbor opportunistic human pathogens, which could lead to infections in immunocompromised individuals. Their presence on public transportation has already been demonstrated. These include multidrug-resistant bacterial pathogens [10–13].

Implementing a multifaceted approach that integrates surface and air cleaning with other active measures can play a crucial role in enhancing microbial safety in the passenger cabin. Additionally, ventilation systems can prevent the spread of airborne microbes [14, 15]. Reducing the dispersion of bioaerosol and the spread of infectious diseases must be considered a key parameter for future ventilation concepts, in addition to reducing energy consumption and thus operating costs. For this reason, we apply a defined bioaerosol to a ventilation concept in a defined experimental environment and compare the bacterial and particle dispersion. Additionally, we evaluate the effectiveness of the chosen air curtain ventilation concept in preventing the spread of airborne bioaerosols. The goal is to apply it to more realistic configurations such as passenger cabins at a later stage. Air curtains are already used in various indoor settings, including shopping malls and hospitals, and have been studied for many years [16]. Recent studies have employed experimental and computational approaches to gain insight into their application against aerosol spread [17, 18].

One recent study [5] demonstrated that the air quality around an orchestra can deteriorate during performances. The authors suggest that assessing bioaerosols may be an appropriate method for modeling exposure to potentially infectious particles from the upper respiratory tract. Unlike the previous study [5], which assessed bacteria sampled from the exhaled air of the musicians, this study uses a newly developed, standardized bioaerosol [19] with a defined, known initial bacterial concentration. The propagation of this bioaerosol is then studied in an experimental chamber. This bioaerosol is based on genera commonly found in public transportation and contains nine bacterial species. This allows us to focus our investigation on this particular environment, which is prone to microbial spread and is therefore relevant to our research. To the best of our knowledge, the controlled distribution of a defined bioaerosol that mimics a specific microbiome, as in this study, has not been conducted before. We will compare the results to particle concentration measurements, a well-known method of evaluating the effectiveness of ventilation concepts [20].

There are a variety of methodologies for evaluating bioaerosol spread. In addition to simulating particle dispersion, analyzing particulate matter (PM) is a reliable method for precise measurement. Various devices are available for measuring PM, ranging from rather expensive, high-resolution detectors to low-cost sensors with lower resolution and precision. Besides measuring PM, culture-based methods can be used to evaluate the spread of bioaerosols and, importantly, the survival of pathogens through air travel. Several studies have been conducted on bioaerosol collection using either passive or active air sampling [21, 22]. Passive air sampling uses Petri dishes containing culture media that allow bacteria to colonize and be cultured for subsequent survival analysis. Active sampling uses air samplers, which are available in a variety of types. The most common air samplers draw air directly onto agar plates using the principle of particle impingement (e.g., MAS-100 Eco, MBV), while others sample the air into a liquid solution (e.g., Coriolis Micro, Bertin Technologies). The advantage of the latter is that the sample can easily be cultured and further analyzed (e.g., by extracting DNA for additional purposes). Selective culture media with antibiotics can be used to analyze specific organisms, while complete media are used to cultivate a broad spectrum of organisms, such as bacteria.

In this study, we use the most common genera from a recent study on public transportation to simulate the public transportation microbiome [19]. This specific simulated microbiome is used as a reference for investigating both time-resolved, sensor-based PM measurements and time-integrated bacterial survival analysis. Our goal is to gain a deeper understanding of how particles and viable bacterial cells propagate through the chamber and the air curtain flow field and to identify the environmental and fluid dynamic properties that affect the two measurement methods. To this end, we create five distinct ventilation cases for air curtain Reynolds numbers $\mathrm{Re} < 11,000$. Two of the five cases include additional HEPA filters to reduce the overall particle concentration and increase the air curtain's effectiveness.

In our study, we focused on three key aspects: (A) the introduction of the defined bioaerosol to serve as a reference for studies on the spread of pathogens in indoor environments, (B) measuring viable bacteria and aerosol particles in a range of $D_p = 0.3$–$4\,\mu$m and comparing them for five different ventilation cases, and (C) evaluating the performance of the two measurement techniques.

2. Materials and Methods

2.1. Experimental Setup. The measurements were performed in a chamber specifically designed for this experiment. The chamber's dimensions are 2 m long, 1 m high, and 1 m wide, as shown in Figure 1. An air curtain was installed at the entrance to a second smaller room R2 at a height of $H =$ 68 cm inside the chamber. Thus, the chamber consisted of two subrooms: one to the left of the air curtain (denoted R1 in Figure 1) and one to the right (denoted R2). A bioaerosol generator with an outlet height of 36.5 cm was placed at the bottom left of the chamber (R1) and emitted aerosols toward the air curtain. High air exchange rates (ACR) of around $300\,\mathrm{h}^{-1}$ were achieved with the maximum volume flow of the air curtain and HEPA filters.

Bacterial samples were collected from four different locations. Active bioaerosol sampling (referred to as sampling location AS) was conducted at one location in R2 using active air sampling on an agar plate with the MAS-100 Eco (MBV) (see Figure 1). Three positions were selected for passive bacterial sampling in the air curtain impingement zone (where the air curtain flow meets the opposing surface and splits into positive and negative x-directions as indicated in Figure 1). The Petri dish (P1) was placed on the left side of the air curtain ($x = +20$ cm) in the subroom R1. It was closer to the aerosol generator than the other Petri dishes. Thus,

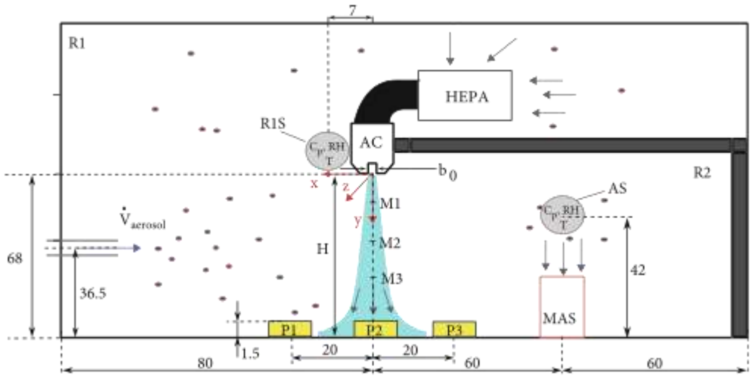

(a)

(b)

Figure 1: (a) 2D sketch of the experimental setup inside the chamber in the center plane ($z = 0$). On the left side of the air curtain (AC) in room R1, the bioaerosol generator, the measurement position (R1S) for aerosol monitoring (C_p, RH, T), the first position for passive sampling on Petri dish (P1), and the HEPA filters are shown. Below the air curtain ($x = 0$) are the locations of the anemometer measurements (M1, M2, and M3) and the second passive sampling position (P2). To the right of the air curtain, in the room (R2), is the third passive sampling position (P3) and the active aerosol sampling position (AS), which is above the mobile aerosol sampler (MAS). Distances are shown in centimeters. (b) A picture of the experimental setup showing the measurement chamber with the aerosol generator, Petri dishes (P1–P3), the air curtain, and the MAS.

the highest bioaerosol concentration was expected at P1. A second Petri dish (P2) was placed directly below the air curtain nozzle ($x = 0$ cm), and a third dish was placed to the right of the air curtain (P3) ($x = -20$ cm) in R2. The Petri dishes had a diameter of 10 cm. A total of six PM sensors were installed in R1 and R2. Two PM sensors were placed to the left of the air curtain at position ($x = +7$ cm, $y = 0$ cm) (denoted as R1S in Figure 1a). These sensors were positioned symmetrically in the z-direction ($z = \pm 17$ cm), as shown in Figure 1b. One sensor was placed to the right of the air curtain (AS), near the inlet of the MAS, and three additional PM sensors were placed 1 cm above the agar plates at positions P1, P2, and P3. Temperature and humidity were also measured at positions R1S and AS.

2.2. Test Organisms, Growth Conditions, and Production of the Simulated Microbiome. The organisms within the used bioaerosol are listed in Table 1 and were grown, as described in [19] using a total of three types of culture media: 2xReasoner's 2A broth (TEKnova), tryptic soy broth (Sigma-Aldrich), and brain heart infusion broth (Sigma-Aldrich). Media compositions are listed in Tables S1–S3. The strains *Burkholderia lata* DSM 23089^T, *Enterococcus viikkiensis* DSM 24043^T, *Propionibacterium cyclohexanicum* DSM 16859^T, *Pseudomonas antarctica* DSM 15318^T, and *Staphylococcus capitis* DSM 111179 were grown for 18 h under constant shaking at 200 rpm, while the strains *Corynebacterium halotolerans* DSM 44683^T, *Flavobacterium frigoris* DSM 15719^T, *Sphingomonas rubra* DSM 26135^T, and

TABLE 1: List of bacterial strains in the standardized bioaerosol with growth conditions and reference. For the cultivation of the bacteria, media broth or agar was used.

Strain	Growth	Reference
Burkholderia lata DSM 23089^T	2xReasoner's 2A (2xR2A) 37°C	[23]
Corynebacterium halotolerans DSM 44683^T	Tryptic soy broth (TSB) or agar (TSA) 37°C	[24]
Enterococcus viikkiensis DSM 24043^T	Brain heart infusion (BHI) 37°C	[25]
Flavobacterium frigoris DSM 15719^T	2xReasoner's 2A (2xR2A) 20°C	[26]
Propionibacterium cyclohexanicum DSM 16859^T	Brain heart infusion (BHI) 37°C	[27]
Pseudomonas antarctica DSM 15318^T	Tryptic soy broth (TSB) or agar (TSA) 20°C	[28]
Sphingomonas rubra DSM 26135^T	2xReasoner's 2A (2xR2A) 20°C	[29]
Staphylococcus capitis DSM 111179	2xReasoner's 2A (2xR2A) 37°C	[30]
Streptococcus halotolerans DSM 101996^T	Brain heart infusion (BHI) 37°C	[31]

Streptococcus halotolerans DSM 101996^T were grown for 48 h at 200 rpm. The composition of the bacterial strains and respective growth conditions used in this study are listed in Table 1.

Each culture (50 mL) was centrifuged at 323 g for 10 min. The supernatant was then discarded, after which the cell pellet was resuspended in 50 mL phosphate-buffered saline (PBS; Na_2HPO_4 7.0 g, KH_2PO_4 3.0 g, NaCl 4.0 g/L, pH 7.5). This step was repeated once. Then, the cell pellet was resuspended in 5–20 mL of PBS, depending on the cell density. For *B. lata* and *S. capitis*, the cell concentration used was ~10^8 CFU/mL, as determined by OD_{600nm} measurement and standard plate count on 2xR2A agar. The other seven strains (see Table 1) were mixed to an equal total concentration of 10^8 cells/mL, which was also confirmed by plate counting on 2xR2A, TSA, and BHI agar. All cell suspensions were equally mixed in artificial saliva, which is based on the work of Woo et al. [32] and described in Table 2.

Bacteria can be classified as either Gram-positive or Gram-negative. This classification offers insight into cell wall and membrane structure. It also influences factors such as antibiotic susceptibility and the ability to withstand stressors like desiccation. To reduce the spread of bacteria and understand the effectiveness of microbial countermeasures, it is essential to test a diverse range of species to obtain comprehensive results.

The bacterial species used in this study varied in size and shape. They ranged from approximately $D_p = 0.5$ to 5.0 μm. *S. capitis* displayed the smallest cells and *P. antarctica* displayed the largest cells (Figure 2). The shapes of the bacterial cells ranged from coccoid to rod-shaped to pleomorphic structures, either as single cells or in the form of diplococci, streptococci, or staphylococci. To determine the bacterial survival, we focused on two of the nine species. The selected bacteria, *B. lata* and *S. capitis*, harbor antibiotic resistance. *B. lata* is resistant to streptomycin, while the *S. capitis* strain used is resistant to rifampicin. This key feature enables clear separation from other airborne bacteria in the bioaerosol or from other sources of pollution during survival assays. Other distinguishing features of these two species are their size and shape (see Figure 2) and their Gram stain (see Table 3).

2.3. Bioaerosol Generation, Sampling, and Survival

2.3.1. Aerosol Generation. The aerosol was generated using a "Blaustein Atomizer" (BLAM, CH Technologies), connected to a control unit (CHƐST, CH Technologies). This setup was used in combination with a syringe pump and a 50 mL syringe containing the bacterial solution. Continuous aerosolization was achieved with an air pressure of 1.24 bar (18 psi). The BLAM nebulized the bacterial solution via four collision nebulization jets in MPA (multipass atomization) mode at a flow rate of 0.5 mL/min. Similar settings were used in the study by Danelli et al. [33], in which the nebulization efficiency for *Escherichia coli* ATCC 25922 was tested, achieving nebulization efficiencies approximately two to four times higher than other nebulizers. According to the manufacturer, the BLAM's output particle diameter is generally between $D_p = 0.001$ and 10 μm. Massabò et al. [34] found that the mean size distribution of the generated particles is 0.45 μm (STD of 0.25 μm). For each ventilation configuration, the bioaerosol was nebulized for 10 min while the air sampler and PM sensors were operated. Before starting a new measurement, the particle concentration C_p ($D_p = 0.3$–10 μm) in the test chamber had to fall below a threshold of $C_p < 20\,cm^{-3}$.

TABLE 2: Composition of artificial saliva based on Woo et al. [32] with modifications. Artificial saliva was adjusted to a final volume of 1 L with dH_2O and sterilized at 121°C for 20 min.

Amount	Chemical component
1.00 mL	Dulbecco's modified Eagle's medium (PAN-Biotech)
0.88 g	NaCl
0.42 g	$NaHCO_3$
0.04 g	$MgCl_2 * 6H_2O$
3.00 g	Mucin

2.3.2. Aerosol Sampling. The MAS-100 Eco was used for active sampling at position AS (see Figure 1). The device collects 100 L of aerosol per minute onto an agar plate. The collected bacteria can be retrieved from the plate afterwards. Thus, a total of 1000 L were sampled during the 10-min measurement intervals. Preliminary measurements were conducted to ensure sufficient bacteria were sampled [35]. The collection efficiency of impaction-based bioaerosol samplers, such as the MAS-100, is defined by the cutoff diameter

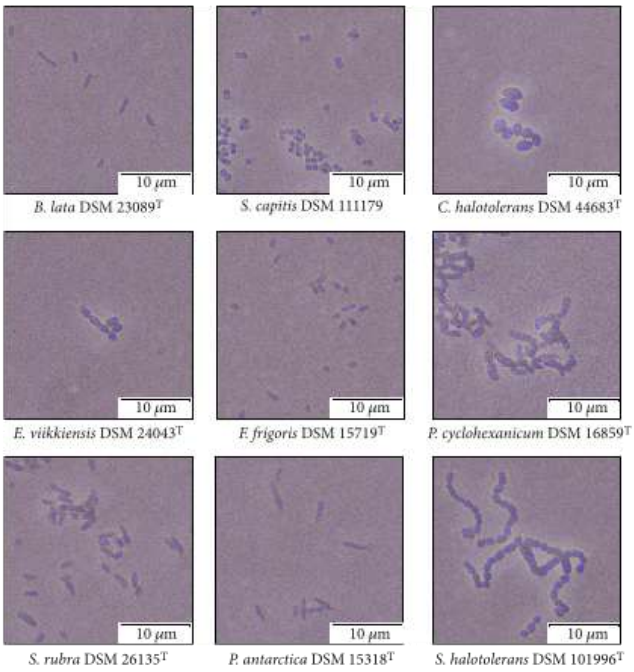

FIGURE 2: Light microscopy pictures of the bacterial species of the reference bioaerosol (100x magnification, Olympus CX43).

TABLE 3: Key characteristics of the cultivated bacterial species *S. capitis* and *B. lata*.

Characteristic	*S. capitis*	*B. lata*
Length/size	0.5–1.2 μm	2.0–2.5 μm
Morphology	Coccoid	Rod-shaped
Antibiotic resistance	Rifampicin	Streptomycin
Gram-stain	Positive	Negative

D_{50}. According to the manufacturer of the MAS, the cutoff diameter is $D_{50} = 1.6\,\mu$m. This means that 50% of the particles with a diameter of 1.6 μm will adhere to the agar plate. Particles with a diameter greater than D_{50}, and therefore greater inertia, are more likely to impact on the agar plates, resulting in a higher collection efficiency. Since *S. capitis* ranges in size from 0.5 to 1.2 μm and *B. lata* ranges from 2.0 to 2.5 μm, it is reasonable to hypothesize that higher concentrations of *B. lata* will be measured at the air sampler position. This assumes that the larger cells of *B. lata* have a higher mass or form larger particles during nebulization than the smaller cells of *S. capitis*.

In passive sampling, particles that result from settling or adhesive forces attach to the agar in the Petri dishes. It is a common technique used in numerous studies [21, 36] and has been known for a long time [37]. However, the quantity of sampled aerosol is usually unknown, which can lead to discrepancies between the different sampling methods. Passive sampling was used at positions P1, P2, and P3 in the impingement zone of the air curtain, where the air curtain flow reaches the bottom of the test chamber (see Figure 1). These positions were selected since Petri dishes are less disruptive to the air curtain flow in the impingement zone than the MAS, and the air curtain's aerodynamic sealing remains undisturbed.

2.3.3. Determination of the Bacterial Survival. To analyze the dispersion of bioaerosols, the previously described bacterial community (see Table 1) was nebulized within the chamber and collected on the agar plates via passive and active sampling. The survival of the key species, which are resistant to antibiotics (see Table 3) on the agar plates, was evaluated exclusively. After each measurement, the agar plates (agar 15 g/L) used for active sampling were retrieved from the chamber, and 1.2 mL of PBS was distributed onto each Petri dish. The cell solution collected from the agar plate was used for survival analysis. To determine the bacterial survival in a cell suspension of *B. lata*, a 10-fold dilution series from 10^{-1} to 10^{-8} was prepared and plated on 2xR2A agar containing 150 μg/mL streptomycin. To grow *S. capitis*, 2xR2A agar containing 5 μg/mL rifampicin was used. The media plates were incubated for 2 days at 37°C. The concentration of surviving bacteria (C_b) was determined by counting colony-

forming units (CFU). Prior to aerosolization, the bacterial community solution was also subjected to CFU per milliliter determination. The concentrations were found to be 7×10^7 CFU/mL for *B. lata* and 1.7×10^8 CFU/mL for *S. capitis*.

2.4. Measurement of the Aerosol Properties. Temperature and relative humidity were measured because they affect water evaporation and, consequently, the final particle size of the aerosol. These parameters also affect the survival of microorganisms and the transmission of infectious diseases, like influenza [38]. SHT85 sensors (Sensirion) were used to measure the temperature and relative humidity in the chamber with respective accuracies of ±0.1°C and ±1.5% RH. The chamber temperature remained nearly constant at 14.7°C (±0.8°C) throughout the measurements. The temperature difference between in front of (R1) and behind the air curtain (R2) was small during each measurement with $\Delta T_{1,2} < 0.4$ K. We measured an average humidity of 63.4% RH (±5.4% RH) for all scenarios. During a single measurement, the humidity increased by approximately 5% RH due to the evaporation of the water within the aerosol particles. The minimum and maximum temperatures in the test chamber were 13.4°C and 15.9°C, respectively, and were directly influenced by the ambient laboratory temperatures.

Additionally, SPS30 PM sensors (Sensirion) were used to monitor the particle concentrations C_p (1/cm^3) for particles with diameters in the size range of $D_p = 0.3$–$10\,\mu$m. These optical sensors measure the scattered light from particles illuminated by a laser diode inside the sensor. According to the signal of the photo diode, each particle is sorted into a specific particle size interval (bin). In our study, we evaluated the following particle size intervals: $D_p = 0.3$–1.0, $D_p = 1.0$–2.5, $D_p = 0.3$–2.5, and $D_p = 2.5$–$4.0\,\mu$m. These intervals cover the sizes of the studied bacterial species *B. lata* and *S. capitis* (see Figure 2) and also the majority (> 99%) of the particles that were generated by the BLAM. The PM sensors provide a number concentration precision for the particle sizes $D_p = 0.3$–$2.5\,\mu$m (PM2.5) of ±100 cm^{-3} for concentrations $C_p <$ 1000 cm^{-3} and ±10% of the measured value (*m.v.*) for concentrations $1000 < C_p < 3000$ cm^{-3}. For $D_p = 2.5$–$4.0\,\mu$m (PM4), the accuracy is lower, with a maximum uncertainty of ±25% *m.v.* It has also been shown [39] that these sensors can be used for PM2.5 at higher concentrations of $3000 < C_p < 20{,}000$ cm^{-3} with deviations from a reference particle sizer (OPS3300, TSI) of less than ±10% *m.v.* We did not observe particle concentrations greater than 18,000 cm^{-3} in our measurements. All sensors were connected to an open-source data acquisition system, and the PM data were recorded at approximately 1 Hz. Data acquisition was facilitated by the use of a mobile measurement system (MMS) developed at the German Aerospace Center (DLR). The MMS is completely open source [40] and includes various sensors that provide mobile, versatile measurement of different indoor air parameters [41].

2.5. Air Curtain. The air curtain device used in our study is a commercial system (MINIBEL 900 E230, Rosenberg) that is typically installed in doorways. The airflow of the device is generated by six fans in a housing by drawing ambient air from one side and expelling it through a rectangular nozzle on the other side. The nozzle has a length of $L_0 = 900$ mm and a width $b_0 = 42$ mm. The air curtain was mounted above the entrance of R2 inside the experimental chamber to generate a planar, downward-facing air jet, as shown in Figure 1. We operated the air curtain in three different power configurations (AC_{off}, AC_{low}, and AC_{high}) by adjusting the current that drives the six fans to study the effect of the volume flow rate. Additionally, we took measurements with the air curtain equipped with H14 HEPA filters for the low and high fan power configurations, $AC_{low+HEPA}$ and $AC_{high+HEPA}$, respectively. This changes the flow dynamics in the experimental chamber by increasing the resistance of the airflow at the air curtain's inlet, resulting in five distinct ventilation configurations, as shown in Table 4. Using HEPA filters substantially lowers particle concentrations in the chamber, especially behind the air curtain, because approximately half of the (filtered) air curtain flow moves in the negative x -direction at the bottom of the chamber (see Figure 1a). Scenarios with HEPA filters introduce two additional flow configurations and extend the range of particle and bacterial concentrations to be compared. However, they must be evaluated separately from the scenarios without HEPA filters when determining the ventilation design's effectiveness. To characterize the resulting flow field, the air velocities were measured at six positions ($z = \pm 17$ cm; $y = +10$, $+30$, $+50$ cm) in the air curtain flow over a period of 30 s at a measurement frequency of 1 Hz using a handheld flow anemometer. The arithmetic means over the 30-s measurement period and along the z-axis are summarized as $\bar{U}_M$ (M1, M2, and M3) and are shown in the last three columns of Table 4. As expected, the obtained mean velocity $\bar{U}_M$ decreases with increasing distance y (M1→M3). Additionally, the mean velocities in the HEPA filter configurations, $AC_{low+HEPA}$ and $AC_{high+HEPA}$, respectively, are reduced compared to the configurations without HEPA filters (see Table 4). This is also evident in the reduction of the measured volume flow $\dot{V}_{ac}$ in Table 4. A common way to characterize an air curtain's flow field is with the deflection modulus which, according to Hayes and Stoecker [16], describes the behavior of the air curtain jet when opposed to a transverse pressure gradient due to buoyancy forces. However, since the differences of the temperatures in the subrooms $\Delta T_{1,2}$ are small (see Section 2.4), the contribution of the buoyancy force is negligible. Thus, we consider the Reynolds number of the air curtain Re_{ac} defined in Equation (1) and realized in this study as listed in Table 4 (Column 3). In Equation (1), $\bar{U}_0$ denotes the average outlet velocity at the nozzle, b_0 is the width of the nozzle, and ν the kinematic viscosity. Additionally, we determine the particle-related air curtain effectiveness E_p in Equation (2), as proposed by Kohl et al. [42].

$$\mathrm{Re}_{ac} = \frac{\bar{U}_0\, b_0}{\nu}. \tag{1}$$

TABLE 4: Information on flow properties of the air curtain for all configurations.

Air curtain configuration:	$\dot{V}_{ac}$ (m^3/h)	Re_{ac}	$\bar{U}_{M1}$ (m/s)	$\bar{U}_{M2}$ (m/s)	$\bar{U}_{M3}$ (m/s)
AC_{off}	0	0	—	—	—
$AC_{low+HEPA}$	244	4000	0.92	0.80	0.61
AC_{low}	344	5700	1.67	1.14	0.60
$AC_{high+HEPA}$	446	7450	2.40	1.52	1.03
AC_{high}	623	10,400	3.46	2.62	1.82

$$E_p = 1 - \frac{\bar{C}_{p,x<0}}{\bar{C}_{p,x>0}}. \quad (2)$$

$$E_b = 1 - \frac{C_{b,x<0}}{C_{b,x>0}}. \quad (3)$$

Similarly to E_p, we also determined the ratio of local bacterial survival, $C_b(x<0)$ to $C_b(x>0)$, as described in Equation (3) and Section 2.3.3. Thus, a higher E_p indicates better protection of the air curtain against the spread of aerosol particles, while a higher E_b indicates better protection against the spread of viable bacteria. In our experimental setup, we calculated E_p and E_b on positions P1 and P3, where the air curtain flow impinges on the floor. The results will be shown and discussed in Section 3.4.

2.6. Statistical Analyses. Regarding the triplicated, time-resolved PM measurements, the ensemble-averaged time series $\langle C_p \rangle(t)$ is shown in Figures 3, 4, and 5 together with the respective standard deviations σ. The measurement of aerosol properties (see Section 2.4) and bacterial survival (see Section 2.3.3) for the five ventilation configurations (see Table 4) was performed in triplicate ($n = 3$). Student's t-tests [43] were used to determine significant differences between the particle and bacteria data, as well as the decrease in particle and bacterial concentrations, respectively. If the variances of the two datasets were unequal, a Welch's t-test [44] was performed instead since Student's t-test assumes equal variance. If one of the datasets was not normally distributed, the Mann–Whitney U-test [45] was performed instead, as this test makes no assumptions about the distribution of the data. The Mann–Whitney U-test is a nonparametric test that does not rely on normal distribution. Significant differences were defined as $p \leq 0.05$ (*), very significant differences as $p \leq 0.01$ (**), and highly significant differences as $p \leq 0.001$ (***). These differences are shown in Figure 6 and subsequent figures. Significance tests were performed between AC_{off} and the scenarios with air curtain, as well as between the two datasets (particle measurements and bacterial survival) for the same ventilation configuration. All statistical analyses were performed using SigmaPlot 14.5 (Systat Software Inc.).

These time series were averaged over time to obtain the mean particle concentration $\overline{C_p}$ and the respective standard deviations, which are shown as bar plots in Figure 6 and subsequent figures.

3. Results and Discussion

The Results and Discussion section is organized as follows: In Section 3.1, we analyze the local particle concentrations $\langle C_p \rangle(t)$ for all ventilation configurations, as this is a common analysis for aerosol spread. Section 3.2 assesses the bacterial survival C_b of our bacterial test species, *B. lata* DSM 23089^T and *S. capitis* DSM 111179, to provide an overview of both the particle concentrations and the bacterial survival. In Section 3.3, the local bacterial survival rates, which are expected to behave similar to the time- and ensemble-averaged local particle concentrations, are analyzed for all air curtain configurations. Finally, in Section 3.4, we evaluate the performance of PM and bacterial survival analysis with and without HEPA filters of varying effectiveness of the air curtain in preventing the passage of particles.

3.1. Evaluation Method 1: Local Particle Concentrations. By measuring the local particle concentrations, we can determine the time-resolved particle dispersion inside our test chamber and quantify the effectiveness of the air curtain against the spreading of particles from the aerosol generator. Since the measured data contains few particles larger than 4 μm in diameter (which is consistent with the literature on the BLAM aerosol generator [35]), we will focus on the size range $D_p = 0.3$–$4.0\,\mu$m. Figure 3 shows the ensemble-averaged concentrations $\langle C_p \rangle(t)$ at positions R1S, AS, P1, P2, and P3 for the reference scenario AC_{off}. Figure 4 shows the results for the active air curtain but without HEPA filters. Figure 5 shows the results for the active air curtain with additional HEPA filters.

Figures 3a, 3b, and 3c are dedicated to particle concentrations for the reference scenario AC_{off}, with a deactivated air curtain ($Re = 0$), and for particle sizes: (a) $D_p = 0.3$–1.0, (b) $D_p = 1.0$–2.5, and (c) $D_p = 2.5$–$4.0\,\mu$m. With the air curtain switched off, there is no additional forced mixing of the air in the test chamber other than the induced airflow induced by the particle source. This results in local particle concentrations differing by a factor of two depending on the particle size and measurement location, as illustrated in Figures 3a, 3b, and 3c). Additionally, local particle concentrations fluctuate significantly over time due to the transport of the turbulent flow structures within the test chamber for the AC_{off} configuration. This is also indicated by the considerable differences in the results obtained in these three individual measurements, shown as dotted lines, indicating the standard deviation of the ensemble average at time t of the measurement. The increase of the particle concentrations

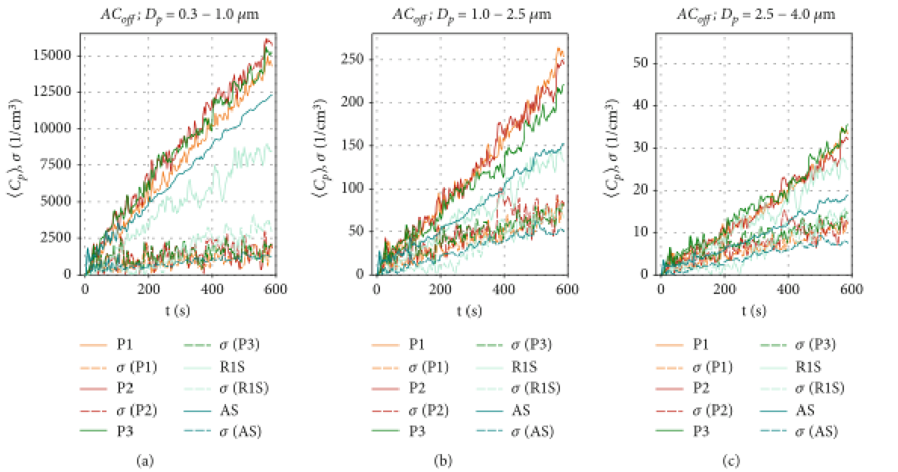

Figure 3: Measured particle concentrations $\langle C_p \rangle(t)$ for ventilation scenario AC_{off} for the particle sizes (a) $D_p = 0.3–1.0\,\mu m$, (b) $D_p = 1.0–2.5\,\mu m$, and (c) $D_p = 2.5–4.0\,\mu m$.

during the observed 600 s is nearly linear in Figure 3b,c. In contrast, a logarithmic increase is observed at R1S for the smaller particles ($D_p = 0.3–1.0\,\mu m$). Since the particle production rate is constant for all measurements due to the constant supply rate from the CHEST, differences in the time development of the particle concentration must result from differences in the settling, evaporation, or agglomeration of individual particles. The main reason for the different behavior of the smaller particles may be their higher sensitivity to turbulence-induced velocity fluctuations in the measurement chamber due to their lower mass and inertia. This could result in increased particle transport toward the chamber walls, where electrostatic or adhesive forces can trap them.

In comparison, Figures 4a, 4b, and 4c show the particle concentrations when the air curtain operates in the AC_{low} configuration. Since there are no HEPA filters installed in this ventilation scenario, particle removal occurs only through gravitational, adhesive, and electrostatic forces. The particle concentration behind the air curtain is significantly lower than in the AC_{off} configuration. The concentrations exhibit a logarithmic increase at all positions, reaching a maximum $\langle C_p \rangle$ between 9000 and 11,000 cm^{-3} for the smallest particles in Figure 4a. This is due to the induced air curtain airflow, which facilitates mixing and reduces an inhomogeneous particle distribution within the measurement chamber for all measured particle sizes, thereby reducing high local maximum particle concentrations. This is supported by the fluctuations of $\langle C_p \rangle(t)$ and also by the standard deviation σ of the ensemble-averaged measurements at all positions P_i, which are reduced compared to the AC_{off} configuration. Figure 4b shows that, for the size range of $D_p = 1.0$ - $2.5\,\mu m$, similar concentrations are measured at all positions ($\langle C_p \rangle(t = 600\,s) = 150$-$260\,cm^{-3}$) compared to the AC_{off} configuration. Only at position R1S, in front of the air curtain, we measure higher values $\langle C_p \rangle(t = 600\,s) \approx 250\,cm^{-3}$ compared to $\sim 150\,cm^{-3}$ in Figure 3b. We attribute this increase to the aerodynamic seal of the air curtain, which results in an increase in the particle-related air curtain effectiveness, E_p, as discussed further in Section 3.4. The lowest particle concentrations are measured at position P3 on the floor behind the air curtain. Figure 4c shows slightly increased particle concentrations for the size range of $D_p = 2.5$ $-4.0\,\mu m$ compared to the reference scenario AC_{off} in Figure 3c. The highest values are measured at R1S with $\langle C_p \rangle(t = 600\,s)$ $= 50\,cm^{-3}$, continuing the trend shown in Figure 4b. Concentrations for this particle size range decrease with distance from the aerosol generator, with only little difference between positions AS and P3 behind the air curtain.

Figures 4d, 4e, and 4f show the particle concentrations when the air curtain is activated at the highest volume flow rate in the configuration AC_{high}. Figure 4d shows that for the size range of $D_p = 0.3–1.0\,\mu m$, the concentrations $\langle C_p \rangle(t)$ are similar to those in Figure 4a. As in Figures 3a and 4a, the increase in particle concentration follows a logarithmic behavior. This behavior is even more pronounced at AC_{high} and is also observable for particles larger than $1.0\,\mu m$ in Figure 4e,f. These results can be attributed to an increased turbulence in the airflow, which increases the transport of particles toward the walls of the chamber, thereby increasing particle removal, as discussed above. The increased turbulence also enhances particles mixing in the chamber. Therefore, the fluctuations of $\langle C_p \rangle(t)$ and of σ are further reduced compared to AC_{low}. Figure 4f shows that for particle sizes of $D_p = 2.5–4.0\,\mu m$, there is only little difference in concentration at positions AS and P3, illustrating the effective mixing of larger particles

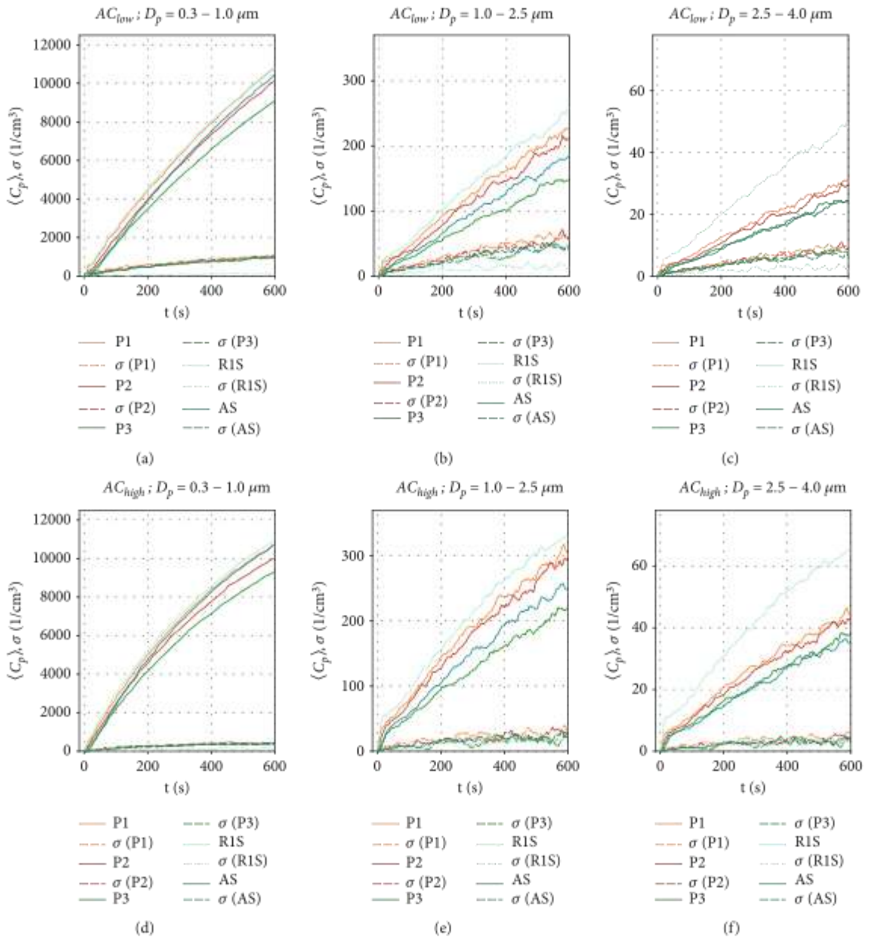

Figure 4: Measured particle concentrations $\langle C_p \rangle (t)$ for ventilation scenarios (a–c) AC_{low} and (d–f) AC_{high} for the particle sizes $D_p = 0.3$–$1.0\,\mu$m (left column), $D_p = 1.0$–$2.5\,\mu$m (middle column), and $D_p = 2.5$–$4.0\,\mu$m (right column).

behind the air curtain. In contrast to that finding, $\langle C_p \rangle (t = 600\,s)$ at R1S, which is in front of the air curtain, is almost twice as high as at positions AS and R3, which are behind the air curtain. This indicates that the air curtain is already effective against larger particles in this ventilation scenario. Additionally, we measure higher total particle concentrations at all positions for the larger particles ($D_p > 1\,\mu$m) than for AC_{off} and AC_{low}. We attribute this result to the induced airflow in the chamber, which prevents particles from settling in R1 and R2.

Figure 5 shows the aerosol particle concentration $\langle C_p \rangle (t)$ for the ventilation configurations with HEPA filters, which provide an additional source of particle removal in addition to the effects described earlier in this section. For the $AC_{low+HEPA}$ configuration in Figures 5a, 5b, and 5c, the particle removal is significantly enhanced, and a steady-state concentration is quickly reached ($t \leq 200\,s$) at all positions P_i, as the particle removal rate reaches equilibrium with the particle production rate in the chamber. The maximum concentrations are reached at position R1S for all particle sizes. As the distance from the BLAM increases, a clear reduction in particle concentrations is evident from in front of the air curtain (R1S), at the bottom (P1), directly under the nozzle (P2), and behind the air curtain (P3 and AS) for all analyzed particle sizes. Therefore, we can conclude that the air curtain significantly reduces the particle spread behind the air curtain ($x < 0$) in this HEPA filter scenario. Thus, an air curtain

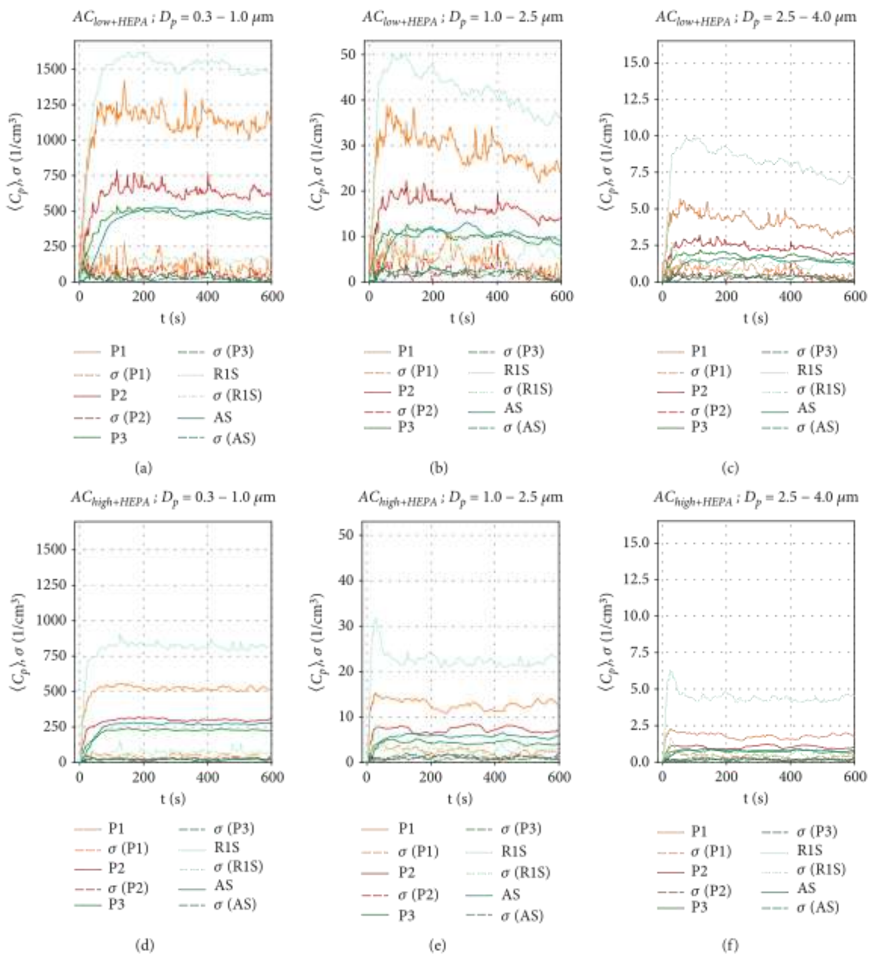

FIGURE 5: Particle concentrations $\langle C_p \rangle(t)$ for ventilation scenario (a–c) $AC_{low+HEPA}$ and (d–f) $AC_{high+HEPA}$ for particle sizes $D_p = 0.3$–$1.0\,\mu m$ (left column), $D_p = 1.0$–$2.5\,\mu m$ (middle column), and $D_p = 2.5$–$4.0\,\mu m$ (right column).

with HEPA filters could serve as an alternative retrofit for a passenger cabin if an additional fresh air supply is unavailable.

For $AC_{high+HEPA}$ in Figures 5d, 5e, and 5f, steady-state particle concentrations were reached even faster ($t \approx 120\,s$), as the particle removal rate has been further increased due to the higher flow rate and therefore higher filtration rates. $AC_{high+HEPA}$ also shows the lowest particle concentration fluctuation and also the lowest σ for all sensor positions, especially for P3 and AS behind the air curtain. As discussed earlier, this is due to the increased mixing, which is enhanced by the higher volume flow configuration compared to $AC_{low+HEPA}$. After particles in the size range of $D_p = 0.3$–$1.0\,\mu m$ reach their maximum concentration, they remain at a constant level, as shown in Figure 5d. The decrease in particle concentration of larger particles ($> 1.0\,\mu m$), shortly after the start of the measurement ($t \approx 30\,s$) in Figure 5e,f for the positions P1, P2, and R1S, requires further investigation, as no reasonable explanation has yet found. It appears that the larger particles exhibit a distinct behavior when HEPA filters are integrated into the air curtain. A more pronounced effect is observed at sensor positions located at $x \geq 0$, directly below and in front of the air curtain.

Figure 6 shows the average particle concentrations $\overline{C_p}$ during the entire 600-s measurement period for all ventilation configurations. To make further comparisons between the two datasets in the following sections, we will compare

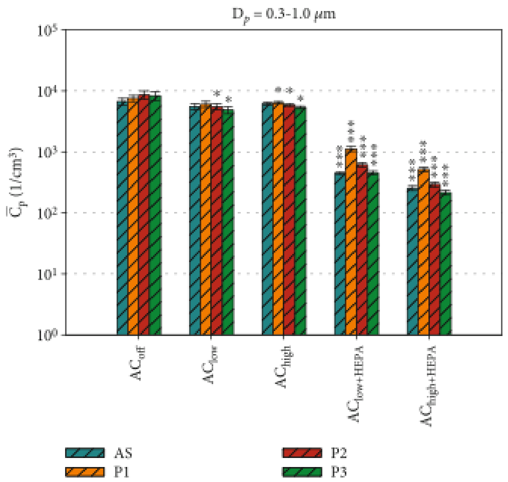

(a)

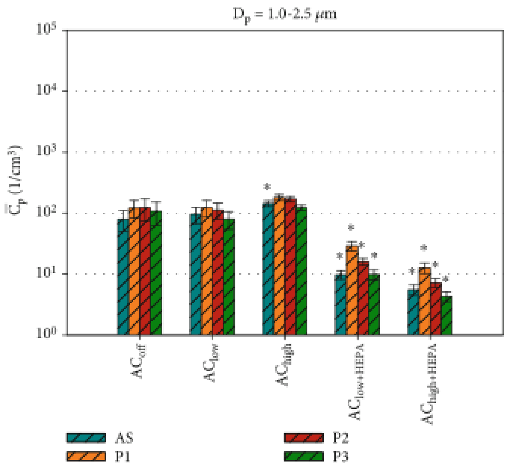

(b)

FIGURE 6: Temporal averaged particle concentrations $\overline{C_p}$ for each ventilation scenario for (a) $D_p = 0.3$–1.0 and (b) $D_p = 1.0$–$2.5\,\mu$m. Significance testing was performed with Student's t-test, comparing data to the control configuration AC$_{off}$. Note: $^{*}p \leq 0.05$, $^{**}p \leq 0.01$, and $^{***}p \leq 0.001$.

the average particle concentrations at positions P1, P2, P3, and AS, where bacterial survival data was collected. Figure 6 shows the average particle concentrations $\overline{C_p}$ for each position and ventilation configuration. These are compared via t-test to our reference configuration, AC$_{off}$. For the smaller particles ($D_p = 0.3$–$1.0\,\mu$m), which make up ~99% of all particles, a highly significant (***) reduction of approximately one log count is found for all ventilation configurations, including HEPA filters at all measurement positions (see Figure 6a). For the AC$_{low}$ and AC$_{high}$ configurations, the local measurements at P2 and P3 show a significant (*) reduction in $\overline{C_p}$. For particle concentrations in the range of $D_p = 1.0$–$2.5\,\mu$m (Figure 6b), significant reductions are only observed for AC$_{low+HEPA}$ and AC$_{high+HEPA}$. A significant increase in particle concentration at AS is found for the AC$_{high}$ configuration in Figure 6b as well as for P1, P2, and P3 for $D_p = 2.5$–$4.0\,\mu$m (see Figure S1). These results demonstrate a significant increase in particles in the size

range of $D_p = 1.0–4.0\,\mu$m for the configurations with an active air curtain but without HEPA filters. This is most likely due to the induced airflow in the chamber, which prevents particles from settling.

This section provided an overview of the dynamic particle behavior in the experimental chamber based on local PM measurements during five distinct ventilation scenarios. Increasing the air curtain volume flow $\dot{V}_{ac}$ ($\propto Re_{ac}$) resulted in an increased air curtain velocity with enhanced particle mixing in the measurement chamber. Without HEPA filters, the air curtain was more effective in reducing the dispersal of larger particles (> 1 μm) than smaller particles (< 1 μm). Scenarios with HEPA filters demonstrated a highly significant reduction in particles, particularly behind the air curtain, due to the additional filtration process.

3.2. Evaluation Method 2: Local Bacterial Survival. The survival of the two key bacterial species selected for this study, *B. lata* and *S. capitis*, represents the second assessment method for measuring the spread of potentially harmful bioaerosols, in addition to PM measurements. In the absence of time-resolved data, the local bacterial survival assessment provides specific insights into the effects of how environmental conditions, such as temperature and humidity, affect bacteria. These conditions were kept constant throughout the study. Figure 7 shows the local bacterial survival C_b at sampling position P_i with the associated standard deviations for all ventilation configurations that were investigated in this study. These were measured in triplicate. As was done for the data in Figure 6, *t*-tests were conducted for C_b at all sampling positions, comparing the data at each position P_i with the control configuration AC_{off}. It should be noted that the initial concentration of *B. lata* within the bacterial community was 7×10^7 CFU/mL, while the concentration of *S. capitis* was 1.7×10^8 CFU/mL. This was due to the limited precision possible in the bioaerosol production process. Regarding the overall bacterial survival achieved, the morphologically smaller species, *S. capitis* exhibits concentrations approximately 10 times higher than those of *B. lata* at all measurement positions in Figure 7. The highest viable cell concentration of *S. capitis* is collected by the MAS across all configurations. This outcome is expected, given the increased particle collection efficiency on the agar plate resulting from active sampling at a flow rate of 100 L/min. Since the air sampler's cutoff diameter (D_{50}) is 1.6 μm, particles smaller than 1.6 μm are collected with lower efficiency, while particles larger than 1.6 μm are collected with higher efficiency. Given the size range of $D_p = 0.5–1.2\,\mu$m for *S. capitis* and $D_p = 2.0–2.5\,\mu$m for *B. lata*, one might expect higher concentrations of *B. lata* to be collected by the MAS compared to *S. capitis*. However, this is not the case. In fact, the concentrations of *S. capitis* are consistently higher than those of *B. lata* across all sampling positions. Although the measured bacterial survival of *B. lata* is lower than that of *S. capitis*, some of these cells may still be metabolically active, as they can adapt to stress by reducing their reproduction rate as a survival strategy [46].

Figure 7a shows a gradual increase in *S. capitis* with increasing distance (P1→P3) for the AC_{off} and air curtain configurations without HEPA filters. This suggests that the air curtain has no measurable impact on the bacterial spread. Adding HEPA filters to the air curtain creates a distinct ventilation scenario, with a highly significant (***) reduction in particles (as shown in Figure 6) and in bacterial survival at position P2, which is directly below the air curtain nozzle. Furthermore, a notable reduction of approximately one log scale is evident at all positions P_i. However, the *t*-test does not consider the reduction to be significant at positions AS and P3 because the standard deviations in the reference configuration AC_{off} are high. For the $AC_{high+HEPA}$ configuration, the highest bacterial survival is observed at P1 (in front of the air curtain), and the lowest is observed at P3 (behind the air curtain). This is consistent with the measured particle concentrations $\overline{C_p}$ in Figure 6.

Figure 7b shows the survival of *B. lata*. The highest concentrations are measured by the MAS behind the air curtain at position AS ($C_b < 10^5$ CFU/mL), while the concentrations at P1, P2, and P3 are below 10^4 CFU/mL. For the AC_{high} ventilation scenario, a clear trend is evident at position P3, where the decrease of C_b is significant (*). For the AC_{low} ventilation scenario, the decrease is very significant (**).

For the configurations with HEPA filters, a very significant reduction is observed for AS, as well as for P1 and P3, with the $AC_{low+HEPA}$ configuration. It is noteworthy that the standard deviations for *B. lata* are increased for $AC_{high+HEPA}$ at P2 and P3. This is hypothesized to be due to the low total bacterial concentration of *B. lata* ($C_b < 400$ CFU/mL), resulting from increased particle removal, as discussed in the previous section. This emphasizes the importance of adapting the initial cell count in the bioaerosol to the ventilation configuration.

The most reasonable explanation for our findings is the correlation between the bacterial size and shape and the particle size distribution of the aerosol generator [34]. *S. capitis* has coccoid cells that are smaller in size, while *B. lata* has slightly larger rod-shaped cells (see Figure 2). It is reasonable to assume that *B. lata* is more susceptible to external forces acting on its cell walls during aerosol generation or sampling. This would ultimately result in a reduced survival rate compared to *S. capitis*. Another possible explanation lies in the characteristics of the cell walls of both species. *S. capitis* is Gram-positive, while *B. lata* is Gram-negative, resulting in different cell wall properties of both species. Gram-positive bacteria are generally more resistant to desiccation than Gram-negative bacteria [47, 48], but further research is necessary to quantify the influence of these parameters.

The survival of the two species differed significantly between the two air sampling methods. This finding is consistent with the fact that passive and active sampling impact microorganisms in distinct ways [49]. For passive air sampling, survival can differ depending on cell size and shape [50]. Mainelis observed that the selection of an air sampler and the selection of the bacteria to be tested both significantly influence survival [51]. We aimed to increase comparability for further studies on airborne bacterial dispersal by

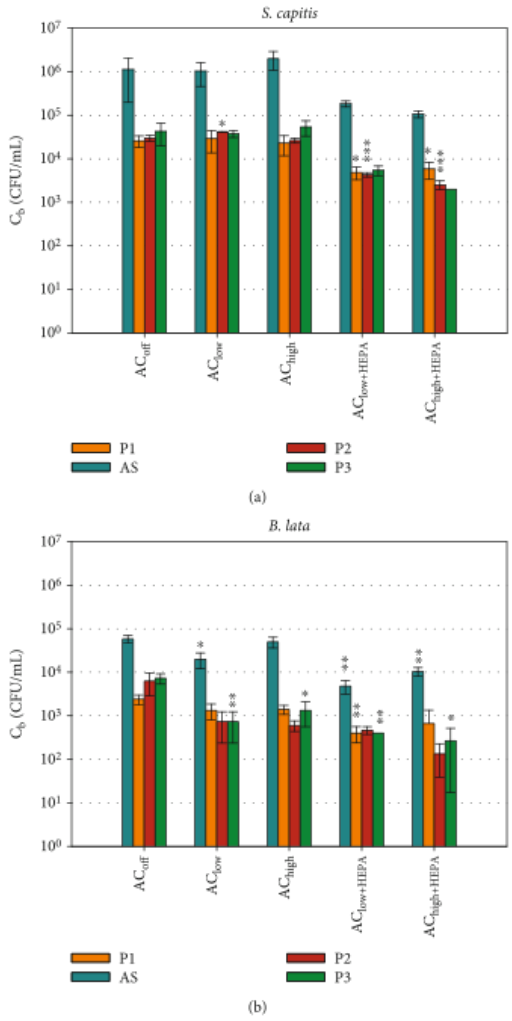

FIGURE 7: C_b of the two bacterial strains, (a) *S. capitis* and (b) *B. lata*, at different air curtain configurations measured in triplicate. Significance testing was performed with Student's *t*-test, comparing the mean data to the control configuration AC_{off}. Note: $^*p \leq 0.05$, $^{**}p \leq 0.01$, and $^{***}p \leq 0.001$.

using a defined bioaerosol in a controlled laboratory setting with controlled environmental conditions under five distinct ventilation scenarios. Our results highlight the importance of considering a diverse range of bacterial species in order to detect variations in survival under different environmental conditions.

3.3. Comparison Between Both Evaluation Methods

3.3.1. Absolute Concentrations. The number of viable bacteria or active virions per particle is an important parameter for calculating infection risks and dose–response models. While the D_{50} of the MAS is known, its collection efficiency across the entire particle size is not. Thus, the following comparison of the two investigated quantities of bioaerosol dispersal is limited to the measured absolute concentrations of particles $\overline{C_p}$, calculated as an average over the course of 600 s of the measurement time, and bacterial survival C_b, representing the total number of sampled bacteria over the entire measurement duration. Nevertheless, active bacterial sampling by the MAS is a more reliable sampling strategy

than passive bacterial sampling in varying ventilation scenarios. For this reason, we focus on the active sampling technique for the comparison of the absolute concentrations in Figure 8. This figure compares the absolute concentrations of sampled particles $\overline{C_p}$ of $D_p = 1.0–2.5\,\mu$m and the survival of the two key bacterial species for all five distinct ventilation scenarios at the AS position. This particular size range was chosen due to the alignment between cell size (see Table 3) and particle size. For completeness, a comparison with the other particle sizes is shown in Figure S2, revealing similar trends in both datasets.

Figure 8a shows a notable agreement between the particle concentration and the bacterial survival of *S. capitis* in configurations without HEPA filters. Both quantities increase in the AC_{high} scenario, and the standard deviation significantly decreases for both datasets. The measured particle concentrations in this size range are approximately four orders of magnitude lower than C_b of *S. capitis*. Therefore, a different scaling was selected for the log-scaled y-axis for both datasets. There is less agreement for the configurations with HEPA filters. Nevertheless, a notable decline of approximately one log count is evident when comparing $AC_{low+HEPA}$ to AC_{high} for both datasets. Furthermore, both bioaerosol dispersion measurement methods demonstrate a reduction toward the $AC_{high+HEPA}$ scenario. The standard deviation for both datasets decreases compared to the ventilation scenarios without HEPA filters.

Figure 8b presents a comparison between *B. lata* and particles with diameters between $D_p = 1.0$ and $2.5\,\mu$m. Given that *B. lata* is slightly larger than *S. capitis* (see Table 3), similar or even better agreement with the particle data of that particular size range was expected. However, the observed agreement between the PM data and C_b is less pronounced, especially in the context of the AC_{low} scenario. A reduction in C_b is evident for the HEPA configurations. The factors contributing to the observed discrepancy in the behavior of the two bacterial species can be attributed to a wide range of potential causes. First, fluctuations in the viable cell concentration of the bioaerosol impact the biological data. Second, the effect of atomization by the four BLAM nozzles on the distinct bacterial species is unknown. Nevertheless, the BLAM was identified as the most suitable and least harmful nebulizer in the study by Danelli et al. [33]. The impact of the nebulization process on the cells was outlined in Section 3.2. Finally, the potential for codependencies among the nine species under study may affect the bacterial viability in the air or on the sampling medium.

3.3.2. Normalized Concentrations. After analyzing the absolute data for bacterial survival and particle concentrations, each dataset (C_b and $\overline{C_p}$) is normalized with the corresponding AC_{off} data, as shown in Figure 9. This allows us to identify the effects of the applied ventilation configuration while reducing the influence of different initial concentrations of *B. lata* and *S. capitis* in the artificial saliva. Therefore, it is reasonable to hypothesize that the normalized evaluation data for each position P_i, $C_{p,\text{norm}} = \bar{C}_{p,i}(AC)/\bar{C}_{p,i}(AC_{off})$ and $C_{b,\text{norm}} = (C_{b,i}(AC)/C_{b,i}(AC_{off})$, will exhibit similar behavior under equal environmental conditions which were achieved inside the experimental chamber. Figure 9 also shows the results of t-tests conducted to analyze the relationship between the normalized particle concentrations and the normalized bacterial survival rates at each position by comparing the two datasets of C_b and $\overline{C_p}$, respectively.

The two methods of assessing bioaerosol dispersion show best agreement for $C_{b,\text{norm}}$ of *S. capitis* (Figure 9a), which displays a pattern comparable to $C_{p,\text{norm}}$ for $D_p = 1.0$ $–2.5\,\mu$m. Notably, the particle concentrations are more similar to those of *S. capitis* than to those of *B. lata* (Figure 9a,b). This can be attributed to the size and shape of the cells of *S. capitis* in comparison to the cells of *B. lata*, as previously described. A comparison to particles in the $0.3–1.0\,\mu$m size range is presented in Figure S3a,b. Regarding *B. lata* (Figure 9b), it is observed that only the HEPA filter configurations of the air curtain result in a comparable reduction of approximately 90% for both bacteria and particles. The agreement between *B. lata* and the particle concentrations of $D_p = 0.3–1.0\,\mu$m (see Figure S3b) is found to be similar to that observed with $D_p = 1.0–2.5\,\mu$m in Figure 9b.

Our findings highlight the heterogeneous behavior of different bacterial species during airborne transmission. Therefore, we recommend implementing a defined testing strategy to evaluate the susceptibility of opportunistic bacteria to environmental conditions during airborne transmission. Our results also demonstrate good agreement between measured bacterial and PM concentrations for *S. capitis*. Thus, its transmission pathways under similar environmental conditions could be traced using only PM measurements. Furthermore, combining both measurement methods allows for the development of optimized microbial countermeasures for future use in indoor environments such as the passenger cabins of trains and aircraft.

3.4. Air Curtain Effectiveness. This final section presents an assessment of the effectiveness of the considered air curtain system in mitigating the spread of the bioaerosol within the test chamber. The particle-based air curtain effectiveness, denoted as E_p, is calculated according to the formulation presented in Equation (2) of Section 2.5. A comparison is made with the bacterial related air curtain effectiveness E_b as defined in Equation (3). These calculations are performed at sampling positions P1 (in front of the air curtain) against P3 (behind the air curtain). Both positions are equidistant from the center plane of the air curtain at a distance of $x = \pm 20$ cm (see Figure 1). It should be noted that active and passive bacterial sampling are subject to different physical effects during the sampling process, as previously discussed. These effects depend heavily on the flow field at the sampling position; thus, the results may vary considerably for the different air curtain Reynolds numbers and for the two sampling methods.

As illustrated in Table 5 (first row) and previously in Figures 3, 4, 5, 6, and 7, a high transport of bioaerosols into R2 was measured when the air curtain was inactive. The data indicate negative effectiveness for both E_p and E_b, meaning

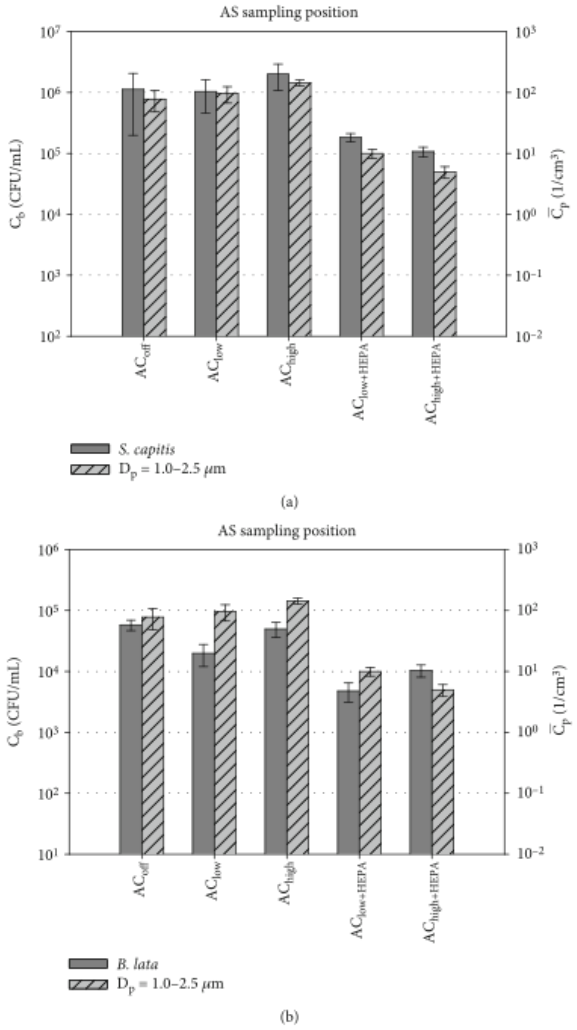

FIGURE 8: Absolute $\overline{C_p}$ of $D_p = 1.0–2.5\,\mu m$ compared to C_b of (a) *S. capitis* and (b) *B. lata* on the sampling position AS. The scaling of the *y*-axis was adjusted for a more accurate and comparable representation of the data.

that there is higher concentration of particles and bacteria at P3 behind the air curtain than at P1 in front of it. The values for E_b for *S. capitis* (−0.64) and *B. lata* (−2.04) are significantly lower than the values for E_p across all particle sizes.

The second row of Table 5 shows the effectiveness of the air curtain for both bacterial species in the AC_{low} configuration. The effectiveness for *S. capitis* ($E_b = -0.3$) differs greatly from that for *B. lata* ($E_b = 0.45$). The same is true for the AC_{high} configuration, as shown in the third row of Table 5. Although the standard deviation of C_b for *S. capitis* (see Figure 7a) were remarkably low for the AC_{high} configuration, future comparisons of active bacterial sampling methods, such as those used by the MAS, may yield more comparable results for E_b than passive sampling on agar plates. Regarding E_p in both configurations, a reduction to $E_p = 0.2–0.36$ for AC_{low} and to $E_p = 0.16–0.33$ for AC_{high} is observed. This indicates that the air curtain is effective in reducing particle spread for both configurations, with a slight advantage for

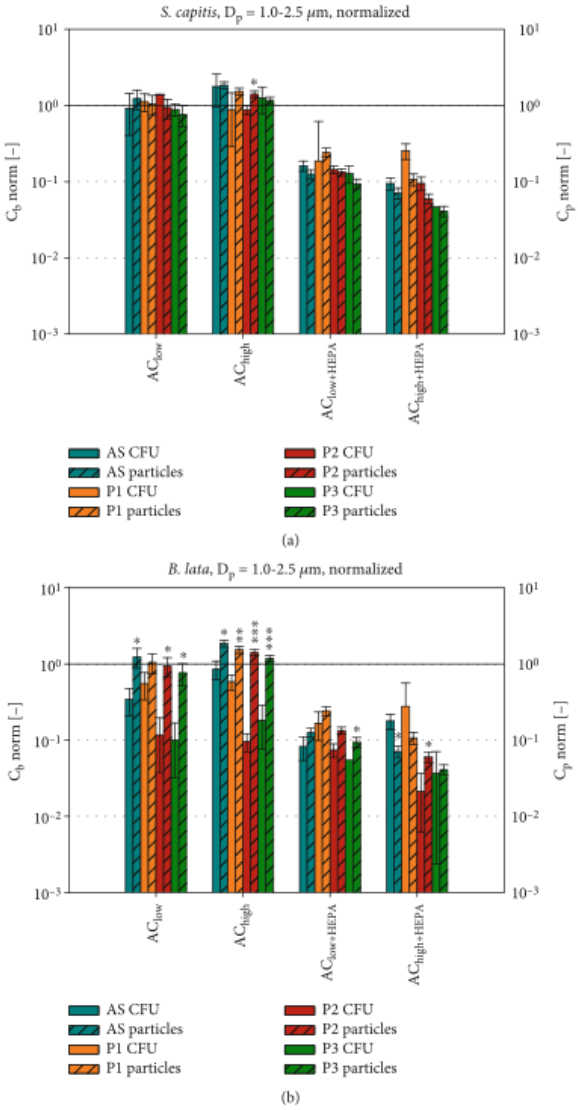

FIGURE 9: Reduction of particle concentrations of sizes 1.0–2.5 μm and the survival fraction of the bacterial strains (a) *S. capitis* and (b) *B. lata*. The bacteria from the air sampler (AS) and Petri dishes (P1–P3) and the average particle concentration $\overline{C_p}(\Delta t)$ for $\Delta t = 600$ s are shown on logarithmic axes. The values are normalized to the respective values obtained for the AC_{off} scenario at each position P_i ($C_{b,norm} = (C_{b,i}(AC)/C_{b,i}(AC_{off})$, $C_{p,norm} = \overline{C}_{p,i}(AC)/\overline{C}_{p,i}(AC_{off})$. Student's t-tests were performed to compare the respective CFU data to the particle concentration data for each configuration. Note: $^{*}p \leq 0.05$, $^{**}p \leq 0.01$, and $^{***}p \leq 0.001$.

TABLE 5: Air curtain effectiveness E_b calculated using bacterial survival and E_p using particle concentration for all air curtain configurations between measurement positions P1 and P3.

	S. capitis E_b (−)	*B. lata* E_b (−)	D_p = 0.3–1.0 μm E_p (−)	D_p = 1.0–2.5 μm E_p (−)	D_p = 2.5–4.0 μm E_p (−)
AC_{off}	−0.64	−2.04	−0.10	0.12	−0.07
AC_{low}	−0.30	0.45	0.20	0.36	0.23
AC_{high}	−1.36	0.05	0.16	0.33	0.20
$AC_{low+HEPA}$	−0.12	0.00	0.60	0.66	0.59
$AC_{high+HEPA}$	0.66	0.60	0.58	0.66	0.60

the lower Reynolds number configuration AC_{low} in our specific geometric setup (see Figure 1). Additionally, a higher E_p is observed for AC_{low} and AC_{high} configurations for particle diameters > 1 μm, as discussed earlier in relation to Figure 4.

In the last row of Table 5, there is good agreement between E_p and E_b for the $AC_{high+HEPA}$ configuration. For both bacterial species and the particle diameters smaller than 4.0 μm, the values range from 0.58 to 0.66. The highest bacterial air curtain effectiveness (E_p = 0.66) is associated with *S. capitis*. This species exhibited lower standard deviations in the triplicate measurements (Figure 7) and also better agreement with the (normalized) particle concentrations in Figures 8 and 9 for D_p = 1.0–2.5 μm. Therefore, a very good agreement with the particle-based effectiveness (E_p = 0.66) for medium-sized particles (D_p = 1.0–2.5 μm) was expected for the $AC_{high+HEPA}$ configuration. For *B. lata*, the highest agreement is observed between E_b and E_p for D_p = 2.5–4.0 μm, with a value of 0.60 for both. This may be attributed to the larger cell size and the rod-shaped morphology of *B. lata* (see Table 3 and Figure 2).

The $AC_{high+HEPA}$ configuration shows nearly identical values to the $AC_{low+HEPA}$ configuration, with regard to E_p for all investigated particle sizes. However, a notable shift is observed in E_b, with the air curtain effectiveness declining for *S. capitis* (−0.12) and *B. lata* (0.00) compared to the $AC_{high+HEPA}$ configuration. As previously mentioned, these discrepancies are due to the different flow regimes of the air curtain (Reynolds number reduction from 7450 to 4000), resulting in different sampling conditions at P1 and P3, respectively.

Further measurement campaigns should include flow field measurements near the Petri dishes to gain a deeper understanding of these findings. The sensor-based results of E_p in Table 5 also elucidate two important findings. First, applying fresh or filtered air when using the air curtain as an indoor ventilation concept is crucial to mitigate the spread of airborne pathogens. Second, increasing the volume flow $\dot{V}_{ac}$ and the Reynolds number Re_{ac} from $AC_{low+HEPA}$ to $AC_{high+HEPA}$ does not necessarily increase the effectiveness of E_p. In fact, it decreases by 0.02 for the particles with D_p = 0.3–1.0 μm, indicating a dependency of E_p (Re, D_p), as discussed in the literature [17, 42]. When considering a potential application in the passenger cabin or other indoor environments, it is important to bear in mind that HEPA filters create additional resistance to airflow. Consequently, more power is needed to operate the air curtain and achieve sufficient airflow for aerodynamic sealing. We recommend using fresh air to power the air curtain; however, this may also depend on the air quality and climatic conditions of the ambient fresh air and may not always be possible, for example, in an air craft cabin or subway train. Regarding E_p and thus E_b, it is difficult to predict the effect of changing to a more realistic geometric scenario. Several studies, for example, the one by Kurec et al. [18], aim to implement air curtains in realistic geometries. However, factors such as the position of the suction ports for the exhaust air remain very relevant. Adapting the flow parameters to the respective geometry and boundary conditions will remain necessary to achieve an optimal balance between energy consumption and reducing bioaerosol dispersal, thereby improving air quality.

4. Conclusions and Outlook

The three main objectives of our study were (A) to implement a defined reference bioaerosol as an assessment tool to measure the spread of pathogens in indoor environments, (B) to compare the survival rates of the two key bacterial species from the reference bacterial community with the well-established method of sensor-based PM measurements, and (C) to evaluate the performance of the PM sensor-based and microbiological sampling techniques considering the effectiveness of the used air curtain system against bioaerosol spread.

A. The bacterial input was a defined mixture of a total of nine bacterial species in artificial saliva, representing genera commonly found in aircraft and subway systems. This approach provides a realistic representation of actual bioaerosols. The bioaerosol was nebulized using a well-established bioaerosol generator. Sampling was performed passively on agar plates positioned in the impingement zone of the air curtain and actively via an aerosol sampling device behind the air curtain. Two species, *B. lata* and *S. capitis* (representing Gram-negative and Gram-positive bacteria, respectively), were subjected to selective evaluation based on their resistance against the antibiotics streptomycin and rifampicin, respectively. Cultivating both species allowed us to determine bacterial survival for all tested air curtain configurations. Significant discrepancies were observed between the two sampling techniques and the two species. The

active aerosol sampling method demonstrated significantly higher bacterial survival due to the increased collection efficiency. In contrast, the passive sampling method yielded bacterial survival counts that were approximately 1.5–2 log counts lower. A comparison of the bacterial survival of *B. lata* and *S. capitis* using both sampling methods revealed lower concentrations of 1–1.5 log counts for *B. lata* than for *S. capitis*. This difference can be attributed to the different characteristics of the species (morphology, size, desiccation resistance, etc.), which influence their survival (e.g., during nebulization). Due to limited precision in the production process, a slightly lower initial concentration of *B. lata* was found in the bioaerosol before nebulization. Additionally, the difference in local survival between the two bacterial genera emphasizes the need for caution when performing quantitative analyses. These results highlight the importance of using a combination of different bacterial strains and standardized methods when investigating the transmission routes of potentially harmful bioaerosols. Nevertheless, our defined bioaerosol remains a suitable tool for analyzing bioaerosol dispersal.

B. The comparison of the local PM measurements with the local bacterial survival (determined by active and passive particle sampling) showed that the particle measurements were more sensitive to the different flow configurations of the air curtain than the biological evaluation tool. Another advantage of the PM measurements is the temporal resolution of the data, which provides additional information on the dynamics of aerosol spread. This makes PM measurements advantageous when designing a specific ventilation system or adjusting its parameters. Including bacterial survival is important when evaluating system parameters that cannot be assessed through aerosol particle counting alone. These factors may include temperature, humidity, radiation, or biochemical reactions, which can affect pathogens during airborne transport from a source of contamination to a potentially susceptible individual. As these parameters did not vary during our measurements, we expected a good agreement between the number of airborne particles and the number of viable bacteria collected. Indeed, the agreement between *S. capitis* and the measured particle concentrations in the size range $D_p = 1.0–2.5\,\mu m$ was remarkable when comparing the bacteria sampled from the air sampler. However, the agreement between the survival rate of *B. lata* and the actively sampled particles in the specified size range was less pronounced. Normalizing the bacterial and particle data to our reference configuration with the air curtain deactivated showed that *S. capitis* reflected changes in particle concentration more accurately than *B. lata* did. These different results highlight the varying behavior of bacterial species, an important consideration when performing and interpreting studies on bioaerosol dispersal.

C. Adjusting the fan speed and using HEPA filters resulted in five distinct air curtain Reynolds numbers ($Re < 11,000$) and a variation of the air curtain flow field. Using the previously described sensor-based and biological evaluation tools at designated points on the floor in front of and behind the air curtain (P1/P3), we assessed the effectiveness of the air curtain in preventing bioaerosol dispersion. When the air curtain was inactive, strong fluctuations in particle concentrations in the chamber were measured over time. Regarding the microbial evaluation method, the air curtain effectiveness reached values of up to −2.04 for *B. lata* and −0.64 for *S. capitis*, indicating that up to 204% more bacteria were sampled behind the air curtain than in front of it. The PM sensor-based evaluation method yielded values of −0.1 for the smaller particles (0.3–1.0 μm) and up to 0.12 for the larger particles (1.0–2.5 μm). The activation of the air curtain resulted in a particle-related effectiveness of 0.2 for smaller ($< 1\,\mu m$) and 0.36 for larger particles $D_p = 1.0–2.5\,\mu m$. Adding HEPA filters significantly increased the effectiveness for the smaller and the larger particles due to particle removal at the air curtain inlet. Therefore, a comparison of the effectiveness between the different configurations was not in the scope of our studies. In the HEPA scenario, the effectiveness against the smaller particles reached 0.58, while the effectiveness against the larger particles reached 0.66. In this configuration, the effectiveness against bacterial spread was evaluated at 0.60 and 0.66 for *B. lata* and *S. capitis*, respectively. The good agreement between the two measurement techniques for this final configuration indicates that the bacterial-based results obtained from the Petri dishes were significantly influenced by the local air velocities, which affected the settling characteristics of the particles on the Petri dishes. Further studies should use multiple active aerosol samplers in front of and behind the air curtain as this method is less sensitive to variations in local air velocity. However, passive sampling, for example, in the air curtain impingement zone can provide valuable information on bioaerosol spread, but quantitative analyses must be carried out with caution.

Our study indicates that the defined bacterial bioaerosol served as an appropriate reference standard that facilitated a deeper understanding of the spread of potentially harmful bioaerosols. Comparing PM concentration with bacterial survival showed better agreement for *S. capitis*. A broader evaluation of all nine bacterial species present in the bioaerosol could provide a more comprehensive understanding of their specific airborne survival and behavior. Studies using single model organisms would be interesting to investigate the effect of using single organisms versus a microbial community that resembles a more realistic reference. The air curtain reduced the spread of bioaerosols in the test chamber. It was most effective with particles between 1.0 and 2.5 μm in diameter. As expected, the configurations that

included additional HEPA filters achieved higher particle removal rates. Changes in environmental parameters such as humidity, temperature, and UV radiation, which directly affect bacterial survival, can be the subject of further measurements. Additionally, conducting experiments in a cabin-like environment can account for factors such as cabin dimensions, seating arrangements, headrests, doors, and other features. Before integrating the air curtain into an overall ventilation strategy, however, the thermal comfort of passengers in the vicinity of the air curtain's strong airflow must be assessed.

This study introduced a standardized bioaerosol and reliable, straightforward detection methods. Using these methods in a defined indoor environment, we compared the spread of two bacterial species from the bioaerosol across five different ventilation scenarios. This comparison allowed us to evaluate the methods against each other and investigate bioaerosol transmission in depth. This study will facilitate the testing and evaluation of novel measures for airborne microbial reduction in future applications.

Data Availability Statement

Data are available on request.

Conflicts of Interest

The authors declare no conflicts of interest.

Author Contributions

Yen-Tran Ly and Andreas Kohl share joint first authorship.

Funding

This work was funded by the GANDALF project of the German Aerospace Center (DLR). Open Access funding was enabled and organized by Projekt DEAL.

Acknowledgments

We thank Felix Werner, Andrea Schroeder, and Alessa Schiele for their help during the experiments and Christoph Steger for building the experimental chamber. We especially thank Ralf Moeller for his unlimited support for this project and beyond. This publication represents a component of Y.-T.L.'s doctoral (Dr. Rer. Nat.) thesis in the Faculty of Natural Science at the Justus Liebig University Giessen, Germany. This publication represents a component of A.K.'s doctoral (Dr. Ing.) thesis in the Faculty of Mechanical Engineering at the Technische Universität Ilmenau, Germany.

Supporting Information

Additional supporting information can be found online in the Supporting Information section. *(Supporting Information)* Table S1: List of ingredients of Reasoner's 2A (1xR2A) ready-mix from TEKnova. Table S2: List of ingredients of tryptic soy media ready-mix from Sigma-Aldrich. Table S3: List of ingredients of brain heart infusion broth ready-mix from Sigma-Aldrich. Figure S1: Average particle concentrations of particle size 2.5–4.0 μm in (a) linear and (b) logarithmic view. Figure S2: Absolute $\overline{C_p}$ of $D_p = 0.3$–$1.0\,\mu$m compared to C_b of (a) *S. capitis* and (b) of *B. lata* on the sampling position AS and $D_p = 2.5$–$4.0\,\mu$m compared to C_b of (c) *S. capitis* and (d) of *B. lata* on the sampling position AS. Figure S3: Bacterial growth (CFU per milliliter) of the bacterial strain *B. lata* and *S. capitis* retrieved from the air sampler and the average particle concentration $\overline{C_p}(\Delta t)$ for $\Delta t = 600\,s$ for the particle size 0.3–1.0 μm for (a) *S. capitis* and (b) *B. lata*.

References

[1] A. L. Byrd, Y. Belkaid, and J. A. Segre, "The Human Skin Microbiome," *Nature Reviews Microbiology* 16, no. 3 (2018): 143–155, https://doi.org/10.1038/nrmicro.2017.157.

[2] E. A. Grice, H. H. Kong, G. Renaud, et al., "A Diversity Profile of the Human Skin Microbiota," *Genome Research* 18, no. 7 (2008): 1043–1050, https://doi.org/10.1101/gr.075549.107.

[3] A. J. Hoisington, C. E. Stamper, K. L. Bates, et al., "Human Microbiome Transfer in the Built Environment Differs Based on Occupants, Objects, and Buildings," *Scientific Reports* 13, no. 1 (2023): 6446, https://doi.org/10.1038/s41598-023-33719-6.

[4] J. Meadow, A. E. Altrichter, S. W. Kembel, et al., "Bacterial Communities on Classroom Surfaces Vary With Human Contact," *Microbiome* 2, no. 1 (2014): 7, https://doi.org/10.1186/2049-2618-2-7.

[5] B. Knobling, G. Franke, L. Beike, T. Dickhuth, and J. K. Knobloch, "Reading the Score of the Air—Change in Airborne Microbial Load in Contrast to Particulate Matter During Music Making," *International Journal of Environmental Research and Public Health* 19, no. 16 (2022): 9939, https://doi.org/10.3390/ijerph19169939.

[6] Y.-T. Ly, F. Arndt, A. L. Boschert, et al., "Nach der Pandemie ist vor der Pandemie: Und wie interdisziplinäre Forschung hier helfen kann," *Flugmedizin·Tropenmedizin Reisemedizin* 30, no. 3 (2023): 122–130, https://doi.org/10.1055/a-2073-2615.

[7] Y.-T. Ly, S. Leuko, and R. Moeller, "An Overview of the Bacterial Microbiome of Public Transportation Systems-Risks, Detection, and Countermeasures," *Frontiers in Public Health* 12 (2024): 1367324, https://doi.org/10.3389/fpubh.2024.1367324.

[8] H. Weiss, V. S. Hertzberg, C. Dupont, et al., "The Airplane Cabin Microbiome," *Microbial Ecology* 77, no. 1 (2019): 87–95, https://doi.org/10.1007/s00248-018-1191-3.

[9] M. H. Leung, D. Wilkins, E. K. Li, F. K. Kong, and P. K. Lee, "Indoor-Air Microbiome in an Urban Subway Network: Diversity and Dynamics," *Applied and Environmental Microbiology* 80, no. 21 (2014): 6760–6770, https://doi.org/10.1128/AEM.02244-14.

[10] E. Afshinnekoo, C. Meydan, S. Chowdhury, et al., "Geospatial Resolution of Human and Bacterial Diversity With City-Scale Metagenomics," *Cell Systems* 1, no. 1 (2015): 72–87.

[11] C. Shen, S. Feng, H. Chen, et al., "Transmission of *mcr-1*-Producing Multidrug-Resistant Enterobacteriaceae in Public Transportation in Guangzhou, China," supplement_2, *Clinical Infectious Diseases* 67, S217–S224, https://doi.org/10.1093/cid/ciy661.

[12] T. Cao, Y. Liu, Y. Li, et al., "A Public Health Concern: Emergence of Carbapenem-Resistant *Klebsiella pneumoniae* in a Public Transportation Environment," *Journal of Antimicrobial Chemotherapy* 75, no. 10 (2020): 2769–2772, https://doi.org/10.1093/jac/dkaa260.

[13] J. Gu, X. J. Xie, J. X. Liu, et al., "Prevalence and Transmission of Antimicrobial-Resistant *Staphylococci* and *Enterococci* From Shared Bicycles in Chengdu, China," *Science of the Total Environment* 738 (2020): 139735, https://doi.org/10.1016/j.scitotenv.2020.139735.

[14] L. Schibuola and C. Tambani, "High Energy Efficiency Ventilation to Limit COVID-19 Contagion in School Environments," *Energy and Buildings* 240 (2021): 110882, https://doi.org/10.1016/j.enbuild.2021.110882.

[15] C.-Y. Chen, P.-H. Chen, J.-K. Chen, and T.-C. Su, "Recommendations for Ventilation of Indoor Spaces to Reduce COVID-19 Transmission," *Journal of the Formosan Medical Association* 120, no. 12 (2021): 2055–2060, https://doi.org/10.1016/j.jfma.2021.08.007.

[16] F. C. Hayes, "Heat Transfer Characteristics of the Air Curtain: A Plane Jet Subjected to Transverse Pressure and Temperature Gradients" University of Illinois at Urbana-Champaign, 1968), Available: https://www.proquest.com/openview/e93713a6260a9634a3555a5724afb0b6/1?cbl=18750%26diss=y%26pq-origsite=gscholar.

[17] S. Ikardouchene, S. Delaby, and X. Nicolas, "Interaction of a Droplet Spray With a Turbulent Plane Air Jet Impacting a Wall: Application to the Confinement of Atmospheres Contaminated With Particles by Air Curtain," *Experiments in Fluids* 64, no. 3 (2023): 51, https://doi.org/10.1007/s00348-023-03585-z.

[18] K. Kurec, B. Olszański, K. Gumowski, et al., "Air Curtain as a SARS-CoV-2 Spreading Mitigation Method in a Small Aircraft Cabin," *Proceedings of the Institution of Mechanical Engineers, Part G: Journal of Aerospace Engineering* 237, no. 11 (2023): 2480–2504, https://doi.org/10.1177/09544100231153703.

[19] Y.-T. Ly, N. Wetzig, J. Holtel, S. Leuko, and R. Moeller, eds., "Modeling the Public Transport Microbiome: Development of a Microbial Reference Community," in *18th International Conference on Indoor Air Quality and Climate, INDOOR AIR 2024* (Elsevier, 2024).

[20] D. Schmeling, M. Kühn, D. Schiepel, et al., "Analysis of Aerosol Spreading in a German Inter City Express (ICE) Train Carriage," *Building and Environment* 222 (2022): 109363, https://doi.org/10.1016/j.buildenv.2022.109363.

[21] C. Napoli, V. Marcotrigiano, and M. T. Montagna, "Air Sampling Procedures to Evaluate Microbial Contamination: A Comparison Between Active and Passive Methods in Operating Theatres," *BMC Public Health* 12, no. 1 (2012): 594, https://doi.org/10.1186/1471-2458-12-594.

[22] W. Przystaś, E. Zabłocka-Godlewska, and E. Melaniuk-Wolny, "A Comparison of Sedimentation Method and Active Sampler Analysis of Microbiological Indoor Air Quality-Case Study," *Ecological Chemistry and Engineering S* 30, no. 1 (2023): 37–48, https://doi.org/10.2478/eces-2023-0009.

[23] E. Vanlaere, A. Baldwin, D. Gevers, et al., "Taxon K, a Complex Within the *Burkholderia cepacia* Complex, Comprises at Least Two Novel Species, *Burkholderia contaminans* sp. nov. and *Burkholderia lata* sp. nov," *International Journal of Systematic and Evolutionary Microbiology* 59, no. 1 (2009): 102–111, https://doi.org/10.1099/ijs.0.001123-0.

[24] H.-H. Chen, W. J. Li, S. K. Tang, et al., "*Corynebacterium halotolerans* sp. nov., Isolated From Saline Soil in the West of China," *International Journal of Systematic and Evolutionary Microbiology* 54, no. 3 (2004): 779–782, https://doi.org/10.1099/ijs.0.02919-0.

[25] R. Rahkila, P. Johansson, E. Säde, and J. Björkroth, "Identification of Enterococci From Broiler Products and a Broiler Processing Plant and Description of *Enterococcus viikkiensis* sp. nov," *Applied and Environmental Microbiology* 77, no. 4 (2011): 1196–1203, https://doi.org/10.1128/AEM.02412-10.

[26] S. Van Trappen, I. Vandecandelaere, J. Mergaert, and J. Swings, "*Flavobacterium degerlachei* sp. nov., *Flavobacterium frigoris* sp. nov. and *Flavobacterium micromati* sp. nov., Novel Psychrophilic Bacteria Isolated From Microbial Mats in Antarctic Lakes," *International Journal of Systematic and Evolutionary Microbiology* 54, no. 1 (2004): 85–92, https://doi.org/10.1099/ijs.0.02857-0.

[27] K. Kusano, H. Yamada, M. Niwa, and K. Yamasato, "*Propionibacterium cyclohexanicum* p. nov., a New Acid-Tolerant ω-Cyclohexyl Fatty Acid-Containing Propionibacterium Isolated From Spoiled Orange Juice," *International Journal of Systematic and Evolutionary Microbiology* 47, no. 3 (1997): 825–831, https://doi.org/10.1099/00207713-47-3-825.

[28] G. S. Reddy, G. I. Matsumoto, P. Schumann, E. Stackebrandt, and S. Shivaji, "Psychrophilic Pseudomonads From Antarctica: *Pseudomonas antarctica* sp. nov., *Pseudomonas meridiana* sp. nov. and *Pseudomonas proteolytica* sp. nov," *International Journal of Systematic and Evolutionary Microbiology* 54, no. 3 (2004): 713–719, https://doi.org/10.1099/ijs.0.02827-0.

[29] Y.-Y. Huo, X. W. Xu, S. P. Liu, H. L. Cui, X. Li, and M. Wu, "*Sphingomonas rubra* sp. nov., Isolated From Bioreactor Wastewater," *International Journal of Systematic and Evolutionary Microbiology* 61, no. 5 (2011): 1028–1032, https://doi.org/10.1099/ijs.0.020958-0.

[30] L.-Y. Sobisch, K. M. Rogowski, J. Fuchs, et al., "Biofilm Forming Antibiotic Resistant Gram-Positive Pathogens Isolated From Surfaces on the International Space Station," *Frontiers in Microbiology* 10 (2019): 543, https://doi.org/10.3389/fmicb.2019.00543.

[31] L. Niu, S. Lu, S. Hu, et al., "*Streptococcus halotolerans* sp. nov. Isolated From the Respiratory Tract of Marmota Himalayana in Qinghai-Tibet Plateau of China," *International Journal of Systematic and Evolutionary Microbiology* 66, no. 10 (2016): 4211–4217, https://doi.org/10.1099/ijsem.0.001337.

[32] M.-H. Woo, Y.-M. Hsu, C.-Y. Wu, B. Heimbuch, and J. Wander, "Method for Contamination of Filtering Facepiece Respirators by Deposition of MS2 Viral Aerosols," *Journal of Aerosol Science* 41, no. 10 (2010): 944–952, https://doi.org/10.1016/j.jaerosci.2010.07.003.

[33] S. G. Danelli, M. Brunoldi, D. Massabò, F. Parodi, V. Vernocchi, and P. Prati, "Comparative Characterization of the Performance of Bio-Aerosol Nebulizers in Connection With Atmospheric Simulation Chambers," *Atmospheric Measurement Techniques* 14, no. 6 (2021): 4461–4470, https://doi.org/10.5194/amt-14-4461-2021.

[34] D. Massabò, S. G. Danelli, P. Brotto, et al., "ChAMBRe: A New Atmospheric Simulation Chamber for Aerosol Modelling and Bio-Aerosol Research," *Atmospheric Measurement Techniques* 11, no. 10 (2018): 5885–5900, https://doi.org/10.5194/amt-11-5885-2018.

[35] A. Kohl, Y.-T. Ly, S. Leuko, D. Schmeling, C. Wagner, and R. Moeller, eds., "Evaluation of Bioaerosol Propagation Through an Air Curtain," in *18th International Conference on Indoor Air Quality and Climate, INDOOR AIR 2024* (Elsevier, 2024).

[36] S. Coldrick, A. Kelsey, M. J. Ivings, et al., "Modeling and Experimental Study of Dispersion and Deposition of Respiratory Emissions With Implications for Disease Transmission," *Indoor Air* 32, no. 2 (2022): e13000, https://doi.org/10.1111/ina.13000.

[37] D. Kingston, "Selective Media in Air Sampling: A Review," *Journal of Applied Microbiology* 34, no. 1 (1971): 221–232, https://doi.org/10.1111/j.1365-2672.1971.tb02280.x.

[38] A. C. Lowen, S. Mubareka, J. Steel, and P. Palese, "Influenza Virus Transmission Is Dependent on Relative Humidity and Temperature," *PLoS Pathogens* 3, no. 10 (2007): e151, https://doi.org/10.1371/journal.ppat.0030151.

[39] D. Schiepel, R. Brinkema, and D. Schmeling, eds., "Artificial Saliva Aerosol Source and Detection System for Spreading Analysis in Indoor Environments," in *17th International Conference on Indoor Air Quality and Climate, INDOOR AIR 2022* (Elsevier, 2022).

[40] K. Niehaus and A. Westhoff, "Mobile Measurement System" 2022, Available from: https://zenodo.org/records/6471391.

[41] K. Niehaus and A. Westhoff, "An Open-Source Data Acquisition System for Laboratory and Industrial Scale Applications," *Measurement Science and Technology* 34, no. 2 (2023): 027001, https://doi.org/10.1088/1361-6501/ac9994.

[42] A. Kohl, D. Schmeling, and C. Wagner, eds., "Interaction of Exhaled Aerosol Particles With the Flow Field of an Air Curtain," in *ICHMT Digital Library Online* (Begel House Inc., 2023).

[43] Student, "The Probable Error of a Mean," *Biometrika* 6, no. 1 (1908): 1–25, https://doi.org/10.2307/2331554.

[44] B. L. Welch, "The Significance of the Difference Between Two Means When the Population Variances Are Unequal," *Biometrika* 29, no. 3-4 (1938): 350–362, https://doi.org/10.1093/biomet/29.3-4.350.

[45] H. B. Mann and D. R. Whitney, "On a Test of Whether One of Two Random Variables Is Stochastically Larger Than the Other," *Annals of Mathematical Statistics* 18, no. 1 (1947): 50–60, https://doi.org/10.1214/aoms/1177730491.

[46] R. R. Colwell, "Viable but Nonculturable Bacteria: A Survival Strategy," *Journal of Infection and Chemotherapy* 6, no. 2 (2000): 121–125, https://doi.org/10.1007/PL00012151.

[47] Y. Hirai, "Survival of Bacteria Under Dry Conditions; From a Viewpoint of Nosocomial Infection," *Journal of Hospital Infection* 19, no. 3 (1991): 191–200.

[48] A. Nocker, P. S. Fernández, R. Montijn, and F. Schuren, "Effect of Air Drying on Bacterial Viability: A Multiparameter Viability Assessment," *Journal of Microbiological Methods* 90, no. 2 (2012): 86–95, https://doi.org/10.1016/j.mimet.2012.04.015.

[49] J. Cox, R. Indugula, S. Vesper, Z. Zhu, R. Jandarov, and T. Reponen, "Comparison of Indoor Air Sampling and Dust Collection Methods for Fungal Exposure Assessment Using Quantitative PCR," *Environmental Science: Processes & Impacts* 19, no. 10 (2017): 1312–1319, https://doi.org/10.1039/c7em00257b.

[50] T. Reponen, K. Willeke, S. Grinshpun, and A. Nevalainen, "Biological Particle Sampling," in *Aerosol Measurement: Principles, Techniques, and Applications* (Wiley, 2011), 549–570, https://doi.org/10.1002/9781118001684.ch24.

[51] G. Mainelis, "Bioaerosol Sampling: Classical Approaches, Advances, and Perspectives," *Aerosol Science and Technology* 54, no. 5 (2020): 496–519, https://doi.org/10.1080/02786826.2019.1671950.

2.5 Comparison of single bacteria and a bacterial reference community in a test against coated surfaces of varying copper content

Title	**Comparison of Single Bacteria and a Bacterial Reference Community in a Test Against Coated Surfaces of Varying Copper Content**
Authors	**Yen Ly-Sauerbrey[1]**, Ronja Anton[2], Laura Kopruch[3], Carolin Luisa Krämer[1,4], Alessa L. Boschert[5,6], Claudio Neidhöfer[7], Oliver Schwengers[8], Daniela Zander[2,3] and Stefan Leuko[1]
Affiliation	[1] Institute of Aerospace Medicine, German Aerospace Center, Cologne, Germany [2] Institute for Frontier Materials on Earth and in Space, German Aerospace Center, Cologne, Germany, [3] Division of Materials Science and Engineering, Chair of Corrosion and Corrosion Protection, Foundry Institute, RWTH Aachen University, Aachen, Germany, [4] Department of Natural Sciences, University of Applied Sciences Bonn-Rhein-Sieg, Rheinbach, Germany, [5] MVZ Laboratory Dr. Limbach and Colleagues eGbR, Heidelberg, Germany, [6] Institute for Medical Microbiology, Immunology and Hygiene, University Hospital of Cologne, Cologne, Germany, [7] Division of Clinical Bacteriology and Mycology, University Hospital of Basel, Basel, Switzerland, [8] Department of Bioinformatics and Systems Biology, Justus Liebig University Giessen, Giessen, Germany
Article type	Original research article
Authorship	Single-first author

Journal	Frontiers in Microbiology
Year	2025
Volume	16
DOI	10.3389/fmicb.2025.1659828
Author Contributions	
YL-S	Conceptualization, Data curation, Formal analysis, Investigation, Methodology, Visualization, Writing - original draft
RA	Conceptualization, Formal analysis, Investigation, Visualization, Writing - review & editing
LK	Formal analysis, Investigation, Writing - review & editing
CK	Conceptualization, Writing - review & editing
AB	Writing - review & editing
CN	Resources, Writing - review & editing
OS	Data curation, Resources, Writing - review & editing
DZ	Writing - review & editing
SL	Supervision, Writing - review & editing

frontiers | Frontiers in Microbiology

TYPE Original Research
PUBLISHED 26 August 2025
DOI 10.3389/fmicb.2025.1659828

OPEN ACCESS

EDITED BY
Mariana Carmen Chifiriuc,
University of Bucharest, Romania

REVIEWED BY
Denny Chin,
Concerto Biosciences, United States
Lamia Benhalima,
8 May 1945 University of Guelma, Algeria

*CORRESPONDENCE
Yen Ly-Sauerbrey
✉ yen-tran.ly@dlr.de

RECEIVED 04 July 2025
ACCEPTED 07 August 2025
PUBLISHED 26 August 2025

CITATION
Ly-Sauerbrey Y, Anton R, Kopruch L, Krämer CL, Boschert AL, Neidhöfer C, Schwengers O, Zander D and Leuko S (2025) Comparison of single bacteria and a bacterial reference community in a test against coated surfaces of varying copper content.
Front. Microbiol. 16:1659828.
doi: 10.3389/fmicb.2025.1659828

Comparison of single bacteria and a bacterial reference community in a test against coated surfaces of varying copper content

Yen Ly-Sauerbrey[1]*, Ronja Anton[2], Laura Kopruch[3], Carolin Luisa Krämer[1,4], Alessa L. Boschert[5,6], Claudio Neidhöfer[7], Oliver Schwengers[8], Daniela Zander[2,3] and Stefan Leuko[1]

[1]Institute of Aerospace Medicine, German Aerospace Center, Cologne, Germany, [2]Institute for Frontier Materials on Earth and in Space, German Aerospace Center, Cologne, Germany, [3]Chair of Corrosion and Corrosion Protection, Foundry Institute, Division of Materials Science and Engineering, RWTH Aachen University, Aachen, Germany, [4]Department of Natural Sciences, University of Applied Sciences Bonn-Rhein-Sieg, Rheinbach, Germany, [5]MVZ Laboratory Dr. Limbach and Colleagues eGbR, Heidelberg, Germany, [6]Institute for Medical Microbiology, Immunology and Hygiene, University Hospital of Cologne, Cologne, Germany, [7]Division of Clinical Bacteriology and Mycology, University Hospital of Basel, Basel, Switzerland, [8]Department of Bioinformatics and Systems Biology, Justus Liebig University Giessen, Giessen, Germany

Introduction: Pathogens can easily transmit via surfaces and objects. In light of the ongoing pandemic of antimicrobial resistance, silently threatening millions worldwide, this is of particular concern in clinical and public environments. Thus, it is crucial to understand how antimicrobial materials influence surface-associated microbes and microbial communities. Copper, known for its antimicrobial activity, has demonstrated effectiveness against numerous clinically relevant pathogens. However, these *in vitro* pure cultures are in stark contrast to the *in vivo* microbial communities. Additionally, the application of pure copper surfaces is high in cost and maintenance.

Methods: Hence, in this study we not only tested the antibacterial effectivity of different copper concentrations against single species, but also against a reference bacterial community representing the most abundant bacterial genera in public transport. This allowed a comparison of the antibacterial efficacy of copper against a bacterial community and against single species. Coatings on glass, which were composed of full copper (100 at.% Cu) and copper-aluminum alloys with different Cu contents (79 at.%, 53 at.% and 24 at.%) were tested with two selected single species (*Burkholderia lata* DSM 23089T and *Staphylococcus capitis* DSM 111179) and those species within the bacterial community.

Results: In general, the survival of the two species within the bacterial community was higher compared to their respective survival as a single species, significantly for *S. capitis*. Surfaces with 100 at.% copper content showed the greatest antibacterial effect in terms of bacterial survival, with a reduced survival of up to 10^{-6}. The 79 at.% Cu coating only had an inhibitory effect on the metabolic activity of *B. lata* when exposed to the surfaces as single species.

Discussion: Our results highlight the benefits of additional testing of microbial communities rather than pure cultures. These experiments allow for enhanced

evaluation of antimicrobial surfaces since they also take complex and diverse interactions within a surface microbiota into account. Therefore, community testing might be the more holistic approach for the testing of antibacterial materials.

KEYWORDS

antimicrobial materials, copper coating, bacterial community, copper gradient, microbial load

1 Introduction

Microbial dispersion naturally accompanies human presence. Through breathing, bioaerosols are spread, and direct contact to the environment causes the distribution of microbes that are harboring the skin. While most microorganisms are harmless or even beneficial, caution is needed when it comes to the spread of (opportunistic) pathogens. The currently ongoing silent pandemic of antimicrobial resistance (AMR) which includes multidrug-resistant bacteria (MDR), is already affecting millions of patients, resulting in limited or no treatment option of infections (Mahoney et al., 2021; Naghavi et al., 2024). Public surfaces play a vital role in the spread of pathogens (Xiao et al., 2019). Therefore, countermeasures to reduce infection transmission are needed. Transmission of pathogens and microorganisms in general is facilitated by many factors. Especially crowded environments, but also confined spaces lacking proper ventilation are hotspots of antimicrobial spread. Public transportation in large cities with millions of daily commuters combines both of the aforementioned features. Hence, it is a key environment for microbial transmission, simultaneously also highlighting the need for effective countermeasures.

Different countermeasures are available to reduce the microbial spread. In terms of air cleaning, disinfection can be performed using fumigation of e.g., hydrogen peroxide (Møretrø et al., 2019). For material disinfection, UV-disinfection, is common in hospital settings (Guettari et al., 2021; Ghosh et al., 2022). Antimicrobial materials are another approach to reduce the bacterial load on fomites. A great variation of antimicrobial materials and surfaces are available and have different antimicrobial mechanisms. For instance, some anti-biofouling surfaces reduce the attachment of microorganisms to the surfaces (Linklater et al., 2021), while others have biocidal species that inactivate microorganisms, like biocidal nanocomposites (Tamayo et al., 2016). Besides biocidal reactives, some surfaces rupture bacterial cells (Luan et al., 2018). Other commonly used antimicrobial materials are metals. So-called "metalloantibiotics" can cause toxicity for cells (Frei et al., 2023). However, while some metals exhibit antimicrobial properties, certain bacteria possess or have developed resistance to high metal ion concentrations (Hobman and Crossman, 2015). Therefore, deliberate and strategic application of these materials is essential.

One of the best-known antimicrobial metals is copper. Although copper is essential for the cells of all aerobic organisms (Festa and Thiele, 2011), toxic concentrations damage cells in various ways. Hence, while copper ultimately results in cell inactivation or death, the point of attack can vary between different types of microorganisms. For instance, viruses are affected by RNA degradation and membrane damage (in enveloped viruses) caused by copper ions. In fungi, on the other hand, copper ions cause physical damage of the cell membranes (Salah et al., 2021). In bacteria, copper not only damages the cell membrane, but also the DNA, due to the intrusion of copper ions and resulting oxidative stress (Grass et al., 2011; Santo et al., 2011; Pramanik et al., 2012). Oxidative stress involves reactive oxygen species (ROS), which are generated by both Fenton-like and Fenton-independent reactions, which cause oxidative damage of the cells through lipid peroxidation, protein oxidation, the above mentioned DNA and membrane damage, ultimately leading to cell death (Barnham et al., 2004; Pham et al., 2013; Salah et al., 2021).

Since copper functions as a cofactor, which catalyzes many redox reactions, high concentrations pose an issue with the copper homeostasis within the cells. High concentrations of copper can become toxic, since it can replace the iron in iron-sulfur clusters of proteins and damage or inactivate those proteins (Chillappagari et al., 2010).

Interestingly, the mechanism behind the antimicrobial copper surfaces is different between wet- and dry-contact killing (Ramos-Zúñiga et al., 2023). While it is not yet fully understood how copper inactivates cells in a wet contact killing setting, even less is known about the mechanism behind dry contact killing (Grass et al., 2011). However, it has been observed, that cells accumulate copper ions much faster during dry contact killing compared to wet contact killing, leading to damage especially of the cell membrane (Santo et al., 2011).

The application of copper as an antimicrobial element dates back to ancient times and has been studied extensively. Nowadays, it is used or tested in different settings, such as in hospitals (Mikolay et al., 2010) or in public transport (Williams et al., 2024). Nevertheless, copper is not a cost-effective element for processing and long-term use. It corrodes easily, and it is therefore not favored to be applied in its pure state. A promising method of enhancing the durability while maintaining cost efficiency is the use of copper alloys. In a past study, the effective antimicrobial copper content was tested by using materials with different copper contents in a hospital setting (Karpanen et al., 2012). In the described study by Karpanen et al. (2012), copper alloys with $\geq$ 58% copper content resulted in a microbial reduction on surfaces. Another study by Mehtar et al. (2008) tested different surfaces against nosocomial pathogens and a minimum copper content of > 55% was determined.

In this study, glass slides were used since glass is not antimicrobial and therefore does not influence the effect of the

coatings. Further, the used glass substrates support reproducibility due to their standardized roughness, which could otherwise influence the settling and behavior of the tested bacteria. Nevertheless, this approach can be applied to various materials. Another benefit of the used coatings is that aluminum is used in the alloy, which is more cost effective than zinc in brass (Westmetall, 2024)[1] which is also the subject of investigations into antimicrobial materials (Timofeev et al., 2025). Further, pure copper oxidizes quickly, which creates a colored surface making the material less user-friendly. Hence, copper-aluminum (Cu-Al) alloy coatings are considered to be highly suitable for real-setting applications.

To test the effectivity of such materials, many studies use microbial model organisms. A common issue of many studies is not the microbial selection for testing, but rather the applicability to real-world settings. A natural microbial environment is shaped by a variation of microorganisms, and the species within a microbial community interact. Microbial communities are complex, therefore studying the effects and the interactions within a microbial community is challenging (Pierce and Dutton, 2022). Many studies exist, that investigate the effect of heavy metals, such as copper, on soil microbial communities (Corcoll et al., 2019; Sutcliffe et al., 2019; Shaw et al., 2020), but the investigation of the surface microbiome of highly touched surfaces is still limited. Yet, especially in hospital settings with an already high selection pressure due to antibiotics and regular disinfection, the risk of giving multi-drug resistance bacteria a further advantage by reducing the total bacterial load of surfaces, has to be considered.

During this study, not only single species, but also a defined bacterial community which simulates the microbiome of public transport was used. This particular bacterial community (Ly et al., 2024) has already been successfully applied as a reference for other experimental settings (Kohl et al., 2024). This approach allows the investigation of differences between single species and a bacterial community after the exposure to copper and copper alloy surface coatings with different copper contents (24 at.%, 53 at.%, 79 at.%, 100 at.%). It enhances our understanding of the antimicrobial effect of copper and deepens the knowledge on what parameters may affect such experimental setups.

The findings of this study aim to contribute to research focused on reducing microbial spread while simultaneously minimizing material costs (full copper vs. copper alloy) and the economic impact of multidrug-resistant (MDR) bacteria.

2 Materials and methods

2.1 Used organisms and preparation of bacterial suspensions

The human skin associated bacterium *S. capitis* was selected for this study, as it is one of the most common genera found in indoor environments. The used strain of *S. capitis* DSM 111179 (*S. capitis*) harbors an antibiotic resistance against rifampicin, which allows selective determination of survival within the simulated bacterial community. Another tested bacterial strain was *B. lata* DSM 23089^T, as a biosafety level 1 strain of *Burkholderia*, allowing straightforward handling. The genus *Burkholderia* is also commonly found in public transport environments. One characteristic of *B. lata* DSM 23089^T (*B. lata*) is its resistance against streptomycin and therefore allowing selective growth. Both strains of *S. capitis* and *B. lata* were purposely chosen for testing, since their morphological composition and therefore the expected reaction to copper surfaces differed. *S. capitis* is gram-positive and coccoid, while *B. lata* is gram-negative and has rod-shaped cells.

TABLE 1 List of strains within the standardized bacterial community, growth conditions and references.

Strain	Growth conditions	References
Burkholderia lata DSM 23089^T	R2A 37 °C	Vanlaere et al., 2009
Corynebacterium halotolerans DSM 44683^T	TSB/TSA 37 °C	Chen et al., 2004
Enterococcus viikkiensis DSM 24043^T	BHI 37 °C	Rahkila et al., 2011
Flavobacterium frigoris DSM 15719^T	R2A 20 °C	Van Trappen et al., 2004
Propionibacterium cyclohexanicum DSM 16859^T	BHI 37 °C	Kusano et al., 1997
Pseudomonas antarctica DSM 15318^T	TSB/TSA 20 °C	Reddy et al., 2004
Sphingomonas rubra DSM 26135^T	R2A 20 °C	Huo et al., 2011
Staphylococcus capitis DSM 111179	R2A 37 °C	Sobisch et al., 2019
Streptococcus halotolerans DSM 101996^T	BHI 37 °C	Niu et al., 2016

R2A, Reasoner's 2A; TSB, tryptic soy broth; TSA, tryptic soy agar; BHI, brain heart infusion.

The species and growth conditions of the bacterial community are listed in Table 1 and are described in greater detail in Ly et al. (2024).

Bacterial strains were grown for 18 h at the respective growth conditions listed in Table 1. The bacterial cells were then harvested in the stationary growth phase. Afterward, the bacterial cultures were centrifuged at 323 *g* for 10 min, and the supernatant was discarded. The cell pellet was resuspended in 50 mL in phosphate buffered saline (PBS; Na_2HPO_4 7.0 g, KH_2PO_4 3.0 g, NaCl 4.0 g, per Liter, pH 7.5). The washing step was repeated once. The cell solutions were set to a concentration of 10^7 cells/60 µL after $OD_{600\ nm}$ measurement. These steps were followed by colony forming unit (CFU) determination on the respective media given in Table 1 to confirm the cell concentration. For the bacterial community, all nine bacterial strains were mixed in equal cell counts with a final concentration of 10^7 cells/mL.

2.2 Copper and aluminum coatings on glass surfaces

The coatings were applied to microscopy slides as substrate material (Labsolute, Th. Geyer) with sample dimensions of 76:

1 Westmetall (2024). Marktdaten [Online]. Available: https://www.westmetall.com/de/markdaten.php [Accessed 23.09.2024].

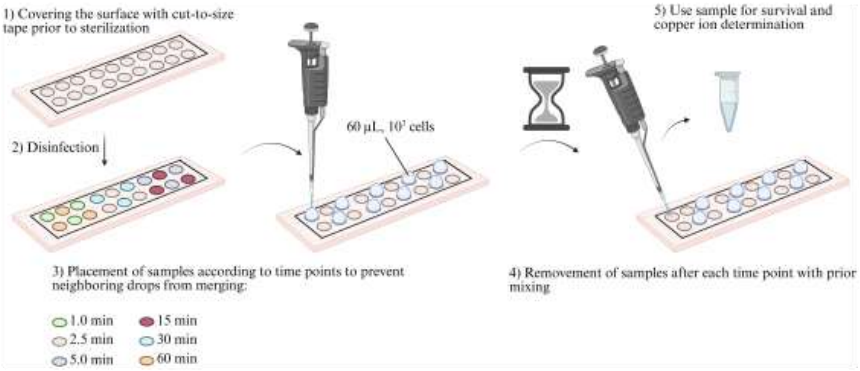

FIGURE 1
Experimental procedure of wet contact killing assay. (1) First, the surfaces were covered with cut-to-size tape with 18 cut-outs with a diameter of 6 mm each. (2) The surface was then disinfected with 99% ethanol and irradiated with germicidal UV-C (254 nm) for 30 min. (3) Then, 60 µL (10^7 cells) of the prepared bacterial solution was applied with a certain time delay to ensure efficient work without the samples merging due to insufficient distance between them. (4) After each time point, the samples were mixed before being transferred to tubes. (5) The obtained samples were then used to determine the survival rate, perform the metabolic activity assay, and ICP-MS measurements.

76: 1 mm. Batch magnetron sputtering (Z400, Systec SVS vacuum coatings, Karlstadt, Germany) was applied for deposition of the coatings. Prior to deposition, one side of the glass substrate was subjected to Ar^+ ion etching for sample surface cleaning and activation. The target material used were dense polycrystalline targets of Cu and Al with a diameter of 100 mm. In order to obtain coatings with different Cu contents, DC co-sputtering was performed at different target powers. The total pressure during deposition was 0.4 Pa in an Ar atmosphere with a constant flow rate of 20 sccm. The coating thickness was 0.8–2.0 µm.

The sputtered coatings were analyzed using an X-ray diffraction (Bruker D8 Advance, Cu Kα radiation, EVA/Topas 4.2 software package, Bruker AXS, Karlsruhe, Germany), which revealed the phases within the deposited coatings. In order to determine the coating thickness, cross sections were analyzed using a scanning electron microscope (SEM) (DSM Ultra 55, Carl Zeiss NTS, Wetzlar, Germany). Additionally, energy-dispersive X-ray spectroscopy (EDS) (Aztec, Oxford Instruments, Abingdon, United Kingdom) was executed at 5 kV to determine the coating content of Cu and Al.

2.3 Wet contact killing

An overview of the experimental procedure is displayed in Figure 1. To prepare the surfaces for the wet contact killing assay, adhesive PVC tape was cut out to defined spots of 6 mm diameter for each bacterial sample, and the surfaces were disinfected with 99% ethanol and subsequent UV-C (254 nm) treatment for 30 min. The microbial samples were prepared in PBS, and 60 µL (10^7 cells/60 µL) were applied on each surface spot for 1, 2.5, and 5 min for *B. lata*, and 15, 30, and 60 min for *S. capitis*. Time points were selected based on survival results of preliminary experiments and allowed the detection of survival within the tested time scale. Of the retrieved samples, 10 µL were used for the determination of bacterial survival, 10 µL for metabolic activity assay, and 10 µL for ICP-MS analysis. The wet contact killing assay was conducted using a minimum of three biological replicates. The experimental setup during the experiment is displayed in Figure 2.

2.4 Determination of bacterial survival

To determine the bacterial survival, a 10-fold serial dilution of each sample was prepared from 10^{-1} to 10^{-8} in PBS and 20 µL of each dilution was plated on respective media plates. For single species testing, R2A agar plates were used. For samples of the bacterial community, selective growth of *B. lata* was performed on R2A containing streptomycin (150 µg/mL), and for *S. capitis* R2A with rifampicin (5 µg/mL) was used. Agar plates were incubated at 37 °C for 48 h. Colony forming units (CFU) were counted afterward to determine the CFU/mL. The survival fraction N/N_0 was then calculated by dividing the CFU/mL of the treatment conditions by the CFU/mL of the initial cell solution.

2.5 Copper ion content detection via ICP-MS

One method of analysis after wet contact killing experiment was the determination of the Cu 63 isotope with Inductively Coupled Plasma - Mass Spectrometry (ICP-MS) analysis, using a NexION® 2000 ICP-MS (Perkin Elmer, Massachusetts, United States). Measurements were performed in the kinetic energy discrimination (KED) mode using Ar (99.999 vol%) as the nebulizer gas and He (99.9999 vol%) as the collision gas. The cell solution was diluted by a factor of 600, using 10 µL of the solution and diluting it in 5,990 µL of 0.69% HNO_3. PBS was used as control sample. For ICP-MS, triplicate samples were used ($n = 3$).

FIGURE 2
Experimental setup during wet contact killing, exemplary on a copper (100 at.%) and aluminum (100 at.%) surface. During the experiment (after step 3 of Figure 1), the surfaces were positioned in petri dishes packed with wet paper towels to maintain constant high humidity. This reduced evaporation of the samples.

2.6 Determination of metabolic activity via resazurin reduction

To investigate the metabolic activity of the bacterial cells after exposure to the tested surface materials, the reduction of resazurin was used as indicator (alamarBlue® Cell Viability Reagent, Thermo Fisher™). This method was used already by Cortesão et al. (2021) with fungal spores. The assay was conducted in a 96-well plate, with a total volume of 200 µL reaction mix per well. The reaction mix consisted of 170 µL culture media with and without antibiotics, as described in see section "2.1 Used organisms and preparation of bacterial suspensions," 10 µL bacterial solution, and 20 µL of alamarBlue. The 96-well plate was incubated at 37 °C for 24 h. The OD_{600nm} and OD_{570nm} were measured every 30 min using a Multi-Detection Microplate Reader (Infinite M200 PRO, Tecan). Before each measurement, the samples were subjected to orbital shaking. To calculate the percentage of resazurin reduction, the standard protocol of the manufacturer was used (Thermo Fisher Scientific, United States)[2]. Each reaction was conducted in biological triplicates ($n = 3$).

2.7 Scanning electron microscopy (SEM)

For the phenotypical analysis of the cells after wet contact killing, scanning electron microscopy was conducted. Sample preparation included the wet contact killing procedure with coatings of 100 at.% Cu and Al, as described in see section "2.3 Wet contact killing," except for the recovery of the samples. The cell solutions were dried on the surfaces for 2 h, followed by fixation using 2% paraformaldehyde (PFA; Merck 104005) in 0.05 M HEPES buffer (pH 7.2) for 1 h (30 min at 25 °C + 30 min at 37 °C). One exception was made for the Cu surface with the bacterial community. Here, the contact time was 1 h and after fixation, the surface was washed three times with PBS and one time with sterile, deionized water.

To examine the surfaces after wet contact killing, a scanning electron microscope (SEM) (DSM Ultra 55, Carl Zeiss NTS, Wetzlar, Germany) was used with the SE detector with a voltage of 5 kV. Prior to the investigations the surfaces were Pt-coated for 80 s to create a conductive surface.

2.8 Sequencing of *B. lata* DSM 23089^T

To identify genes which are potentially related to copper defense or tolerance within the genomes of *B. lata* and *S. capitis*, the following process was conducted. The genome of *S. capitis* DSM 111179 was already submitted by the German Aerospace Center and is accessible as NCBI RefSeq assembly GCF_025272695.1 on NCBI. For *B. lata* DSM 23089^T, no whole genome sequence data was available. We conducted nanopore sequencing as well as whole genome sequencing prior to hybrid assembly. For whole genome sequencing, DNA was extracted using the QIAGEN Genomic-tip 20/G in combination with the Genomic DNA buffer Set, according to the manufacturer's instructions (QIAGEN, Hilden, Germany). Further processing for Illumina sequencing was performed by the Cologne Center for Genomics as described in the following. Libraries were prepared with the TruSeq DNA Nano library preparation kit (Illumina)[3] without PCR, starting with 1 µg gDNA input. Library preparation was followed by clean up and size selection using SPRI beads (Beckman Coulter Genomics) aiming for an insert size of 350 bp. After library quantification (Qubit, Life Technologies) and validation (Tape Station, Agilent), equimolar amounts of library were pooled. The library pool was quantified by real-time PCR using the Peqlab KAPA Library Quantification Kit and the Applied Biosystems 7900HT Sequence Detection System and then sequenced on an Illumina NovaSeq6000 sequencing instrument with a paired-end 2 × 150 bp.

Nanopore sequencing was conducted by Noscendo GmbH, Germany. DNA isolation, library preparation, and sequencing on the MinION benchtop sequencer were carried out as described in Neidhöfer et al. (2023). All genomes were assembled following a

2 ThermoFisher Scientific (2025). alamarBlue Assays for Cell Viability Protocol, for Microplates [Online]. Available: https://www.thermofisher.com/de/de/home/references/protocols/cell-and-tissue-analysis/protocols/alamarblue-cell-viability-reagent-for-microplates-protocol.html [Accessed 04-15 2025].

3 https://support.illumina.com/content/dam/illumina-support/documents/documentation/chemistry_documentation/samplepreps_truseq/truseqnanodna/truseq-nano-dna-library-prep-guide-15041110-d.pdf [Accessed 07-23 2025].

hybrid long-read-first assembly approach using Hybracter v0.11.0 (Bouras et al., 2024). Resulting genomes were annotated using Bakta v1.11.0 (Schwengers et al., 2021) via Bakta Web (Beyvers et al., 2025).

2.9 Statistical analysis

Student's *t*-tests were performed to calculate the level of significance between treated and untreated samples. Untreated samples were not exposed to any wet contact killing and treated samples were exposed to wet contact killing. If the equal variance test (Brown-Forsythe) failed between the two data sets, Welch's *t*-test were performed instead of Student's *t*-test, since the latter assumes that the variances of the two samples are equal. If the data of both data sets were not normally distributed, the Mann-Whitney Rank Sum test was performed instead, as this test makes no assumptions about the distribution of the data. To calculate the significant differences within the alamarBlue data sets, two-way Repeated Measures (RM) ANOVA was performed to compare the positive control to respective bacterial samples. The control samples (PBS) of the ICP-MS measurements were compared to the bacterial samples by paired *t*-test. Significant differences were defined with $p \leq 0.05$ (*), $p \leq 0.01$ (**) and $p \leq 0.001$ (***). All statistical analyses were executed with SigmaPlot 14.5 (Systat Software Inc).

3 Results

3.1 Analysis of coating

The deposited coatings were crystallin after deposition. The phases of the coatings formed during processing were determined using X-Ray measurements. The 100 at.% Cu coating and the 100 at.% Al coating consisted of only one phase of Cu or Al. For the alloy coatings with variation of Cu content intermetallic phases of Cu and Al were analyzed.

In order to determine the thickness of each coating type, cross sections were investigated in the SEM. Table 2 shows the coating thicknesses. Due to its ductility, Cu is difficult to prepare by metallographic preparation methods, therefore the coatings had a slight difference in thickness as a sputtering rate could not be determined without intensive preparation methods. However, this subtle variation in thickness was not expected to play any role in the antimicrobial behavior.

TABLE 2 Coating thickness of each coating type measured in cross section via scanning electron microscope (SEM).

Coating (Cu content in at.%)	Coating thickness (μm)
100	~1.4
79	~0.8
53	~1.4
24	~0.8
0	~2.0

3.2 Bacterial survival on surfaces with different copper contents

The bacterial community and the single species *S. capitis* and *B. lata* were exposed to a variation of surfaces for different time periods and their survival was determined. Results of the survival, survival fraction N/N_0 and significance tests are summarized in Supplementary Tables 1–7. Over the maximum time tested of 60 min, the survival fraction of *S. capitis* was significantly reduced ($p < 0.001$) on the 100 at.% copper coating in both tested scenarios (single vs. within bacterial community, Figures 3a, b). Comparing the survival of *S. capitis* as single species and within the bacterial community, first differences were observed from the second time point at 30 min. Here, the survival reduction as single species was 2-log scales (10^{-2}), while within the bacterial community, the survival fraction dropped to less than 10^{-3} cells/mL. Contrarily, after 60 min of exposure, *S. capitis* showed less reduction within the bacterial community when compared to its testing in pure culture. This observation was reflected in a difference of 2-log scales. The direct comparison of single species and bacterial community survival on the different surface types was conducted for the last time point (60 min) (Figure 3c). On the one hand, no significant difference was observed between *S. capitis* as single species and within the bacterial community after contact killing on 100 at.% Al and 53 at.% Cu. On the other hand, a significant difference was observed for the 79 at.% Cu ($p = 0.021$, survival single 42.3%; within bacterial community 161%) and 100 at.% Cu surface ($p = 0.013$, survival single 6.9×10^{-5}%; within bacterial community 8.8×10^{-3}%). Therefore, *S. capitis* showed improved survival within the bacterial community.

The survival fraction of *B. lata* was determined based on the exposure of the bacteria for 1, 2.5, and 5 min (see Figures 3d, e), based on preliminary experiments conducted, which showed no detectable survival of *B. lata* after 15 min of 100 at.% Cu surface contact (data not shown). Within (Figure 3d), the survival fraction is displayed for the testing of *B. lata* as a single species. Several similar trends were observed in the survival of *B. lata* as a single species as well as within the bacterial community when compared to *S. capitis*. For one, they were both significantly affected in the survival by the 100 at.% Cu coatings ($p < 0.001$, survival fraction *B. lata* single 3.74×10^{-5}). This was also the case for *B. lata* within the bacterial community ($p < 0.001$, survival fraction 5.33×10^{-3}, Figure 3e). Focusing on the last time point (5 min), a 2.5-log discrepancy was shown between survival as single species and within the bacterial community. Another akin tendency between *S. capitis* and *B. lata* was that single strains and the strains within the community were affected similarly at the first time point after 1.0 min. The last time point (60 and 5 min) showed better survival of the bacteria within the community, also for both selected species (Figures 3b, e). However, as displayed in Figure 3f, there was no significant difference in survival after 5 min of contact killing between *B. lata* as singles species and *B. lata* within the bacterial community.

Overall, *B. lata* showed a higher susceptibility to the copper coated surfaces compared to *S. capitis*. Our results showed that

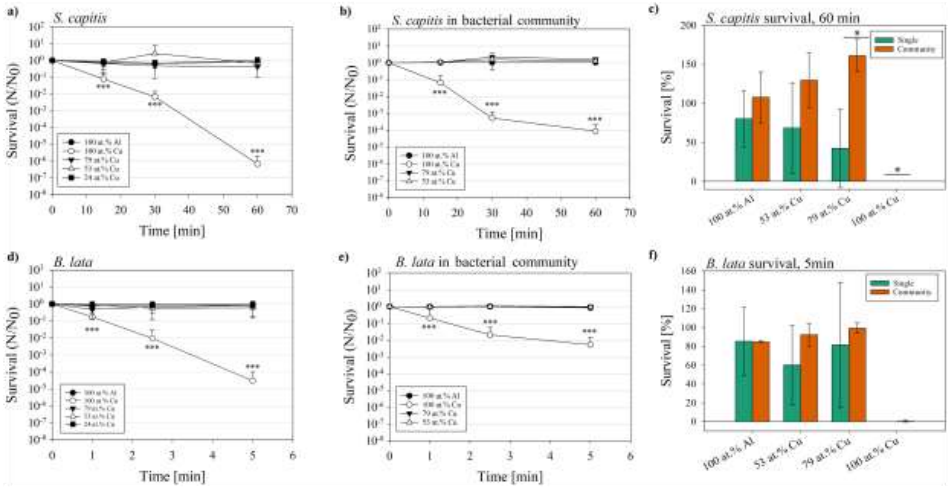

FIGURE 3
Survival fraction (N/N_0) of the species *S. capitis* and *B. lata* after exposure to glass slides coated with copper gradients of 100 at.%; 79 at.%, 53 at.%, and 24 at.%, or coated with 100 at.% aluminum as negative control. Survival fraction of *S. capitis* as **(a)** single species and **(b)** within the bacterial community, survival **(c)** after 60 min of contact killing. *B. lata* as **(d)** single species and **(e)** within the bacterial community, and **(f)** survival after 5 min of contact killing. Results shown are mean and standard deviation of three biological replicates. Statistically significant differences in survival fraction relative to the 100 at.% Al control **(a,b,d,e)**, and the differences in survival between single species and respective species within the bacterial community **(c,f)** are displayed. Significant differences were defined with $p \leq 0.05$ (*), $p \leq 0.01$ (**) and $p \leq 0.001$ (***).

both *B. lata* and *S. capitis* survived a longer exposure to copper surfaces better within a bacterial community compared to exposure as a single species. However, we only saw significant differences for *S. capitis*.

3.3 Metabolic activity after wet contact killing

To evaluate the metabolic activity of *S. capitis* and *B. lata* after exposure to the coated surfaces as single species and within the bacterial community, an alamarBlue assay was performed over 20 h.

Figure 4 displays the measured metabolic activity via alamarBlue assay of the single species *S. capitis* (Figure 4a) and *B. lata* (Figure 4c) and the species within the bacterial community after exposure to the surfaces and settings as described earlier. Significance was tested and p-values were summarized in Supplementary Tables 8, 9. In the alamarBlue assay for samples of the bacterial community, rifampicin was supplemented in the media in samples which were exposed to 60 min of wet contact killing for selective growth and measurement of *S. capitis* (Figure 4b). Streptomycin was added into the media of samples that were prolonged 5 min of wet contact killing to select for *B. lata* (Figure 4d).

Pure cultures of *S. capitis* (Figure 4a) that were exposed to either the control material 100 at.% Al, 53 at.% Cu, 24 at.% Cu, as well as the positive control (untreated bacteria) increased their metabolic activity exponentially during the early phase: The alamarBlue reduction for those samples reached nearly 100% after ~7 h into measurement. Interestingly, the *S. capitis* single species 79 at.% Cu sample showed a delayed metabolic activity (8.5 h until maximum alamarBlue reduction). The greatest affected samples were those after exposure to the 100 at.% Cu coated surface, which, for the *S. capitis* single species only showed slight increase up to ~22% after 20 h of incubation and displayed very significant ($p = 0.003$) differences compared to the positive control.

In contrast, *S. capitis* within bacterial community (Figure 4b) exposed to 79 at.% Cu and 53 at.% Cu reached a maximum alamarBlue reduction of 84.8% and 87.6%, respectively, only after 9–10 h of measurement. The positive control showed an even stronger alamarBlue reduction after 8 h. As for the 100 at.% Cu samples, the reduction started after approximately 15 h of incubation.

Figure 4c displays the metabolic activity of *B. lata* after 5 min of wet contact killing on all tested surface types, while (Figure 4d) shows it for *B. lata* within the bacterial community on 100 at.% Cu, 79 at.% Cu, and 53 at.% Cu. A maximum alamarBlue reduction was reached by the *B. lata* single species samples after ~8 h into measurement for the positive control, 53 at.% Cu, 24 at.% Cu, and 100 at.% Al treated samples. For *B. lata*, pure cultures that were exposed to 79 at.% Cu surface, a linear increase of the metabolic activity was followed by an exponential rise after 18 h of incubation, resulting in a highly significant ($p < 0.001$; 20 h into alamarBlue: 79 at.% Cu 58%; PC 113%) difference compared to the positive control. Minimal increase of the alamarBlue reduction was observed for the 100 at.% Cu coated samples, resulting in a

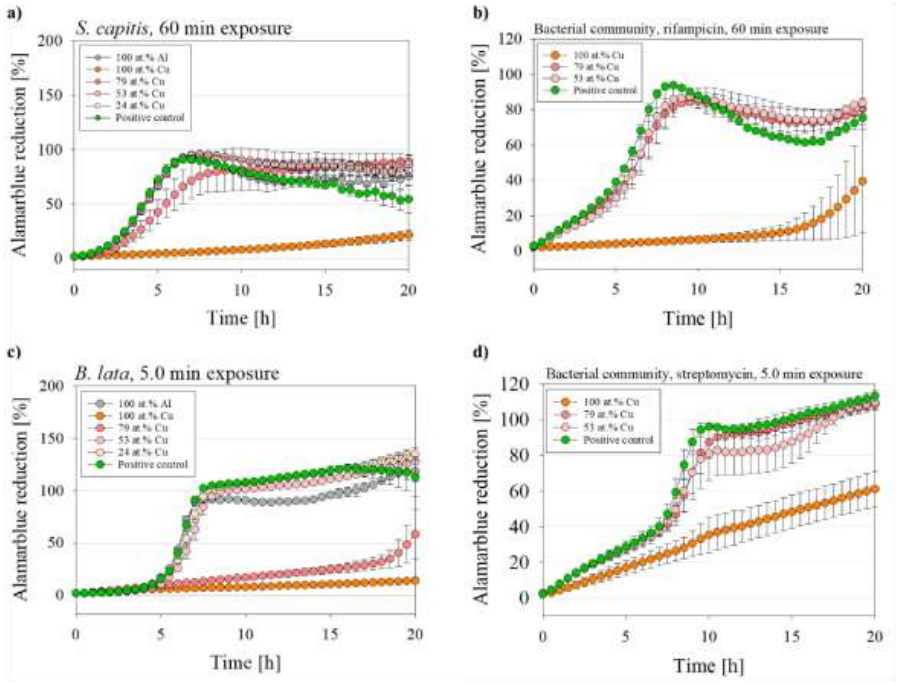

FIGURE 4
Metabolic activity of *B. lata* and *S. capitis* as single species and within the bacterial community after wet contact killing assay. The species **(a)** *S. capitis* and **(b)** *S. capitis* within the bacterial community (medium supplemented with rifampicin) were treated on the surfaces for 60 min. The species **(c)** *B. lata* and **(d)** *B. lata* within the bacterial community (medium supplemented with streptomycin) were tested for 5 min to the surfaces prior to the metabolic activity measurement. The contact killing was performed with coatings with varying copper content, aluminum and positive control (= untreated bacterial sample with no wet contact killing). The data is displayed as mean and standard error (n = 3).

reduction of approximately 14% after 20 h of incubation and a very significant difference (p = 0.002; 20 h into alamarBlue: 100 at.% Cu 14%; PC 113%) compared to the positive control. Similar to the positive control, other samples, such as 53 at.% Cu and 24 at.% Cu, showed an alamarBlue reduction of over 100%. This was also observed in the advanced measurement times in Figure 4d. This oversaturation can be traced back to different reasons. For instance, accumulation of the reduced product resorufin, or the over-reduction of alamarBlue to hydroresorufin, which can be avoided by a shorter incubation time (O'Brien et al., 2000).

For the samples of *B. lata* within the bacterial community, the maximum metabolic activity was reached two hours later compared to the pure culture, after ~10–11 h, for the positive control and 53 at.% Cu surface samples. A great difference between single species and bacterial community samples was displayed for the 79 at.% Cu and 100 at.% Cu surfaces. In contrast to the single species exposed to 100 at.% Cu with 14% maximum alamarBlue reduction, *B. lata* within the bacterial community resulted in a linear increase of alamarBlue reduction, with a final reduction of approximately 60% after 20 h of incubation. Further, the results of the 79 at.% Cu sample of the bacterial community were comparable to the 53 at.% Cu sample with increased metabolic activity, whereas as pure culture, the sample exposed to 79 at.% Cu showed significantly reduced metabolic activity.

To rule out any effects of the addition of the antibiotics, the metabolic activity assay was conducted without antibiotics too. The results showed no significant difference between the trend of the alamarBlue reduction (Supplementary Figure 3). However, other bacteria within the bacterial community could have contributed to the alamarBlue reduction in this case.

The metabolic activity of both *S. capitis* and *B. lata* reduced with increasing copper content, as indicated by decreased reduction of resazurin. The metabolic activity was also measured for each time point that was tested in section 3.1 (1 min, 2.5 min for *B. lata* and 15 min, 30 min for *S. capitis*), showing mostly similar behavior of the resazurin reduction (Supplementary Figures 1, 2).

To conclude this section, the metabolic activity assay showed that the 100 at.% Cu surface treatment led to a decreased alamarBlue reduction for all single species and bacterial community when compared to the positive controls. As for *S. capitis* single species, the maximum metabolic activity was 22% after 20 h into the assay. The samples exposed to the other materials showed high resazurin reduction after only 7.0–8.5 h. These results were similar for *S. capitis* within the bacterial community.

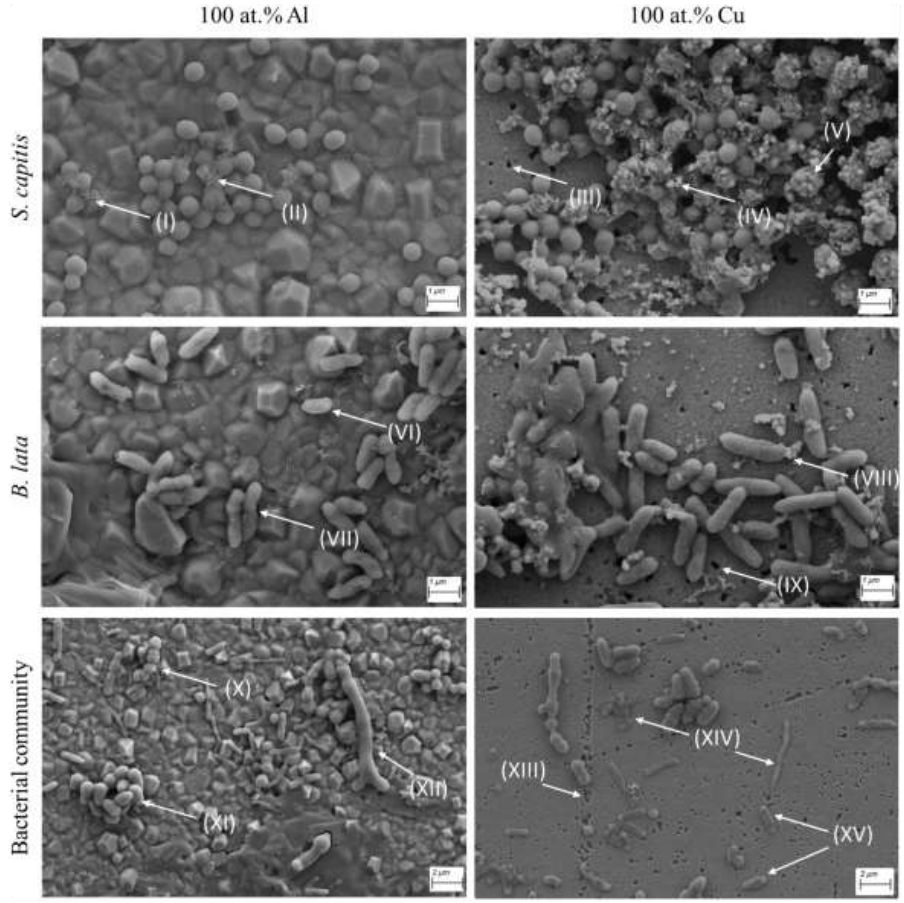

FIGURE 5
Scanning electron microscopy (SEM) imaging of *S. capitis*, *B. lata*, and the bacterial community on 100 at.% Al and 100 at.% Cu surfaces after 2 h of contact (1 h for the bacterial community on copper). (I, II, IV, V) cell debris, (III, IX, XIII) indication of surface degradation, (VI, VII, VIII, XIV) visibly damaged cells, (X, XI, XII, XV) intact cells.

For the single species *B. lata*, a maximum alamarBlue reduction of 14% was reached after 20 h of measurement after wet contact killing on 100 at.% Cu. The sample treated with 79 at.% Cu surface also exhibited a significantly reduced metabolic activity with a maximum of 58% after 20 h of measurement. The other materials and the positive control showed peak reduction only after 10-11 h of measurement. Compared to the single species, the bacterial community samples showed higher metabolic activity for the 100 at.% Cu and 79 at.% Cu samples.

Lastly, the bacterial community samples (5 min and 60 min wet contact killing) treated with 100 at.% Cu surface coating, showed a maximum alamarBlue reduction of 40% and 60%, respectively. In contrast, the single species *S. capitis* and *B. lata* exhibited a maximum alamarBlue reduction of only 22% and 14%, respectively.

3.4 SEM imaging of bacterial cells on copper and aluminum containing coatings

While the results above present an overview of what effect the copper containing surfaces have on the survival and metabolic activity of the cells, SEM imaging of selected samples was conducted to gain further insights. Cell suspensions of *S. capitis*, *B. lata* and the bacterial community were applied on 100 at.% Cu and 100 at.% Al surface coatings, respectively (Figure 5). A contact time of approximately 2 h was selected for full evaporation of the sample prior to sample fixation for SEM. Only for the bacterial community sample on 100 at.% Cu, the contact time was limited to 1 h due to protocol optimization. This difference in time has to be taken into

account for the following observations and consecutive comparison of the samples.

The exposure of *S. capitis* on surfaces containing aluminum and copper showed distinct differences: First, only little damage of the cells or products of the cells were observed for *S. capitis* on 100 at.% Al (I, II). In contrast, on 100 at.% Cu surface, cells of *S. capitis* were found surrounded or completely covered by potential cellular debris or other organic material (IV, V). However, the cells showed no striking anomalies when compared to the cells that were exposed to 100 at.% Al surface coatings. It was noticeable that degradation of the copper coatings occurred, leaving holes of varying diameters within the coatings (III).

For *B. lata*, which was observed to be the more susceptible species according to the survival after exposure on copper surfaces, morphological damage was visible for both surface types, aluminum (VI, VII) and copper (VIII). Interestingly, most cells seemed to be phenotypically intact. Similar to *S. capitis*, some extracellular debris was observed next to or on the cells on the copper coating. Additionally, signs of degradation in the surface coating were also observed (IX).

The last tested condition was the bacterial community. The different cell types and morphologies were observed (X, XI, XII), showing no morphological impact or damage on 100 at.% Al surface coating. Again, as with the two tested pure cultures, the surface of the 100 at.% Cu coating showed characteristics of degradation (XIII). Comparable to the aluminum surface image of the two strains, both, damaged and dead cells (XIV), as well as seemingly intact cells (XV) were observed.

3.5 Copper tolerance and defense related genes in *S. capitis* and *B. lata*

To explain the higher susceptibility of *B. lata* for copper related stress compared to *S. capitis*, genes that are related to copper tolerance or defense, and genes known for coping with oxidative stress were identified in both strains' genomes (Table 3). Multiple genes were detected in both strains. Surprisingly, more potential copper and oxidative stress response genes were detected in *B. lata* than in *S. capitis*. It should be noted, that the presence of genes in the genome alone does not guarantee their expression. It is, therefore, difficult to make strong interpretations based on this information. Nevertheless, as for *S. capitis*, the copper-sensing transcriptional operon repressor gene *csoR*, has been identified. This gene represents one of the main copper regulators in Gram-positive bacteria (Baker et al., 2011).

3.6 Copper ion content in the cell solution after wet contact killing

The copper ion release is relevant for the contact killing effectivity. The results of the copper ion release after different time periods of wet contact killing on the 100 at.% Cu surface coating is displayed in Figure 6. Overall, the highest copper ion concentrations were reached in the control samples, containing no bacteria and only PBS (buffer), with 21.22 mg/L after 60 min on the surface.

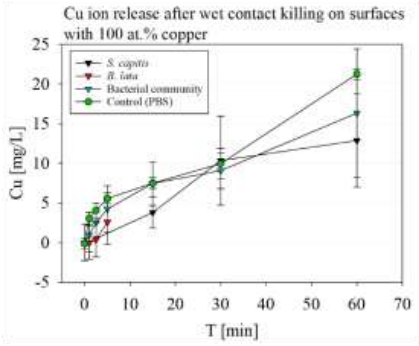

FIGURE 6
Copper ion release detection via ICP-MS after wet contact killing on surfaces with 100 at.% Cu content coatings, testing *S. capitis*, *B. lata*, bacterial community and the control containing only PBS buffer.

The copper ion release after wet contact killing with *S. capitis* over a course of 60 min showed overall high standard deviations. The first time point of 15 min pended slightly lower than 5 mg/L, and increased to a similar copper-ion concentration compared to the buffer control to 10 mg/L at 30 min. After 60 min, the copper ion concentration reached ~13 mg/L.

For *B. lata* samples, only a slight increase of copper-ions was observed after 5 min of wet contact killing, but no significance was determined.

The copper ion release of the surfaces after exposure of the bacterial community to the surfaces over 60 min showed similar concentrations compared to the control, while exhibiting high standard deviations.

The results showed that highest copper ion release was detected in the control solution, PBS. PBS is a salt containing solution, which leads to a corrosion effect, triggering an increased ion release (Luo et al., 2019). Although the copper ion concentration was highest for the PBS control, no significant difference was determined by paired *t*-test compared to the bacterial samples.

4 Discussion

In this study, bacterial species were exposed to surface coatings which contained different copper concentrations and aluminum as control element. The tested microorganisms were *S. capitis* DSM 111179, *B. lata* DSM 23089^T and a bacterial community containing the two strains mentioned above and seven other species whose genera are most abundant in public transport environments. These species were selected due to the relevance of reducing microbial spread in public transportation environments, where many people come into contact with and transmit microorganisms. Since humans shape an environments' microbiome, indoor environments have many similarities, as typical skin microorganisms. The microbial composition of an environment can be influenced by surface materials, (Hsu et al., 2016) as well as temperature, relative humidity, and ventilation

TABLE 3 Copper tolerance and oxide stress related genes and functions found in the genomes of *S. capitis* and *B. lata*.

Gene	Protein function	*S. capitis*	*B. lata*
copC	copper resistance protein; copper homeostasis periplasmic binding protein	×	×
pcoD	copper resistance protein D	–	×
copD	located in the inner membrane together with pcoD with yet unclear function	–	×
copZ	copper chaperone; copper chaperone & heavy metal transport/detoxification protein	×	×
cycoC	Heme/copper-type cytochrome/quinol oxidase subunit 3-like	–	×
cirA	TonB-dependent copper receptor	–	×
ompR	Two-component system copper resistance phosphate regulon response regulator	–	×
cueR	Cu(I)-responsive transcriptional regulator	–	×
soxR	redox-sensitive transcriptional activator SoxR	–	×
csoR	copper-sensing transcriptional repressor	×	–
csoZ	putative copper chaperone	×	–
	Copper binding protein	–	×
	Copper transporter	–	×
sufI	Multicopper oxidase, type 3	–	×
sodC	superoxide dismutase [Cu-Zn]	×	×
	catalase	×	×
katG, katE, btaE	Glutathione peroxidase	–	×
	Glutathione peroxidase	×	–
gstA, yfcF	Glutathione-S-transferase, glutathione transferase	–	×

(Rai et al., 2021). Although the microbial communities vary within different environments, such as public transportation, a core microbiome of the public transport exists which differs to other distinct environments (Danko et al., 2021). Indoor settings such as offices are more likely to have a lower outdoor/indoor exchange compared to mass transit, where doors open every few minutes. Commuters lead to a higher number of people and more variable composition in the cabin environment compared to other indoor settings.

The investigation of the public transport microbiome and the microbial reduction in these settings is relevant for groups of the population that are susceptible to (opportunistic) pathogens, such as elderly and other immune compromised patients. The performed experimental design was carried out to test the difference between the effectiveness of antimicrobial properties against single organisms and organisms within a bacterial community, with the latter closely mimicking real environments. The second aim of the study was to investigate the effectivity of novel surface coatings as a sustainable alternative to full copper materials to investigate the minimal copper concentration for antibacterial effects for more economical and efficient usage.

4.1 100 at.% Cu coatings show highest antibacterial activity

The results of the bacterial survival after wet contact killing showed, that only the 100 at.% Cu coating had significant antibacterial effect on both tested strains, as single species and in the bacterial community. The 79 at.% Cu coating only affected the *S. capitis* as single species significantly more than within the bacterial community, but not compared to the control 100 at.% Al. In contrast, previous studies showed that copper alloys with $\geq$ 58% copper content showed microbial reduction on surfaces (Karpanen et al., 2012). However, the tested surfaces in the study by Karpanen et al. (2012) were investigated over a course of 12 weeks in a real setting with no defined bacterial inoculum, and the overall study design and aims differed. Therefore, it would be of interest to expose cells on the different surfaces used in our study over a longer time period. Another approach to test the antibacterial activity of the surfaces would be dry contact killing, which is closer to real environment settings and has shown to be more effective (Santo et al., 2011). This could be explained by fast copper intake which leads to high copper susceptibility. Furthermore, the bacteria within our study were harvested at the stationary growth phase. Consequently, it would be of interest to perform the wet contact killing experiments with bacteria within the exponential growth phase, since a higher level of sensitivity is expected (Battesti et al., 2011).

In a study by Fowler et al. (2019), the minimum inhibitory concentrations (MIC) of Cu ions were investigated on *Staphylococcus epidermidis*, showing an inhibitory effect after 5 h of exposure to 90 mg/L Cu ions within the sample solution. This result was not observed within the experimental setup of our study. However, both study designs differed. Fowler et al. (2019) conducted direct treatment of Cu ions in culture media, while the bacteria in our study were in PBS, aggravating the Cu ion stress tolerance. We measured Cu ion concentrations between ~1 and 21 mg/L with bacterial exposure times of 1.0–60 min on 100 at.% Cu. It is noticeable, that the measured Cu ion concentrations

were higher compared to other wet contact killing studies, which measured maximum Cu ion concentrations of ~20 µg/L after 60 min of wet contact killing range (Timofeev et al., 2025). Whereas in our study, Cu ion concentrations reached 21 mg/L. The sample preparation was similar, although different organisms and materials (full copper, no coatings) were used in the study by Timofeev et al. (2025). Interestingly, the detected Cu ion concentrations are more comparable to a wet contact killing study, which was conducted with *Escherichia coli* K12 (Luo et al., 2017).

It shows, that Cu ions seem to have a different weight of effect on the different bacterial species, which can be attributed to the variability of copper defense mechanisms and their effectivity, as described in following discussion (Solioz et al., 2010; Bondarczuk and Piotrowska-Seget, 2013; Giachino and Waldrom, 2020; Lima et al., 2022).

The decreased antibacterial effect of the Cu-Al alloy coatings could be traced back to the significantly lower Cu ion release of the alloys compared to the 100 at.% Cu coatings (Supplementary Figure 4). The reason for the lower Cu ion release could be related to the intermetallic phases between Cu and Al, which are strongly bound and allows for only reduced Cu ion release (Shi et al., 2020). For more detailed investigation of the antibacterial properties of the surfaces, a closer look to oxidative stress caused by ROS will be helpful. This could be performed indirectly by the investigation of possible protein oxidation or DNA damage using gel electrophoresis, or membrane damage could be observed by fluorescence microscopy and LIVE/DEAD staining (Fernández et al., 2011; Berney et al., 2007). A direct detection of ROS could be conducted using oxidative stress markers (Li et al., 2016).

4.2 Different genotypes result in different survival

The wet contact killing experiments showed that both tested bacterial strains were not similar in their susceptibility to copper. Although *B. lata* was exposed to an overall low copper ion concentration of 5 mg/L after 5 min, its susceptibility to the 100 at.% copper containing surface was significantly higher with a > 4-log reduction in survival, compared to *S. capitis*, which was exposed to ~13 mg/L after 60 min. The survival of *S. capitis* after 15 min of wet contact killing was similar to the survival of *B. lata* after only 2.5 min of wet contact killing on 100 at.% copper content surface. The high susceptibility of *B. lata* to copper was already observed in preliminary tests, exhibiting a 100% reduction after only 15 min of exposure (data not shown). This observation is not reflected in studies that have tested different strains of *Burkholderia glumae*. In a study which conducted contact killing assay with strains of *Burkholderia glumae*, survival was still detectable after 4 h of contact time (Cui et al., 2014). However, membrane damage was already observed after 1 min of contact, visualized by LIVE/DEAD staining. This was not clearly shown in our study by SEM of *B. lata* after 5 min of contact, indicating a high variability of behavior even among the same genus. A reason for this discrepancy related to copper tolerance could be manifold. Different species can differ drastically due to their different isolation and genotypes. The isolation sides differ between *B. glumae* (rice seeds) and *B. lata* (forest soil) and therefore selective pressure led to a different set of genes. Additionally, the genome sizes of *B. glumae* LMG 2196 with 6.8 Mbp and *B. glumae* AU6208 with 6.1 Mbp are smaller compared to *B. lata* with 8.6 Mbp allowing a greater gene number. While the authors found *copC* in the tested strains of *B. glumae*, we found multiple genes related to copper tolerance and defense in *B. lata* and *S. capitis*. Nevertheless, *B. glumae* equipped with only *copC* lead to a higher copper tolerance compared to *B. lata*. It is remarkable, that more copper resistance-related genes are encoded in *B. lata* compared to *B. glumae* and *S. capitis* despite its decreased survival after copper contact. The genes found in *B. lata* were e.g. *copC, copD, copZ, pcoD, sufI*, and *cirA* and in *S. capitis*, relevant genes such as *copC, csoZ, copZ*, and *csoR* were found. However, the actual expression of those genes is unclear and needs to be investigated in future studies. Further, the function of these genes can differ between genera. Consequently, the function of those genes can only be assumed based on available findings that investigated other bacterial species and genera. The occurrence of copper- and oxidative stress related genes in both *B. lata* and *S. capitis* was compared with existing data on similar species, if information was available. For *B. lata*, the gene *copC*, coding for the copper resistance protein or copper homeostasis periplasmic binding protein was detected. It has been shown on *Burkholderia cenocepacia*, that copC functions as a Cu ion binding protein, allowing copper detoxification (Higgins et al., 2020). *copC* was also detected in *Staphylococcus aureus*, acting as a copper transport gene (Kinnevey et al., 2013). Other genes that were detected in the tested *S. capitis* such as *csoZ*, *copZ*, and *csoR* were found in *S. aureus* before (Baker et al., 2011). The *csoR* gene, encoding for the copper-sensing transcriptional repressor, is considered as one of the main copper regulators in Gram-positive bacteria (Baker et al., 2011), which we assume to be significant in the great survival of *S. capitis* compared to *B. lata*.

4.3 Gram-negative vs. gram-positive bacteria in their copper defense

As shown above, even species of one genus can differ in their survivability against antibacterial copper surfaces. What distinguishes *B. lata* from *S. capitis*, is their gram stain and therefore their bacterial structure. *S. capitis* is gram-positive and *B. lata* is gram-negative. Other gram-negative strains such as the model organism *Escherichia coli* or *Pseudomonas aeruginosa* have been tested in previous studies on surfaces with different copper contents. *E. coli* showed total inactivation varying between 15 and 180 min (Wilks et al., 2005; Różańska et al., 2017). *P. aeruginosa* showed an inhibition of 99.9% when treated with 800 µg/mL of copper nanoparticles, while *S. capitis* could endure this concentration (Betancourt-Galindo et al., 2014). The difficulty of comparing study designs and model organisms is highlighted by the observed differences in antimicrobial effectivity of surfaces across studies. The high survival of *S. capitis* was anticipated due to a thick layer of peptidoglycan, which has been suggested to be the reason for better survival compared to gram-negative *Pseudomonas aeruginosa* after treatment with copper nanoparticles (Betancourt-Galindo et al., 2014). Studies such as Różańska et al. (2017) showed, similar to our results, that *Staphylococcus* survived on surfaces for long periods of time, ranging from ~45 to ~220 min,

depending on the copper alloys tested. Although both gram-positive (*S. capitis*) and gram-negative (*B. lata*) bacteria were susceptible to copper toxicity, the gram-negative strain used in our study showed significantly higher susceptibility, which may be due to increased lipid peroxidation, leading to membrane damage, DNA damage and cell death (San et al., 2015). Further, the above-mentioned genes related to copper tolerance and defense could be higher regulated in *S. capitis* compared to *B. lata*. This has to be investigated in future studies. Nevertheless, gram-negative bacteria are not expected to be more susceptible to copper stress compared to gram-positive in general. Gram-negative bacteria are able to provide active control through the outer- and inner membrane and are equipped with a strong efflux pump system (Bondarczuk and Piotrowska-Seget, 2013). Under consideration of the cell sizes (*S. capitis* 1 μm, coccoid; *B. lata* 2 μm, rod-shaped), 83.4% of 10^7 cells of *S. capitis* were expected to occur as a monolayer on the 6 mm diameter surface contact area, while 89.4% were calculated for *B. lata*. This could enhance the higher susceptibility of *B. lata* to copper compared to *S. capitis*, but only to some extent, since the calculations are based on one selected size and without taking the cell shape into account. However, the cell size varies, e.g., it can be between 0.5 and 1.0 μm for *S. capitis*.

4.4 Bacterial survival after long exposure times is higher within a bacterial community

As shown by Salah et al. (2021), many studies have tested the antimicrobial effectiveness of different copper and copper alloy materials and surfaces. However, while most studies were conducted with strains of *E. coli* or *S. aureus,* none of them tested the effectiveness against microbial communities. In this study, we tested a bacterial consortium of nine bacterial strains with different genera, based on Ly et al. (2024). The results of this work showed the reduced antibacterial effectivity of the test surfaces on the bacterial community in comparison to single species.

With long term use of antimicrobial materials, it should be noted that the microbiome of surfaces change. The composition can change and the diversity has been observed to lower within microbial communities that have been exposed to increased copper concentrations (Schmidt et al., 2012; Sutcliffe et al., 2019; Shaw et al., 2020). Occurring species that were copper sensitive decreased, and copper tolerant species occurred to be more dominant in the microbiome (Gustavson et al., 1999; Serra et al., 2009; Ancion et al., 2010; Corcoll et al., 2019). These studies did not investigate associated resistance to antibiotics, although it displays an important aspect that was shown in a study by Arndt et al. (2025, unpublished manuscript). The authors demonstrated the risk of antibiotic resistance enhancing the copper tolerance in strains of *Enterococcus faecium*, highlighting the conscious application of countermeasures and drug use. This specific combination of antibiotic resistance and surface transmission has been subject of many studies within the clinical environment (Stephens et al., 2019; Xiao et al., 2019). However, the transmission of (opportunistic) pathogens is not limited to the clinical environment, but is relevant for all public environments, where the spread and emergence of antibiotic resistances needs to be reduced.

Within our used study design, cell layering on the surface was expected and intended for a more realistic approach. The determination of the actual multilayer was a challenge within this study, since the different cell sizes and shapes vary enormously and therefore error would be expected. One hypothesis for the increased survival of the selected species *B. lata* and especially *S. capitis* within the bacterial community is the cell layering and reduced contact to the surfaces. Due to varying cell morphologies of the different used bacterial species (as shown in see section "3.4 SEM imaging of bacterial cells on copper and aluminum containing coatings"), layers could be thicker than those resulting from layering of single species. Thus, less cells of *S. capitis* and *B. lata* were exposed to the surfaces when the bacterial community was tested. As a result, less cells could be damaged.

Another hypothesis is based on the metabolic interaction between the bacterial species. Metabolic interaction can lead to the spread and use of metabolic compounds that help cells which are normally more susceptible to copper (Williams et al., 2016). Copper defense mechanisms by bacteria within the bacterial community, such as the production of extracellular vesicles to secrete copper out of cells, could also benefit other bacterial species due to a lower toxic copper concentration in the environment (Lima et al., 2022). Inter-bacterial interactions and metabolic changes are already known among bacteria against toxic compounds (Hong et al., 2018; Dai et al., 2024). Since the survival of *B. lata* within the bacterial community was higher compared to the single exposure of *B. lata* to copper even after only 5 min of contact, rapid metabolic changes and inter-bacterial interactions could have impacted the increased survival besides the cell layering as described in the previous section.

The formation of biofilms is a common structure which leads to the resistance of bacterial cells against antibacterial compounds. However, this is not expected for the experiments, since the cells were present in PBS, a low nutrient solution. Therefore, potential biofilm formation by e.g., biofilm forming species *S. capitis* was not expected for the copper exposure times of up to 5 and 60 min, respectively.

4.5 Metabolic activity after surface exposure corresponds with bacterial survival

After wet contact killing on 100 at.% copper surface, the metabolism of both species *S. capitis* and *B. lata* showed significantly reduced and delayed activity in both scenarios as single species and within the bacterial community corresponding with results of their respective bacterial survival. The single species testing showed reduced metabolic activity compared to the bacterial community, especially for *B. lata*. Here, even the 79 at.% copper surface caused a delayed metabolic activity of the cells, although it was not reflected in the survival data. This could be explained by the strategic metabolic downregulation to preserve important functions for survival while minimizing cell damage (Traxler et al., 2011; Qi et al., 2023). However, a decrease would also be observed in the survival, which was not the case in our study. Another mechanism which maintains survivability and simultaneously alters the metabolic activity of bacterial cells is

antioxidant response. The oxidative stress that is induced by copper might have caused a temporary metabolic downregulation and, therefore, delay of the alamarBlue metabolization. Simultaneously, oxidative stress response would activate the production of antioxidants, such as glutathione peroxidase, superoxide dismutase and catalase, which are genes found in *S. capitis* and *B. lata*. Beside the oxidative stress response, multiple genes related to copper defense that were found in both genomes, such as *copC* and *copZ* are assumed to be upregulated during copper stress, as well as active copper transport (Teitzel et al., 2006). The *cirA* gene was found in *B. lata*, and is evidently downregulated in *Acidithiobacillus ferrooxidans* D2 during copper stress. *cirA* is a TonB-dependent copper receptor, which restricts copper uptake by the regulation of transporters (Salazar et al., 2013).

A clear determination and overview of genes, which are up- and downregulated during copper stress in the tested species within this study is not given and, therefore, poses a limitation of this study. Nevertheless, we assume that the metabolic upregulation of genes related to copper stress was not significant, especially in *B. lata* due to its high susceptibility to the wet contact killing assay, which was reflected in the reduced metabolic activity on the 79 at.% Cu and 100 at.% Cu surfaces. In general, the metabolic activity assay confirmed the survival data, and showed additional susceptibility of the tested strains toward exposure to copper surfaces that was not visible by bacterial survival alone.

4.6 Intact cell morphology after copper exposure

The SEM imaging of the 100 at.% copper and 100 at.% aluminum coatings after contact killing, showed a slight increase of extracellular products and other organic matrix surrounding the cells on copper surfaces. Those accumulations could be determined as extracellular vesicles, which form after stress response and have been observed both in gram-positive and gram-negative bacteria (Kim et al., 2015; Bose et al., 2020; Briaud and Carroll, 2020). Such structures have been shown in a cyanobacterial strain and were identified as a copper-secretion mechanism (Lima et al., 2022). Especially for *S. capitis*, the accumulation of the vesicles was increased on the copper surfaces, indicating the stress response. EDS analysis of the material showed occurrence of sulfur (Supplementary Figure 5), which has been observed in extracellular vesicles before (Noundou et al., 2024). However, sulfur containing extracellular vesicles are rare. Therefore, a likely possibility would be that the accumulations are copper oxides, as shown in Akintelu et al. (2020).

The cell morphology showed only little visual damage, or no significant damage compared to the cells observed on the 100 at.% Al coated surface, which may be attributed to the multilayer of cells on the surface. This observation should be deeper investigated in future studies. Contrary to these results, cell disruption was clearly observed in a study by Gopinath et al. (2016) after 60 min exposure to CuO nanoparticles. A reason for the observed cell disruption could be due to the exposure to the bacterial species MIC concentrations of the CuO nanoparticles, whereas in our study, no defined copper concentration but rather time was set. Further, the authors study conducted experiments in CuO nanoparticle solution, in contrast to our study on surfaces.

4.7 Potential for further enhancements of copper coatings

So far, various studies have been conducted with copper alloys. We created and tested Cu-Al-coatings as a feasible but more sustainable approach. To our dissatisfaction, only 100 at.% Cu coatings were sufficient for bacterial reduction. However, we were able to identify options for improvements: Firstly, another metal than aluminum could be used to create copper alloys, since it is a rather soft material.

Next, the coatings were generated by magnetron sputtering. This is a well-established method for creating coatings, such as implant coatings (Tian et al., 2007; Ferraris and Spriano, 2016). However, intermetallic phases formed during the deposition of the Cu-Al alloys. Since Cu-atoms are rigidly situated within these structures, Cu ions are less likely to be released (Shi et al., 2020). This is in accordance with our Cu ion content measurement of the PBS and bacterial solution after wet contact killing on Cu-Al alloy samples (Supplementary Figure 4), which is most likely contributing to the lower antibacterial effect, as described in see section "4.4 Bacterial survival after long exposure times is higher within a bacterial community." Another alloy of interest would be Al-Ag-Cu, which has shown to have a greater antibacterial effect compared to Cu-Al alloys on strains of *E. coli*, explained by the higher proportion of antimicrobial metals within the Al phase (Hahn et al., 2018). However, since aluminum proposes a rather soft material which is prone to damage, other metals such as zinc (Almoudi et al., 2018) could be used.

The durability and stability under real-life conditions of the coatings have to be addressed in future studies, as the focus of this study was on the antibacterial activity and effectivity. Glass slides were purposely selected as substrate material, since they compose of standardized roughness and therefore support reproducibility of the results. Therefore, the mechanical and tribological properties of the coatings should be studied as well as corrosion under conditions involving cleaning agents, operational environments, and microbial biofilms.

5 Conclusion and outlook

In this study, the bacterial community showed greater survival after exposure to the Cu and Cu-Al coatings, demonstrating the importance of testing not only single species. The coatings showed highest antibacterial activity when the Cu content was 100 at.%. Metabolic activity measurements supported the bacterial survival data.

Scanning electron microscope imaging revealed that cells exhibited morphological damage on the 100 at.% Cu coatings, although this damage was not differing significantly from the 100 at.% Al coatings after 1–2 h of contact time. While more genes related to copper and oxidative stress defense were found in *B. lata*, survival of *S. capitis* was significantly higher. This observation will be focused on in future studies by investigating the gene expression.

The copper ion content following wet contact killing on 100 at.% Cu coatings was comparatively high compared to other studies, but could be explained by the coatings showing early degradation under the SEM. However, Cu-Al alloy coatings exhibited significantly reduced copper ion release compared to the 100 at.% Cu coating. This phenomenon can be attributed to the formation of a robust intermetallic phase between Cu and Al, which hinders ion release, explaining the weak antibacterial activity of these alloy coatings.

In subsequent studies, a more thorough examination of the wet contact killing process, as well as the dry contact killing process, could provide additional information about the test materials and their antibacterial activity. An additional approach would be to investigate the expression of copper tolerance or copper defense related genes to better understand the differential survival of species within the bacterial community. These approaches can be evaluated using current methodologies and also with new synthesized surface coatings incorporating other metals.

To conclude, this study provided new findings on wet contact killing effects on bacteria, both as pure culture and as bacterial community. Additionally, novel copper-based surface coatings were tested and will be improved in future investigations. Our study on this topic contributes to the understanding of copper as an antibacterial countermeasure, with the aim to combat the transmission of opportunistic bacteria that pose a human health risk.

Data availability statement

The datasets presented in this study can be found in online repositories. The names of the repository/repositories and accession number(s) can be found below: https://www.ncbi.nlm.nih.gov/, PRJNA1283126.

Author contributions

YL-S: Conceptualization, Data curation, Formal analysis, Investigation, Methodology, Visualization, Writing – original draft. RA: Conceptualization, Formal analysis, Investigation, Visualization, Writing – review & editing. LK: Formal analysis, Investigation, Writing – review & editing. CK: Conceptualization, Writing – review & editing. AB: Writing – review & editing. CN: Resources, Writing – review & editing. OS: Data curation, Resources, Writing – review & editing. DZ: Writing – review & editing. SL: Supervision, Writing – review & editing.

Funding

The author(s) declare that financial support was received for the research and/or publication of this article. This work was supported by the DLR internal grant DLR-VO: GANDALF and the data will be included in the Ph.D. thesis of YL-S. Further support was granted for CK by the German Space Agency at the German Aerospace Center (Grant 50WB2230). SL was supported by the German Aerospace Center (Deutsches Zentrum für Luft- und Raumfahrt, DLR) and the Traffic grants RoSto and VmO4Orte. This work was supported by the DFG Research Infrastructure West German Genome Center (project 407493903) as part of the Next Generation Sequencing Competence Network (project 423957469).

Acknowledgments

We thank Katharina Utens, Alina Auerhammer, and Amelie Tuerling for their assistance and support in the laboratory. Further, we thank Franca Arndt for her advisory support. NGS analyses were carried out at the production site Cologne [Cologne Center for Genomics (CCG)]. Figure 1 was created in BioRender.com. Last, we thank Prof. Ralf Möller†, who accompanied and guided the first steps of this work. We are deeply grateful for his commitment and for being an exceptional group leader, colleague and mentor.

Conflict of interest

AB was employed by MVZ Laboratory Dr. Limbach and Colleagues eGbR.

The remaining authors declare that the research was conducted in the absence of any commercial or financial relationships that could be construed as a potential conflict of interest.

Generative AI statement

The authors declare that no Generative AI was used in the creation of this manuscript.

Any alternative text (alt text) provided alongside figures in this article has been generated by Frontiers with the support of artificial intelligence and reasonable efforts have been made to ensure accuracy, including review by the authors wherever possible. If you identify any issues, please contact us.

Publisher's note

Supplementary material

The Supplementary Material for this article can be found online at: https://www.frontiersin.org/articles/10.3389/fmicb.2025.1659828/full#supplementary-material

References

Akintelu, S. A., Folorunso, A. S., Folorunso, F. A., and Oyebamiji, A. K. (2020). Green synthesis of copper oxide nanoparticles for biomedical application and environmental remediation. *Heliyon* 6:e04508. doi: 10.1016/j.heliyon.2020.e04508

Almoudi, M. M., Hussein, A. S., Hassan, M. I. A., and Zain, N. M. (2018). A systematic review on antibacterial activity of zinc against *Streptococcus mutans*. *Saudi Dental J.* 30, 283–291. doi: 10.1016/j.sdentj.2018.06.003

Ancion, P.-Y., Lear, G., and Lewis, G. D. (2010). Three common metal contaminants of urban runoff (Zn, Cu & Pb) accumulate in freshwater biofilm and modify embedded bacterial communities. *Environ. Pollut.* 158, 2738–2745. doi: 10.1016/j.envpol.2010.04.013

Arndt, F., Siems, K., Timofeev, S. M., Baumann, P., Ahmed, A. S., Müller, D. W., et al. (2025). Copper stress response of antibiotic-resistant and copper-tolerant E. faecium and the antibacterial efficacy of functionalized copper surfaces. *Adv. Materials Interfaces*. (in press).

Baker, J., Sengupta, M., Jayaswal, R. K., and Morrissey, J. A. (2011). The *Staphylococcus aureus* CsoR regulates both chromosomal and plasmid-encoded copper resistance mechanisms. *Environ. Microbiol.* 13, 2495–2507. doi: 10.1111/j.1462-2920.2011.02522.x

Barnham, K. J., Masters, C. L., and Bush, A. I. (2004). Neurodegenerative diseases and oxidative stress. *Nat. Rev. Drug Discov.* 3, 205–214. doi: 10.1038/nrd1330

Battesti, A., Majdalani, N., and Gottesman, S. (2011). The RpoS-mediated general stress response in *Escherichia coli*. *Annu. Rev. Microbiol.* 65, 189–213. doi: 10.1146/annurev-micro-090110-102946

Berney, M., Hammes, F., Bosshard, F., Weilenmann, H., and Egli, T. (2007). Assessment and interpretation of bacterial viability by using the LIVE/DEAD baclight kit in combination with flow cytometry. *Appl. Environ. Microbiol.* 73, 3283–3290. doi: 10.1128/AEM.02750-06

Betancourt-Galindo, R., Reyes-Rodriguez, P., Puente-Urbina, B., Avila-Orta, C., Rodriguez-Fernández, O., Cadenas-Pliego, G., et al. (2014). Synthesis of copper nanoparticles by thermal decomposition and their antimicrobial properties. *J. Nanomaterials* 2014:980545. doi: 10.1155/2014/980545

Beyvers, S., Jelonek, L., Goesmann, A., and Schwengers, O. (2025). Bakta Web–rapid and standardized genome annotation on scalable infrastructures. *Nucleic Acids Res.* 53, W51–W56. doi: 10.1093/nar/gkaf335

Bondarczuk, K., and Piotrowska-Seget, Z. (2013). Molecular basis of active copper resistance mechanisms in Gram-negative bacteria. *Cell Biol. Toxicol.* 29, 397–405. doi: 10.1007/s10565-013-9262-1

Bose, S., Aggarwal, S., Singh, D. V., and Acharya, N. (2020). Extracellular vesicles: An emerging platform in gram-positive bacteria. *Microbial Cell* 7:312. doi: 10.15698/mic2020.12.737

Bouras, G., Houtak, G., Wick, R. R., Mallawaarachchi, V., Roach, M. J., Papudeshi, B., et al. (2024). Hybracter: Enabling scalable, automated, complete and accurate bacterial genome assemblies. *Microbial Genom.* 10:001244. doi: 10.1099/mgen.0.001244

Briaud, P., and Carroll, R. K. (2020). Extracellular vesicle biogenesis and functions in gram-positive bacteria. *Infect. immunity* 88:e00433-20. doi: 10.1128/iai.00433-20

Chen, H.-H., Li, W.-J., Tang, S.-K., Kroppenstedt, R. M., Stackebrandt, E., Xu, L.-H., et al. (2004). *Corynebacterium halotolerans* sp. nov., isolated from saline soil in the west of China. *Int. J. Syst. Evol. Microbiol.* 54, 779–782. doi: 10.1099/ijs.0.02919-0

Chillappagari, S., Seubert, A., Trip, H., Kuipers, O. P., Marahiel, M. A., and Miethke, M. (2010). Copper stress affects iron homeostasis by destabilizing iron-sulfur cluster formation in *Bacillus subtilis*. *J. Bacteriol.* 192, 2512–2524. doi: 10.1128/jb.00058-10

Corcoll, N., Yang, J., Backhaus, T., Zhang, X., and Eriksson, K. M. (2019). Copper affects composition and functioning of microbial communities in marine biofilms at environmentally relevant concentrations. *Front. Microbiol.* 9:3248. doi: 10.3389/fmicb.2018.03248

Cortesão, M., Siems, K., Koch, S., Beblo-Vranesevic, K., Rabbow, E., Berger, T., et al. (2021). MARSBOx: Fungal and bacterial endurance from a balloon-flown analog mission in the stratosphere. *Front. Microbiol.* 12:601713. doi: 10.3389/fmicb.2021.601713

Cui, Z., Ibrahim, M., Yang, C., Fang, Y., Annam, H., Li, B., et al. (2014). Susceptibility of opportunistic *Burkholderia glumae* to copper surfaces following wet or dry surface contact. *Molecules* 19, 9975–9985. doi: 10.3390/molecules19079975

Dai, W., Xie, C., Xiao, Y., Ma, Y., Ding, Y., Song, Z., et al. (2024). Bacterial susceptibility to ceria nanoparticles: The critical role of surrounding molecules. *Environ. Sci. Technol.* 58, 12390–12399. doi: 10.1021/acs.est.4c02396

Danko, D., Bezdan, D., Afshin, E. E., Ahsanuddin, S., Bhattacharya, C., Butler, D. J., et al. (2021). A global metagenomic map of urban microbiomes and antimicrobial resistance. *Cell* 184, 3376–3393. doi: 10.1016/j.cell.2021.05.002

Fernández, L. L., Montes-Bayón, M., González, E. B., Sierra, L. M., Sanz-Medel, A., and Bettmer, J. (2011). Initial studies on quantitative DNA induced oxidation by gel electrophoresis (GE)-ICP-MS. *J. Anal. Atomic Spectrom.* 26, 195–200. doi: 10.1039/C0JA00163E

Ferraris, S., and Spriano, S. (2016). Antibacterial titanium surfaces for medical implants. *Materials Sci. Eng. C* 61, 965–978. doi: 10.1016/j.msec.2015.12.062

Festa, R. A., and Thiele, D. J. (2011). Copper: An essential metal in biology. *Curr. Biol.* 21, R877–R883. doi: 10.1016/j.cub.2011.09.040

Fowler, L., Engqvist, H., and Öhman-Mägi, C. (2019). Effect of copper ion concentration on bacteria and cells. *Materials* 12:3798. doi: 10.3390/ma12223798

Frei, A., Verderosa, A. D., Elliott, A. G., Zuegg, J., and Blaskovich, M. A. (2023). Metals to combat antimicrobial resistance. *Nat. Rev. Chem.* 7, 202–224. doi: 10.1038/s41570-023-00463-4

Ghosh, S., Chen, Y., and Hu, J. (2022). Application of UVC and UVC based advanced disinfection technologies for the inactivation of antibiotic resistance genes and elimination of horizontal gene transfer activities: Opportunities and challenges. *Chem. Eng. J.* 450:138234. doi: 10.1016/j.cej.2022.138234

Giachino, A., and Waldron, K. J. (2020). Copper tolerance in bacteria requires the activation of multiple accessory pathways. *Mol. Microbiol.* 114, 377–390. doi: 10.1111/mmi.14522

Gopinath, V., Priyadarshini, S., Al-Maleki, A., Alagiri, M., Yahya, R., Saravanan, S., et al. (2016). *In vitro* toxicity, apoptosis and antimicrobial effects of phyto-mediated copper oxide nanoparticles. *RSC Adv.* 6, 110986–110995. doi: 10.1039/C6RA13871C

Grass, G., Rensing, C., and Solioz, M. (2011). Metallic copper as an antimicrobial surface. *Appl. Environ. Microbiol.* 77, 1541–1547. doi: 10.1128/AEM.02766-10

Guettari, M., Gharbi, I., and Hamza, S. (2021). UVC disinfection robot. *Environ. Sci. Pollut. Res. Int.* 28, 40394–40399. doi: 10.1007/s11356-020-11184-2

Gustavson, K., Petersen, S., Pedersen, B., Stuer-Lauridsen, F., Pedersen, S., and Wängberg, S. (1999). Pollution-induced community tolerance (PICT) in coastal phytoplankton communities exposure to copper. *Hydrobiologia* 416, 125–138. doi: 10.1023/A:1003811419842

Hahn, C., Hans, M., Hein, C., Dennstedt, A., Mücklich, F., Rettberg, et al. (2018). Antimicrobial properties of ternary eutectic aluminum alloys. *BioMetals* 31, 759–770. doi: 10.1007/s10534-018-0119-1

Higgins, S., Gualdi, S., Pinto-Carbó, M., and Eberl, L. (2020). Copper resistance genes of *Burkholderia cenocepacia* H111 identified by transposon sequencing. *Environ. Microbiol. Reports* 12, 241–249. doi: 10.1111/1758-2229.12828

Hobman, J. L., and Crossman, L. C. (2015). Bacterial antimicrobial metal ion resistance. *J. Med. Microbiol.* 64, 471–497. doi: 10.1099/jmm.0.023036-0

Hong, W., Karanja, C. W., Abutaleb, N. S., Younis, W., Zhang, X., Seleem, M. N., et al. (2018). Antibiotic susceptibility determination within one cell cycle at single-bacterium level by stimulated Raman metabolic imaging. *Anal. Chem.* 90, 3737–3743. doi: 10.1021/acs.analchem.7b03382

Hsu, T., Joice, R., Vallarino, J., Abu-Ali, G., Hartmann, E. M., Shafquat, A., et al. (2016). Urban transit system microbial communities differ by surface type and interaction with humans and the environment. *mSystems* 1:e00018-16. doi: 10.1128/mSystems.00018-16

Huo, Y.-Y., Xu, X.-W., Liu, S.-P., Cui, H.-L., Li, X., and Wu, M. (2011). *Sphingomonas rubra* sp. nov., isolated from bioreactor wastewater. *Int. J. Syst. Evol. Microbiol.* 61, 1028–1032. doi: 10.1099/ijs.0.020958-0

Karpanen, T. J., Casey, A., Lambert, P. A., Cookson, B., Nightingale, P., Miruszenko, L., et al. (2012). The antimicrobial efficacy of copper alloy furnishing in the clinical environment: A crossover study. *Infect. Control Hosp. Epidemiol.* 33, 3–9. doi: 10.1086/663644

Kim, J. H., Lee, J., Park, J., and Gho, Y. S. (2015). Gram-negative and Gram-positive bacterial extracellular vesicles. *Semin. Cell Dev. Biol.* 40, 97–104. doi: 10.1016/j.semcdb.2015.02.006

Kinnevey, P. M., Shore, A. C., Brennan, G. I., Sullivan, D. J., Ehricht, R., Monecke, S., et al. (2013). Emergence of sequence type 779 methicillin-resistant *Staphylococcus aureus* harboring a novel pseudo staphylococcal cassette chromosome mec (SCC mec)-SCC-SCC CRISPR composite element in Irish hospitals. *Antimicrob. Agents Chemother.* 57, 524–531. doi: 10.1128/aac.01689-12

Kohl, A., Ly, Y.-T., Leuko, S., Schmeling, D., Wagner, C., and Moeller, R. (2024). "Evaluation of bioaerosol propagation through an air curtain," in *Proceedings of the 18th International Conference on Indoor Air Quality and Climate, INDOOR AIR 2024*, (Hoboken, NJ: Wiley).

Kusano, K., Yamada, H., Niwa, M., and Yamasato, K. (1997). *Propionibacterium cyclohexanicum* sp. nov., a new acid-tolerant ω-cyclohexyl fatty acid-containing *propionibacterium* isolated from spoiled orange juice. *Int. J. Syst. Evol. Microbiol.* 47, 825–831. doi: 10.1099/00207713-47-3-825

Li, M., Ma, Z., Zhu, Y., Xia, H., Yao, M., Chu, X., et al. (2016). Toward a molecular understanding of the antibacterial mechanism of copper-bearing titanium alloys against *Staphylococcus aureus*. *Adv. Healthc. Mater.* 5, 557–566. doi: 10.1002/adhm.201500712

Lima, S., Matinha-Cardoso, J., Giner-Lamia, J., Couto, N., Pacheco, C. C., Florencio, F. J., et al. (2022). Extracellular vesicles as an alternative copper-secretion mechanism in bacteria. *J. Hazardous Mater.* 431:128594. doi: 10.1016/j.jhazmat.2022.128594

Linklater, D. P., Baulin, V. A., Juodkazis, S., Crawford, R. J., Stoodley, P., and Ivanova, E. P. (2021). Mechano-bactericidal actions of nanostructured surfaces. *Nat. Rev. Microbiol.* 19, 8–22. doi: 10.1038/s41579-020-0414-z

Luan, Y., Liu, S., Pihl, M., van der Mei, H. C., Liu, J., Hizal, F., et al. (2018). Bacterial interactions with nanostructured surfaces. *Curr. Opin. Colloid Interface Sci.* 38, 170–189. doi: 10.1016/j.cocis.2018.10.007

Luo, J., Hein, C., Mücklich, F., and Solioz, M. (2017). Killing of bacteria by copper, cadmium, and silver surfaces reveals relevant physicochemical parameters. *Biointerphases* 12:020301. doi: 10.1116/1.4980127

Luo, J., Hein, C., Pierson, J.-F., and Mücklich, F. (2019). Localised corrosion attacks and oxide growth on copper in phosphate-buffered saline. *Mater. Characterization* 158:109985. doi: 10.1016/j.matchar.2019.109985

Ly, Y.-T., Wetzig, N., Holtel, J., Leuko, S., and Moeller, R. (2024). "Modeling the public transport microbiome: development of a microbial reference community," in *18th International Conference on Indoor Air Quality and Climate, INDOOR AIR 2024*, (Hoboken, NJ: Wiley).

Mahoney, A. R., Safaee, M. M., Wuest, W. M., and Furst, A. L. (2021). The silent pandemic: Emergent antibiotic resistances following the global response to SARS-CoV-2. *IScience* 24:102304. doi: 10.1016/j.isci.2021.102304

Mehtar, S., Wiid, I., and Todorov, S. (2008). The antimicrobial activity of copper and copper alloys against nosocomial pathogens and *Mycobacterium tuberculosis* isolated from healthcare facilities in the Western Cape: An in-vitro study. *J. Hosp. Infect.* 68, 45–51. doi: 10.1016/j.jhin.2007.10.009

Mikolay, A., Huggett, S., Tikana, L., Grass, G., Braun, J., and Nies, D. H. (2010). Survival of bacteria on metallic copper surfaces in a hospital trial. *Appl. Microbiol. Biotechnol.* 87, 1875–1879. doi: 10.1007/s00253-010-2640-1

Møretrø, T., Fanebust, H., Fagerlund, A., and Langsrud, S. (2019). Whole room disinfection with hydrogen peroxide mist to control *Listeria monocytogenes* in food industry related environments. *Int. J. Food Microbiol.* 292, 118–125. doi: 10.1016/j.ijfoodmicro.2018.12.015

Naghavi, M., Vollset, S. E., Ikuta, K. S., Swetschinski, L. R., Gray, A. P., Wool, E. E., et al. (2024). Global burden of bacterial antimicrobial resistance 1990–2021: A systematic analysis with forecasts to 2050. *Lancet* 404, 1199–1226. doi: 10.1016/S0140-6736(24)01867-1

Neidhöfer, C., Neuenhoff, M., Jozić, R., Atangcho, B., Unsleber, S., Neder, U., et al. (2023). Exploring clonality and virulence gene associations in bloodstream infections using whole-genome sequencing and clinical data. *Front. Cell. Infect. Microbiol.* 13:1274573. doi: 10.3389/fcimb.2023.1274573

Niu, L., Lu, S., Hu, S., Jin, D., Lai, X., Yang, J., et al. (2016). *Streptococcus halotolerans* sp. nov. isolated from the respiratory tract of Marmota himalayana in Qinghai-Tibet Plateau of China. *Int. J. Syst. Evol. Microbiol.* 66, 4211–4217. doi: 10.1099/ijsem.0.001337

Noundou, V. L., Levy, A., Modla, S., Yu, Y., Qu, J., and Hanson, T. E. (2024). *Chlorobaculum tepidum* outer membrane vesicles are likely a significant route for biogenic sulfur transport. *bioRxiv [Preprint]* doi: 10.1101/2024.09.30.615447

O'Brien, J., Wilson, I., Orton, T., and Pognan, F. (2000). Investigation of the Alamar Blue (resazurin) fluorescent dye for the assessment of mammalian cell cytotoxicity. *Eur. J. Biochem.* 267, 5421–5426. doi: 10.1046/j.1432-1327.2000.01606.x

Pham, A. N., Xing, G., Miller, C. J., and Waite, T. D. (2013). Fenton-like copper redox chemistry revisited: Hydrogen peroxide and superoxide mediation of copper-catalyzed oxidant production. *J. Catal.* 301, 54–64. doi: 10.1016/j.jcat.2013.01.025

Pierce, E. C., and Dutton, R. J. (2022). Putting microbial interactions back into community contexts. *Curr. Opin. Microbiol.* 65, 56–63. doi: 10.1016/j.mib.2021.10.008

Pramanik, A., Laha, D., Bhattacharya, D., Pramanik, P., and Karmakar, P. (2012). A novel study of antibacterial activity of copper iodide nanoparticle mediated by DNA and membrane damage. *Colloids Surfaces B Biointerfaces* 96, 50–55. doi: 10.1016/j.colsurfb.2012.03.021

Qi, Z., Sun, N., and Liu, C. (2023). Glyoxylate cycle maintains the metabolic homeostasis of *Pseudomonas aeruginosa* in viable but nonculturable state induced by chlorine stress. *Microbiol. Res.* 270:127341. doi: 10.1016/j.micres.2023.127341

Rahkila, R., Johansson, P., Säde, E., and Björkroth, J. (2011). Identification of enterococci from broiler products and a broiler processing plant and description of *Enterococcus viikkiensis* sp. nov. *Appl. Environ. Microbiol.* 77, 1196–1203. doi: 10.1128/AEM.02412-10

Rai, S., Singh, D. K., and Kumar, A. (2021). Microbial, environmental and anthropogenic factors influencing the indoor microbiome of the built environment. *J. Basic Microbiol.* 61, 267–292. doi: 10.1002/jobm.202000575

Ramos-Zúñiga, J., Bruna, N., and Pérez-Donoso, J. M. (2023). Toxicity mechanisms of copper nanoparticles and copper surfaces on bacterial cells and viruses. *Int. J. Mol. Sci.* 24:10503. doi: 10.3390/ijms241310503

Reddy, G. S., Matsumoto, G. I., Schumann, P., Stackebrandt, E., and Shivaji, S. (2004). Psychrophilic pseudomonads from Antarctica: *Pseudomonas antarctica* sp. nov., *Pseudomonas meridiana* sp. nov. and *Pseudomonas proteolytica* sp. nov. *Int. J. Syst. Evol. Microbiol.* 54, 713–719. doi: 10.1099/ijs.0.02827-0

Różańska, A., Chmielarczyk, A., Romaniszyn, D., Sroka-Oleksiak, A., Bulanda, M., Walkowicz, M., et al. (2017). Antimicrobial properties of selected copper alloys on *Staphylococcus aureus* and *Escherichia coli* in different simulations of environmental conditions: With vs. without organic contamination. *Int. J. Environ. Res. Public Health* 14:813. doi: 10.3390/ijerph14070813

Salah, I., Parkin, I. P., and Allan, E. (2021). Copper as an antimicrobial agent: Recent advances. *RSC Adv.* 11, 18179–18186. doi: 10.1039/D1RA02149D

Salazar, C. N., Acosta, M., Galleguillos, P. A., Shmaryahu, A., Quatrini, R., Holmes, D. S., et al. (2013). Analysis of gene expression in response to copper stress in *Acidithiobacillus ferrooxidans* strain D2, isolated from a copper bioleaching operation. *Adv. Mater. Res.* 825, 157–161. doi: 10.4028/www.scientific.net/AMR.825.157

San, K., Long, J., Michels, C. A., and Gadura, N. (2015). Antimicrobial copper alloy surfaces are effective against vegetative but not sporulated cells of gram-positive *Bacillus subtilis*. *Microbiologyopen* 4, 753–763. doi: 10.1002/mbo3.276

Santo, C. E., Lam, E. W., Elowsky, C. G., Quaranta, D., Domaille, D. W., Chang, C. J., et al. (2011). Bacterial killing by dry metallic copper surfaces. *Appl. Environ. Microbiol.* 77, 794–802. doi: 10.1128/AEM.01599-10

Schmidt, M. G., Attaway, H. H., Terzieva, S., Marshall, A., Steed, L. L., Salzberg, D., et al. (2012). Characterization and control of the microbial community affiliated with copper or aluminum heat exchangers of HVAC systems. *Curr. Microbiol.* 65, 141–149. doi: 10.1007/s00284-012-0137-0

Schwengers, O., Jelonek, L., Dieckmann, M. A., Beyvers, S., Blom, J., and Goesmann, A. (2021). Bakta: Rapid and standardized annotation of bacterial genomes via alignment-free sequence identification. *Microbial Genomics* 7:000685. doi: 10.1099/mgen.0.000685

Serra, A., Corcoll, N., and Guasch, H. (2009). Copper accumulation and toxicity in fluvial periphyton: The influence of exposure history. *Chemosphere* 74, 633–641. doi: 10.1016/j.chemosphere.2008.10.036

Shaw, J., Ernakovich, J. G., Judy, J., Farrell, M., Whatmuff, M., and Kirby, J. (2020). Long-term effects of copper exposure to agricultural soil function and microbial community structure at a controlled and experimental field site. *Environ. Pollut.* 263:114411. doi: 10.1016/j.envpol.2020.114411

Shi, A., Zhu, C., Fu, S., Wang, R., Qin, G., Chen, D., et al. (2020). What controls the antibacterial activity of Ti-Ag alloy, Ag ion or Ti2Ag particles? *Mater. Sci. Eng. C* 109:110548. doi: 10.1016/j.msec.2019.110548

Sobisch, L.-Y., Rogowski, K. M., Fuchs, J., Schmieder, W., Vaishampayan, A., Oles, P., et al. (2019). Biofilm forming antibiotic resistant gram-positive pathogens isolated from surfaces on the international space station. *Front. Microbiol.* 10:543. doi: 10.3389/fmicb.2019.00543

Solioz, M., Abicht, H. K., Mermod, M., and Mancini, S. (2010). Response of Gram-positive bacteria to copper stress. *JBIC J. Biol. Inorganic Chem.* 15, 3–14. doi: 10.1007/s00775-009-0588-3

Stephens, B., Azimi, P., Thoemmes, M. S., Heidarinejad, M., Allen, J. G., and Gilbert, J. A. (2019). Microbial exchange via fomites and implications for human health. *Curr. Pollut. Rep.* 5, 198–213. doi: 10.1007/s40726-019-00123-6

Sutcliffe, B., Hose, G., Harford, A., Midgley, D., Greenfield, P., Paulsen, I., et al. (2019). Microbial communities are sensitive indicators for freshwater sediment copper contamination. *Environ. Pollut.* 247, 1028–1038. doi: 10.1016/j.envpol.2019.01.104

Tamayo, L., Azócar, M., Kogan, M., Riveros, A., and Páez, M. (2016). Copper-polymer nanocomposites: An excellent and cost-effective biocide for use on antibacterial surfaces. *Mater. Sci. Eng. C* 69, 1391–1409. doi: 10.1016/j.msec.2016.08.041

Teitzel, G. M., Geddie, A., De Long, S. K., Kirisits, M. J., Whiteley, M., and Parsek, M. R. (2006). Survival and growth in the presence of elevated copper: Transcriptional profiling of copper-stressed *Pseudomonas aeruginosa*. *J. Bacteriol.* 188, 7242–7256. doi: 10.1128/jb.00837-06

ThermoFisher Scientific. (2025). *alamarBlue assays for cell viability protocol, for microplates*. Available: https://www.thermofisher.com/de/de/home/references/protocols/cell-and-tissue-analysis/protocols/alamarblue-cell-viability-reagent-for-microplates-protocol.html (accessed April 15 2025)

Tian, X., Wang, Z., Yang, S., Luo, Z., Fu, R. K., and Chu, P. K. (2007). Antibacterial copper-containing titanium nitride films produced by dual magnetron sputtering. *Surface Coatings Technol.* 201, 8606–8609. doi: 10.1016/j.surfcoat.2006.09.322

Timofeev, S. M., Siems, K., Müller, D. W., Ahmed, A. S., Schiele, A., Brix, K., et al. (2025). Stress response of *Aspergillus niger* spores to copper surfaces and the implications for antifungal surface functionalization. *Adv. Mater. Interfaces* 12:2400852. doi: 10.1002/admi.202400852

Traxler, M. F., Zacharia, V. M., Marquardt, S., Summers, S. M., Nguyen, H. T., Stark, S. E., et al. (2011). Discretely calibrated regulatory loops controlled by ppGpp partition gene induction across the 'feast to famine' gradient in *Escherichia coli*. *Mol. Microbiol.* 79, 830–845. doi: 10.1111/j.1365-2958.2010.07498.x

Van Trappen, S., Vandecandelaere, I., Mergaert, J., and Swings, J. (2004). *Flavobacterium degerlachei* sp. nov., *Flavobacterium frigoris* sp. nov. and *Flavobacterium micromati* sp. nov., novel psychrophilic bacteria isolated from microbial mats in Antarctic lakes. *Int. J. Syst. Evol. Microbiol.* 54, 85–92. doi: 10.1099/ijs.0.02857-0

Vanlaere, E., Baldwin, A., Gevers, D., Henry, D., De Brandt, E., LiPuma, J. J., et al. (2009). Taxon K, a complex within the *Burkholderia cepacia* complex, comprises at

least two novel species, *Burkholderia* contaminans sp. nov. and *Burkholderia lata* sp. nov. *Int. J. Syst. Evol. Microbiol.* 59, 102–111. doi: 10.1099/ijs.0.001123-0

Westmetall (2024). *Marktdaten*. Available: https://www.westmetall.com/de/markdaten.php (accessed September 23, 2024)

Wilks, S., Michels, H., and Keevil, C. (2005). The survival of *Escherichia coli* O157 on a range of metal surfaces. *Int. J. Food Microbiol.* 105, 445–454. doi: 10.1016/j.ijfoodmicro.2005.04.021

Williams, C. L., Neu, H. M., Gilbreath, J. J., Michel, S. L., Zurawski, D. V., and Merrell, D. S. (2016). Copper resistance of the emerging pathogen *Acinetobacter baumannii*. *Appl. Environ. Microbiol.* 82, 6174–6188. doi: 10.1128/AEM.01813-16

Williams, T. C., Asselin, E., Mazzulli, T., Woznow, T., Hamzeh, H., Nahkaie, D., et al. (2024). One-year trial evaluating the durability and antimicrobial efficacy of copper in public transportation systems. *Sci. Rep.* 14:6765. doi: 10.1038/s41598-024-56225-9

Xiao, S., Jones, R. M., Zhao, P., and Li, Y. (2019). The dynamic fomite transmission of Methicillin-resistant *Staphylococcus aureus* in hospitals and the possible improved intervention methods. *Building Environ.* 161:106246. doi: 10.1016/j.buildenv.2019.106246

2.6 Short-time thermal inactivation of surrogates of the public transport microbiome with a low-cost thermoresistometer

Title	**Short-time thermal inactivation of surrogates of the public transport microbiome with a low-cost thermoresistometer**
Authors	**Henrik Grübbel**[1], Yen Ly-Sauerbrey[2], Franca Arndt[2], Bruno Pavletic[2], Stefan Leuko[2], and Frank Rinderknecht[1]
Affiliation	[1] Institute of Vehicle Concepts, German Aerospace Center, Stuttgart, Germany [2] Institute of Aerospace Medicine, German Aerospace Center, Cologne, Germany
Article type	Original research article
Authorship	Co-author
Journal	Scientific Reports
Year	2026
Volume	16
DOI	10.1038/s41598-026-35087-3
Author Contributions	
HG	Conceptualization, Data curation, Formal analysis, Investigation, Methodology, Visualization, Writing - original draft
YL-S	Investigation, Data curation, Formal analysis, Methodology, Writing - review & editing
FA	Investigation, Data curation, Formal analysis, Methodology, Writing - review & editing
BP	Investigation, Data curation, Formal analysis, Methodology, Writing - review & editing

SL	Supervision, Writing - review & editing
FR	Supervision, Writing - review & editing

www.nature.com/scientificreports

scientific reports

Check for updates

OPEN

Short-time thermal inactivation of surrogates of the public transport microbiome with a low-cost thermoresistometer

Henrik Grübbel[1], Yen Ly-Sauerbrey[2], Franca Arndt[2], Bruno Pavletić[2], Stefan Leuko[2] & Frank Rinderknecht[1]

In this study, the thermal inactivation of the bacterial genera *Staphylococcus*, *Enterococcus* and *Burkholderia*, which can be found in public transportation environments, as well as the bacteriophage MS2 as a surrogate for potential viral pathogens are investigated. To quantify the thermal inactivation characteristic, an automated and inexpensive thermoresistometer is constructed and set up, which enables the microorganisms to be exposed to short-term thermal shocks. The time dependent temperature curves were measured to account for heat-up and cooling times. Afterwards, the microorganisms were exposed to temperatures in the range of 50 °C to 85 °C for durations of 2 s up to 10 s and the thermal inactivation of the respective microorganisms was measured by counting colony forming units (CFU) and plague forming units (PFU). The data was visualized and fitted to an analytical thermodynamic model based on a first-order reaction and the Arrhenius equation to predict thermal inactivation times. This study reports the first measured thermal inactivation values for *E. viikkiensis* and *B. lata*, which have not been studied before. The results for MS2 and *S. capitis* show significantly shorter inactivation times than previous experiments. After exposure to 85 °C for 2 s there was no measurable survival of all tested microorganisms. The semi-automated test setup used allows for consistent measurements and can be adapted by other research groups.

Keywords Thermal inactivation, Microorganims, Microbiome, Thermoresistometer, Short-time, Public transport

Human passengers are the primary source of airborne and surface-bound microorganisms in public transport environments, which are introduced through skin contact, respiratory droplets or aerosols[1]. In addition to known pathogens such as SARS-CoV-2, several studies have characterized the microbiomes of indoor air and surfaces in transport systems, frequently identifying genera such as *Staphylococcus*, *Enterococcus*, *Sphingomonas*, and *Streptococcus*[2–4]. Of particular concern are the so-called ESKAPE pathogens: *Enterococcus faecium*, *Staphylococcus aureus*, *Klebsiella pneumoniae*, *Acinetobacter baumannii*, *Pseudomonas aeruginosa* and *Enterobacter* species. These bacteria are known for their ability to develop multidrug resistances and are primarily associated with hospital settings, but have also been found in public transport environments, likely due to frequent use by healthcare workers and patients[5–7]. To mitigate aerosol-based transmission in public transport, several countermeasures have been proposed, such as the use of high-efficiency particulate air (HEPA) filters[8], increasing the fresh air supply[9], or requiring passengers to wear masks[10]. An alternative approach is the thermal inactivation of potentially infectious aerosols. Heat can damage cell membranes, denature enzymes or degrade DNA/RNA, leading to microbial inactivation. This principle is already widely applied in food safety (e.g. pasteurization) and in sterilization processes in laboratories and medical facilities. While thermal inactivation is not yet established for aerosol disinfection, it has been proposed by various authors[11–13]. One of the main challenges of thermal inactivation is its high energy demand. However, in winter conditions, when cabin heating is already required, the existing thermal energy could be harnessed for microbial inactivation without significantly increasing energy consumption. Despite their small interior volumes, battery-electric public transport vehicles require high heating capacities, leading to significant energy consumption for climate control

[1]German Aerospace Center (DLR), Institute of Vehicle Concepts, Stuttgart, Germany. [2]German Aerospace Center (DLR), Institute of Aerospace Medicine, Cologne, Germany. email: henrik.gruebbel@dlr.de

and reduced driving range in winter[14]. Compared to buildings, this makes thermal inactivation particularly promising for public transport environments.

To implement thermal inactivation effectively, a comprehensive understanding of the temperature-dependent inactivation kinetics of the target microorganisms is required. Microbial inactivation typically follows first-order reaction kinetics[15], which can be described by:

$$\ln\left(\frac{C_t}{C_0}\right) = -kt \tag{1}$$

where C_t is the microbial concentration at time t, C_0 is the initial concentration, and k is the reaction rate constant. While the natural logarithm (ln) is used here, the term "log-linear model" in microbiology often refers to the same first-order behavior expressed with base-10 logarithms. The two forms differ only by a constant factor (ln 10). This model has been widely applied to describe the thermal inactivation behavior of both viruses[16] and bacteria[17]. First-order reaction kinetics are commonly employed to model thermal inactivation, but they may fail to capture complex patterns such as shoulder and tailing effects or variability within microbial populations[18]. The temperature dependency of k can be modeled using the Arrhenius equation[16]. Here, A is the frequency factor, E_a the activation energy, R the universal gas constant, and T the absolute temperature:

$$k = A\exp\left(-\frac{E_a}{RT}\right) \tag{2}$$

Accurate modeling of microbial inactivation requires experimental data regarding the thermal resistance of microorganisms commonly encountered in public transport environments. While previous studies have applied such models to experimental data, for example, on SARS-CoV-2[19], data remain scarce for most microorganisms, particularly regarding short-term exposure to thermal shocks. For disinfection of vehicle cabin air, as well as for other applications such as fluid treatment, only short exposure times are available for microbial inactivation due to spatial and thermal constraints. A system capable of applying rapid, near-isothermal thermal shocks is required to assess microbial inactivation at discrete temperatures while avoiding bias from slow temperature transitions. Previous studies have employed various methods to investigate short-duration thermal inactivation. These include manually immersing glass capillaries into hot water baths[20], using computer-controlled thermoresistometers with steam heating[21], or mixing microbial solutions with pre-heated liquids and sampling at intervals[22,23]. Another approach involves flowing microbial suspensions through heated and cooled capillaries to simulate controlled thermal shocks[24]. Manual immersion is the simplest method for testing microbial resistance to thermal shock and has the advantage of requiring only relatively small quantities of microorganisms. However, its reproducibility is limited, particularly for short exposure times. In this study, we present a semi-automated thermoresistometer that retains the simplicity of manual immersion while significantly improving repeatability. This enables the systematic investigation of short-term thermal inactivation. Sealed glass capillaries filled with microbial suspensions are automatically immersed into a heated water bath and subsequently cooled by forced convection using ambient air. The proposed thermoresistometer can be easily constructed and operated by other research groups. Microbial reduction is quantified via dilution series and the plate count method. The organisms used in this study–*Enterococcus vitikkiensis* DSM 24043^T, *Staphylococcus capitis* DSM 111179, *Burkholderia lata* DSM 23089^T, and the *Escherichia* bacteriophage MS2 DSM 13767–are all classified as Biosafety Level 1 (BSL-1) according to German regulations, allowing experiments to be conducted in a BSL-1 laboratory.

The experimental setup of the thermoresistometer is not directly applicable for use in public transportation environments but it provides a crucial data baseline of the thermal inactivation kinetics of relevant microorganisms, addressing current gaps in literature. Additional studies are needed to discuss the potential integration in public transport vehicles and to compare its benefits and limitations to currently used technologies like HEPA-filters. The findings are not limited to applications in public transportation and can be extended to estimate thermal inactivation in a variety of systems, including water and wastewater treatment processes and thermal disinfection strategies used in medical and healthcare environments.

To the best of our knowledge, this study is the first to examine the short-term thermal inactivation of *B. lata*, *E. vikkiensis*, and *S. capitis*. It also introduces a low-cost, semi-automated thermoresistometer designed to improve experimental accuracy compared to manual immersion approaches.

Methods

Microorganisms and growth media

As previously discussed, the following microorganisms in Table 1 were used in the experiment. The microorganisms were obtained from the Leibniz Institute DSMZ German Collection of Microorganisms and

Strain	Growth	Reference
Burkholderia lata DSM 23089^T	R2A 37 °C	Vanlaere et al., 2009[29]
Enterococcus vitikkiensis DSM 24043^T	BHI 37 °C	Rahkila et al., 2011[30]
Staphylococcus capitis DSM 111179	R2A 37 °C	Sobisch et al., 2019[31]
Escherichia Phage MS2 DSM 13767	NZCYM 37 °C	Emslander et al., 2022[32]

Table 1. Microorganisms used in the experiment.

Cell Cultures (Braunschweig, Germany). The strain *Enterococcus viikkiensis* DSM 24043^T was isolated from the air of a broiler processing facility in Finland. The strain *Staphylococcus capitis* DSM 111179 was isolated from surfaces on the International Space Station. They serve as surrogates for more pathogenic *Enterococci*, such as *Enterococcus faecium*, and *Staphylococci*, such as *Staphylococcus aureus*, both of which are members of the ESKAPE pathogens. The strain *Burkholderia lata* DSM 23089^T was isolated from forest soil and represents the genus *Burkholderia*, which has also been detected in public transport environments[1,25]. The isolation place of the bacteriophage MS2 remains unknown. However, MS2 is a commonly used surrogate for more dangerous viruses such as SARS-CoV-2[26] or the Norovirus[27]. The bacterial species (*E. viikkiensis, S. capitis, B. lata*) were grown for 18 h under constant shaking at 200 revolutions per minute (rpm) at 37 °C on 2x Reasoner's 2A (TEKnova) and Brain Heart Infusion medium (Sigma-Aldrich) as shown in Table 1. The MS2 phages were grown in the presence of host *Escherichia coli* DSM 5695 in NZCYM medium (Sigma-Aldrich). The host was allowed to grow until the exponential phase for two hours, when the infection started. After 18 hours of growth in liquid culture shaking at 125 rpm, the phages were precipitated with polyethylene glycol (PEG) and diluted in phosphate buffered saline (PBS) buffer (PBS: Na_2HPO_4 7.0 g, KH_2PO_4 3.0 g, NaCl 4.0 g, per Liter, pH 7.5). To determine the phage titer, a double-layered agar method with NZCYM was utilized as described by Kropinski et. al. 2009[28]. The cell number was adjusted to $10^5 - 10^6$ colony forming units (CFU)/plaque forming units (PFU) in phosphate buffered saline.

Thermoresistometer and determination of thermal resistance

To expose the microorganisms to thermal shocks, glass capillaries were immersed in a temperature-controlled heating bath. Compared to conventional plastic test tubes, glass capillaries offer the advantages of lower wall thickness and reduced thermal mass, enabling faster and more uniform heat transfer. The capillaries were secured within a clamping block, which could be precisely lowered into and withdrawn from the heating bath via a linear guide mechanism. A schematic representation of the mode of operation is shown in Fig. 1.

To determine the thermal resistance in the experiment, the glass capillaries (*a*; HIRSCHMANN ringcaps REF 9600150, Germany) were filled with 50 μL of microbial solution with an initial CFU/PFU of $10^5 - 10^6$ using a pipette controller for capillaries (BRAND pipette controller micro, Germany). The glass capillaries were sealed using a flame and it was verified that the sealing had no significant influence on the viable count of the microorganisms. As a control, two samples of each microorganism were sealed in a glass capillary, stored in it during the experiments and then analysed together with the thermally treated samples via plate count. Heat treatment was done by submerging the class capillaries in a temperature controlled water bath (*b*) using a magnet hotplate stirrer (*c*; IKA rct basic, Germany) with a PT100 probe. The magnetic stirrer was set to 160 rpm to improve heat transfer and prevent thermal stratification of the water. By using a solenoid (*d*; Intertec ITS-LS-4035, Germany) and a digital timing relays (*e*; Crouzet DZ1R, France) operated with an 24 V laboratory power supply the submerging was automated for repeatability. The solenoid is connected to a rocker arm with a linear guide (*f*), which in turn is linked to a 3D-printed holder (*g*) that clamps the capillaries at their upper end. After the programmed exposure time, the glass capillaries are retracted to their original position by spring force and removed from the water bath. The full submerging of the glass capillaries takes approximately 0.23 s and the removal takes approximately 0.16 s, both measured by frame by frame analysis of a 30 fps video. When not submerged, the glass capillaries are constantly cooled with ambient air by a 24 V fan (*h*; ebmpapst 8414 NH, Germany). The temperature of the water bath is constantly monitored during the experiments by a datalogger (*i*; Ahlborn Almemo 710, Germany) and a type N thermocouple (*j*; Electronic Sensor, Germany). Compared to manual immersion of the glass capillaries, this experimental setup allows greater repeatability. Due to the standard components used, the setup is simple and inexpensive. The actual setup used in the experiments is shown in Fig. 2.

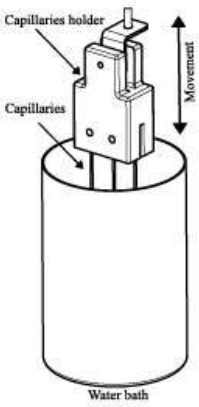

Fig. 1. Functional principle of the thermoresistometer.

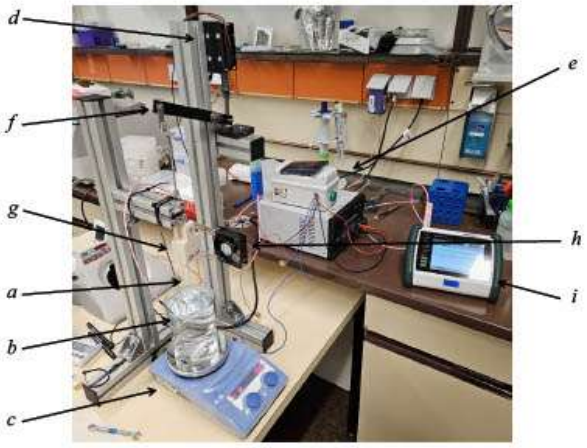

Fig. 2. Experimental setup of the thermoresistometer for controlled thermal exposure; *a* 50 µL capillary; *b* water bath; *c* hotplate stirrer; *d* solenoid; *e* timing relays; *f* capillary holder; *g* rocker arm; *h* cooling fan; *i* datalogger.

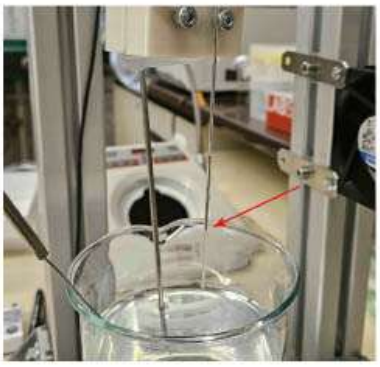

Fig. 3. Type N thermocouple in glass capillary for temperature curve measurement.

In order to quantify and verify the thermal stress to which the microorganisms were exposed, the temperature curve was measured using a 0.5 mm thermocouple type N, which was inserted into a glass capillary filled with water. The temporal resolution of the measurement was 0.1 s. The thermocouple inside the glass capillary is shown in Fig. 3.

After the heat exposure, the glass capillaries were opened with a diamond needle file and the samples were retrieved. To determine the survival, a 10-fold dilution series from 10^{-1} to 10^{-8} was prepared and plated on respective media plates. After incubation at 37 °C for 48 h, colonies were counted and CFU/ml or PFU/ml were calculated. To determine the phage titer, a double-layered agar method with NZCYM was utilized as described before.

All experiments were done in technical triplicates. The decimal reduction times (D-value) were calculated according to the following equation:

$$D = \frac{t}{log_{10}N_0 - log_{10}N} \tag{3}$$

Where t is the exposure time, $logN_0$ the logarithmic initial cell concentration and $logN$ the logarithmic final population. The D-value represents the time required to achieve a one-log (10-fold) reduction in the number of viable microorganisms under specified conditions.The results were analyzed using Microsoft Excel 2019 for

Microorganism	Timepoints			
	50 °C	60 °C	70 °C	85 °C
Enterococcus viikkiensis	-	4 s, 6 s, 8 s	2 s, 3 s, 4 s	2 s, 3 s, 4 s
Staphylococcus capitis K1	-	6 s, 8 s, 10 s	2 s, 3 s, 4 s, 6s	2 s, 3 s, 4 s
Burkholderia lata	-	2 s, 4 s, 6 s	2 s, 3 s, 4 s	2 s, 3 s, 4 s
MS2	3 s, 5 s, 7 s	3 s, 4 s	2 s, 3 s, 4 s	2 s, 3 s, 4 s

Table 2. Temperatures and time intervals investigated in the experiments.

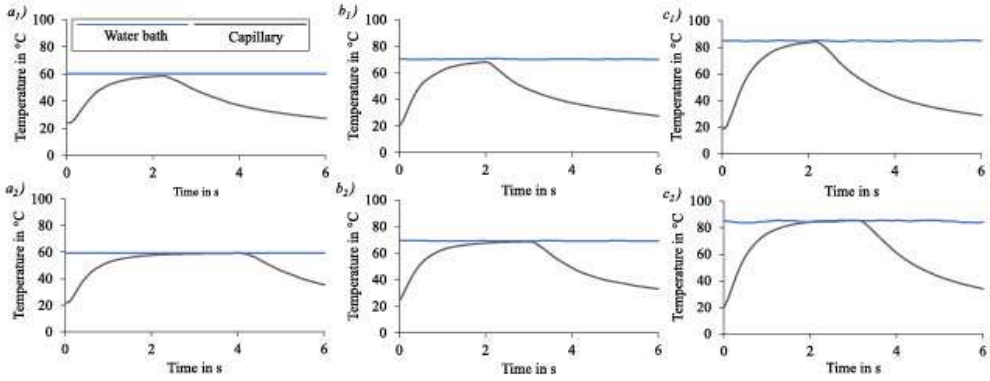

Fig. 4. Temperature of the water bath (blue) and the buffer medium in the glass capillary (grey) when submerged in water bath with the set temperature of 60 °C for 2 s (a_1) and 4 s (a_2), 70 °C for 2 s (b_1) and 3 s (b_2) and 85 °C for 2 s (c_1) and 3 s (c_2).

general data handling and R 4.5.1 for statistical evaluation. To assess the significance of the findings, an analysis of variance (ANOVA) was conducted, followed by a Tukey HSD post hoc test, using a significance level of 5 %.

Experimental procedure

First, the thermal load on the samples was assessed by measuring the temperature inside the capillary, as previously described. Three target temperatures 60 °C, 70 °C, and 85 °C were selected for analysis. Subsequently, the thermal shock resistance of the microorganisms *E. viikkiensis*, *B. lata*, *S. capitis*, and MS2 was evaluated at varying exposure times and temperatures, as outlined in Table 2. Additionally, the temperature of 50 °C was tested for MS2.

Results

Temperature measurements

Figure 4 presents the results of the temperature measurements. The blue curve shows the measured temperature of the water bath and the grey curve the measured temperature of the buffer medium in the capillary submerged and extracted from the water bath. The graph starts at $t = 0\,s$ with the submersion of the capillary. The data obtained at 60 °C (2 s, 4 s), 70 °C (2 s, 3 s), and 85 °C (2 s, 3 s) demonstrate that the heating and cooling of the glass capillary are not instant due to the thermal mass. As expected, this prevents the achievement of an ideal thermal shock. The temperature curves exhibit a rapid initial increase, which gradually levels off before reaching the target temperature. This behavior is attributed to the decreasing temperature gradient between the heating medium and the sample. The target temperature is typically reached after approximately 2 s. Cooling occurs rapidly through forced convection. For example, following 1 s of cooling at a bath temperature of 60 °C, the sample temperature drops to approximately 40 °C. At a bath temperature of 70 °C, this takes about 1.5 s, while at 85 °C, around 2 s are required.

A thermal tolerance was defined to take into account the heating and cooling time. The tolerance limit was defined as 5 % of the target temperature in °C, so that only the time during which the sample reached at least 95 % of the target temperature in °C is counted as exposure time. Therefore the exposure time is calculated as follows:

$$t_{exp} = t_{set} + \Delta t \tag{4}$$

Where t_{exp} is the exposure time of the microorganism after the correction, t_{set} is the set time of the submersion in the water bath and Δt the time correction, which is calulated as follows:

$$\Delta t = t_1\,(\vartheta > 0.95\vartheta_{set}) - t_2\,(\vartheta < 0.95\vartheta_{set}) \tag{5}$$

Where t_1 is the time when the probe reached 95 % and t_2 the time when the temperature ϑ falls below 95 % of the set exposure temperature ϑ_{set} in °C. This calculation was carried out for the considered times and temperatures respectively. The mean value of the time deviation is $\Delta t = -1.3\,s$. As this value was derived directly from the measured sample temperature, the duration of immersion and removal of the sample are already included.

Thermal inactivation of microorganisms

Enterococcus viikkiensis

Enterococcus viikkiensis was tested at temperatures and set exposure times of 60 °C (4 s, 6 s, 8 s), 70 °C (2 s, 3 s, 4 s) and 85 °C (2 s, 3 s, 4 s). At 85 °C there was no measurable survival detected. The resulting concentrations in CFU/ml are displayed as bars in Fig. 5 in dependence of the exposure time and temperature. The measurements were performed in triplicates and the error bars show the standard deviation of each sample (n=3). The initial CFUs differ as the experiments were conducted on different days. At 60 °C the rate of inactivation increases with extended exposure time. The calculated D-value at $t_{set} = 4\,s$ is $D_{4\,s,60\,°C} = 51.68$ s and decreased to $D_{8\,s,60\,°C} = 9.49$ s with $t_{set} = 8$ s. The D-values were calculated with the mean of the 3 samples and the corrected actual exposure time t_{exp}. After 8 s of exposure, thermal inactivation reaches approximately 80 %. According to the ANOVA analysis, this reduction is statistically significant ($p = 0.045$). At 70 °C the rate of inactivation increases between $t_{set} = 2$ s and $t_{set} = 3$ s with with D-Values of $D_{2\,s,70\,°C} = 1.28$ and $D_{3\,s,70\,°C} = 0.73$ s. After 4 s of set exposure time the inactivation is estimated at 99.9 %. At 70 °C the thermal inactivation was significant after all durations ($p_{2\,s} = 0.00022, p_{3\,s} = 0.00002, p_{4\,s} = 0.00002$). However, the differences between the thermally treated microorganisms at 70 °C were not significant.

Staphylococcus capitis

Staphylococcus capitis was tested at temperatures and set exposure times of 60 °C (6 s, 8 s, 10 s), 70 °C (2 s, 3 s, 4 s, 6 s) and 85 °C (2 s, 3 s, 4 s). Compared to the previous tests, the exposure times were adjusted due to the higher thermal resistance. The concentration results are shown in Fig. 6, using the same format as previously. Again as with *E. viikkiensis* at 85 °C, there was no measurable survival detected. The data show some inconsistencies, with a higher CFU count observed after 8 seconds of exposure at 60 °C than after 6 seconds. However, the difference was not significant. The calculated D-value at $t_{set} = 6\,s$ and $t_{set} = 8$ s where therefore $D_{6\,s,60\,°C} = 10.77$ s and $D_{8\,s,60\,°C} = 16.56$ s. All thermal inactivations at 60 °C were statistically significant ($p_{6\,s} = 0.005, p_{8\,s} = 0.006, p_{10\,s} = 0.001$). Similar behaviour is observed after 3 and 4 s of set exposure time at 70 °C. The thermal inactivation after 2 s of set exposure time was statistically not significant ($p_{2\,s} = 0.44$). After 3 s and 4 s the inactivation was significant with ($p_{3\,s} = 0.01, p_{4\,s} = 0.01$). When treated for 6 seconds of set exposure time t_{set} at 70 °C, there was no measurable survival. The differences between all thermally threated probes were not significant.

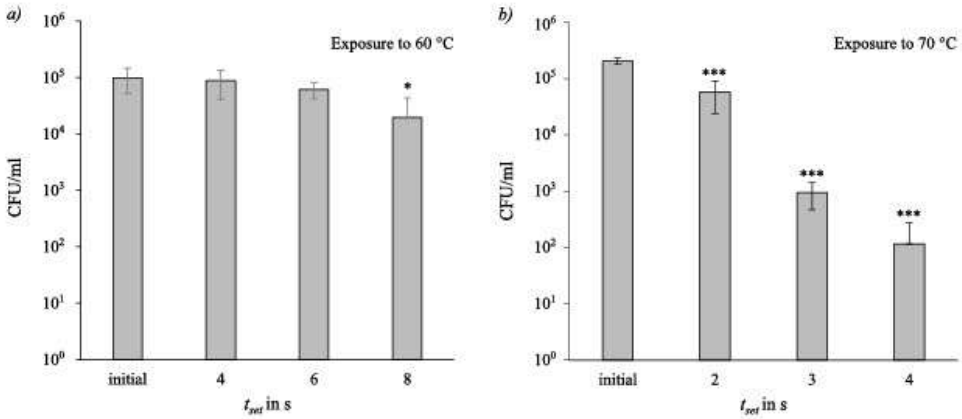

Fig. 5. Survival of *Enterococcus viikkiensis*; *a)* after exposure to 60 °C for a set exposure time of (4 s, 6 s, 8 s); *b)* after exposure to 70 °C for (2 s, 3 s, 4 s). Significance level compared to initial (ANOVA): $^{*}p \leq 0.05$; $^{***}p \leq 0.001$.

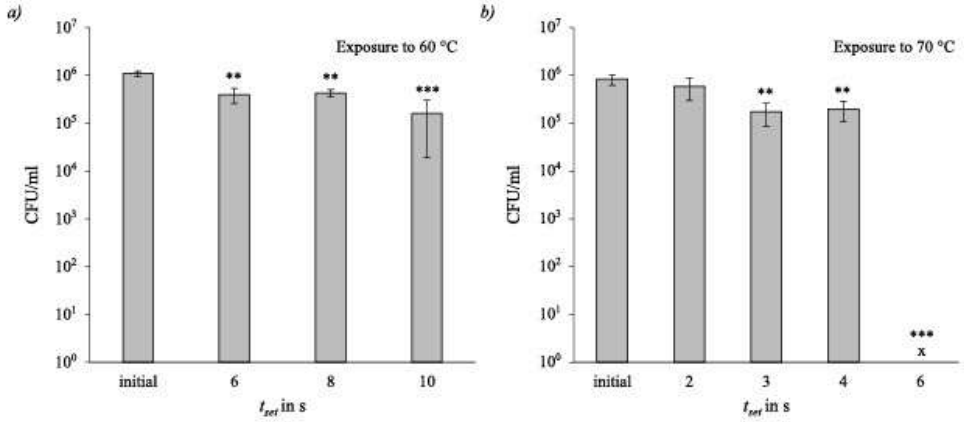

Fig. 6. Survival of *Staphylococcus capitis*; *a* after exposure to 60 °C for a set exposure time of (6 s, 8 s, 10 s); *b* after exposure to 70 °C for (2 s, 3 s, 4 s, 6 s). Significance level compared to initial (ANOVA): $^{**}p \leq 0.01$; $^{***}p \leq 0.001$.

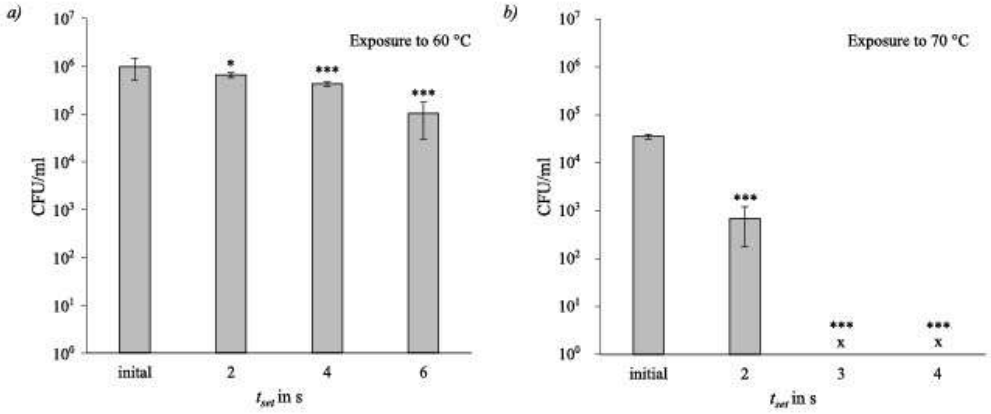

Fig. 7. Survival of *Burkholderia lata*; *a* after exposure to 60 °C for a set exposure time of (2 s, 4 s, 6 s); *b* after exposure to 70 °C for (2 s, 3 s, 4 s). Significance level compared to initial (ANOVA): $^{*}p \leq 0.05$; $^{***}p \leq 0.001$.

Burkholderia lata

Burkholderia lata was tested at temperatures and set exposure times of 60 °C (2 s, 4 s, 6 s), 70 °C (2 s, 3 s, 4 s) and 85 °C (2 s, 3 s, 4 s). Figure 7 displays the concentration results in the previously used format. As with both previously tested microorganisms, there was no measurable survival at 85 °C. The initial concentrations at 60°C and 70°C differ due to the experiments being conducted on separate days. After exposure times of 3s and 4s at 70 °C there was also no measurable activity. The thermal inactivation after all exposure times at 60 °C ($p_{2\,s} = 0.019, p_{4\,s} = 0.001, p_{6\,s} = 0.0001$) and 70 °C ($p_{2\,s,3\,s,4\,s} < 0.0001$) was significant.

MS2

MS2 was tested at temperatures and set exposure times of 50 °C (3 s, 5 s, 7 s), 60 °C (3 s, 4 s), 70 °C (2 s, 3 s, 4 s) and 85 °C (2 s, 3 s). The results are displayed in Plague Forming Units per ml (PFU/ml) in Fig. 8. No measurable survival was detected at any given exposure time after heat treatment at 70 °C and 85 °C. At 50 °C there was no measurable inactivation after 3 and 5 seconds. After 7 s exposure time at 50 °C the inactivation was 91.4 % with a calculated D-value of $D_{7\,s,50\,°C} = 5.34\,s$ and significant ($p_{7\,s} = 0.01$). Exposure to 60 °C

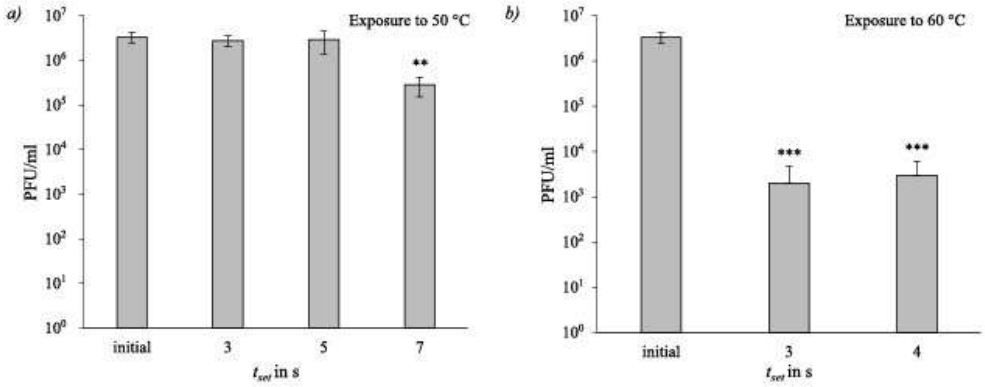

Fig. 8. Survival of MS2; *a* after exposure to 50 °C for a set exposure time of (3 s, 5 s, 7 s); *b* after exposure to 60 °C for (3 s, 4 s). Significance level compared to initial (ANOVA): $^{**}p \leq 0.01$; $^{***}p \leq 0.001$.

Microorganism	D-Value			
	50 °C	60 °C	70 °C	85 °C
Enterococcus viikkiensis	not tested	27.7 ± 20.0	0.9 ± 0.3	fully inactivated
Staphylococcus capitis	not tested	12.6 ± 3.2	3.8 ± 1.0	fully inactivated
Burkholderia lata	not tested	5.4 ± 1.7	0.4 ± 0.1	fully inactivated
MS2	31.1 ± 29.4	0.7 ± 0.2	fully inactivated	fully inactivated

Table 3. D-Values of the tested microorganisms.

Microorganism	Activation Energy E_a in J/mol	Frequency factor $ln(a)$ in 1/s
Enterococcus viikkiensis	302611.3	107.0
Staphylococcus capitis	114257.5	39.6
Burkholderia lata	239738.5	85.7
MS2	335847.6	122.9

Table 4. Average activation energy E_a and frequency factor $ln(a)$ for the tested microorganisms.

resulted in a statistically significant ($p_{3\,s,4\,s} < 0.0001$) inactivation of 99.9 % after 3 and 4 seconds with D-values of $D_{3\,s,60\,°C} = 0.53\,s$ and $D_{4\,s,60\,°C} = 0.89\,s$.

Decimal reduction times and modelling

An average for the decimal reduction time was calculated for the tested temperatures. The results are listed in Table 3 with the according 95 % confidence intervals (CI). As only short periods of thermal inactivation up to 10 s were tested, the confidence interval is larger for higher D-values, such as the thermal inactivation of MS2 at 50 °C or *E. viikkiensis* at 60 °C, due to the relatively low thermal inactivation and high deviation in the experiments.

Among all tested microorganisms, bacteriophage MS2 exhibited the highest sensitivity to thermal shock. Due to complete inactivation after the selected exposure periods, it was not possible to determine decimal reduction times (D-values) at 70 °C. Among the bacterial strains, *B. lata* was the most susceptible to thermal treatment at both 60 °C and 70 °C, exhibiting the lowest D-values. At 60 °C, *E. viikkiensis* demonstrated the highest thermal resistance, while at 70 °C, *S. capitis* exhibited the highest D-value. To predict the temperature-dependent inactivation times of the microorganisms, the reaction rate constant was determined and modeled using the Arrhenius equation (Equation 2). The resulting average activation energy E_a and frequency factor $\ln(a)$ are summarized in Table 4.

To estimate the required exposure time for a 3-log reduction as a function of temperature, calculations based on the previously described Arrhenius model were performed. The results for the tested microorganisms are shown in Fig. 9. At 85 °C, all microorganisms except *S. capitis* reach a 3-log inactivation after $\approx 1\,s$ or less.

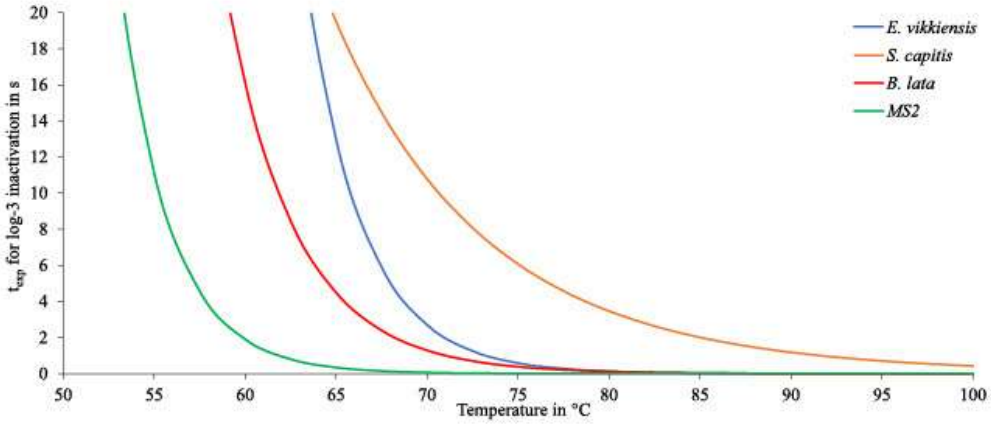

Fig. 9. Exposure time for a 3-log inactivation of *E. viikkiensis*, *S. capitis*, *B. lata* and MS2 in dependence of the temperature.

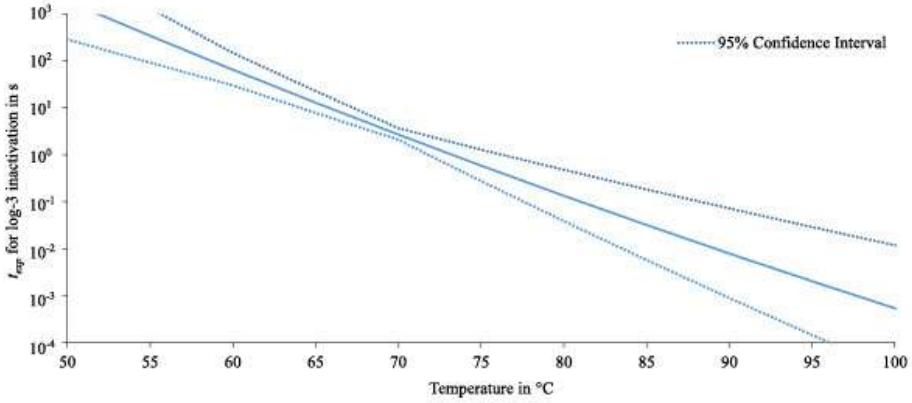

Fig. 10. Exposure time for a 3-log inactivation of *E. viikkiensis* in dependence of the temperature with the according 95 % confidence intervall.

Since experimental data were only available for 60 °C and 70 °C, the predictive accuracy decreases at temperatures outside this range. Therefore, the 95 % confidence intervall was calculated according to the experimental results of *E. viikkiensis* as it had the highest D-value and widest confidence interval at 60 °C and *S. capitis* as it had he highest D-value and widest confidence interval at 70 °C. The results for the thermal inactivation of *E. viikkiensis* including the 95 % confidence interval are shown in Fig. 10. According to the upper bound of the 95 % confidence interval, an exposure time of less than 0.1 s is required to achieve a 3-log reduction at 100 °C.

The predicted exposure times required for a 3-log reduction of *S. capitis* including the 95 % confidence interval are presented in Fig 11. Similar to *E. viikkiensis*, model predictions for *S. capitis* are based on experimental data obtained at 60 °C and 70 °C. Consequently, the reliability of the extrapolated values decreases at temperatures outside this interval. The 95 % confidence intervall is smaller here, as the data showed less variability. Based on the upper limit of the 95 % confidence interval, an exposure time of approximately 2.7 s is estimated to be sufficient for a 3-log reduction at 100 °C. However, according to the experimental results no survival was measurable after exposure to 85 °C for 2 s.

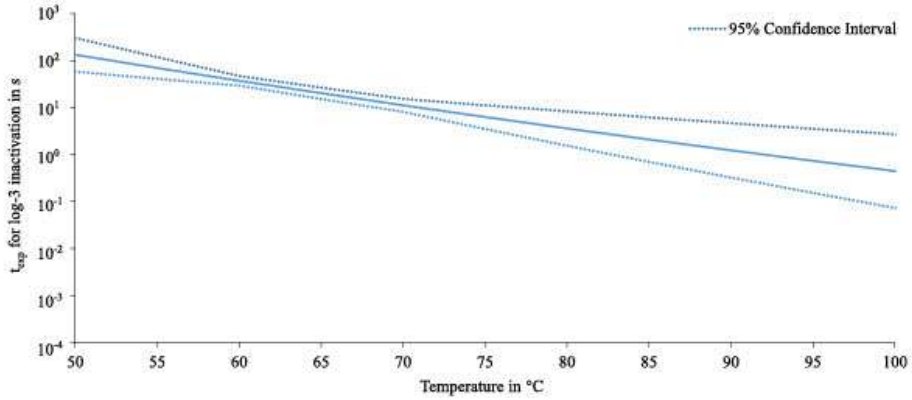

Fig. 11. Exposure time for a 3-log inactivation of *S. capitis* in dependence of the temperature with the according 95 % confidence intervall.

Discussion

This study presented an experimental setup for investigating the thermal inactivation of microorganisms through short-duration thermal shocks. The thermal shock was measured using a thermocouple placed in the buffer medium. In the conducted experiments, microorganisms were exposed to a thermal shock with an initial time span of approximately 0.7 s. However, due to non-ideal heat transfer conditions, this duration was corrected from the actual submersion time in the heating bath as detailed in the methods section. To evaluate the resistance of microorganisms to thermal shocks, a literature review was conducted for comparison. Our experimental setup produced significantly shorter exposure times than those typically reported.

For *E. viikkiensis*, no literature data were found regarding resistance to thermal shocks. However, *Enterococcus faecium* is one of the most studied species in this context. Freeman et al.[33] exposed *E. faecium* in broth culture to 65–80 °C, with survival reported up to 20 min at 65–75 °C and 3 min at 80 °C. The method of heating was not specified. Martinez et al.[34] showed that the D-values of *E. faecium* at 70 °C are dependent on growth temperature and duration. Reported D_{70} values ranged from 0.33 to 1.73 min across growth temperatures of 5–45 °C and times from 1 to 1200 h. At 37 °C and 24 h growth, a D_{70} of 0.97 ± 0.06 min was observed. Heat treatment was performed using a TR-SC thermoresistometer, where inocula were injected into pre-heated buffer with neutral pH. Coe et al.[35] examined thermal inactivation of *E. faecium* on mash feed, using a heated air stream followed by cooling. A D_{70} value of 135.7 s was reported. In contrast, our study revealed much shorter thermal inactivation times for *E. viikkiensis*, with a D_{70} of 0.9 ± 0.3 s. This discrepancy may be due to the intense, short-term thermal shock applied in our experiments, or inherent differences between *E. faecium* and *E. viikkiensis*.

For staphylococci, the potentially vancomycin-resistant *Staphylococcus aureus* has been widely studied. Kennedy et al.[36] reported D-values between 4.8 and 6.5 min at 60 °C in soy broth. Montanari et al.[37] examined various staphylococcal strains at 80 °C. Test tubes were submerged in a water bath, reaching target temperature within 1.5 min. A 6-log reduction in bacterial count occurred within 2–4 min, although survival was observed up to 20 min. In our study, *S. capitis* K1 exhibited significantly shorter inactivation times. The D-values were 12.6 ± 3.2 s at 60 °C and 3.8 ± 1.0 s at 70 °C. Complete inactivation was achieved after 2 s treatment time in the 85 °C water bath. These differences are likely attributable to the shorter, more intense heat exposure in our setup or species-specific heat resistance.

Only limited data exist regarding thermal inactivation of *Burkholderia* species. No D-values were found in the literature. Schroeder and Loparev[38] achieved complete inactivation of a high-density suspension (10^{10} CFU/ml) of *Burkholderia cepacia* at 95 °C after 45 s using a Denator Stabilizer T1. Perrett and Mawhinney[39] studied inactivation of *Burkholderia mallei* in equine serum. A suspension ($\geq 10^{6}$ CFU/ml) was heated to 56 °C for up to 30 min. Complete inactivation was observed after 20–30 min, while viable colonies were detected after 10 min. In our study, *B. lata* was the most susceptible bacterium to thermal shocks. D-values were 5.4 ± 1.7 s at 60 °C and 0.4 ± 0.1 s at 70 °C. Complete inactivation occurred after 2 s at 85 °C.

The MS2 bacteriophage, commonly used as a surrogate for more dangerous viruses such as SARS-CoV-2[26], was found by Shaffer et al.[40] to be significantly more heat-resistant than norovirus. They reported D-values of 354.2 min at 50 °C, 51.6 min at 60 °C, and 14.4 min at 70 °C. Heating was performed using a block heater in which the testing tubes reached the target temperature in approximately 2 min. In contrast, our results showed D-values of 31.1 ± 1.7 s at 50 °C and 0.7 ± 0.2 s at 60 °C. No viable MS2 particles were detected after 2 s at 70 °C. This suggests MS2 may be particularly susceptible to thermal shocks. Furthermore, Dolan et al.[41] reported a D-value of 0.64 s at 60 °C during microwave treatment of frozen strawberries, though the extent to which microwaves contributed to inactivation is unclear. Grinshpun et al.[42] studied MS2 inactivation in an airstream

and found that exposure times of 0.24–0.33 s at approximately 75 °C reduced virus viability by 1-log. In our experiments, no viable MS2 particles were detectable after exposure to 70 °C for 2 s.

Compared to literature values, our setup consistently achieved shorter inactivation times across all tested organisms. This is likely due to the rapid application of thermal energy, as opposed to gradual heating and cooling phases used in other studies. The described system is both cost-effective and suitable for replication by other research groups investigating thermal shock inactivation. To test temperatures above 100 °C, the water could be replaced with a heating bath fluid with a higher boiling point. This change could also improve the heat-up phase if the fluid has a higher thermal conductivity. However the cool-down phase could be extended as the evaporation of the water contributes to cooling down the capillary. Furthermore, immersing the glass capillary horizontally rather than vertically would allow the entire liquid column to be uniformly exposed to the thermal medium. This orientation helps prevent displacement of the liquid column caused by uneven heating and the expansion of air bubbles. For improved modeling and understanding of the underlying mechanisms, further experiments should explore a broader range of temperatures and exposure times. This would also help verify the appropriateness of the log-linear inactivation model used, or suggest alternatives. Especially at lower temperatures the decay curve showed a shoulder effect at short exposure times, which cannot be represented by the model. Extrapolations should be treated with caution, especially outside the tested temperature ranges (50–60 °C for MS2 and 60–70 °C for other microorganisms), where uncertainty is greater. Nevertheless, results at 85 °C indicate that all microorganisms tested experienced $>$ log 3 reductions after less than 0.7 s of corrected or 2 s of actual submersion time.

The collected data can inform the design of public transport vehicle heating systems aimed at achieving thermal inactivation. Specifically, it enables the estimation of relevant parameters such as air volume, exposure duration, and the temperatures required to inactivate potential pathogens. The proposed system is primarily suited for cold climates, where substantial heating capacity is already required. In warmer regions, alternative approaches such as HEPA filtration are likely to be more advantageous.These questions, however, require further investigation to determine whether thermal inactivation of indoor air in public transport vehicles is more energy-efficient or more effective than existing systems. Further research is also necessary to characterize the behavior and thermal response of microorganisms when exposed to heat in aerosolized form. Furthermore, relevant pathogens should also be tested to validate the results obtained with their surrogate organisms. Other potential applications can also be evaluated based on the data obtained. These include the treatment of microbiologically contaminated liquids, such as wastewater, and the thermal inactivation of microorganisms in clinical or healthcare environments. However, the energy efficiency of such approaches must be carefully assessed, as sufficient waste heat is typically not available and active heating of the medium would be required.

Conclusion

This study investigated thermal inactivation using harmless (BSL-1) surrogates of pathogens and developed an optimized setup in which thermal shocks achieve rapid inactivation. Our findings confirm that significant microbial inactivation can be achieved in short time frames, suggesting that integration into heating, ventilation and air conditioning (HVAC) systems of public transport vehicles is technically viable. At 85 °C, all tested microorganisms exhibited more than a 3-log reduction after less than 0.7 s of corrected exposure time, corresponding to 2 s of actual submersion. However, the potential integration of such a system, as well as its advantages and limitations compared to existing technologies, still require further investigation. Compared to previous literature values, the application of thermal shocks with a very rapid heating and cooling phase results in faster thermal inactivation. To further assess the applicability of thermal inactivation for aerosolized microorganisms in the cabin air of public transport vehicles, dedicated experiments using aerosolized microorganisms should be conducted. These studies are necessary to verify whether the same inactivation mechanisms and timeframes observed in liquid media also apply under aerosolized conditions. Furthermore also relevant pathogens should be investigated regarding their thermal inactivation characteristics and should be compared to their selected surrogates. While the proposed application focuses on public transport, the findings can be extended to other contexts, such as thermal inactivation in water and wastewater treatment or disinfection strategies in medical and healthcare environments.

Data Availability

Data is provided within the manuscript. Additional datasets used and analyzed during the current study are available from the corresponding author on reasonable request.

Received: 12 August 2025; Accepted: 2 January 2026
Published online: 09 January 2026

References

1. Ly, Y.-T., Leuko, S. & Moeller, R. An overview of the bacterial microbiome of public transportation systems-risks, detection, and countermeasures. *Front. Public Health* **12**, 1367324. https://doi.org/10.3389/fpubh.2024.1367324 (2024).
2. Gohli, J. et al. The subway microbiome: seasonal dynamics and direct comparison of air and surface bacterial communities. *Microbiome* **7**, 160. https://doi.org/10.1186/s40168-019-0772-9 (2019).
3. Grydaki, N., Colbeck, I., Mendes, L., Eleftheriadis, K. & Whitby, C. Bioaerosols in the Athens metro: Metagenetic insights into the PM10 microbiome in a naturally ventilated subway station. *Environ. Int.* **146**, 106186. https://doi.org/10.1016/j.envint.2020.106186 (2021).
4. Leung, M. H. Y., Wilkins, D., Li, E. K. T., Kong, F. K. F. & Lee, P. K. H. Indoor-air microbiome in an urban subway network: diversity and dynamics. *Appl. Environ. Microbiol.* **80**, 6760–6770. https://doi.org/10.1128/AEM.02244-14 (2014).
5. Miller, W. R. & Arias, C. A. ESKAPE pathogens: antimicrobial resistance, epidemiology, clinical impact and therapeutics. *Nat. Rev. Microbiol.* **22**, 598–616. https://doi.org/10.1038/s41579-024-01054-w (2024).

6. Mendes, Å. et al. Contamination of public transports by *Staphylococcus aureus* and its carriage by biomedical students: point-prevalence, related risk factors and molecular characterization of methicillin-resistant strains. *Public Health*129, 1125–1131. https://doi.org/10.1016/j.puhe.2015.05.010 (2015).
7. Lutz, J. K. et al. Methicillin-resistant *Staphylococcus aureus* in public transportation vehicles (buses): another piece to the epidemiologic puzzle. *Am. J. Inf. Control*42, 1285–1290. https://doi.org/10.1016/j.ajic.2014.08.016 (2014).
8. Nazarenko, Y. Air filtration and SARS-CoV-2. *Epidemiol. Health*42, e2020049. https://doi.org/10.4178/epih.e2020049 (2020).
9. Moreno, T. et al. Tracing surface and airborne SARS-CoV-2 RNA inside public buses and subway trains. *Environ. Int.*147, 106326. https://doi.org/10.1016/j.envint.2020.106326 (2021).
10. Howard, J. et al. An evidence review of face masks against COVID-19. *Proc. Natl. Acad. Sci. U. S. A.* https://doi.org/10.1073/pnas.2014564118 (2021).
11. Vlaskin, M. S. Review of air disinfection approaches and proposal for thermal inactivation of airborne viruses as a life-style and an instrument to fight pandemics. *Appl. Therm. Eng.*202, 117855. https://doi.org/10.1016/j.applthermaleng.2021.117855 (2022).
12. Canpolat, M. et al. Rapid thermal inactivation of aerosolized SARS-CoV-2. *J. Virol. Methods*301, 114465. https://doi.org/10.1016/j.jviromet.2022.114465 (2022).
13. Busto, M., Tarifa, E. E., Cristaldi, M., Badano, J. M. & Vera, C. R. Simulation of thermal sanitization of air with heat recovery as applied to airborne pathogen deactivation. *Int. J. Environ. Sci. Technol.: IJEST* https://doi.org/10.1007/s13762-022-03948-9 (2022).
14. Vehviläinen, M. et al. Setting up and operating electric city buses in harsh winter conditions. *Appl. Sci.*12, 2762. https://doi.org/10.3390/app12062762 (2022).
15. Erkmen, O. & Bozoglu, T. F. (eds) *Food Microbiology: Principles into Practice* (Wiley, 2016).
16. Price, W. C. Thermal inactivation rates of four plant viruses. *Arch. die Gesamte Virusforsch.*1, 373–386. https://doi.org/10.1007/BF01245548 (1940).
17. Villa-Rojas, R. et al. Thermal inactivation of salmonella enteritidis pt 30 in almond kernels as influenced by water activity. *J. Food Prot.*76, 26–32. https://doi.org/10.4315/0362-028X.JFP-11-509 (2013).
18. Aspridou, Z. & Koutsoumanis, K. P. Individual cell heterogeneity as variability source in population dynamics of microbial inactivation. *Food Microbiol.*45, 216–221. https://doi.org/10.1016/j.fm.2014.04.008 (2015).
19. Yap, T. F., Liu, Z., Shveda, R. A. & Preston, D. J. A predictive model of the temperature-dependent inactivation of coronaviruses. *Appl. Phys. Lett.*117, 060601. https://doi.org/10.1063/5.0020782 (2020).
20. Gędas, A., Schmidt, H. & Weiss, A. Identification and evaluation of Escherichia coli strain atcc 8739 as a surrogate for thermal inactivation of enterohemorrhagic Escherichia coli in fruit nectars: Impact of applied techniques on the decimal reduction time. *Food Microbiol.*122, 104544. https://doi.org/10.1016/j.fm.2024.104544 (2024).
21. Brown, K. L., Gaze, J. E., McClement, R. H. & Withers, P. Construction of a computer-controlled thermoresistometer for the determination of the heat resistance of bacterial spores over the temperature range 100 to 150° c . *Int. J. Food Sci. Technol.*23, 361–371. https://doi.org/10.1111/j.1365-2621.1988.tb00590.x (1988).
22. Condón, S., Arrizubieta, M. J. & Sala, F. J. Microbial heat resistance determinations by the multipoint system with the thermoresistometer TR-SC improvement of this methodology. *J. Microbiol. Methods*18, 357–366. https://doi.org/10.1016/0167-7012(93)90017-C (1993).
23. Conesa, R., Andreu, S., Fernández, P. S., Esnoz, A. & Palop, A. Nonisothermal heat resistance determinations with the thermoresistometer Mastia. *J. Appl. Microbiol.*107, 506–513. https://doi.org/10.1111/j.1365-2672.2009.04236.x (2009).
24. Jiang, Y. et al. Sub-second heat inactivation of coronavirus using a betacoronavirus model. *Biotechnol. Bioeng.*118, 2067–2075. https://doi.org/10.1002/bit.27720 (2021).
25. Weiss, H. et al. The airplane cabin microbiome. *Microb. Ecol.*77, 87–95. https://doi.org/10.1007/s00248-018-1191-3 (2019).
26. Domingues, J. M. et al. Inhibition of Escherichia virus MS2, surrogate of SARS-CoV-2, via essential oils-loaded electrospun fibrous mats: Increasing the multifunctionality of antivirus protection masks. *Pharmaceutics* https://doi.org/10.3390/pharmaceutics14020303 (2022).
27. Dawson, D. J., Paish, A., Staffell, L. M., Seymour, I. J. & Appleton, H. Survival of viruses on fresh produce, using ms2 as a surrogate for norovirus. *J. Appl. Microbiol.*98, 203–209. https://doi.org/10.1111/j.1365-2672.2004.02439.x (2005).
28. Kropinski, A. M., Mazzocco, A., Waddell, T. E., Lingohr, E. & Johnson, R. P. Enumeration of bacteriophages by double agar overlay plaque assay. *Methods Mol. Biol. (Clifton, N.J.)*501, 69–76. https://doi.org/10.1007/978-1-60327-164-6_7 (2009).
29. Vanlaere, E. et al. Taxon k, a complex within the *Burkholderia cepacia* complex, comprises at least two novel species, *Burkholderia contaminans* sp. nov. and *Burkholderia lata* sp. nov. *Int. J. Syst. Evol. Microbiol.*59, 102–111. https://doi.org/10.1099/ijs.0.001123-0 (2009).
30. Rahkila, R., Johansson, P., Säde, E. & Björkroth, J. Identification of enterococci from broiler products and a broiler processing plant and description of *Enterococcus viikkiensis* sp. nov. *Appl. Environ. Microbiol.*77, 1196–1203. https://doi.org/10.1128/AEM.02412-10 (2011).
31. Sobisch, L.-Y. et al. Biofilm forming antibiotic resistant gram-positive pathogens isolated from surfaces on the international space station. *Front. Microbiol.*10, 543. https://doi.org/10.3389/fmicb.2019.00543 (2019).
32. Emslander, Q. et al. Cell-free production of personalized therapeutic phages targeting multidrug-resistant bacteria. *Cell Chem. Biol.*29, 1434-1445.e7. https://doi.org/10.1016/j.chembiol.2022.06.003 (2022).
33. Freeman, R., Kearns, A. M. & Lightfoot, N. F. Heat resistance of nosocomial Enterococci. *The Lancet*344, 64–65. https://doi.org/10.1016/S0140-6736(94)91091-X (1994).
34. Martínez, S., López, M. & Bernardo, A. Thermal inactivation of *Enterococcus faecium*: effect of growth temperature and physiological state of microbial cells. *Lett. Appl. Microbiol.*37, 475–481. https://doi.org/10.1046/j.1472-765X.2003.01431.x (2003).
35. Coe, C. et al. Thermal inactivation of Salmonella surrogate, *Enterococcus faecium*, in mash broiler feed pelleted in a university pilot feed mill: Microbiology and food safety section. *Poult. Sci.*104, 104998. https://doi.org/10.1016/j.psj.2025.104998 (2025).
36. Kennedy, J., Blair, I. S., McDowell, D. A. & Bolton, D. J. An investigation of the thermal inactivation of *Staphylococcus aureus* and the potential for increased thermotolerance as a result of chilled storage. *J. Appl. Microbiol.*99, 1229–1235. https://doi.org/10.1111/j.1365-2672.2005.02697.x (2005).
37. Montanari, C. et al. New insights in thermal resistance of staphylococcal strains belonging to the species *Staphylococcus epidermidis*, *Staphylococcus lugdunensis* and *Staphylococcus aureus*. *Food Control*50, 605–612. https://doi.org/10.1016/j.foodcont.2014.09.039 (2015).
38. Schroeder, M. R. & Loparev, V. Rapid inactivation of non-endospore-forming bacterial pathogens by heat stabilization is compatible with downstream next-generation sequencing. *Appl. Biosaf.: J. Am. Biol. Saf. Assoc.*24, 129–133. https://doi.org/10.1177/1535676019861261 (2019).
39. Perrett, L. & Mawhinney, I. Inactivation of *Burkholderia mallei* in equine serum for laboratory use. *J. Clin. Microbiol.*53, 1456–1457. https://doi.org/10.1128/jcm.03141-14 (2015).
40. Shaffer, M., Huynh, K., Costantini, V., Vinjé, J. & Bibby, K. Heat inactivation of aqueous viable norovirus and MS2 bacteriophage. *J. Appl. Microbiol.* https://doi.org/10.1093/jambio/lxae033 (2024).
41. Dolan, K. D., Miranda, R. & Schaffner, D. W. Estimation of bacteriophage MS2 inactivation parameters during microwave heating of frozen strawberries. *J. Food Prot.*86, 100032. https://doi.org/10.1016/j.jfp.2022.100032 (2023).
42. Grinshpun, S. A. et al. Inactivation of aerosolized viruses in continuous air flow with axial heating. *Aerosol Sci. Technol.*44, 1042–1048. https://doi.org/10.1080/02786826.2010.509119 (2010).

Acknowledgements
The authors express their heartfelt gratitude to the deceased Prof. Ralf Möller who was the founder of the graduate school GANDALF. His enthusiasm and curiosity have inspired and guided our work. We miss him, both as a mentor and supervisor and as a friend.

Author contributions
H.G. conceived the experiment, H.G., Y.L.-S., F.A., B.P. prepared the experiment, H.G., Y.L.-S., F.A., B.P. conducted the experiment, H.G., Y.L.-S., F.A., B.P. analysed the results, H.G. wrote the manuscript, F.R. and S.L. supervised the study, all authors reviewed and approved the final manuscript.

Funding
Open Access funding enabled and organized by Projekt DEAL. This study received funding by the interdisciplinary graduate school GANDALF of the German Aerospace Center (DLR).

Declarations

Competing interests
The authors declare no competing interests.

Additional information
Correspondence and requests for materials should be addressed to H.G.

Reprints and permissions information is available at www.nature.com/reprints.

Publisher's note Springer Nature remains neutral with regard to jurisdictional claims in published maps and institutional affiliations.

2.7 Other publications

Co-authored peer-reviewed articles

- Ramos-Nascimento, A., Grenga, L., Haange, S. B., Himmelmann, A., Arndt, F. S., **Ly, Y. T.**, ... & Moeller, R. (2023). Human gut microbiome and metabolite dynamics under simulated microgravity. *Gut microbes*, *15*(2), 2259033.

- Boschert, A. L., Leuko, S., Krämer, C. L., Siems, K., **Ly-Sauerbrey, Y. T.**, Arndt, F. (2025). Spaceflight and Medical Microbiology: Possible Implications for Standard Infection Diagnostics and Therapy. *MDPI life*.

Scientific outreach

- **Ly, Y. T.***, Arndt, F.*, Boschert, A. L.*, Pavletić, B., Webner, F., Kohl, A., ... & Moeller, R. (2023). Nach der Pandemie ist vor der Pandemie: Und wie interdisziplinäre Forschung hier helfen kann. *Flugmedizin· Tropenmedizin· Reisemedizin-FTR*, *30*(03), 122-130.
  (also published 2024 in the journal *Laryngo-Rhino-Otologie*)

- Leuko, S., **Ly, Y. T.**, Timofeev, S. M., Auerhammer, A., Malzacher, G., & Moeller, R. (2024). Mikrobielle Welt auf Reisen: Die unsichtbare Begleitung im öffentlichen Nahverkehr und ihre Auswirkungen. *ZEVrail-Zeitschrift für das gesamte System Bahn*.

*Joint first authorship

Scientific conferences

Conference papers

- Koch, S. M.*, **Ly, Y. T.***, Arndt, F. S.*, Müller, D., Schmeling, D., & Moeller, R. (2022). Evaluating decontamination and prevention techniques by establishing standardized broad-range microbial testing platforms. In *17th International Conference on Indoor Air Quality and Climate, INDOOR AIR 2022*.

- Kohl, A.*, **Ly, Y. T.***, Leuko, S., Schmeling, D., Wagner, C., & Moeller, R. (2024). Evaluation of bioaerosol propagation through an air curtain. In *18th International Conference on Indoor Air Quality and Climate, INDOOR AIR 2024*.

  *Joint first authorship

Poster presentations

- Indoor Air 2022 (online): Evaluating decontamination and prevention techniques by establishing standardized broad-range microbial testing platforms
- VAAM 2022 (online): Standardized microbial mock community against pandemic threats
- Gordon Research Conference 2022 (Waterville Valley, USA): Development of a standardized and synthetic public transportation microbial community as a reference tool
- DGLRM 2023 (Cologne, Germany): DLR's Graduate School GANDALF: Awareness and fighting pandemic threats
- Indoor Air 2024 (Honolulu, USA): Modeling the public transport microbiome: Development of a microbial reference community
- VAAM 2025 (Bochum, Germany): Copper vs. Bacteria: Who Wins on the Surface? Antimicrobial effectiveness across copper content gradients on surfaces against a reference microbial community

Oral presentation

- Indoor Air 2024 (Honolulu, USA): Evaluation of bioaerosol propagation through an air curtain

3 Discussion

The scientific contributions of this thesis are summarized in **Figure 5** and will be discussed, based on the previously stated research questions.

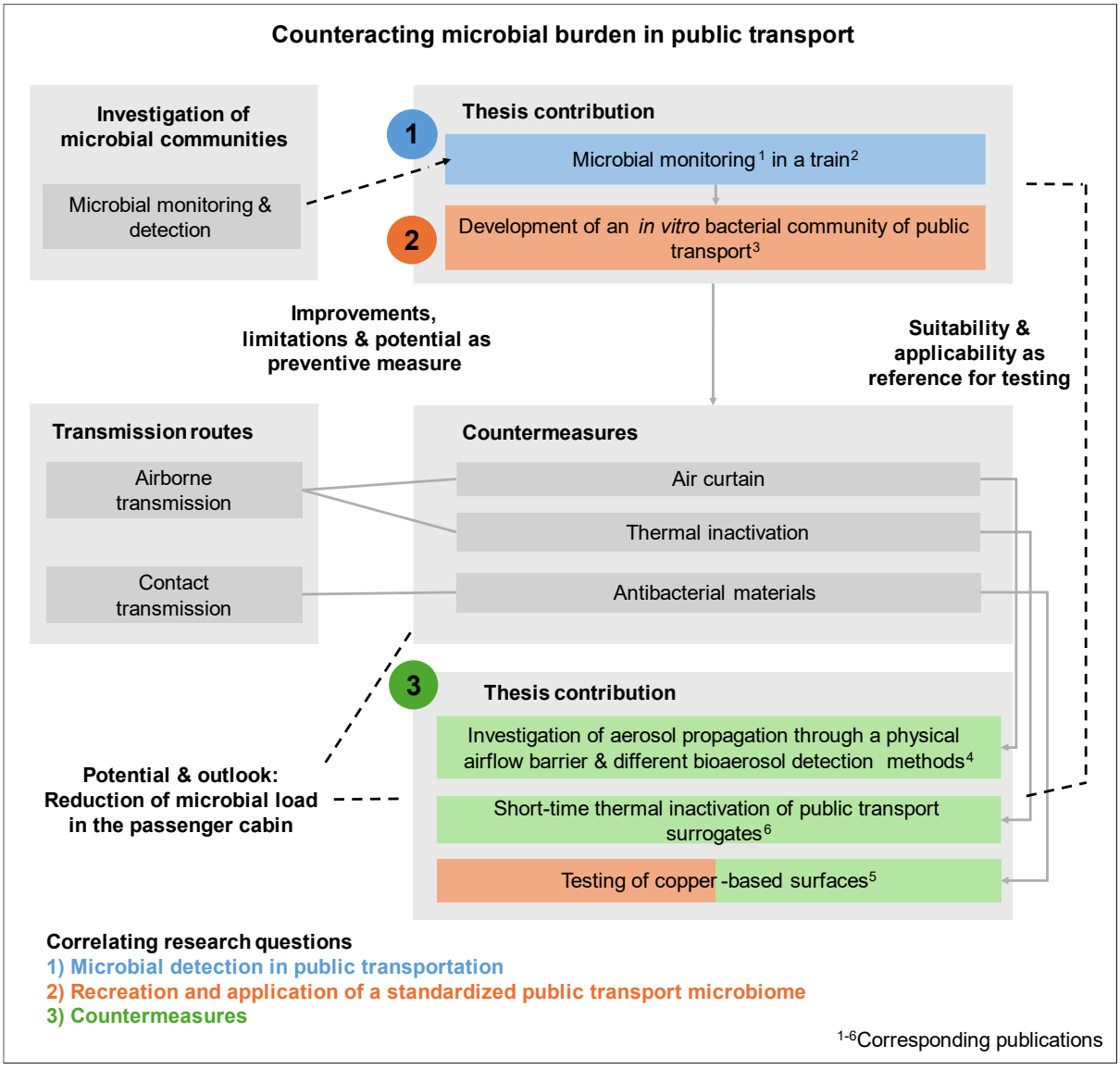

Figure 5: Overview of this thesis' contributions and discussion points, indicated by dotted lines. Based on Figure 1. Corresponding publications: [1]An overview of the bacterial microbiome of public transportation systems (2.1), [2]Microbial communities in local train cabins remain stable through the seasons during one year of monitoring (2.2), [3]Modeling the public transport microbiome (2.3), [4]Aerosol propagation through an air curtain (2.4), [5]Testing antibacterial effectivity of copper coated surfaces (2.5), [6]Short-time thermal inactivation of surrogates of the public transport microbiome (2.6).

3.1 Microbial surveillance as a preventive measure

Public transport passenger cabins represent an environment, which can facilitate transmission of infectious diseases. Therefore, the first research question within the frame of this dissertation focused on the detection of microbes within this environment.

RQ1) What microbiome are we facing in public transport systems, and how can we reliably detect it?

3.1.1 The public transport microbiome

A passenger cabin is defined by its confined space, human crowds of varying individuals, fomites, and limited air circulation. Similar confined environments which are important to monitor with the aim of infection control, safety of humans and products, or resistance tracking, that already underlie regular microbial monitoring, are e.g. intensive care units (ICUs), clean rooms, or the ISS, as concluded by Mora et al. (141). Onboard the ISS, health risks are shown by increased AMR compared to Earth analog, and a changed microbial composition, highlighting the importance of monitoring (142). This is conducted every 90 days, added by weekly cleaning, and biweekly disinfection (141). Microbial monitoring is also conducted in hospitals (143), where strict cleaning protocols, especially in ICUs, exist (141).

Microbiome studies help to detect and understand microbial taxa and dynamics, indicating potential transmission pathways and guiding the development of targeted countermeasures. This work conducted microbial monitoring under real-life conditions by sampling train cabins over the course of one year, every two months. To answer the first part of the research question, the results revealed, similar to previous studies, human-associated taxa throughout most sampling locations. This was expected, since humans shape their environmental microbiome, as shown in **Table 1** of the introduction. This observation is highlighted when we compare most abundant taxa from different studies on a variation of human-shaped environments (see **Table 3**). Four genera, namely *Corynebacterium, Staphylococcus*, *Streptococcus,* and *Pseudomonas* are highly abundant in all listed environments. Other highly abundant genera are *Micrococcus* and *Kocuria*. Since **Table 3** consists of data from multiple previous studies (and our study, chapter 2.2), a variation due to sampling substrate (surface, air, dust) and detection (sequencing technology, data analysis) is present, which influence the outcome of microbiome studies.

Nevertheless, clear similarities were observed throughout the train cabin, outside the passenger cabins (subway station), aircraft cabin, and even onboard the ISS.

Table 3: Most abundant taxa in selected human-shaped environments. Green highlights similar taxa in all categories.

Train cabin (this work)	**Subway station and cabin**	**Aircraft cabin**	**ISS**
Cutibacterium	*Staphylococcus*	*Staphylococcus*	*Corynebacterium*
Corynebacterium	*Acinetobacter*	*Pseudomonas*	*Streptococcus*
Acinetobacter	*Corynebacterium*	*Corynebacterium*	*Staphylococcus*
Staphylococcus	*Micrococcus*	*Streptococcus*	*Propionibacterium*
Streptococcus	*Propionibacterium*	*Enterobacteriaceae*	*Faecalibacterium*
JC017	*Pseudomonas*	*Flavobacterium*	*Haemophilus*
Pseudomonas	*Sphingomonas*	*Kocuria*	*Actinomyces*
Paracoccus	*Flavobacterium*	*Micrococcus*	*Pseudomonas*
Kocuria	*Streptococcus*	*Sphingomonas*	*Micrococcus*
Prevotella	*Kocuria*	*Stenotrophomonas*	*Bacillus*

References: **Subway** – Afshinnekoo et al., 2018 (64), Kang et al., 2018 (65), Gohli et al., 2019 (66), Zhao et al., 2019 (67), Hernández et al., 2020 (68). **Aircraft cabin** – Weiss et al., 2019 (62), Liu et al., 2020 (63), Sun et al., 2020 (60). **ISS**: Mora et al., 2019 (144), Venkateswaran et al., 2014 (145), Lang et al., 2017 (146), Avila-Herrera et al., 2020 (147).

To the best of my knowledge, no other longitudinal study similar to our train microbiome study has been conducted before, since most previous studies focused on the subway station rather than passenger cabins (66, 148-150). Studies, such as by Hsu et al. (2016) (151), investigated both train cabins and stations within three samplings (2x May, 1x October). Similar observations to our study were shown, such as the abundant detection of *Propionibacterium acnes*. An advantage of our study was the collection of in total six samplings (1x spring, 2x summer, 1x fall, 2x winter), allowing for the investigation of influences by temperature and relative humidity fluctuations. This can be of great relevance, as both factors influence microbial transmission and infection risk, and can vary between bacterial species, as concluded by Hiwar et al. (2021) (152). Bacterial strains of *Staphylococcus aureus*, *Pseudomonas aeruginosa* and *Acinetobacter baumannii*, all species of the ESKAPE pathogens, showed improved survival on high-touch dry surfaces at low temperature and relative humidity (153),

favoring outbreaks in cold seasons. This was also observed for two strains of *E. coli.* In contrast, *E. coli* within an aerosol showed higher survival at higher relative humidity (154). Viruses, such as Influenza survive and transmit better at low relative humidity and temperatures (155-157). Further, low relative humidity can enhance the susceptibility of the host by drying out mucous membranes and impairing mucociliary clearance (158, 159). No significant different seasonal changes in diversity were found within the train cabins. Although the measured relative humidity highly varied throughout the sampling times, no correlation between the train cabin air diversity and the relative humidity was observed. Since the indoor temperature in the cabin was constant, it can be suggested that the detected bacteria were also less influenced by the relative humidity. Sampling locations showed higher variation compared to the sampling season. Since sampling took place at midday and cleaning occurs at night, evening sampling could have affected the results due to higher passenger traffic.

3.1.2 Microbial detection – lack of standards and limited by resources

The second part of RQ1 addresses the detection of the public transport microbiome. The methodical approach for microbial detection can influence the results of microbiome studies and is therefore important to discuss. For sampling, swabs are widely used in similar studies and were also used in this work for surface sampling. The handling of swabs is simple, and only requires minimal training. Especially for hard-to-reach spots, such as the louvers in the passenger cabin, swabs are suitable. Compared to swabs, wipes are better suited for sampling large (nonporous) surfaces and are therefore a good alternative for microbial monitoring. However, they can be more prone to contamination during sampling, their handling is less standardized and more laborious, and they can be more expensive than swabs. For air collection, active air or dust sampling are widely spread, but the selection of the sampling method can highly influence the outcome of the detected microbiome (160). The same accounts for DNA extraction, which can influence the yield and diversity (161). As expected, this applies for the data analysis, too. Within this work, 16S rRNA sequencing of the V1-V2 region was performed. The selection of the V1-V2 region as target was based on high taxonomic resolution of respiratory samples (162) and suitability for low-biomass samples (163). Sequencing of variable regions of the 16S rRNA gene in similar microbiome studies is common, as shown by Ly et al. (2021) (36). Many studies on the subway microbiome were performing 16S rRNA sequencing of the V3-V4 (66, 164, 165) or only the V4 region (149, 151, 166). Less frequent was the investigation of the whole 16S gene or metagenome sequencing. Both, however, allow

a deeper analysis of the microbiome and are able to reliably identify bacterial species. Although these methods generate detailed information, high-throughput is bound to high cost and might not be feasible for regular monitoring. An issue that can overestimate the abundance of bacteria and affects sequencing, is the intragenomic heterogeneity of 16S rRNA genes (167). The degree of overestimation differs for phyla, targeted variable region and full length 16S rRNA gene. Another common approach to investigate the microbiome is cultivation and subsequent sequencing (for identification). This can be less expensive, but the detection is limited to cultivable species. Besides the sequencing technique, data analysis can influence the results, for example, due to varying bioinformatic pipelines that process raw data differently or due to multiple available databases for feature assignment (168). It shows, that a comparison between studies can be difficult at some point due to the variation of used methodologies. Therefore, standardization for distinct targets is important. Standardized protocols have been developed within the MetaSUB Consortium (169, 170) and are important for conducting microbial monitoring studies. However, sample processing within this consortium is conducted in distinct laboratories and, therefore, bound to a certain capacity. Thus, the standardization cannot be implemented in every microbiome research study. Besides research-driven standard protocols, there are no legal guidelines for microbial monitoring in public transport settings.

For targeted detection of distinct pathogenic species, performing qPCR is a good method that stands in contrast to the general detection of the all-over environmental microbiome. This was utilized to detect *S. capitis* and *S. aureus* in the train cabin, as a low-cost alternative to sequencing at species level. Low levels of both species were observed, while *S. aureus* was found in less sampling locations than *S. capitis*. Besides species specific targets, markers like antibiotic resistance genes can additionally be addressed. Although conducting qPCR is less labor and cost intensive compared to sequencing, only a few species can be targeted due to limited DNA of the swab samples. Alternatively, selective cultivation of potential pathogens can be conducted and is aimed for future studies.

Based on the findings, it is not easy to tell if the public transport microbiome poses a human health threat. It is important to conduct microbial monitoring to control and be aware of the possible hotspots and behavioral measures that reduce microbial transmission. At which concentration a pathogen is stated as infectious cannot be answered easily, as it depends on host and pathogen, and in case of airborne transmission, on factors like exposure time, CO_2 levels and relative humidity (171, 172). Based on that, the infectious dose can range greatly, as shown in a review on foodborne pathogens with a dose between <10 to over 10^5 organisms (173). The

results of our study revealed, that the diversity of the train cabin microbiome was dependent on the sampling position and not the sampling season. This information can be further targeted to identify microbial hotspots, for example via targeted detection of potential pathogens. In the end, obtained data can be used to determine surfaces, that should be considered for antimicrobial coatings or intensified cleaning protocols. These interventions can be tested using an *in vitro* model of the environment, which can help to test and optimize them under controlled conditions. In this work, this was performed with a variation of countermeasures.

3.2 *In vitro* bacterial community of the public transport microbiome

One important element of this work was the establishment and application of the *in vitro* bacterial community. Single species from this community as well as the community as a whole were used in all tested microbial countermeasures (air curtain, thermal inactivation, antibacterial materials). Learnings and findings based on the created bacterial community are discussed in the following, pointing out its suitability, applicability and distinct variations between it and single species experiments.

RQ2) From *in vivo* to *in vitro*: Is it possible to recreate and apply a standardized public transport microbiome as a simplified, yet realistic reference model for experimental testing?

3.2.1 Suitability & applicability as a reference

As the title of this thesis suggests, one central aim is to improve detection and inspire prevention measures against bacterial contaminants in public transportation using an *in vitro* bacterial community. It was decided to use a community rather than single model organisms, since the latter are unable to properly reflect the actual response to distinct stressors compared to their response in a real environmental setting. This is due to community effects, which can be synergistic or antagonistic interactions, or genotypic and phenotypic diversity (174). Therefore, an approach closer to real-life settings was introduced in order to investigate and test the effectivity of potential microbial countermeasures. The idea is not new, as *in vitro* microbiomes exist, based on the gut (70, 175) or soil (176) microbiome. However, this is the first time that

such a bacterial community has been developed in regards to the public transport environment (177). The *in vitro* bacterial community resembles abundant and relevant bacterial taxa of known public transport microbiomes. Its composition is based on previously conducted studies presented in this work (see chapter 1.3, 2.1). Those include genera like *Pseudomonas*, *Staphylococcus*, *Propionibacterium*, *Streptococcus*, *Sphingomonas*, and *Corynebacterium*. Representatives such as *Enterococcus* and *Flavobacterium* are not the most abundant according to literature, but are nevertheless considered as relevant. For instance, *Flavobacterium* and *Burkholderia* were found to be abundant in a distinct publication on the aircraft cabin microbiome (62). Further, *Enterococcus* represents a genus of the ESKAPE pathogens, which are highly relevant due to their remarkable antibiotic resistance.

A key advantage of the created bacterial community is its biosafety level. All community members have been chosen specifically to be BSL-1, which makes handling in the laboratory straightforward and, therefore, enhances reproducibility by other scientists. Exchanging single species for those that are easier to cultivate would optimize reproducibility, since *S. halotolerans* DSM 101996^T and *P. cyclohexanicum* DSM 16859^T, as well as *F. frigoris* DSM 15719^T and *S. rubra* DSM 26135^T to a certain extent, exhibited aggravated cultivation.

But to what extent is this model reflecting the microbiome of real public transport or passenger cabins, and what are its limitations? First of all, most genera in the *in vitro* bacterial community are represented in the public transport microbiome, like skin-associated genera *Staphylococcus* or *Propionibacterium*. However, only bacteria and no other microorganisms such as fungal species or viral particles, and no anaerobic species were included. Furthermore, highly prevalent bacterial taxa in public transport environments such as *Micrococcus* and *Kocuria* were not selected for the bacterial community due to temporal expenditure and handling in the laboratory. Therefore, it was decided to limit the community to nine bacterial genera, and thus not all abundant taxa could be considered. It has to be noted, that the selection of the species within the bacterial community can greatly influence its behavior and reaction of it in different settings due to the production of potentially harmful metabolites, as reviewed by Hibbing et al. (2010) (178). The composition of genera of the *in vitro* community was intended to be equal in cell concentrations, although in nature, the microbiome is composed of a combination of highly abundant and rare taxa, with no equal distribution and depending on their environment (179, 180). As it is not possible to determine the exact abundance of each genus, an equally distributed bacterial composition was selected. The bacterial community members were carefully chosen, since there are many factors that need to be taken into account. Besides the reproducibility, two

species were selected to be distinguishable after cultivation in the bacterial community. Therefore, the antibiotic resistances of *B. lata* DSM 23089^T to streptomycin and *S. capitis* DSM 111179 to rifampicin was utilized. It was of great importance that other community members were not resistant to these antibiotics as well. To create a realistic substrate for the bacterial community, particularly for experiments in which the community was aerosolized to mimic exhalation, artificial saliva based on Woo et al. was used (2010) (181). At this point, a distinct difference to *in vitro* gut microbiomes is apparent. While *in vitro* gut microbiomes are often cultivated in one container with a special medium (182, 183), the bacterial community of this work was created by single cultivation of all species and mixture afterwards in PBS or artificial saliva. The cultivation poses one limitation of this work, as no co-cultivation was tested, which is expected to impact the results. Previous studies have demonstrated the impact of co-cultivation on the increased chemical diversity of microbial compounds, which cannot be detected in pure cultures (184). Although co-cultivation was not in the scope of this work, as this thesis presents the development and first experiments with the *in vitro* community, future studies should address this issue to gain further insights into the dynamics within the community. This presents a great challenge, since fast- and slow-growing species are included in the community, which facilitates artificial dominance. Further, the species grow under certain temperature and media. Creating specific media that imitate the oral environment, for example, would facilitate new applications of the *in vitro* bacterial community by providing even more realistic surroundings. But even at this point, the applications of the bacterial community are manifold: Various microbial interventions can be tested using the community as reference, such as disinfection and cleaning agents, that are used for passenger cabins.

It shows, that there are many obstacles that came along the development of the *in vitro* bacterial community. The "correct" selection of the species, cultivation of each species, and the approach to create equal distributions within the mixture. Despite the difficulties and limitations of the *in vitro* bacterial community, this model and similar studies are important to understand the bacterial reaction to certain stressors in a controlled setting.

To conclude and address RQ2 regarding the development and applicability of an *in vitro* bacterial community: Although certain limitations remain, as this is the first *in vitro* bacterial community to simulate the public transport microbiome, it has been well characterized and is suitable to use as a reference for different experimental tests.

3.2.2 Single vs. bacterial community testing

Focusing on the applicability of the created *in vitro* bacterial community (RQ2), a distinct driver of its creation is the investigation of stressors and effects on bacteria under more realistic settings. Single species can help to understand basic mechanisms and responses to stressors or conditions. However, a bacterial community adds more complexity, which has been demonstrated in this work in the form of synergistic behavior after wet contact killing on copper-containing (Cu-Al) surface coatings (see chapter 2.5) or within the investigations into air curtain effectivity and bioaerosol detection (see chapter 2.4). One advantage, that enhances applicability of the *in vitro* bacterial community, is the possibility to distinguish target species of the bacterial community by selective growth of the species *S. capitis* DSM 111179 and *B. lata* DSM 23089^T. It was shown throughout all studies, that *B. lata* DSM 23089^T was more susceptible to stressors or treatments, like desiccation (air curtain) and copper stress (Cu-Al coatings). This behavior can be traced back to the species' desiccation and copper tolerance, based on genetic settings and Gram-staining, as discussed in chapter 2.5 (185). Another factor, that influences the species survival, is the bacterial community. The community showed significant shielding against copper stressors for *S. capitis* DSM 111179. With a different community composition, varying shielding effects can be expected due to antagonist effects that different species can bring, e.g. through the reinforcement of antagonistic dynamics or modification of pairwise interactions (186). Further influence within bacterial communities and in single species is quorum sensing. It is a type of communication between bacteria, which allows a quicker activation of specific stress responses (187). Additionally, metabolites can be exchanged which also favor bacteria in vicinity (188). However, metabolites can also be harmful, as previously described. Antagonistic interactions can be further displayed by environmental modifications, such as changes in pH, caused by certain metabolites, leading to unfavorable growth conditions (189). The microbiome is also shaped by the competition for resources, overgrowth of low abundant species and selective pressure (140, 190). Additional investigation of the bacterial community is necessary to better understand community dynamics and their influence on the survival of distinct species. Synergies, competition, and biofilm formation are effects that were not investigated but should be addressed in the future, as they provide important insight into real-life environments and behaviors.

The developed simulated bacterial community allowed for the evaluation of different microbial countermeasures under controlled conditions. In the following section, intervention strategies are discussed in terms of their effectivity and applicability to public transport settings.

3.3 Reduction of microbial load in passenger cabins

Different interventions were tested to reduce microbial load in hypothetical passenger cabins by mitigating the microbial transmission through airborne and via surface pathways.

RQ3) To what extent can physical and material-based interventions reduce microbial load in passenger cabins?

3.3.1 Intervention of airborne transmission

Different physical-based interventions were tested to investigate their effectivity and applicability in passenger cabins. The first and major investigated physical-based intervention was the **air curtain**, equipped with HEPA filters (see chapter 2.4). For that, two different detection methods were employed: sensor-based particle measurement and CFU-based bacterial survival determination. This combination allowed for a differentiated analysis of the bioaerosol propagation in a closed environment. The outcome of the microbial assessment was dependent on the test microorganisms' tolerance to shear forces during bioaerosol generation. Since the used device (BLAM, CH Technologies) was designed for the aerosolization with low impact on microorganisms and has been tested in a previous study (191), the shear forces were expected to be little. Further, during the process of aerosolization, impingement, and continued presence on the petri dishes until retrieval, the bacteria are exposed to desiccation. The desiccation tolerance of distinct members of the bacterial community was investigated in pure cultures. *P. antarctica* DSM 15318^{T}, *S. halotolerans* DSM 101996^{T}, and *P. cyclohexanicum* DSM16859^{T} showed no detectable survival after up to 7 days of desiccation. In contrast, *S. capitis* DSM 111179 showed survival up to 28 days of desiccation, with a significant decline of CFU/mL (192). This observation can likely be explained by the origin of these species. More susceptible species were initially isolated from environments with high humidity, such as orange juice (193) or the respiratory tract (194). Therefore, they are expected to be less adapted to desiccation (193, 194). The used strain for the air curtain studies, *S. capitis* DSM 111179 was first isolated from stainless steel (type V2A) aboard the ISS (195) and is therefore adapted to rather dry environments. Previous work (196) has shown its desiccation tolerance. According to the genome annotation of *S. capitis* DSM 111179 (annotation name: GCF_025272695.1-RS_2024_10_12), it has similar genes as highly desiccation tolerant *S. aureus* that are relevant for its desiccation tolerance (197): *clpX*, coding for ATP-dependent Clp protease ATP-binding

subunit ClpX, *sigB* coding for RNA polymerase sigma factor SigB, and *yjbH*, coding for a protease adaptor protein. Of the mentioned genes, *B. lata* DSM 23089^{T} only has *clpx*, potentially explaining its lower desiccation tolerance. This section presents one limitation of the bacterial community. Depending on the species' isolation sites, their reaction to certain stressors can be highly variable and might be less close to their relatives in a real passenger cabin environment.

Different factors, like temperature, relative humidity, and positioning and flow velocity of the aerosol source and air curtain influence the outcome of such studies and were not changed in this work for a better comparability between the different air curtain scenarios tested. Besides, as described in the first chapter of the discussion, the infectiousness and bioaerosol spread are influenced by above mentioned factors (198), which should be addressed in future experiments to move towards application in a real passenger cabin. However, this study focused on initial testing of the bioaerosol detection and air curtain setup to determine its effectiveness against bioaerosol spread and therefore its feasibility to be used in a passenger cabin. Rooting back to RQ3, to what extent physical-based interventions can reduce the microbial load in passenger cabins? Combining the air curtain with HEPA filters was shown to reduce particles and bacteria by up to 66%. Although no standards exist, that prescribe a minimum effectivity for microbial reduction of ventilation or air purification systems, particularly for public transport, 66 % effectivity can be considered low. However, the experimental settings included high-dose bacterial concentrations for facilitated detection (~2.36×10^{9} CFU/m^{3} (*B. lata* DSM 23089^{T}), ~5.7×10^{9} CFU/m^{3} (*S. capitis* DSM 111179)), higher than can be expected to be realistically exhaled by one person during 10 minutes of breathing (up to ~2.3×10^{4} CFU/m^{3}, calculated based on max. concentrations of 7×10^{3} CFU/m^{3} after 3 min of breathing) (199). Therefore, more realistic settings with lower bacteria concentrations would most likely result in a higher air curtain effectivity.

Besides the mechanical approach to reduce bioaerosol transmission in a passenger cabin, other strategies were tested in this work. **Thermal inactivation** of microorganisms has been long known, and is most popular for its application in food industry, e.g. for pasteurization of milk or other products. During high heat exposure, bacterial cell damage is caused on structural and genetic level, resulting in membrane disruption, generation of oxidative stress, as well as protein denaturation and aggregation (200). The aim was to use this known microbial countermeasure and characterize the heat tolerance of microorganisms, that are not typical food contaminants, but more relevant for public transport settings and pathogenic outbreaks. For this purpose, a

heated water bath was used in combination with bacterial solutions sealed in glass capillaries. This approach allowed fast heat transmission and a controlled setting. A great advantage of thermal inactivation is the short time period it takes to inactivate microorganisms. Results showed no detectable survival of the tested microorganisms after exposure to 85 °C for 2 s, promoting the potential of short-time thermal inactivation as a microbial intervention in passenger cabins. However, there are heat resistant microorganisms, that cannot be inactivated by this approach. For example, spores from bacteria or fungi are highly resistant to heat (201, 202). Future experiments should test not only the microorganisms as single species, but also together in a bacterial community, including vegetative cells and heat-resistant spores. The obtained data can be compared to the next step – thermal inactivation of aerosolized microorganisms – for future applications in passenger cabins for air decontamination. In theory, the aim is to use such a setup in an electric people mover during the cold seasons when heating is required. Simultaneously, the heat inactivation supplies the cabin with air with lower microbial burden. The additional application of air curtains would enhance this effect by generating invisible barriers for bioaerosols.

Besides thermal inactivation, preliminary tests using **non-thermal plasma** were performed as another measure to reduce microbial contaminants in the air. The antimicrobial properties of non-thermal plasma have many similarities to those of copper. The mechanisms include the generation of reactive oxygen and nitrogen species (RONS), UV photons, charged particles (203-205), leading to oxidative stress, damage of cell membranes, DNA and protein damage. In an experimental setup (see **Figure 6**), the bioaerosol source was positioned at the left site with a flow direction to the right. Within the flow field, three built-in plasma units were distributed. In the end (right site), a ventilation system enforced the flow direction of the bioaerosol and petri dishes were positioned to collect the bioaerosol.

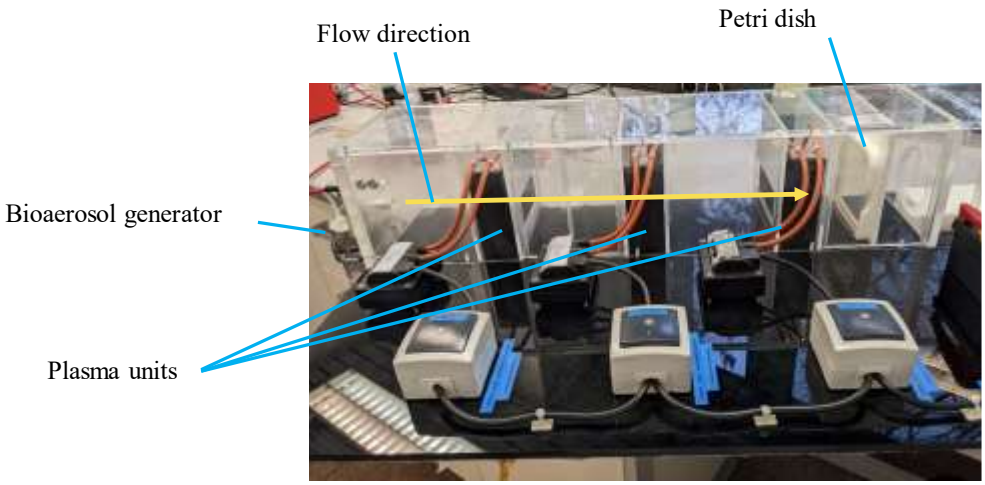

Figure 6: Experimental setup of plasma-based decontamination.

The preliminary tests showed great antibacterial effects, when using one of the three plasma units on a *S. capitis* DSM 111179 bioaerosol (10^6 CFU/mL) after five minutes of exposure. After incubation, 508 CFU were detected without any plasma intervention, whereas only 13 CFU were counted with one active plasma unit. This data already shows the great potential of non-thermal plasma as a method for a reduced microbial burden. However, the synthesis of side products of plasma, such as ozone or RONS have to be addressed, since they could irritate human air ways (206). Therefore, filter systems and degradation systems exist and are important before application in public settings (207). Nevertheless, as shown by Zhang et al. (2024) (208) or Jangra et al. (2023) (209), non-thermal plasma is already an effective method for air disinfection. It shows, that there are different possibilities to reduce the microbial load in the passenger cabin.

3.3.2 Intervention of contact transmission

The material-based intervention to reduce microbial load in passenger cabins were copper-based surface coatings. Fomites play a great role in the microbial transmission. Through the identification of hotspots and frequently touched surfaces in passenger cabins, targeted application of antimicrobial materials or coatings could be applied. Previous studies have tested different copper coatings, highlighting the importance of testing different microorganisms. Those were for instance fungal spores (210) or healthcare-related *Enterococcus faecium* strains, focusing on the impact of antimicrobial resistance and copper tolerance (211). Besides *in vitro* studies, experiments with potential antimicrobial surfaces have been conducted in real-life settings (e.g. public transport, hospital, schools, ISS) and have been shown to be effective (212-216). This work focused on the effectivity of copper and copper-alloy coatings against bacterial species within the *in vitro* bacterial community and as pure cultures. The results have shown that 100 at.% copper-coated surfaces had a significant antibacterial effect on the reference bacterial community. However, coatings with 79 at.% or less Cu content showed no significant effect on the survival of the tested species within the bacterial community and in single species testings, leaving space for improvement. It should be noted, that no long-term effects were tested. Therefore, it cannot be stated definitely that there is no antibacterial effect at all. With this work, extended data on the effectivity of copper and copper-alloys on bacteria within a bacterial community in comparison to pure cultures were provided.

There are different factors that influence the antibacterial properties of copper. The physical transmission efficiency of microorganisms depends on surface material, hand condition or coverings, and humidity (217-219). Another important factor is the surface type in terms of complexity, since flat surfaces, like tables, are easier to clean than door knobs or irregularly shaped objects (220). Long-term use is accompanied with debris, oxidation, biofilm formation and damage of material, which can reduce the antibacterial effectivity (221), when no proper cleaning or maintenance is given. Copper oxidation can reduce antibacterial properties by decreased Cu-ion release depending on the type of oxide and surface composition. The formation of a passivation layer of oxidized copper can constitute a problem by decreasing the ion release and therefore the antibacterial properties (222).

But overall, long-term use of copper surfaces still shows high antibacterial effectivity, as demonstrated by previous studies. In a study, a combination of bacterial cellulose and CuNPs was used for up to 90 days, which exhibited sustained antibacterial activity (223). Another study tested copper-coated door handles for three years, which were more effective against MRSA than glass and stainless steel (215). Anodic aluminum oxide-copper coatings were more effective than zincated Cu coatings after polishing in a study by Chen et al. (2023) (221). However, those results were highly dependent on the used test organisms. For example, a study using copper-doped Ti alloys for 14 days showed an antibacterial rate (based on untreated and treated bacterial count) of 100 % against *S. aureus*, but only 12 % against *Escherichia coli* (224). This observation can be attributed to the different properties and defense mechanisms of bacteria.

As shown by Novoa-Aponte et al. (2022) (104), bacteria differ in their genetic features and, therefore, capabilities to conquer copper stress. The difference in copper-tolerance was also observed in this thesis between *S. capitis* DSM 111179 and *B.* lata DSM 23089^{T}. Within the community, members carry different sets of genes related to copper tolerance, which could benefit species within the community, for example, by producing helpful metabolites, binding or sequestrating copper. The identification of copper-related genes in all bacterial community members was performed by WGS (Nanopore & Illumina) with subsequent hybrid assembly and annotation using Bakta (225), or based on publicly available annotated data from NCBI. The results are summarized in **Table 4**. The most abundant gene among the community members is the widely distributed copper-stress related *copZ*, which functions as a metallochaperone (226-230). It was found in six out of nine bacterial species in the community.

Table 4. Selection of copper tolerance and oxide stress related genes found in the genomes of the bacterial community. BL: *Burkholderia lata* DSM 23089^T, SC: *Staphylococcus capitis* DSM 111179, CH: *Corynebacterium halotolerans* DSM 44683^T, EV: *Enterococcus viikkiensis* DSM 24043^T, FF: *Flavobacterium frigoris* DSM 15719^T, PA: *Pseudomonas antarctica* DSM 15318^T, PC: *Propionibacterium cyclohexanicum* DSM 16859^T, SH: *Streptococcus halotolerans* DSM 101996^T, SR: *Sphingomonas rubra* DSM 26135^T.

Genes	**BL**	**SC**	**CH**	**EV**	**FF**	**PA**	**PC**	**SH**	**SR**
copC	×	×	×			×			×
copD	×					×			×
copY				×				×	
copZ	×	×		×	×	×	×		
pcoD	×								
cycoC	×								
cirA	×					×			
ompR	×					×			
cueR	×					×			
soxR	×					×			
csoR		×							
csoZ		×							
sufI	×								
cutC	×			×				×	
Other proteins									
Cu oxidase	×		×		×	×	×	×	×
Cu-containing nitrite reductase					×		×		
Cu binding protein			×		×			×	×
Cu resistance protein	×					×			×
Cu chaperone Pcu (A) C	×		×			×			×

Interestingly, *B. lata* DSM 23089^{T} displayed the highest number of copper-related genes (14), but was evidently less tolerant to copper stress than *S. capitis* DSM 111179, with four identified genes. Therefore, as expected, the coded genes and their transcription should be investigated further to understand the defense mechanisms behind the single species and the bacterial community.

To what extent can the coatings reduce the microbial load in passenger cabins? To conclude, antimicrobial surfaces pose a promising measure to reduce contact transmission. In contrast to alternative strategies against contact transmission, they display a continuous, passive measure, are independent from user's behavior, and are a good addition to public transport areas with high fluctuation of passengers. Only few long-term experiments (16 weeks to at least 18 months) have been conducted (212, 231), and results have shown positive effects compared to controls. However, little is known about the effectivity over long periods (several years), corrosion (especially for copper), and the effect on antibacterial properties. More research is needed on the influence of coated materials and the effects of relative humidity and temperature. Further, it is important to investigate adaptation strategies of bacterial communities. In the end, antibacterial coatings represent an addition to active measures, such as cleaning, which is inevitable. Although standardized test methods to assess the antibacterial activity of surfaces, such as ISO 22196 (232), the given experimental conditions do not cover real-world environments, for example due to high prescribed temperatures (~37 °C) and high relative humidity (> 90 %) (233). So far, commonly used model organisms are *E. coli* or *S. aureus*, and there is no standard that investigates bacterial interactions. In 2023, the ISO 7581:2023 standard was released to evaluate bactericidal activity of surfaces (234), which comes closer to realistic settings through testing under dry conditions. However, further improvements are needed to, for example, simulate high-touch settings and other realistic environmental conditions.

3.3.3 Safe passenger cabin of the future

Based on current knowledge and the results of this work, which countermeasure is feasible and effective in a passenger cabin (RQ3)? There is no easy answer to this question. There are many considerations, that cannot be easily evaluated: costs for integration into cabin systems, impact on heating, ventilation and air conditioning (HVAC), regulatory constraints, maintenance requirements, etc. To make well-founded estimates, more research is needed. Measures, such as the thermal inactivation of the cabin air during cold months, need to be further developed to be considered for application in a passenger cabin ventilation system. Despite all the factors that are difficult to assess, a few can be categorized based on the current state of knowledge (**Table 5**). In addition to the novel countermeasures that were investigated in this work, the comparison shown in **Table 5** includes more established methods such as UV-C and fogging with chemicals like H_2O_2.

Of the countermeasures investigated, passive approaches, such as antibacterial surfaces and airflow-based strategies, are particularly well-suited for passenger cabins. These approaches can be applied continuously during operation without compromising passenger safety or comfort. A great advantage of the air curtain is that no chemicals and, therefore, no safety measures are required. However, the correct positioning for the most effective use needs to be determined without impairing passengers' comfort. This study has shown that thermal inactivation, intended as a measure during the cold months when heating is required, is effective within seconds. However, further testing of bioaerosols is needed. A main drawback of this method is that the cabin air is not decontaminated when the cabin is not heated. If the system is used regardless, high energy consumption is to be expected. Non-thermal plasma has shown to be effective, too. Similar to the thermal inactivation, not much is known about its use in public transportation and testing in this setting is insufficient. However, its effectivity to reduce microbial loads in indoor settings has been shown (207, 235). UV-C is another method for surface and air disinfection, which is particularly relevant in healthcare settings (236, 237). Nevertheless, there are certain limitations, such as maintenance requirements, safety measures, variable effectivity across pathogen and surface types (238), limited surface coverage, and shadowing. Another established and effective intervention, fogging of H_2O_2, can only be used in public transport settings, when no passengers are present. Therefore, the operating time of the cabins is impaired, posing a downside of this method. In addition, the application of this measure is bound to staff-costs and, therefore, less suitable for passenger cabins.

Table 5: Comparison of bacterial interventions for passenger cabins.

Intervention	Target (air/surface)	Mode of action	Integration into passenger cabin	Effectivity	Continuous effect	Passengers allowed during use	Passenger comfort impaired	Safety considerations
Air curtain	Air	Physical barrier, dilution	Moderate	Moderate	Yes	Yes	Yes	Low
Thermal inactivation	Air	Protein denaturation	Complex	High	Yes	Yes	No	Low
Non-thermal plasma	Air	ROS, RNS	Complex	High	Yes	Yes	No	Medium
Antibacterial surfaces	Surface	Cu-ions, ROS	Easy	Moderate	Yes	Yes	No	Low
UV-C irradiation	Air/surface	DNA/RNA damage, ROS	Moderate	High	No	No	No	Medium
H_2O_2 fogging	Air/surface	Oxidative chemical disinfection	Moderate	High	No	No	No	Medium

In regards to the industry or operator perspective, measures that are low-cost in all aspects, system integration, maintenance, and operation, are important. In addition, passenger comfort should not be impaired, or passengers should feel even safer with integrated measures. Considering these factors, the integration of antimicrobial surfaces would be a reasonable choice. However, to reduce not only contact, but also airborne transmission of pathogens, further measures need to be added. Hence, additional strategies should be considered: Basic hand hygiene is important to reduce contact transmission of pathogens (239). Other behavioral measures, such as wearing masks while sick, practicing social distancing, showed high effectivity in previous studies (240, 241), but require active participation of people. Further, regular surface disinfection can be time- and staff-limited, yet highly effective (242). Combining methods that require different defense mechanisms of microorganisms, such as antimicrobial surfaces (Cu-homeostasis), air curtains (desiccation tolerance), non-thermal plasma (oxidative stress response), or thermal inactivation (heat shock response) can pose an effective measure against microbial spread.

4 Conclusion and outlook

Despite declining public attention since the peak of the corona pandemic, infectious diseases remain a relevant health risk, especially for vulnerable people with a compromised immune system. There is a high chance for new upcoming pathogenic species that can cause outbreaks and pandemics. Zoonotic spillovers and emerging infections are driven by factors, such as climate change, biodiversity loss, and increased wildlife contacts (243, 244). Therefore, understanding human indoor built environments and their microbiome is essential to inform and develop new measures that can reduce microbial transmission, especially in critical infrastructures.

A **key element** in this work was posed by the *in vitro* bacterial community. It is based on the most abundant and relevant bacterial genera found in public transport. This approach allowed a simulation of this environment and helped to gain insights to the effects of the intervention strategies, that would be limited for the use of single model organisms. It is standardized and reproducible, making it suitable as a reference for various applications. The bacterial community or parts of it were used for all following investigations, and constitutes a powerful tool to test and evaluate existing and new microbial countermeasures.

This work contributed the investigation of three interventions for reduced microbial spread. 1) An air curtain to reduce bioaerosol propagation, 2) antibacterial surface coatings to conquer contact transmission, and 3) thermal inactivation of different microorganisms.

The **first** intervention successfully applied the *in vitro* bacterial community to investigate bacterial spread in a closed chamber, influenced by an air curtain as a physical barrier for the bioaerosol. Bacterial detection was compared to sensor-based particle measurement, and similar trends in bacterial survival and particle concentrations were revealed for *S. capitis* DSM 111179. *B. lata* DSM 23089^{T} showed lower survival due to increased desiccation susceptibility. Overall, the air curtain reached a maximum effectivity of 66 % in the reduction of bacterial and particle concentrations.

The evaluation of bioaerosol spread by both particle measurement and bacterial survival helped to understand the complementing data we obtained from those measurements. We have to be aware of the different factors (desiccation tolerance, size, shape, etc.) that influence the survival and pathogenicity of bacteria, and that particle measurements create useful additional data that help to visualize the bioaerosol spread. In addition, an air curtain was tested as a measure to

reduce bioaerosol propagation within a closed room. In future perspective, it could be applied in passenger cabins to reduce airborne transmission of infectious agents.

The **second** microbial intervention that was investigated were copper-aluminum-based antibacterial surface coatings. For exposure times up to 60 min, 100 at.% Cu coatings showed the highest antibacterial activity. Comparing the survival of pure cultures to the bacterial community, a significant protective effect by the community was evident for *S. capitis* DSM 111179. This research highlighted the importance of testing communities instead of single model organisms, as they can highly influence the survival of single species. The novel alloy surface coatings are subject to improvement, but pose a helpful measure to reduce contact transmission of bacterial species. Future applications could be frequently-touched surfaces in public transport or healthcare settings. Long-term experiments are still needed, but we created a useful foundation that can be build up upon.

The **third** measure was thermal inactivation of a set of microorganisms, including three bacteria of the *in vitro* bacterial community and a bacteriophage. The used experimental setup facilitated fast heat transfer to the test organisms, enabling the characterization of the target species‘ heat tolerance. In future studies, this approach should be tested on a broader range of species and bacterial communities, and subsequently compared to the thermal inactivation of airborne microorganisms. The long-term vision of this project lies in its application within heated passenger cabins, particularly during winter.

Rooting back to the research topic and questions, what was accomplished in this work to detect and prevent bacterial contaminants in public transport? Microbial monitoring in a train cabin using 16S rRNA sequencing revealed additional data to present research findings. Those include high abundance of human-associated taxa, and sampling location dependent microbiomes. Detection can be performed using various methodologies, that offer respective advantages and disadvantages. For microbial monitoring on species-level and specific pathogens, qPCR has been proven as a possible approach. It was further shown in this thesis, that it is possible to recreate and apply a standardized public transport microbiome as a reference model for experimental testing. A series of potential countermeasures were tested with this *in vitro* bacterial community, and more can be tested in future experiments, also in other laboratories. As nature is truly complex, certain limitations cannot be avoided within the developed community. Finally, it was demonstrated that there is no single microbial intervention that can build the perfectly safe passenger cabin, but by combining interventions, multiple attack sites against bacteria can be created.

This thesis presents a variety of potential countermeasures, and future studies should deepen the investigations. Important work remains to be conducted on the long-term effects before these measures can be applied in real passenger cabins. It needs to be studied, how the bacterial community changes after prolonged exposure, for example to antimicrobial surfaces. The potential formation of biofilms should be further investigated, as these can impact the materials durability and effectivity. In addition, the behavior of the bacterial community on materials currently or potentially used in passenger cabins should be addressed in terms of survival and persistence following controlled touch events. This also accounts for cleaning agents, which can be tested solely or in combination with antimicrobial materials to assess their impact on the materials' effectivity. Furthermore, the survival of species and colonies after exposure to several cycles of short-time thermal inactivation or non-thermal plasma should be explored. In addition, potential development of resistances or tolerances should be investigated to evaluate the feasibility of the tested countermeasures in real-life settings. Prior to the application of air curtains in passenger cabins, the experiments conducted in this work should be upscaled to include more realistic room dimensions, and different temperature and relative humidity settings. In regards to the *in vitro* bacterial community, conducting co-cultivation experiments would provide an even more realistic approach, opening new research questions and topics related to bacterial interactions, such as synergies, competition, and the secretion of metabolites.

This work highlights the importance of multimodal microbial reduction strategies for public transport systems, addressing both air and surfaces. It has deepened our knowledge of microbial dynamics in such environments and demonstrates the strong potential of the *in vitro* bacterial community for future research. These insights contribute to the development of protective measures for vulnerable populations and improved preparedness for future pandemics.

5 Acknowledgements

This work would not exist as it is, without the following people mentioned. First of all, I want to thank Prof. Dr. Ralf Möller. He was determined in his actions and had a contagious passion for science. He offered me a huge opportunity and thanks to him, I was able to start my journey at the DLR. To the grief of us all, my PhD journey ended without him as a group leader, mentor, and respected colleague. I thank Prof. Dr. Alexander Goesmann for his support throughout the beginning of my work and critical thinking as my doctoral advisor at the Justus Liebig University Giessen. I am thankful for the amount of support that I did not take for granted from Prof. Dr. Stefan Janssen, as my second reviewer. I also thank Dr. Christine Hellweg and Dr. Torsten Hain for being examiners of my thesis defense.

I would like to express my gratitude to the leaders of the Institute of Aerospace Medicine, thanking Dr. Christine Hellweg, Dr. Christian Liemersdorf and Prof. Dr. Jens Jordan. A great thank you goes to Dr. Stefan Leuko, stepping in as a group leader, and Dr. Kristina Beblo-Vranesevic as supporting group leader. Further, but very importantly, I would like to thank the past and current members of the aerospace microbiology research group, especially Katharina Runzheimer as my partner in crime and both Katha and Franca Arndt, as my greatest companions going through every phase of the master and doctoral time together, Carolin Krämer & Fiona Douglas, as my best office buddies that make time fly, Stella Timofeev & Dr. Katharina Siems, for their best supervision and support from my beginning times at the DLR till now, Johanna Piepjohn, Tommaso Zaccaria, Denise Engel, Erika Muratov, and last but not least, Andrea Schröder for both scientific, laboratory and mental support throughout the whole journey, accompanied by the best working environment. I thank Christoph Steger for his technical support at all times. I am grateful for Dr. Alessa Boschert for her continuous support, valuable feedback and mentorship. During all sorts of projects, I always got support by Dr. Claudio Neidhöfer, thank you!

I also thank the warm welcome and constructive meetings at the Giessen University by Stefan, Alex, and Julia. I sincerely thank Anna Rehm, who kindly introduced me to sequencing data analysis and endured all my questions. Thanks to Dr. Oliver Schwengers for sharing his expertise and giving lessons on genome assemblies.

The journey was accompanied by cooperation, and I would like to thank Dr. Ronja Anton for the fun and cold hours during electron microscopy and the generation of the surface coatings. I

thank Dr. Julia Holtel and Nina Wetzig for supporting my very first sequencing approaches. Without the interest and curiosity of people at National express and goRheinland, there would not have been the opportunity to collect samples in the train cabin throughout years. Therefore, thank you Wilfried Koenen and Florian Schütz.

My PhD was funded by the GANDALF Graduate School, which was brought to life by Ralf and supported by the senior members of the graduate school. I thank all PhD students, Andreas and Henrik for the successful collaboration, Dr. Daniel Schmeling for being my DLR-mentor, and all the seniors that accompanied the last years with fun meetings all across Germany.

Most importantly, I want to thank my family and friends, who supported me since the beginning and throughout the last years. Natalie, thank you for always believing in me and motivating me.

6 Bibliography

1. Ly Y-T, Arndt F, Boschert AL, Pavletić B, Webner F, Kohl A, et al. Nach der Pandemie ist vor der Pandemie: Und wie interdisziplinäre Forschung hier helfen kann. *Flugmedizin· Tropenmedizin· Reisemedizin-FTR* (2023) 30(03):122–30. doi: 10.1055/a-2073-2615.
2. To KK-W, Sridhar S, Chiu KH-Y, Hung DL-L, Li X, Hung IF-N, et al. Lessons learned 1 year after SARS-CoV-2 emergence leading to COVID-19 pandemic. *Emerging microbes & infections* (2021) 10(1):507–35. doi: 10.1080/22221751.2021.1898291.
3. Rehman S. A parallel and silent emerging pandemic: Antimicrobial resistance (AMR) amid COVID-19 pandemic. *Journal of Infection and Public Health* (2023) 16(4):611–7. doi: 10.1016/j.jiph.2023.02.021.
4. Mahoney AR, Safaee MM, Wuest WM, Furst AL. The silent pandemic: Emergent antibiotic resistances following the global response to SARS-CoV-2. *IScience* (2021) 24(4). doi: 10.1016/j.isci.2021.102304.
5. Fu K, Zhou Q, Wang H. Variability in Microbial Communities Driven by Particulate Matter on Human Facial Skin. *Toxics* (2024) 12(7). doi: 10.3390/toxics12070497.
6. Dietert RR. Safety and risk assessment for the human superorganism. *Taylor & Francis* (2017). p. 1819–29. doi: 10.1080/10807039.2017.1356683.
7. Naik S, Bouladoux N, Linehan JL, Han S-J, Harrison OJ, Wilhelm C, et al. Commensal–dendritic-cell interaction specifies a unique protective skin immune signature. *Nature* (2015) 520(7545):104–8. doi: 10.1038/nature14052.
8. D'Amelio P, Sassi F. Gut microbiota, immune system, and bone. *Calcified tissue international* (2018) 102(4):415–25. doi: 10.1007/s00223-017-0331-y.
9. Yoo JY, Groer M, Dutra SVO, Sarkar A, McSkimming DI. Gut microbiota and immune system interactions. *Microorganisms* (2020) 8(10):1587. doi: 10.3390/microorganisms8101587.
10. Nakatsuji T, Chen TH, Narala S, Chun KA, Two AM, Yun T, et al. Antimicrobials from human skin commensal bacteria protect against *Staphylococcus aureus* and are deficient in atopic dermatitis. *Science translational medicine* (2017) 9(378):eaah4680. doi: 10.1126/scitranslmed.aah4680.
11. Sandiford S, Upton M. Identification, characterization, and recombinant expression of epidermicin NI01, a novel unmodified bacteriocin produced by *Staphylococcus*

epidermidis that displays potent activity against Staphylococci. *Antimicrobial agents and chemotherapy* (2012) 56(3):1539–47. doi: 10.1128/aac.05397-11.

12. Thursby E, Juge N. Introduction to the human gut microbiota. *Biochemical journal* (2017) 474(11):1823–36. doi: 10.1042/BCJ20160510.
13. Bilbo SD, Wray GA, Perkins SE, Parker W. Reconstitution of the human biome as the most reasonable solution for epidemics of allergic and autoimmune diseases. *Medical Hypotheses* (2011) 77(4):494–504. doi: 10.1042/BCJ20160510.
14. Rook GA. The old friends hypothesis: evolution, immunoregulation and essential microbial inputs. *Frontiers in Allergy* (2023) 4:1220481. doi: 10.3389/falgy.2023.1220481.
15. Song SJ, Lauber C, Costello EK, Lozupone CA, Humphrey G, Berg-Lyons D, et al. Cohabiting family members share microbiota with one another and with their dogs. *elife* (2013) 2:e00458. doi: 10.7554/eLife.00458.
16. Chen YE, Fischbach MA, Belkaid Y. Skin microbiota–host interactions. *Nature* (2018) 553(7689):427–36. doi: 10.1038/nature25177.
17. Boxberger M, Cenizo V, Cassir N, La Scola B. Challenges in exploring and manipulating the human skin microbiome. *Microbiome* (2021) 9(1):125. doi: 10.1186/s40168-021-01062-5.
18. Tulchinsky TH. John Snow, cholera, the broad street pump; waterborne diseases then and now. *Case studies in public health* (2018):77. doi: 10.1016/B978-0-12-804571-8.00017-2.
19. Lai C-C, Chen S-Y, Ko W-C, Hsueh P-R. Increased antimicrobial resistance during the COVID-19 pandemic. *International journal of antimicrobial agents* (2021) 57(4):106324. doi: 10.1016/j.ijantimicag.2021.106324.
20. Jeon K, Jeong S, Lee N, Park M-J, Song W, Kim H-S, et al. Impact of COVID-19 on antimicrobial consumption and spread of multidrug-resistance in bacterial infections. *Antibiotics* (2022) 11(4):535. doi: 10.3390/antibiotics11040535.
21. Samreen, Iqbal A, Hesham A. M, Hussein H. A. Environmental antimicrobial resistance and its drivers: a potential threat to public health. *Journal of Global Antimicrobial Resistance* (2021) 27:101–11. doi: 10.1016/j.jgar.2021.08.001.
22. Huemer M, Mairpady Shambat S, Brugger SD, Zinkernagel AS. Antibiotic resistance and persistence—Implications for human health and treatment perspectives. *EMBO reports* (2020) 21(12):e51034. doi: 10.15252/embr.202051034.

23. Naghavi M, Vollset SE, Ikuta KS, Swetschinski LR, Gray AP, Wool EE, et al. Global burden of bacterial antimicrobial resistance 1990–2021: a systematic analysis with forecasts to 2050. *The Lancet* (2024) 404(10459):1199–226. doi: 10.1016/S0140-6736(24)01867-1.
24. Rice LB. Federal funding for the study of antimicrobial resistance in nosocomial pathogens: no ESKAPE. *The University of Chicago Press* (2008). p. 1079–81. doi: 10.1086/533452.
25. De Oliveira DM, Forde BM, Kidd TJ, Harris PN, Schembri MA, Beatson SA, et al. Antimicrobial resistance in ESKAPE pathogens. *Clinical microbiology reviews* (2020) 33(3): e00181–19. doi: 10.1128/cmr.00181-19.
26. Pendleton JN, Gorman SP, Gilmore BF. Clinical relevance of the ESKAPE pathogens. *Expert review of anti-infective therapy* (2013) 11(3):297–308. doi: 10.1586/eri.13.12.
27. World Health Organization. Prioritization of pathogens to guide discovery, research and development of new antibiotics for drug-resistant bacterial infections, including tuberculosis. *World Health Organization*, (2017) ISBN: 978-92-4-002643-8.
28. WHO bacterial priority list. Bacterial Pathogens of Public Health Importance to Guide Research, Development and Strategies to Prevent and Control Antimicrobial Resistance. *World Health Organization: Geneva, Switzerland* (2024).
29. Ahmad M, Khan AU. Global economic impact of antibiotic resistance: A review. *Journal of global antimicrobial resistance* (2019) 19:313–6. doi: 10.1016/j.jgar.2019.05.024.
30. Yiek W-K, Coenen O, Nillesen M, van Ingen J, Bowles E, Tostmann A. Outbreaks of healthcare-associated infections linked to water-containing hospital equipment: a literature review. *Antimicrobial Resistance & Infection Control* (2021) 10(1):77. doi: 10.1186/s13756-021-00935-6.
31. Wulf M, Markestein A, Van der Linden F, Voss A, Klaassen C, Verduin C. First outbreak of methicillin-resistant *Staphylococcus aureus* ST398 in a Dutch hospital, June 2007. *Euro surveillance: bulletin Europeen sur les maladies transmissibles= European communicable disease bulletin* (2008) 13(9):8051. doi: 10.2807/ese.13.09.08051-en.
32. Breathnach A, Cubbon M, Karunaharan R, Pope C, Planche T. Multidrug-resistant *Pseudomonas aeruginosa* outbreaks in two hospitals: association with contaminated hospital waste-water systems. *Journal of Hospital Infection* (2012) 82(1):19–24. doi: 10.1016/j.jhin.2012.06.007.

33. Valencia R, Arroyo LA, Conde M, Aldana JM, Torres M-J, Fernández-Cuenca F, et al. Nosocomial outbreak of infection with pan–drug-resistant *Acinetobacter baumannii* in a tertiary care university hospital. *Infection Control & Hospital Epidemiology* (2009) 30(3):257–63. doi: 10.1086/595977.
34. Johnson PD, Ballard SA, Grabsch EA, Stinear TP, Seemann T, Young HL, et al. A sustained hospital outbreak of vancomycin-resistant *Enterococcus faecium* bacteremia due to emergence of *vanB E. faecium* sequence type 203. *The Journal of infectious diseases* (2010) 202(8):1278–86. doi: 10.1086/656319.
35. Snitkin ES, Zelazny AM, Thomas PJ, Stock F, Program NCS, Henderson DK, et al. Tracking a hospital outbreak of carbapenem-resistant *Klebsiella pneumoniae* with whole-genome sequencing. *Science translational medicine* (2012) 4(148):148ra16–ra16. doi: 10.1126/scitranslmed.3004129.
36. Ly Y-T, Leuko S, Moeller R. An overview of the bacterial microbiome of public transportation systems-risks, detection, and countermeasures. *Frontiers in Public Health* (2024) 12:1367324. doi: 10.3389/fpubh.2024.1367324.
37. Webner F, Shishkin A, Schmeling D, Wagner C. A Direct Infection Risk Model for CFD Predictions and Its Application to SARS-CoV-2 Aircraft Cabin Transmission. *Indoor Air* (2024) 2024(1):9927275. doi: 10.1155/2024/9927275.
38. Chain of Infection Components: CDC National Institute for Occupational Safety and Health (2022) [cited 2025-12-18]. Available from: https://www.cdc.gov/niosh/learning/safetyculturehc/module-2/3.html#print.
39. Li Y, Leung M, Tang J, Yang X, Chao CYH, Lin JZ, et al. Role of ventilation in airborne transmission of infectious agents in the built environment–a multidisciplinary systematic review. *Indoor air* (2007) 17(1). doi: 10.1111/j.1600-0668.2006.00445.x.
40. Li Y, Qian H, Hang J, Chen X, Cheng P, Ling H, et al. Probable airborne transmission of SARS-CoV-2 in a poorly ventilated restaurant. *Building and environment* (2021) 196:107788. doi: 10.1016/j.buildenv.2021.107788.
41. Knobling B, Franke G, Beike L, Dickhuth T, Knobloch JK. Reading the Score of the Air—Change in Airborne Microbial Load in Contrast to Particulate Matter during Music Making. *International Journal of Environmental Research and Public Health* (2022) 19(16):9939. doi: 10.3390/ijerph19169939.
42. Whitby C, Ferguson RM, Colbeck I, Dumbrell AJ, Nasir ZA, Marczylo E, et al. Compendium of analytical methods for sampling, characterization and quantification of

bioaerosols. *Advances in Ecological Research* (2022) 67:101–229. doi: 10.1016/bs.aecr.2022.09.004.

43. Arumuru V, Pasa J, Samantaray SS. Experimental visualization of sneezing and efficacy of face masks and shields. *Physics of Fluids* (2020) 32(11). doi: 10.1063/5.0030101.
44. Fontes D, Reyes J, Ahmed K, Kinzel M. A study of fluid dynamics and human physiology factors driving droplet dispersion from a human sneeze. *Physics of Fluids* (2020) 32(11). doi: 10.1063/5.0032006.
45. Kwok YLA, Gralton J, McLaws M-L. Face touching: a frequent habit that has implications for hand hygiene. *American journal of infection control* (2015) 43(2):112–4. doi: 10.1016/j.ajic.2014.10.015.
46. Weber DJ, Rutala WA, Miller MB, Huslage K, Sickbert-Bennett E. Role of hospital surfaces in the transmission of emerging health care-associated pathogens: norovirus, *Clostridium difficile*, and *Acinetobacter* species. *American journal of infection control* (2010) 38(5):S25–S33. doi: 10.1016/j.ajic.2010.04.196.
47. Sanborn LWR. The relation of surface contamination to the transmission of disease. *American Journal of Public Health and the Nations Health* (1963) 53(8):1278–83. doi: 10.2105/ajph.53.8.1278.
48. Rozman U, Pušnik M, Kmetec S, Duh D, Šostar Turk S. Reduced susceptibility and increased resistance of bacteria against disinfectants: A systematic review. *Microorganisms* (2021) 9(12):2550. doi: 10.3390/microorganisms9122550.
49. Donaghy JA, Jagadeesan B, Goodburn K, Grunwald L, Jensen ON, Jespers A, et al. Relationship of sanitizers, disinfectants, and cleaning agents with antimicrobial resistance. *Journal of Food Protection* (2019) 82(5):889–902. doi: 10.4315/0362-028X.JFP-18-373.
50. Kramer A, Schwebke I, Kampf G. How long do nosocomial pathogens persist on inanimate surfaces? A systematic review. *BMC infectious diseases* (2006) 6:1–8. doi: 10.1186/1471-2334-6-130.
51. Örgütü DT. UNWTO tourism highlights, 2016 Edition. *UNWTO* (2016) doi*:* 1018111/9789284418145 (2016).
52. Jenelius E, Cebecauer M. Impacts of COVID-19 on public transport ridership in Sweden: Analysis of ticket validations, sales and passenger counts. *Transportation Research Interdisciplinary Perspectives* (2020) 8:100242. doi: 10.1016/j.trip.2020.100242.

53. Pozo RF, Wilby MR, Díaz JJV, González ABR. Data-driven analysis of the impact of COVID-19 on Madrid's public transport during each phase of the pandemic. *Cities* (2022) 127:103723. doi: 10.1016/j.cities.2022.103723.
54. Suzumura T, Kanezashi H, Dholakia M, Ishii E, Napagao SA, Pérez-Arnal R, et al., editors. The impact of COVID-19 on flight networks. *2020 ieee international conference on big data* (2020).
55. Statistisches Bundesamt (Destatis). Fluggäste im Jahr 2024 [cited 2026-01-07]. Available from: https://www.destatis.de/DE/Presse/Pressemitteilungen/2025/01/PD25_042_464.html.
56. Statistisches Bundesamt (Destatis). Liniennahverkehr 2024 [cited 2026-01-07]. Available from: https://www.destatis.de/DE/Presse/Pressemitteilungen/2025/10/PD25_365_461.html.
57. Statistisches Bundesamt (Destatis). EU-Flugverkehr: Mehr Passagiere als vor der Corona-Pandemie [cited 2026-01-07]. Available from: https://www.destatis.de/Europa/DE/Thema/Verkehr/flugpassagiere.html.
58. Findlater A, Bogoch II. Human mobility and the global spread of infectious diseases: a focus on air travel. *Trends in parasitology* (2018) 34(9):772–83. doi: 10.1016/j.pt.2018.07.004.
59. Mangili A, Gendreau MA. Transmission of infectious diseases during commercial air travel. *The Lancet* (2005) 365(9463):989–96. doi: 10.1016/S0140-6736(05)71089-8.
60. Sun Y, Fu X, Li Y, Yuan Q, Ou Z, Lindgren T, et al. Shotgun metagenomics of dust microbiome from flight deck and cabin in civil aviation aircraft. *Indoor Air* (2020) 30(6):1199–212. doi: 10.1111/ina.12707.
61. Korves T, Piceno Y, Tom L, DeSantis T, Jones B, Andersen G, et al. Bacterial communities in commercial aircraft high-efficiency particulate air (HEPA) filters assessed by PhyloChip analysis. *Indoor air* (2013) 23(1):50–61. doi: 10.1111/j.1600-0668.2012.00787.x.
62. Weiss H, Hertzberg VS, Dupont C, Espinoza JL, Levy S, Nelson K, et al. The airplane cabin microbiome. *Microbial ecology* (2019) 77:87–95. doi: 10.1007/s00248-018-1191-3.
63. Liu M, Liu J, Ren J, Liu L, Chen R, Li Y. Bacterial community in commercial airliner cabins in China. *International Journal of Environmental Health Research* (2020) 30(3):284–95. doi: 10.1080/09603123.2019.1593329.

64. Afshinnekoo E, Meydan C, Chowdhury S, Jaroudi D, Boyer C, Bernstein N, et al. Geospatial Resolution of Human and Bacterial Diversity with City-Scale Metagenomics. *Cell Systems* (2015) 1(1):72–87. doi: 10.1016/j.cels.2015.01.001.

65. Kang K, Ni Y, Li J, Imamovic L, Sarkar C, Kobler MD, et al. The Environmental Exposures and Inner- and Intercity Traffic Flows of the Metro System May Contribute to the Skin Microbiome and Resistome. *Cell Reports* (2018) 24(5):1190–202 e5. doi: 10.1016/j.celrep.2018.06.109.

66. Gohli J, Boifot KO, Moen LV, Pastuszek P, Skogan G, Udekwu KI, et al. The subway microbiome: seasonal dynamics and direct comparison of air and surface bacterial communities. *Microbiome* (2019) 7(1):160. doi: 10.1186/s40168-019-0772-9.

67. Zhao B, Dewald C, Hennig M, Bossert J, Bauer M, Pletz MW, et al. Microorganisms@ materials surfaces in aircraft: Potential risks for public health?–A systematic review. *Travel medicine and infectious disease* (2019) 28:6–14. doi: 10.1016/j.tmaid.2018.07.011.

68. Hernández AM, Vargas-Robles D, Alcaraz LD, Peimbert M. Station and train surface microbiomes of Mexico City's metro (subway/underground). *Scientific Reports* (2020) 10(1):8798. doi: 10.1038/s41598-020-65643-4.

69. Li L, Abou-Samra E, Ning Z, Zhang X, Mayne J, Wang J, et al. An in vitro model maintaining taxon-specific functional activities of the gut microbiome. *Nature communications* (2019) 10(1):4146. doi: 10.1038/s41467-019-12087-8.

70. Venema K, Van den Abbeele P. Experimental models of the gut microbiome. *Best Practice & Research Clinical Gastroenterology* (2013) 27(1):115–26. doi: 10.1016/j.bpg.2013.03.002.

71. Aranda-Díaz A, Ng KM, Thomsen T, Real-Ramírez I, Dahan D, Dittmar S, et al. Establishment and characterization of stable, diverse, fecal-derived *in vitro* microbial communities that model the intestinal microbiota. *Cell Host & Microbe* (2022) 30(2):260–72. e5. doi: 10.1016/j.chom.2021.12.008.

72. Birkett M, Dover L, Cherian Lukose C, Wasy Zia A, Tambuwala MM, Serrano-Aroca A. Recent Advances in Metal-Based Antimicrobial Coatings for High-Touch Surfaces. *International Journal of Molecular Sciences* (2022) 23(3). doi: 10.3390/ijms23031162.

73. Kalb L, Bassler P, Schneider-Brachert W, Eckl DB. Antimicrobial Photodynamic Coatings Reduce the Microbial Burden on Environmental Surfaces in Public Transportation-A Field Study in Buses. *International Journal of Environmental Research and Public Health* (2022) 19(4). doi: 10.3390/ijerph19042325.

74. Poku E, Cooper K, Cantrell A, Harnan S, Sin MA, Zanuzdana A, et al. Systematic review of time lag between antibiotic use and rise of resistant pathogens among hospitalized adults in Europe. *JAC-Antimicrobial Resistance* (2023) 5(1):dlad001. doi: 10.1093/jacamr/dlad001.

75. Stennett HL, Back CR, Race PR. Derivation of a precise and consistent timeline for antibiotic development. *Antibiotics* (2022) 11(9):1237. doi: 10.3390/antibiotics11091237.

76. Hasman H, Aarestrup FM. *tcrB*, a gene conferring transferable copper resistance in *Enterococcus faecium*: occurrence, transferability, and linkage to macrolide and glycopeptide resistance. *Antimicrobial agents and chemotherapy* (2002) 46(5):1410–6. doi: 10.1128/aac.46.5.1410-1416.2002.

77. Aarestrup FM, Hasman H. Susceptibility of different bacterial species isolated from food animals to copper sulphate, zinc chloride and antimicrobial substances used for disinfection. *Veterinary microbiology* (2004) 100(1-2):83–9. doi: 10.1016/j.vetmic.2004.01.013.

78. Festa RA, Thiele DJ. Copper: an essential metal in biology. *Current Biology* (2011) 21(21):R877–R83. doi: 10.1016/j.cub.2011.09.040.

79. Grass G, Rensing C, Solioz M. Metallic copper as an antimicrobial surface. *Applied and environmental microbiology* (2011) 77(5):1541–7. doi: 10.1128/AEM.02766-10.

80. Santo CE, Lam EW, Elowsky CG, Quaranta D, Domaille DW, Chang CJ, et al. Bacterial killing by dry metallic copper surfaces. *Applied and environmental microbiology* (2011) 77(3):794–802. doi: 10.1128/AEM.01599-10.

81. Nathan C, Ding A. SnapShot: reactive oxygen intermediates (ROI). *Cell* (2010) 140(6):951–. e2. doi: 10.1016/j.cell.2010.03.008.

82. Sutton HC, Winterbourn CC. On the participation of higher oxidation states of iron and copper in Fenton reactions. *Free Radical Biology and Medicine* (1989) 6(1):53–60. doi: 10.1016/0891-5849(89)90160-3.

83. Warnes S, Caves V, Keevil C. Mechanism of copper surface toxicity in *Escherichia coli* O157: H7 and *Salmonella* involves immediate membrane depolarization followed by slower rate of DNA destruction which differs from that observed for Gram-positive bacteria. *Environmental microbiology* (2012) 14(7):1730–43. doi: 10.1111/j.1462-2920.2011.02677.x.

84. Liochev SI, Fridovich I. The Haber-Weiss cycle—70 years later: an alternative view. *Redox report* (2002) 7(1):55–7. doi: 10.1179/135100002125000190.

85. Pham AN, Xing G, Miller CJ, Waite TD. Fenton-like copper redox chemistry revisited: Hydrogen peroxide and superoxide mediation of copper-catalyzed oxidant production. *Journal of catalysis* (2013) 301:54–64. doi: 10.1016/j.jcat.2013.01.025.
86. Salah I, Parkin IP, Allan E. Copper as an antimicrobial agent: Recent advances. *RSC advances* (2021) 11(30):18179–86. doi: 10.1039/D1RA02149D.
87. Barnham KJ, Masters CL, Bush AI. Neurodegenerative diseases and oxidative stress. *Nature reviews Drug discovery* (2004) 3(3):205–14. doi: 10.1038/nrd1330.
88. Meyer TJ, Ramlall J, Thu P, Gadura N. Antimicrobial properties of copper in gram-negative and gram-positive bacteria. *International Journal of Pharmacy and Pharmaceutical Sciences* (2015) 9(3):274–8.
89. Keyer K, Imlay JA. Superoxide accelerates DNA damage by elevating free-iron levels. *Proceedings of the National Academy of Sciences* (1996) 93(24):13635–40. doi: 10.1073/pnas.93.24.13635.
90. Gaupp R, Ledala N, Somerville GA. Staphylococcal response to oxidative stress. *Frontiers in cellular and infection microbiology* (2012) 2:33. doi: 10.3389/fcimb.2012.00033.
91. Ramos-Zúñiga J, Bruna N, Pérez-Donoso JM. Toxicity mechanisms of copper nanoparticles and copper surfaces on bacterial cells and viruses. *International Journal of Molecular Sciences* (2023) 24(13):10503. doi: 10.3390/ijms241310503.
92. Chang T, Babu RP, Zhao W, Johnson CM, Hedstrom P, Odnevall I, et al. High-resolution microscopical studies of contact killing mechanisms on copper-based surfaces. *ACS applied materials & interfaces* (2021) 13(41):49402–13. doi: 10.1021/acsami.1c11236.
93. Christena LR, Mangalagowri V, Pradheeba P, Ahmed KBA, Shalini BIS, Vidyalakshmi M, et al. Copper nanoparticles as an efflux pump inhibitor to tackle drug resistant bacteria. *Rsc Advances* (2015) 5(17):12899–909. doi: 10.1039/C4RA15382K.
94. Ruparelia JP, Chatterjee AK, Duttagupta SP, Mukherji S. Strain specificity in antimicrobial activity of silver and copper nanoparticles. *Acta biomaterialia* (2008) 4(3):707–16. doi: 10.1016/j.actbio.2007.11.006.
95. Beveridge TJ. Structures of gram-negative cell walls and their derived membrane vesicles. *Journal of bacteriology* (1999) 181(16):4725–33. doi: 10.1128/jb.181.16.4725-4733.1999.

96. Swoboda JG, Campbell J, Meredith TC, Walker S. Wall teichoic acid function, biosynthesis, and inhibition. *Chembiochem: a European journal of chemical biology* (2010) 11(1):35. doi: 10.1002/cbic.200900557.

97. Matias VR, Beveridge TJ. Cryo-electron microscopy reveals native polymeric cell wall structure in *Bacillus subtilis* 168 and the existence of a periplasmic space. *Molecular microbiology* (2005) 56(1):240–51. doi: 10.1111/j.1365-2958.2005.04535.x.

98. Xia J, Wang W, Hai X, Shuang E, Shu Y, Wang J. Improvement of antibacterial activity of copper nanoclusters for selective inhibition on the growth of gram-positive bacteria. *Chinese Chemical Letters* (2019) 30(2):421–4. doi: 10.1016/j.cclet.2018.07.008.

99. Cremin K, Jones BA, Teahan J, Meloni GN, Perry D, Zerfass C, et al. Scanning ion conductance microscopy reveals differences in the ionic environments of gram-positive and negative bacteria. *Analytical chemistry* (2020) 92(24):16024–32. doi: 10.1021/acs.analchem.0c03653.

100. Giachino A, Waldrom KJ. Copper tolerance in bacteria requires the activation of multiple accessory pathways. *Molecular microbiology* (2020) 114(3):377–90. doi: 10.1111/mmi.14522.

101. Pontel LB, Soncini FC. Alternative periplasmic copper-resistance mechanisms in Gram negative bacteria. *Molecular microbiology* (2009) 73(2):212–25. doi: 10.1111/j.1365-2958.2009.06763.x.

102. Grass G, Rensing C. Genes involved in copper homeostasis in *Escherichia coli*. *Journal of bacteriology* (2001) 183(6):2145–7. doi: 10.1128/jb.183.6.2145-2147.2001.

103. Baker J, Sitthisak S, Sengupta M, Johnson M, Jayaswal R, Morrissey JA. Copper stress induces a global stress response in *Staphylococcus aureus* and represses sae and agr expression and biofilm formation. *Applied and environmental microbiology* (2010) 76(1):150–60. doi: 10.1128/AEM.02268-09.

104. Novoa-Aponte L, Argüello JM. Unique underlying principles shaping copper homeostasis networks. *JBIC Journal of Biological Inorganic Chemistry* (2022) 27(6):509–28. doi: 10.1007/s00775-022-01947-2.

105. Farr SB, Kogoma T. Oxidative stress responses in *Escherichia coli* and *Salmonella typhimurium*. *Microbiological reviews* (1991) 55(4):561–85. doi: 10.1128/mr.55.4.561-585.1991.

106. Lima S, Matinha-Cardoso J, Giner-Lamia J, Couto N, Pacheco CC, Florencio FJ, et al. Extracellular vesicles as an alternative copper-secretion mechanism in bacteria. *Journal of Hazardous Materials* (2022) 431:128594. doi: 10.1016/j.jhazmat.2022.128594.

107. Lee J, Lee E-Y, Kim S-H, Kim D-K, Park K-S, Kim KP, et al. *Staphylococcus aureus* extracellular vesicles carry biologically active β-lactamase. *Antimicrobial agents and chemotherapy* (2013) 57(6):2589–95. doi: 10.1128/aac.00522-12.

108. Bondarczuk K, Piotrowska-Seget Z. Molecular basis of active copper resistance mechanisms in Gram-negative bacteria. *Cell biology and toxicology* (2013) 29:397–405. doi: 10.1007/s10565-013-9262-1.

109. Franke S, Grass G, Rensing C, Nies DH. Molecular analysis of the copper-transporting efflux system CusCFBA of *Escherichia coli*. *Journal of bacteriology* (2003) 185(13):3804–12. doi: 10.1128/jb.185.13.3804-3812.2003.

110. Venter H, Mowla R, Ohene-Agyei T, Ma S. RND-type drug efflux pumps from Gram-negative bacteria: molecular mechanism and inhibition. *Frontiers in microbiology* (2015) 6:377. doi: 10.3389/fmicb.2015.00377.

111. Agreles MAA, de Moura ALP, Lima KFA, Aires CAM, de Almeida Campos LA, Cavalcanti IMF. Resistance in gram-negative bacilli: the emergence of RND efflux pumps. *Future Microbiology* (2025):1–15. doi: 10.1080/17460913.2025.2536375.

112. Yang Y, Yin J, Liu J, Xu Q, Lan T, Ren F, et al. The copper homeostasis transcription factor CopR is involved in H_2O_2 stress in *Lactobacillus plantarum* CAUH2. *Frontiers in Microbiology* (2017) 8:2015. doi: 10.3389/fmicb.2017.02015.

113. Zheng C, Jia M, Lu T, Gao M, Li L. CopA protects *Streptococcus suis* against copper toxicity. *International journal of molecular sciences* (2019) 20(12):2969. doi: 10.3390/ijms20122969.

114. Solioz M, Abicht HK, Mermod M, Mancini S. Response of Gram-positive bacteria to copper stress. *JBIC Journal of Biological Inorganic Chemistry* (2010) 15:3–14. doi: 10.1007/s00775-009-0588-3.

115. He M, Tao Y, Mu K, Feng H, Fan Y, Liu T, et al. Coordinated regulation of chemotaxis and resistance to copper by CsoR in *Pseudomonas putida*. *bioRxiv* (2024):2024.07. 28.605504. doi: 10.1101/2024.07.28.605504.

116. Rensing C, Grass G. *Escherichia coli* mechanisms of copper homeostasis in a changing environment. *FEMS microbiology reviews* (2003) 27(2-3):197–213. doi: 10.1016/S0168-6445(03)00049-4.

117. Grass G, Rensing C. CueO is a multi-copper oxidase that confers copper tolerance in *Escherichia coli*. *Biochemical and biophysical research communications* (2001) 286(5):902–8. doi: 10.1006/bbrc.2001.5474.

118. Lushchak VI. Adaptive response to oxidative stress: Bacteria, fungi, plants and animals. *Comparative Biochemistry and Physiology Part C: Toxicology & Pharmacology* (2011) 153(2):175–90. doi: 10.1016/j.cbpc.2010.10.004.

119. Borisov VB, Siletsky SA, Nastasi MR, Forte E. ROS defense systems and terminal oxidases in bacteria. *Antioxidants* (2021) 10(6):839. doi: 10.3390/antiox10060839.

120. Noh J, Kwon B, Han E, Park M, Yang W, Cho W, et al. Amplification of oxidative stress by a dual stimuli-responsive hybrid drug enhances cancer cell death. *Nature communications* (2015) 6(1):6907. doi: 10.1038/ncomms7907 (2015).

121. Yan J, Ralston MM, Meng X, Bongiovanni KD, Jones AL, Benndorf R, et al. Glutathione reductase is essential for host defense against bacterial infection. *Free Radical Biology and Medicine* (2013) 61:320–32. doi: 10.1016/j.freeradbiomed.2013.04.015.

122. Bi Y, Hu N, Sadeghian P, Sadrizadeh S, Asuero Von Munthe Af Morgenstierne M, Mathisen HM, et al., editors. Numerical study on the application of low-turbulence air curtain surrounding laminar airflow distribution in operating rooms. *Building Simulation* (2025) 18:601-617. doi: 10.1007/s12273-024-1229-7.

123. Costa J, Oliveira L, Silva M. Energy savings by aerodynamic sealing with a downward-blowing plane air curtain—A numerical approach. *Energy and buildings* (2006) 38(10):1182–93. doi: 10.1016/j.enbuild.2006.02.003.

124. Isaäcson M. Airport malaria: a review. *Bulletin of the World Health Organization* (1989) 67(6):737. PMID: 2699278.

125. Carlson DA, Hogsette JA, Kline DL, Geden CD, Vandermeer RK. Prevention of mosquitoes (Diptera: Culicidae) and house flies (Diptera: Muscidae) from entering simulated aircraft with commercial air curtain units. *Journal of Economic Entomology* (2006) 99(1):182–93. doi: 10.1093/jee/99.1.182.

126. Kohl A, Schmeling D, Wagner C, editors. Interaction of exhaled aerosol particles with the flow field of an air curtain. *10th International Symposium on Turbulence, Heat and Mass Transfer, THMT-23, Rome, Italy, 11-15 September 2023*; *Begel House Inc* (2023).

127. Ly Y-T, Kohl A, Schmeling D, Leuko S, Wagner C. Comparative Assessment of Bioaerosol Propagation Through an Air Curtain Using Microbiological Methods and Particulate Matter Sensors. *Indoor Air* (2025) 2025(1):8825442. doi: 10.1155/ina/8825442.

128. European Union. Consolidated text: Commission Regulation (EC) No 2073/2005 of 15 November 2005 on microbiological criteria for foodstuffs (Text with EEA relevance)

[cited 2026 19-01]. Available from: http://data.europa.eu/eli/reg/2005/2073/2020-03-08.

129. COSPAR Policy on Planetary Protection (2024) [cited 2026-01-19]. Available from: https://cosparhq.cnes.fr/assets/uploads/2024/07/PP-Policy_SRT_220-July-2024.pdf.

130. Johnson JS, Spakowicz DJ, Hong B-Y, Petersen LM, Demkowicz P, Chen L, et al. Evaluation of 16S rRNA gene sequencing for species and strain-level microbiome analysis. *Nature communications* (2019) 10(1):5029. doi: 10.1038/s41467-019-13036-1.

131. Wang S, Sun B, Tu J, Lu Z. Improving the microbial community reconstruction at the genus level by multiple 16S rRNA regions. *Journal of Theoretical Biology* (2016) 398:1–8. doi: 10.1016/j.jtbi.2016.03.016.

132. Chakravorty S, Helb D, Burday M, Connell N, Alland D. A detailed analysis of 16S ribosomal RNA gene segments for the diagnosis of pathogenic bacteria. *Journal of microbiological methods* (2007) 69(2):330–9. doi: 10.1016/j.mimet.2007.02.005.

133. Elbrecht V, Leese F. Can DNA-based ecosystem assessments quantify species abundance? Testing primer bias and biomass—sequence relationships with an innovative metabarcoding protocol. *PLOS One* (2015) 10(7):e0130324. doi: 10.1371/journal.pone.0130324.

134. Glassing A, Dowd SE, Galandiuk S, Davis B, Chiodini RJ. Inherent bacterial DNA contamination of extraction and sequencing reagents may affect interpretation of microbiota in low bacterial biomass samples. *Gut pathogens* (2016) 8(1):24. doi: 10.1186/s13099-016-0103-7.

135. Arya M, Shergill IS, Williamson M, Gommersall L, Arya N, Patel HR. Basic principles of real-time quantitative PCR. *Expert review of molecular diagnostics* (2005) 5(2):209–19. doi: 10.1586/14737159.5.2.209.

136. Maurin M. Real-time PCR as a diagnostic tool for bacterial diseases. *Expert review of molecular diagnostics* (2012) 12(7):731–54. doi: 10.1586/erm.12.53.

137. Parida M, Sannarangaiah S, Dash PK, Rao P, Morita K. Loop mediated isothermal amplification (LAMP): a new generation of innovative gene amplification technique; perspectives in clinical diagnosis of infectious diseases. *Reviews in medical virology* (2008) 18(6):407–21. doi: 10.1002/rmv.593.

138. Duschek F, Fellner L, Gebert F, Grünewald K, Köhntopp A, Kraus M, et al. Standoff detection and classification of bacteria by multispectral laser-induced fluorescence. *Advanced Optical Technologies* (2017) 6(2):75–83. doi: 10.1515/aot-2016-0066.

139. Ezzat S, Samad FA, El-Gendy AO, Mohamed T. Femtosecond laser-induced fluorescence spectroscopy for the rapid detection of pathogenic bacteria. *Optical and Quantum Electronics* (2024) 56(6):977. doi: 10.1007/s11082-024-06781-1.

140. Becker J, Eisenhauer N, Scheu S, Jousset A. Increasing antagonistic interactions cause bacterial communities to collapse at high diversity. *Ecology Letters* (2012) 15(5):468–74. doi: 10.1111/j.1461-0248.2012.01759.x.

141. Mora M, Mahnert A, Koskinen K, Pausan MR, Oberauner-Wappis L, Krause R, et al. Microorganisms in confined habitats: microbial monitoring and control of intensive care units, operating rooms, cleanrooms and the International Space Station. *Frontiers in microbiology* (2016) 7:1573. doi: 10.3389/fmicb.2016.01573.

142. Singh NK, Wood JM, Karouia F, Venkateswaran K. Succession and persistence of microbial communities and antimicrobial resistance genes associated with International Space Station environmental surfaces. *Microbiome* (2018) 6(1):204. doi: 10.1186/s40168-018-0585-2.

143. Li K, Zhu Q, Jiang F, Li H, Liu J, Yu T, et al. Monitoring microbial communities in intensive care units over one year in China. *Science of The Total Environment* (2022) 811:152353. doi: 10.1016/j.scitotenv.2021.152353.

144. Mora M, Wink L, Kögler I, Mahnert A, Rettberg P, Schwendner P, et al. Space Station conditions are selective but do not alter microbial characteristics relevant to human health. *Nature communications* (2019) 10(1):3990. doi: 10.1038/s41467-019-11682-z.

145. Venkateswaran K, Vaishampayan P, Cisneros J, Pierson DL, Rogers SO, Perry J. International Space Station environmental microbiome—microbial inventories of ISS filter debris. *Applied microbiology and biotechnology* (2014) 98(14):6453–66. doi: 10.1007/s00253-014-5650-6.

146. Lang JM, Coil DA, Neches RY, Brown WE, Cavalier D, Severance M, et al. A microbial survey of the International Space Station (ISS). *PeerJ* (2017) 5:e4029. doi: 10.7717/peerj.4029.

147. Avila-Herrera A, Thissen J, Urbaniak C, Be NA, Smith DJ, Karouia F, et al. Crewmember microbiome may influence microbial composition of ISS habitable surfaces. *PLOS One* (2020) 15(4):e0231838. doi: 10.1371/journal.pone.0231838.

148. Zhou F, Wang Y. Characteristics of antibiotic resistance of airborne *Staphylococcus* isolated from metro stations. *International Journal of Environmental Research and Public Health* (2013) 10(6):2412–26. doi: 10.3390/ijerph10062412.

149. Klimenko NS, Tyakht AV, Toshchakov SV, Shevchenko MA, Korzhenkov AA, Afshinnekoo E, et al. Co-occurrence patterns of bacteria within microbiome of Moscow subway. *Computational and Structural Biotechnology Journal* (2020) 18:314–22. doi: 10.1016/j.csbj.2020.01.007.

150. Grydaki N, Colbeck I, Mendes L, Eleftheriadis K, Whitby C. Bioaerosols in the Athens Metro: Metagenetic insights into the PM(10) microbiome in a naturally ventilated subway station. *Environment International* (2021) 146:106186. doi: 10.1016/j.envint.2020.106186.

151. Hsu T, Joice R, Vallarino J, Abu-Ali G, Hartmann EM, Shafquat A, et al. Urban Transit System Microbial Communities Differ by Surface Type and Interaction with Humans and the Environment. *mSystems* (2016) 1(3). doi: 10.1128/mSystems.00018-16.

152. Hiwar W, King MF, Shuweihdi F, Fletcher LA, Dancer SJ, Noakes CJ. What is the relationship between indoor air quality parameters and airborne microorganisms in hospital environments? A systematic review and meta-analysis. *Indoor air* (2021) 31(5):1308–22. doi: 10.1111/ina.12846.

153. Konno A, Okubo T, Enoeda Y, Uno T, Sato T, Yokota S-i, et al. Human pathogenic bacteria on high-touch dry surfaces can be controlled by warming to human-skin temperature under moderate humidity. *PLOS One* (2023) 18(9):e0291765. doi: 10.1371/journal.pone.0291765.

154. Lin K, Marr LC. Humidity-dependent decay of viruses, but not bacteria, in aerosols and droplets follows disinfection kinetics. *Environmental Science & Technology* (2019) 54(2):1024–32. doi: 10.1021/acs.est.9b04959.

155. Marr LC, Tang JW, Van Mullekom J, Lakdawala SS. Mechanistic insights into the effect of humidity on airborne influenza virus survival, transmission and incidence. *Journal of the Royal Society Interface* (2019) 16(150). doi: 10.1098/rsif.2018.0298.

156. Polozov IV, Bezrukov L, Gawrisch K, Zimmerberg J. Progressive ordering with decreasing temperature of the phospholipids of influenza virus. *Nature chemical biology* (2008) 4(4):248–55. doi: 10.1038/nchembio.77.

157. Lowen AC, Mubareka S, Steel J, Palese P. Influenza virus transmission is dependent on relative humidity and temperature. *PLOS pathogens* (2007) 3(10):e151. doi: 10.1371/journal.ppat.0030151.

158. Eccles R. An explanation for the seasonality of acute upper respiratory tract viral infections. *Acta oto-laryngologica* (2002) 122(2):183–91. doi: 10.1080/00016480252814207.

159. Moriyama M, Hugentobler WJ, Iwasaki A. Seasonality of respiratory viral infections. *Annual review of virology* (2020) 7(1):83–101. doi: 10.1146/annurev-virology-012420-022445.

160. Adams RI, Tian Y, Taylor JW, Bruns TD, Hyvärinen A, Täubel M. Passive dust collectors for assessing airborne microbial material. *Microbiome* (2015) 3(1):46. doi: 10.1186/s40168-015-0112-7.

161. Bjerre RD, Hugerth LW, Boulund F, Seifert M, Johansen JD, Engstrand L. Effects of sampling strategy and DNA extraction on human skin microbiome investigations. *Scientific reports* (2019) 9(1):17287. doi: 10.1038/s41598-019-53599-z.

162. López-Aladid R, Fernández-Barat L, Alcaraz-Serrano V, Bueno-Freire L, Vázquez N, Pastor-Ibáñez R, et al. Determining the most accurate 16S rRNA hypervariable region for taxonomic identification from respiratory samples. *Scientific reports* (2023) 13(1):3974. doi: 10.1038/s41598-023-30764-z.

163. Walker SP, Barrett M, Hogan G, Flores Bueso Y, Claesson MJ, Tangney M. Non-specific amplification of human DNA is a major challenge for 16S rRNA gene sequence analysis. *Scientific reports* (2020) 10(1):16356. doi: 10.1038/s41598-020-73403-7.

164. Vargas-Robles D, Gonzalez-Cedillo C, Hernandez AM, Alcaraz LD, Peimbert M. Passenger-surface microbiome interactions in the subway of Mexico City. *PLOS One* (2020) 15(8):e0237272. doi: 10.1371/journal.pone.0237272.

165. Hernández AM, Vargas-Robles D, Alcaraz LD, Peimbert M. Station and train surface microbiomes of Mexico City's metro. *Scientific Reports* (2019) 10(8798). doi: 10.1101/735027.

166. Leung MH, Wilkins D, Li EK, Kong FK, Lee PK. Indoor-air microbiome in an urban subway network: diversity and dynamics. *Applied and Environmental Microbiology* (2014) 80(21):6760–70. doi: 10.1128/AEM.02244-14.

167. Sun D-L, Jiang X, Wu QL, Zhou N-Y. Intragenomic heterogeneity of 16S rRNA genes causes overestimation of prokaryotic diversity. *Applied and Environmental Microbiology* (2013) 79(19):5962–9. doi: 10.1128/AEM.01282-13.

168. O'Sullivan DM, Doyle RM, Temisak S, Redshaw N, Whale AS, Logan G, et al. An inter-laboratory study to investigate the impact of the bioinformatics component on microbiome analysis using mock communities. *Scientific Reports* (2021) 11(1):10590. doi: 10.1038/s41598-021-89881-2.

169. Ryon KA, Tierney BT, Frolova A, Kahles A, Desnues C, Ouzounis C, et al. A history of the MetaSUB consortium: Tracking urban microbes around the globe. *Iscience* (2022) 25(11). doi: 10.1016/j.isci.2022.104993

170. The Meta Sub International Consortium. The Metagenomics and Metadesign of the Subways and Urban Biomes (MetaSUB) International Consortium inaugural meeting report. *Microbiome* (2016) 4(1):24. doi: 10.1186/s40168-016-0168-z.

171. Haddrell A, Oswin H, Otero-Fernandez M, Robinson JF, Cogan T, Alexander R, et al. Ambient carbon dioxide concentration correlates with SARS-CoV-2 aerostability and infection risk. *Nature Communications* (2024) 15(1):3487. doi: 10.1038/s41467-024-47777-5.

172. Webner F, Shishkin A, Schmeling D, Wagner C. Airborne SARS-CoV-2 in aircraft cabins: new inactivation data significantly influences infection risk predictions. *CEAS aeronautical journal* (2025):1–6. doi: 10.1007/s13272-025-00822-5.

173. Kothary MH, Babu US. Infective dose of foodborne pathogens in volunteers: a review. *Journal of food safety* (2001) 21(1):49–68. doi: 10.1111/J.1745-4565.2001.TB00307.X.

174. Rocca JD, Simonin M, Blaszczak JR, Ernakovich JG, Gibbons SM, Midani FS, et al. The microbiome stress project: toward a global meta-analysis of environmental stressors and their effects on microbial communities. *Frontiers in microbiology* (2019) 9:3272. doi: 10.3389/fmicb.2018.03272.

175. Liu L, Firrman J, Tanes C, Bittinger K, Thomas-Gahring A, Wu GD, et al. Establishing a mucosal gut microbial community in vitro using an artificial simulator. *PLOS One* (2018) 13(7):e0197692. doi: 10.1371/journal.pone.0197692.

176. Coker J, Zhalnina K, Marotz C, Thiruppathy D, Tjuanta M, D'Elia G, et al. A reproducible and tunable synthetic soil microbial community provides new insights into microbial ecology. *Msystems* (2022) 7(6):e00951–22. doi: 10.1128/msystems.00951-22.

177. Ly Y-T, Wetzig N, Holtel J, Leuko S, Moeller R, editors. Modeling the Public Transport Microbiome: Development of a Microbial Reference Community. *18th International Conference on Indoor Air Quality and Climate, INDOOR AIR 2024* (2024).

178. Hibbing ME, Fuqua C, Parsek MR, Peterson SB. Bacterial competition: surviving and thriving in the microbial jungle. *Nature reviews microbiology* (2010) 8(1):15–25. doi: 10.1038/nrmicro2259.

179. Rivett DW, Bell T. Abundance determines the functional role of bacterial phylotypes in complex communities. *Nature microbiology* (2018) 3(7):767–72. doi: 10.1038/s41564-018-0180-0.

180. Jiao S, Chen W, Wei G. Biogeography and ecological diversity patterns of rare and abundant bacteria in oil-contaminated soils. *Molecular ecology* (2017) 26(19):5305–17. doi: 10.1111/mec.14218.

181. Woo M-H, Hsu Y-M, Wu C-Y, Heimbuch B, Wander J. Method for contamination of filtering facepiece respirators by deposition of MS2 viral aerosols. *Journal of aerosol science* (2010) 41(10):944–52. doi: 10.1016/j.jaerosci.2010.07.003.

182. Yousi F, Kainan C, Junnan Z, Chuanxing X, Lina F, Bangzhou Z, et al. Evaluation of the effects of four media on human intestinal microbiota culture *in vitro*. *Amb Express* (2019) 9(1):69. doi: 10.1186/s13568-019-0790-9.

183. Esmail GA, Uriot O, Mottawea W, Denis S, Sultan S, Njoku EN, et al. Western diet-based NutriCol medium: A high-pectin, low-inulin culture medium promoted gut microbiota stability and diversity in PolyFermS and M-ARCOL continuous *in vitro* models. *Food Research International* (2025) 206:115993. doi: 10.1016/j.foodres.2025.115993.

184. Marmann A, Aly AH, Lin W, Wang B, Proksch P. Co-cultivation—A powerful emerging tool for enhancing the chemical diversity of microorganisms. *Marine drugs* (2014) 12(2):1043–65. doi: 10.3390/md12021043.

185. Ly-Sauerbrey Y, Anton R, Kopruch L, Krämer CL, Boschert AL, Neidhöfer C, et al. Comparison of Single Bacteria and a Bacterial Reference Community in a Test Against Coated Surfaces of Varying Copper Content. *Frontiers in Microbiology* (2025) 16:1659828. doi: 10.3389/fmicb.2025.1659828.

186. Bairey E, Kelsic ED, Kishony R. High-order species interactions shape ecosystem diversity. *Nature communications* (2016) 7(1):12285. doi: 10.1038/ncomms12285.

187. Joelsson A, Kan B, Zhu J. Quorum sensing enhances the stress response in *Vibrio cholerae*. *Applied and environmental microbiology* (2007) 73(11):3742–6. doi: 10.1128/AEM.02804-06.

188. Williams CL, Neu HM, Gilbreath JJ, Michel SL, Zurawski DV, Merrell DS. Copper resistance of the emerging pathogen *Acinetobacter baumannii*. *Applied and environmental microbiology* (2016) 82(20):6174–88. doi: 10.1128/AEM.01813-16.

189. Ratzke C, Gore J. Modifying and reacting to the environmental pH can drive bacterial interactions. *PLOS biology* (2018) 16(3):e2004248. doi: 10.1371/journal.pbio.2004248.

190. Rivett DW, Scheuerl T, Culbert CT, Mombrikotb SB, Johnstone E, Barraclough TG, et al. Resource-dependent attenuation of species interactions during bacterial succession. *The ISME journal* (2016) 10(9):2259–68. doi: 10.1038/ismej.2016.11.

191. Danelli SG, Brunoldi M, Massabò D, Parodi F, Vernocchi V, Prati P. Comparative characterization of the performance of bio-aerosol nebulizers in connection with atmospheric simulation chambers. *Atmospheric Measurement Techniques* (2021) 14(6):4461–70. doi: 10.5194/amt-14-4461-2021.

192. Maier M. Establishing and Characterizing of a synthetic ISS bacterial community for spaceflight applications: Stress responses and countermeasure. University of Applied Sciences Bonn-Rhein-Sieg (2025).

193. Kusano K, Yamada H, Niwa M, Yamasato K. *Propionibacterium cyclohexanicum* sp. nov., a new acid-tolerant ω-cyclohexyl fatty acid-containing propionibacterium isolated from spoiled orange juice. *International Journal of Systematic and Evolutionary Microbiology* (1997) 47(3):825–31. doi: 10.1099/00207713-47-3-825.

194. Niu L, Lu S, Hu S, Jin D, Lai X, Yang J, et al. *Streptococcus halotolerans* sp. nov. isolated from the respiratory tract of Marmota himalayana in Qinghai-Tibet Plateau of China. *International journal of systematic and evolutionary microbiology* (2016) 66(10):4211–7. doi: 10.1099/ijsem.0.001337.

195. Sobisch L-Y, Rogowski KM, Fuchs J, Schmieder W, Vaishampayan A, Oles P, et al. Biofilm forming antibiotic resistant gram-positive pathogens isolated from surfaces on the international space station. *Frontiers in microbiology* (2019) 10:543. doi: 10.3389/fmicb.2019.00543.

196. Siems K, Runzheimer K, Rehm A, Schwengers O, Heidler von Heilborn D, Kaser L, et al. Phenotypic and genomic assessment of the potential threat of human spaceflight-relevant *Staphylococcus capitis* isolates under stress conditions. *Frontiers in Microbiology* (2022) 13:1007143. doi: 10.3389/fmicb.2022.1007143.

197. Chaibenjawong P, Foster SJ. Desiccation tolerance in *Staphylococcus aureus*. *Archives of microbiology* (2011) 193(2):125–35. doi: 10.1007/s00203-010-0653-x.

198. Duan X, Shen C, Chen D, Zhai Z. Effect of environmental factors on the concentration distribution of bioaerosols with different particle sizes in an enclosed space. *Indoor and Built Environment* (2023) 32(2):408–24. doi: 10.1177/1420326X221115613.

199. Xu Z, Shen F, Li X, Wu Y, Chen Q, Jie X, et al. Molecular and microscopic analysis of bacteria and viruses in exhaled breath collected using a simple impaction and

condensing method. *PLOS One* (2012) 7(7):e41137. doi: 10.1371/journal.pone.0041137.

200. Cebrián G, Condón S, Mañas P. Physiology of the inactivation of vegetative bacteria by thermal treatments: Mode of action, influence of environmental factors and inactivation kinetics. *Foods* (2017) 6(12):107. doi: 10.3390/foods6120107.
201. Setlow P. Spores of *Bacillus subtilis*: their resistance to and killing by radiation, heat and chemicals. *Journal of applied microbiology* (2006) 101(3):514–25. doi: 10.1111/j.1365-2672.2005.02736.x.
202. Dijksterhuis J. Fungal spores: Highly variable and stress-resistant vehicles for distribution and spoilage. *Food microbiology* (2019) 81:2–11. doi: 10.1016/j.fm.2018.11.006.
203. Gallagher MJ, Vaze N, Gangoli S, Vasilets VN, Gutsol AF, Milovanova TN, et al. Rapid inactivation of airborne bacteria using atmospheric pressure dielectric barrier grating discharge. *IEEE Transactions on Plasma Science* (2007) 35(5):1501–10. doi: 10.1109/TPS.2007.905209.
204. Laroussi M. Low temperature plasma-based sterilization: overview and state-of-the-art. *Plasma processes and polymers* (2005) 2(5):391–400. doi: 10.1002/ppap.200400078.
205. Liang Y, Wu Y, Sun K, Chen Q, Shen F, Zhang J, et al. Rapid inactivation of biological species in the air using atmospheric pressure nonthermal plasma. *Environmental science & technology* (2012) 46(6):3360–8. doi: 10.1021/es203770q.
206. Andreadis AA, Hazen SL, Comhair SA, Erzurum SC. Oxidative and nitrosative events in asthma. *Free Radical Biology and Medicine* (2003) 35(3):213–25. doi: 10.1016/S0891-5849(03)00278-8.
207. Mu Y, Williams PT. Recent advances in the abatement of volatile organic compounds (VOCs) and chlorinated-VOCs by non-thermal plasma technology: A review. *Chemosphere* (2022) 308:136481. doi: 10.1016/j.chemosphere.2022.136481.
208. Zhang L, Wang K, Wu K, Guo Y, Liu Z, Yang D, et al. Air disinfection by nanosecond pulsed DBD plasma. *Journal of Hazardous Materials* (2024) 472:134487. doi: 10.1016/j.jhazmat.2024.134487.
209. Jangra R, Ahlawat K, Dixit A, Prakash R. Efficient deactivation of aerosolized pathogens using a dielectric barrier discharge based cold-plasma detergent in environment device for good indoor air quality. *Scientific Reports* (2023) 13(1):10295. doi: 10.1038/s41598-023-37014-2.

210. Timofeev SM, Siems K, Müller DW, Ahmed AS, Schiele A, Brix K, et al. Stress Response of *Aspergillus niger* Spores to Copper Surfaces and the Implications for Antifungal Surface Functionalization. *Advanced Materials Interfaces* (2025):2400852. doi: 10.1002/admi.202400852.

211. Arndt F, Siems K, Timofeev SM, Baumann P, Ahmed AS, Müller DW, et al. Copper Stress Response of Antibiotic-Resistant and Copper-Tolerant *Enterococcus faecium* and the Antibacterial Efficacy of Functionalized Copper Surfaces. *Advanced Materials Interfaces* (2025):e00430. doi: 10.1002/admi.202500430.

212. Mikolay A, Huggett S, Tikana L, Grass G, Braun J, Nies DH. Survival of bacteria on metallic copper surfaces in a hospital trial. *Applied microbiology and biotechnology* (2010) 87:1875–9. doi: 10.1007/s00253-010-2640-1.

213. Williams TC, Asselin E, Mazzulli T, Woznow T, Hamzeh H, Nahkaie D, et al. One-year trial evaluating the durability and antimicrobial efficacy of copper in public transportation systems. *Scientific Reports* (2024) 14(1):6765. doi: 10.1038/s41598-024-56225-9.

214. Karpanen TJ, Casey AL, Lambert PA, Cookson BD, Nightingale P, Miruszenko L, et al. The antimicrobial efficacy of copper alloy furnishing in the clinical environment: a crossover study. *Infection Control & Hospital Epidemiology* (2012) 33(1):3–9. doi: 10.1086/663644.

215. Colin M, Klingelschmitt F, Charpentier E, Josse J, Kanagaratnam L, De Champs C, et al. Copper alloy touch surfaces in healthcare facilities: An effective solution to prevent bacterial spreading. *Materials* (2018) 11(12):2479. doi: 10.3390/ma11122479.

216. Krämer CL, Müller DW, Arndt F, Rehm A, Walkenfort B, Ahmed AS, et al. Touching Surfaces–Presence of microorganisms on antimicrobial metal surfaces on the International Space Station and in German schools. *BMC microbiology* (2025) 25(1):631. doi: 10.1186/s12866-025-04316-6.

217. Greene C, Vadlamudi G, Eisenberg M, Foxman B, Koopman J, Xi C. Fomite-fingerpad transfer efficiency (pick-up and deposit) of *Acinetobacter baumannii*—with and without a latex glove. *American journal of infection control* (2015) 43(9):928–34. doi: 10.1016/j.ajic.2015.05.008.

218. Herzog AB, Pandey AK, Reyes-Gastelum D, Gerba CP, Rose JB, Hashsham SA. Evaluation of sample recovery efficiency for bacteriophage P22 on fomites. *Applied and environmental microbiology* (2012) 78(22):7915–22. doi: 10.1128/AEM.01370-12.

219. Sze-To GN, Yang Y, Kwan JK, Yu SC, Chao CY. Effects of surface material, ventilation, and human behavior on indirect contact transmission risk of respiratory infection. *Risk analysis* (2014) 34(5):818–30. doi: 10.1111/risa.12144.

220. Goodman ER, Piatt R, Bass R, Onderdonk AB, Yokoe DS, Huang SS. Impact of an environmental cleaning intervention on the presence of methicillin-resistant *Staphylococcus aureus* and vancomycin-resistant enterococci on surfaces in intensive care unit rooms. *Infection Control & Hospital Epidemiology* (2008) 29(7):593–9. doi: 10.1086/588566.

221. Chen J, He Z, Liu J, Wang Y, Hodgson M, Gao W. Antibacterial anodic aluminium oxide-copper coatings on aluminium alloys: preparation and long-term antibacterial performance. *Chemical Engineering Journal* (2023) 461:141873. doi: 10.1016/j.cej.2023.141873.

222. Elguindi J, Moffitt S, Hasman H, Andrade C, Raghavan S, Rensing C. Metallic copper corrosion rates, moisture content, and growth medium influence survival of copper ion-resistant bacteria. *Applied microbiology and biotechnology* (2011) 89(6):1963–70. doi: 10.1007/s00253-010-2980-x.

223. He W, Huang X, Zheng Y, Sun Y, Xie Y, Wang Y, et al. In situ synthesis of bacterial cellulose/copper nanoparticles composite membranes with long-term antibacterial property. *Journal of Biomaterials Science, Polymer Edition* (2018) 29(17):2137–53. doi: 10.1080/09205063.2018.1528518.

224. Liang T, Wang Y, Zeng L, Liu Y, Qiao L, Zhang S, et al. Copper-doped 3D porous coating developed on Ti-6Al-4V alloys and its *in vitro* long-term antibacterial ability. *Applied Surface Science* (2020) 509:144717. doi: 10.1016/j.apsusc.2019.144717.

225. Schwengers O, Jelonek L, Dieckmann MA, Beyvers S, Blom J, Goesmann A. Bakta: rapid and standardized annotation of bacterial genomes via alignment-free sequence identification. *Microbial genomics* (2021) 7(11):000685. doi: 10.1099/mgen.0.000685.

226. Baker J, Sengupta M, Jayaswal RK, Morrissey JA. The *Staphylococcus aureus* CsoR regulates both chromosomal and plasmid-encoded copper resistance mechanisms. *Environmental microbiology* (2011) 13(9):2495–507. doi: 10.1111/j.1462-2920.2011.02522.x.

227. Corbett D, Schuler S, Glenn S, Andrew PW, Cavet JS, Roberts IS. The combined actions of the copper-responsive repressor CsoR and copper-metallochaperone CopZ modulate CopA-mediated copper efflux in the intracellular pathogen *Listeria monocytogenes*. *Molecular microbiology* (2011) 81(2):457–72. doi: 10.1111/j.1365-2958.2011.07705.x.

228. Young CA, Gordon LD, Fang Z, Holder RC, Reid SD. Copper tolerance and characterization of a copper-responsive operon, *copYAZ*, in an M1T1 clinical strain of *Streptococcus pyogenes*. *Journal of bacteriology* (2015) 197(15):2580–92. doi: 10.1128/jb.00127-15.

229. Quintana J, Novoa-Aponte L, Argüello JM. Copper homeostasis networks in the bacterium *Pseudomonas aeruginosa*. *Journal of Biological Chemistry* (2017) 292(38):15691–704. doi: 10.1074/jbc.M117.804492.

230. Rademacher C, Masepohl B. Copper-responsive gene regulation in bacteria. *Microbiology* (2012) 158(10):2451–64. doi: 10.1099/mic.0.058487-0.

231. Colin M, Charpentier E, Klingelschmitt F, Bontemps C, De Champs C, Reffuveille F, et al. Specific antibacterial activity of copper alloy touch surfaces in five long-term care facilities for older adults. *Journal of Hospital Infection* (2020) 104(3):283–92. doi: 10.1016/j.jhin.2019.11.021.

232. International Organization for Standardization. ISO 22196:2011 Measurement of antibacterial activity on plastics and other non-porous surfaces (2011) [cited 2025-12-18]. Available from: https://www.iso.org/standard/54431.html#:~:text=ISO%2022196:2011%20is%20an%20international%20standard%20that,products%20*%20Cover%20photocatalytic%20materials%20and%20products.

233. Ojeil M, Jermann C, Holah J, Denyer SP, Maillard J-Y. Evaluation of new *in vitro* efficacy test for antimicrobial surface activity reflecting UK hospital conditions. *Journal of Hospital Infection* (2013) 85(4):274–81. doi: 10.1016/j.jhin.2013.08.007.

234. International Organization for Standardization. ISO 7581:2023 Evaluation of bactericidal activity of a non-porous antimicrobial surface used in a dry environment (2023) [cited 2025-12-18]. Available from: https://www.iso.org/standard/83386.html.

235. Li Y, Wei L, Lin J, Xie Z, Lu L, Pan X, et al. Nonthermal plasma air disinfection for the inactivation of airborne microorganisms in an experimental chamber and indoor air. *Journal of Applied Microbiology* (2024) 135(4):lxae078. doi: 10.1093/jambio/lxae078.

236. Andersen B, Bånrud H, Bøe E, Bjordal O, Drangsholt F. Comparison of UV C light and chemicals for disinfection of surfaces in hospital isolation units. *Infection Control & Hospital Epidemiology* (2006) 27(7):729–34. doi: 10.1086/503643.

237. de Oliveira Pantoja Freire J, Paes GO, Gonzalez CM, da Gloria Carvalho Barreiros M, Ferreira ALP. UVC light as a strategy for disinfection of hospital air and surfaces. *Acta*

Paulista de Enfermagem (2024) 37:eAPE002191. doi: 10.37689/acta-ape/2024AO000121911.

238. Mosena A, Breyer G, Zitelli L, Menetrier L, de Paula I, Siqueira F, et al. Substrate influence in viral and bacteria UV-C disinfection. *International Journal of Environmental Science and Technology* (2025) 22(4):2531–8. doi: 10.1007/s13762-024-05792-5.

239. Nicolaides C, Avraam D, Cueto-Felgueroso L, González MC, Juanes R. Hand-hygiene mitigation strategies against global disease spreading through the air transportation network. *Risk Analysis* (2020) 40(4):723–40. doi: 10.1111/risa.13438.

240. Catching A, Capponi S, Yeh MT, Bianco S, Andino R. Examining the interplay between face mask usage, asymptomatic transmission, and social distancing on the spread of COVID-19. *Scientific reports* (2021) 11(1):15998. doi: 10.1038/s41598-021-94960-5.

241. Chu DK, Akl EA, Duda S, Solo K, Yaacoub S, Schünemann HJ, et al. Physical distancing, face masks, and eye protection to prevent person-to-person transmission of SARS-CoV-2 and COVID-19: a systematic review and meta-analysis. *The lancet* (2020) 395(10242):1973–87. doi: 10.1016/S0140-6736(20)31142-9.

242. Lei H, Jones RM, Li Y. Exploring surface cleaning strategies in hospital to prevent contact transmission of methicillin-resistant *Staphylococcus aureus*. *BMC infectious diseases* (2017) 17(1):85. doi: 10.1186/s12879-016-2120-z.

243. Morse SS, Mazet JA, Woolhouse M, Parrish CR, Carroll D, Karesh WB, et al. Prediction and prevention of the next pandemic zoonosis. *The Lancet* (2012) 380(9857):1956–65. doi: 10.1016/S0140-6736(12)61684-5.

244. Schmeller DS, Courchamp F, Killeen G. Biodiversity loss, emerging pathogens and human health risks. *Biodiversity and conservation* (2020) 29(11):3095–102. doi: 10.1007/s10531-020-02021-6.